

61
2/5/81.5

0

01.2269

DOE/SF/10534-1

ALTERNATE CENTRAL RECEIVER POWER SYSTEM, PHASE II

MASTER

Midterm Topical Report

March 1980

REMIT/AM/SD

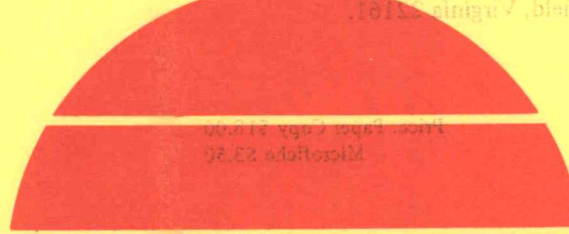
2/5/2/29/0
2/15/2/25/3

Work Performed Under Contract No. AC03-79SF10534

Martin Marietta Aerospace
Denver Division
Denver, Colorado

DOE/SF/10534-1

DOE/SF/10534-1



U.S. Department of Energy



Solar Energy

DISCLAIMER

"This book was prepared as an account of work sponsored by an agency of the United States Government. Neither the United States Government nor any agency thereof, nor any of their employees, makes any warranty, express or implied, or assumes any legal liability or responsibility for the accuracy, completeness, or usefulness of any information, apparatus, product, or process disclosed, or represents that its use would not infringe privately owned rights. Reference herein to any specific commercial product, process, or service by trade name, trademark, manufacturer, or otherwise, does not necessarily constitute or imply its endorsement, recommendation, or favoring by the United States Government or any agency thereof. The views and opinions of authors expressed herein do not necessarily state or reflect those of the United States Government or any agency thereof."

This report has been reproduced directly from the best available copy.

Available from the National Technical Information Service, U. S. Department of Commerce, Springfield, Virginia 22161.

Price: Paper Copy \$18.00
Microfiche \$3.50

DOE-SF-10534-1
MCR-80-1321
Contract DE-AC03-79SF 10534

March 1980

MIDTERM TOPICAL REPORT

ALTERNATE CENTRAL RECEIVER
POWER SYSTEM, PHASE II

Martin Marietta Aerospace
Denver Division
P.O. Box 179
Denver, Colorado 80201

FOREWORD

Martin Marietta Aerospace, Denver Division, submits this report in accordance with Department of Energy Contract DE-AC03-79SF 10534. This satisfies the contractual requirement of a Midterm Topical Report on the Alternate Central Receiver Power System, Phase II program.

TABLE OF CONTENTS

	<u>Page</u>
I. INTRODUCTION	I-1 to I-2
II. SUMMARY	II-1 to II-9
III. RECEIVER SRE.	III-1 to III-164
A. Requirements.	III-1
B. SRE Configuration Selection	III-1
1. Review of Commercial Receiver Selection	III-1
2. Receiver SRE Selection.	III-2
C. SRE System Design	III-10
1. Overall System Description.	III-10
2. Detailed System Description	III-14
3. Receiver Pre-Heat, Fill and Drain	III-17
4. Equipment Layout.	III-19
5. SRE Components.	III-21
a. Receiver.	III-21
b. Sump.	III-29
c. Pump.	III-30
d. Structure	III-30
e. Valves.	III-30
f. Piping.	III-30
g. Cooler.	III-30
h. Calibration flowmeter	III-36
i. Cavity assembly	III-36
D. Failure Modes and Effects Analysis.	III-41
E. Thermal/Hydraulic Analyses.	III-53
1. Receiver Sizing	III-53
2. Flux Analysis	III-61
a. Receiver thermal design	III-68
b. Partial load studies.	III-70
c. Flug gage correlations.	III-105
d. Partial cloud cover	III-107
3. Detailed Receiver Analyses.	III-107
a. Receiver tube warm-up with hot air.	III-107
b. Thermal analysis of welded tubes.	III-116
c. Salt cooldown analysis.	III-116
d. Sudden flow stoppage analysis	III-116
e. Receiver calorimeter cooling system	III-122
f. Two-dimensional steady state tube thermal model .	III-122
4. Air Cooler Thermal Analysis	III-122
5. System Drain Time Analysis.	III-127

TABLE OF CONTENTS (continued)

	<u>Page</u>
6. System Level Analysis	III-127
7. Experimental Uncertainties	III-131
8. Additional Thermal/Hydraulic Analyses	III-136
F. Stress Analyses	III-142
1. Creep-Fatigue of Receiver Tubes	III-142
2. Receiver Structural	III-144
3. Receiver and Cavity Support Structures.	III-145
G. Test Planning	III-147
1. Test Plan Summary	III-147
2. Test Procedures	III-149
3. Data Package.	III-149
H. Fabrication	III-149
1. Receiver Subassembly.	III-149
2. Main Structure.	III-153
3. Air Cooled Heat Exchanger	III-153
4. Pump/Sump	III-158
5. Consoles and Cabinets	III-162
6. Cavity.	III-162
7. Plans for Assembly at CRTF.	III-164
IV. MATERIALS TESTS	IV-1 to IV-35
A. Long-Term Molten Salt Fluid Loop.	IV-1
1. Objectives.	IV-1
2. System Design	IV-2
3. System Operation.	IV-13
4. Results	IV-13
B. Static Materials Tests.	IV-17
1. Objectives.	IV-17
2. Test Descriptions and Results	IV-17
a. Trace Contaminants Test	IV-17
b. On-going Materials Tests (Long Term Tests)	IV-20
c. Stress Corrosion Test	IV-20
d. Carbon Dioxide-Water Vapor Effects on Salt Chemistry	IV-27
e. Salt Treatment Techniques	IV-27
f. Tensile/Intergranular Corrosion Test.	IV-32
g. Corrosion Fatigue Test.	IV-32
h. Thermal Cycling of Test Coupons	IV-32
i. Nitrate Salt Decomposition Test	IV-34
j. Special Purpose Materials Immersion Tests	IV-34
V. COMMERCIAL SYSTEM UPDATE.	V-1
APPENDIX A - RECEIVER SRE TEST PLAN.	A-1
APPENDIX B - MATERIALS TESTS SRE TEST PLAN	B-1

FIGURES

	<u>Page</u>
II-1 Receiver SRE Schematic	II-2
II-2 Artist's Concept of Receiver SRE - Exposed Configuration . .	II-3
II-3 Artist's Concept of Receiver SRE - Cavity Configuration. . .	II-4
II-4 Molten Salt Flow Loop Schematic.	II-6
II-5 Molten Salt Flow Loop.	II-7
III-1 Cavity vs Exposed Receiver Annual Losses - Commercial System.	III-4
III-2 Effect of Absorptivity Degradation on Receiver Performance .	III-5
III-3 Receiver Tube Cooldown After Power Loss.	III-6
III-4 Receiver SRE Candidate Configurations.	III-8
III-5 Receiver SRE Schematic	III-11
III-6 Artist's Concept of Receiver SRE - Exposed Configuration . .	III-12
III-7 Artist's Concept of Receiver SRE - Cavity Configuration. . .	III-13
III-8 Receiver SRE Control Console	III-15
III-9 Receiver SRE Equipment Layout - Plan View.	III-20
III-10 Receiver SRE Equipment Layout - Elevation View	III-22
III-11 Receiver SRE Piping Layout - Plan View	III-23
III-12 Receiver SRE Piping Layout - Elevation View.	III-25
III-13 Receiver Header Tube Assembly.	III-27
III-14 Receiver Tube Heat Flux Sensor	III-28
III-15 Molten Salt Sump	III-31
III-16 Receiver Main Support Towers	III-32
III-17 Cross-Section of Molten Salt Valves.	III-33
III-18 Air Cooler Tube Bundle	III-35
III-19 Calibration Pot Flowmeter Concept.	III-37
III-20 Cavity Assembly.	III-38
III-21 Cavity Front Assembly.	III-39
III-22 Cavity Door Assembly	III-40
III-23 Water-Cooled Aperture.	III-41
III-24 Receiver Tube Layout Analysis.	III-54
III-25 Tube Metal Temperature vs Fluid Temperature - Cavity Configuration at 100% Load	III-56
III-26 Tube Metal Temperature vs Fluid Temperature - Partially Exposed Configuration at 100% Load	III-57
III-27 Tube Metal Temperature vs Fluid Temperature - Fully Exposed Configuration at 100% Load	III-58
III-28 Performance Map - Cavity Configuration	III-59
III-29 Performance Map - Partially Exposed Configuration.	III-60
III-30 Flux Distribution - Horizontal Slice 40 cm Above Aim Point .	III-62
III-31 Flux Distribution - Horizontal Slice 20 cm Above Aim Point .	III-63
III-32 Flux Distribution - Horizontal Slice 20 cm Below Aim Point .	III-64
III-33 Flux Distribution - Vertical Slice 50 cm East of Aim Point .	III-65
III-34 Flux Distribution - Vertical Slice Through Aim Point . . .	III-66
III-35 Flux Distribution - Vertical Slice 50 cm West of Aim Point .	III-67
III-36 Nondimensionalized Heliostat Field Map - SRE vs Full Scale Radiation Geometries	III-69

FIGURES (continued)

	<u>Page</u>
III-37 Incident Fluxes Inside Cavity.	III-71
III-38 Incident Fluxes Outside of Cavity.	III-73
III-39 Incident Fluxes on Aperture Doors and RTAF	III-75
III-40 Receiver Flux Levels - Cavity, 100% Load	III-77
III-41 Receiver Flux Levels - Fully Exposed, 100% Load.	III-79
III-42 Receiver Flux Levels - Partially Exposed, 100% Load.	III-81
III-43 Receiver Flux Levels - Cavity, 75% Load.	III-83
III-44 Receiver Flux Levels - Cavity, 50% Load.	III-85
III-45 Receiver Flux Levels - Cavity, 25% Load.	III-87
III-46 Receiver Flux Levels - Partially Exposed, 75% Load	III-89
III-47 Receiver Flux Levels - Partially Exposed, 50% Load	III-91
III-48 Receiver Flux Levels - Cavity, Warm-up A	III-93
III-49 Receiver Flux Levels - Cavity, Warm-up B	III-95
III-50 Receiver Flux Levels - Cavity, Warm-up C	III-97
III-51 Receiver Flux Levels - Partially Exposed, Warm-up E.	III-99
III-52 Receiver Flux Levels - Partially Exposed, Warm-up F.	III-101
III-53 Receiver Flux Levels - Partially Exposed, Warm-up G.	III-103
III-54 Deleted	
III-55 Heliostat Field Regions for Transfer Function Calculations	III-106
III-56 Flux Levels @ Flux Gage Locations - Cavity Configuration, Maximum Input.	III-108
III-57 Flux Levels @ Flux Gage Locations - Fully Exposed Configuration, Maximum Input, Dual Aim	III-110
III-58 Flux Levels @ Flux Gage Locations - Partially Exposed Configuration, Maximum Input	III-112
III-59 Effect of Partial Cloud Coverage of Heliostat Field on Receiver Fluxes.	III-114
III-60 Thermal Model for Receiver Tube Air Heating.	III-115
III-61 Receiver Tube Air Heating System - Temperatures Across Tube Wall.	III-117
III-62 Receiver Tube Air Heating System Performance - Insulation Temperatures	III-118
III-63 Weld Temperature Analysis - Worst Case	III-119
III-64 Receiver Salt Cooldown Transients.	III-121
III-65 Receiver Tube Thermal Model for Sudden Flow Stoppage	III-123
III-66 Receiver Tube Temperature After Sudden Flow Stoppage	III-124
III-67 Calorimeter Cooling System - Temperatures and Pressures.	III-125
III-68 Two-Dimensional Receiver Tube Temperature Thermal Model.	III-126
III-69 Air Cooler Performance	III-128
III-70 Air Cooler Preheat Power Requirements.	III-129
III-71 Receiver SRE System Drain Time Thermal Model	III-130
III-72 Receiver SRE System Thermal Model.	III-132
III-73 Receiver SRE System Hydraulic Flow Transients.	III-133
III-74 Receiver Transient Performance During Cloud Passage.	III-134
III-75 Receiver Efficiency Uncertainty Analysis	III-135

FIGURES (continued)

	<u>Page</u>
III-76 Receiver Convection Experiment Parameters.	III-138
III-77 Receiver Convection Experiment Uncertainty Analysis.	III-139
III-78 Receiver Convection Experiment Uncertainty Analysis.	III-140
III-79 Receiver Convection Experiment Uncertainty Analysis.	III-141
III-80 Finite Element Model for Receiver Tube Stress Analysis . .	III-143
III-81 Receiver Tubes and Headers Subassembly	III-151
III-82 Receiver Tube Weld Requirements.	III-154
III-83 Welded Receiver Tubes.	III-155
III-84 Receiver Main Support Structure.	III-156
III-85 Air-Cooled Heat Exchanger.	III-157
III-86 Air Cooler Tube Bundle Assembly.	III-159
III-87 Air Cooler Controllable Louvers.	III-160
III-88 Molten Salt Sump and Vertical Cantilever Pump.	III-161
III-89 Receiver SRE Main Control Console.	III-163
IV-1 Long-Term Molten Salt Flow Loop Schematic.	IV-3
IV-2 Long-Term Molten Salt Flow Loop	IV-4
IV-3 Molten Salt Loop Sump and Pump	IV-5
IV-4 Trace Heating Being Installed on Counterflow Heat Exchanger Leg.	IV-6
IV-5 Copper Busbars on Molten Salt Loop Line Heater	IV-8
IV-6 Closeup of Copper Busbars Brazed to Incoloy 800 Tube . . .	IV-9
IV-7 Line Heater with Incoloy 800 Tabs.	IV-10
IV-8 Closeup of Molten Salt Flow Loop Finned Air Cooler Tubes .	IV-11
IV-9 Air Cooler and Fans Showing Insulated Panels	IV-12
IV-10 Removable Materials Sample Holder, with Samples.	IV-14
IV-11 Removal of Materials Sample Holder from Flow Loop.	IV-15
IV-12 Molten Salt Flow Loop Control Console.	IV-16
IV-13 Test Vessel for Trace Contaminants Test.	IV-18
IV-14 Incoloy 800 Materials Samples Immersion Trays in Test Oven	IV-22
IV-15 Dog-Bone Sample for Stress Corrosion Test.	IV-24
IV-16 Stress Corrosion Test Fixture.	IV-25
IV-17 Test Fixture for Effects of CO ₂ -Water Vapor on Salt Chemistry.	IV-28
IV-18 Nitrate Salt Decomposition Test Fixture.	IV-35

TABLES

	<u>Page</u>
II-1 Static Materials Tests and Status.	II-9
III-1 Cavity vs Exposed Receiver Cost - Commercial System.	III-3
III-2 Comparison of Receiver SRE Candidate Configurations.	III-9
III-3 Failure Modes and Effects Analysis	III-43
III-4 Thermal and Wind Stresses on Receiver Tubes.	III-146
III-5 Receiver SRE Tests	III-148
III-6 Receiver SRE Data Package Contents	III-150
IV-1 Test Matrix for Trace Contaminants Test.	IV-19
IV-2 Weight Change Data for Trace Contaminants Tests After 2000 Hours	IV-21
IV-3 Visual Results of Ongoing Materials Tests - 2000-hr Examination.	IV-23
IV-4 Test Matrix for Stress Corrosion Test.	IV-26
IV-5 Test Matrix for CO ₂ -Water Vapor Test	IV-29
IV-6 Test Results for CO ₂ -Water Vapor Test.	IV-30
IV-7 Test Matrix for Salt Treatment Techniques.	IV-31
IV-8 Test Matrix for Tensile/Intergranular Corrosion Test . . .	IV-33
IV-9 Test Matrix for Corrosion Fatigue Test	IV-33

I. INTRODUCTION

The objective of the Phase II program is to prove the feasibility of the molten salt central receiver power system by conducting a series of experiments and using results to update the commercial system developed during Phase I. The experiments are:

- 1) Receiver Subsystem Research Experiment (SRE),
- 2) Long-term molten salt flow loop, and
- 3) Materials test program.

The primary objectives of the receiver SRE are:

- 1) Demonstrate the safe, reliable, and efficient operation of a solar receiver using molten salt (60% NaNO₃, 40% KNO₃) as the heat transfer fluid under operating conditions that simulate a commercial receiver including:
 - Fluid temperatures,
 - Heat flux,
 - Realistic transients (start-up, shutdown, and cloud interruption),
 - Steady-State operation; and
- 2) Demonstrate the fabrication processes and quality control techniques required for a commercial receiver.

The primary objectives of the molten salt loop are:

- 1) Determine if there is any significant mass transport of material that could effect the life of a molten salt system;
- 2) Determine if corrosion rates in a flowing system differ significantly from those in static tests;
- 3) Establish the chemical stability of molten salt in a system with flow and temperature excursions; and
- 4) Gain more experience in the design, construction and operation of molten salt systems.

The primary objective of the materials test program is to provide materials test data needed to commercialize a solar power plant using molten salt.

Specific objectives of this program are:

- 1) Demonstrate compatibility of construction materials with molten salt under anticipated conditions including temperature, fluid velocity, galvanic potentials, salt impurities, and stress;
- 2) Demonstrate stability of molten salt under all anticipated operating conditions;
- 3) Determine effects of CO₂ and water vapor in air on the chemistry of the salt in a vented system; and
- 4) Develop an economical method of treating the salt in a vented system if required.

In this program we are supported by Badger Energy, Inc. Boston, MA, and the Arizona Public Service (APS) Co. Badger provides design input for the molten salt systems, and APS reviews the design and test programs to assure that the program will satisfy the needs of a utility.

II. SUMMARY

We conducted a tradeoff study early in the Phase II program and showed that a four-cavity receiver is more cost effective than an exposed receiver for a commercial solar central receiver power system using molten salt. We then did another study to determine the best of five configurations for the receiver SRE to be tested at the Central Receiver Test Facility (CRTF) in Albuquerque, NM. We decided that a combined cavity-exposed receiver best met the criteria of ability to measure performance, simplicity, compatibility with CRTF, cost and schedule, risk in extrapolating results, and ability to provide comparative data between exposed and cavity receivers.

A simplified schematic of the receiver SRE is shown in Figure II-1. Molten salt (60% NaNO₃, 40% KNO₃) is maintained at 288°C (550°F) in the sump. A vertical cantilever pump circulates the molten salt through the receiver, which consists of 18 serpentine passes of Incoloy 800 tubes. The active area of the receiver panel is approximately 5.5-m (18-ft) wide and 4.0-m (13-ft) high. Solar energy from the CRTF heliostats is directed onto the receiver panel and heats the circulating salt to 566°C (1050°F). The salt then passes through a forced-draft, air-cooled heat exchanger where it is cooled to 288°C (550°F) before being returned to the sump.

Figure II-2 is an artist's concept of the receiver SRE in the exposed configuration atop the CRTF tower. The sump/pump assembly is located to the right of the receiver and the air cooler is located behind it.

Figure II-3 is an artist's concept of the cavity configuration. The cavity assembly is a separate structure that mounts in front of the exposed receiver. In front of the cavity's water-cooled aperture is the Real Time Aperture Flux (RTAF) device used to make power and flux measurements. Pneumatically-operated, insulated doors are seen on either side of the aperture.

We designed the SRE receiver to duplicate larger, commercial receivers with respect to inlet and outlet salt temperatures, maximum solar flux, salt heat transfer coefficients, and power rise rates. Several thermal and hydraulic analyses were done in support of the system design including response to start-up and shutdown transients, sudden flow stoppage, and partial cloud cover of the heliostat field, and a system drain time analysis. We also performed detailed thermal and mechanical stress analyses and a failure modes and effects analysis to identify all the single-point failure modes, their impact on the system, and the corrective measures to be taken.

The receiver was designed and coded to ASME Section VIII, Division 2, and was fabricated with methods we expect will be used to build commercial receivers. Each of the 288 receiver absorber tubes is welded to the adjacent tubes by a tungsten inert gas (TIG) welding process.

II-2

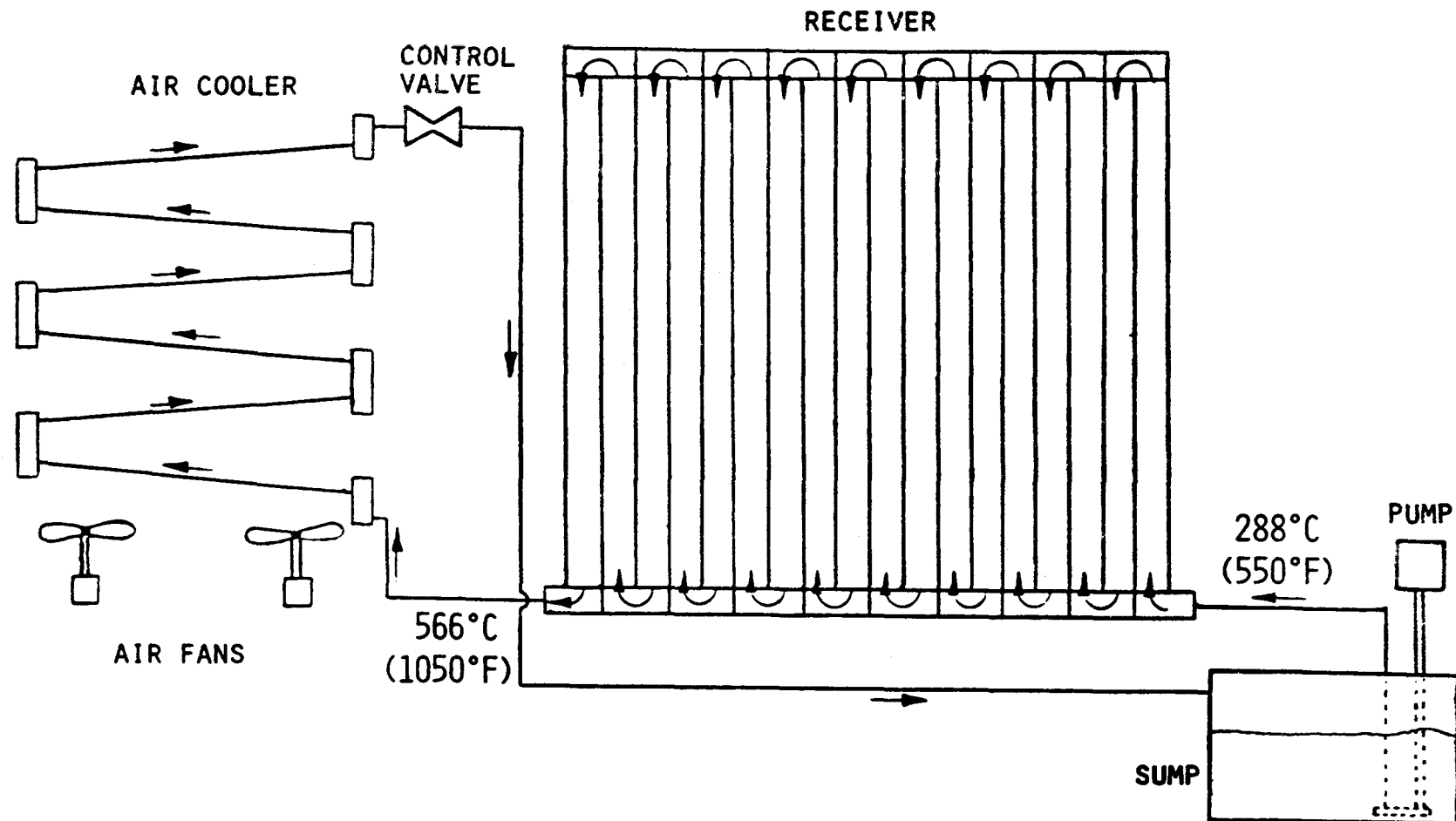


Figure II-1 Receiver SRE Schematic

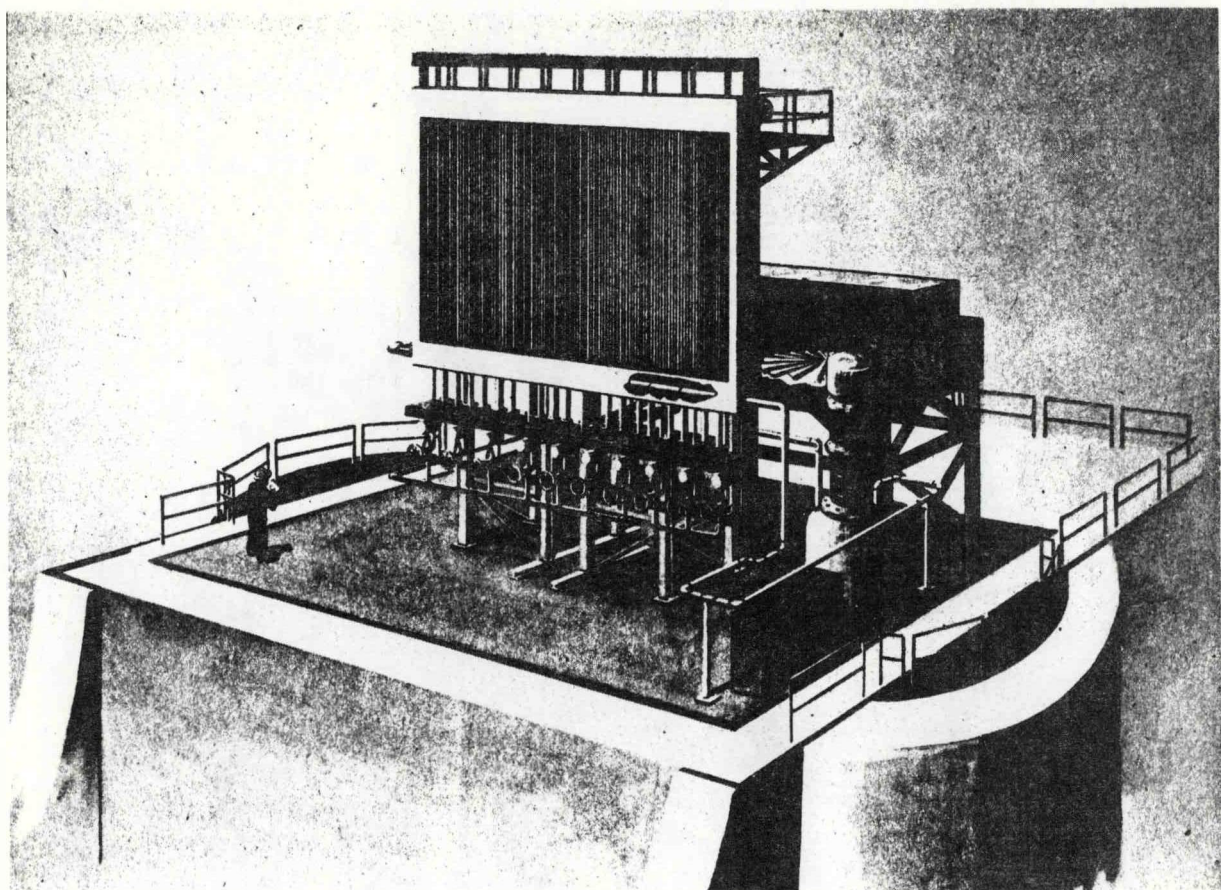


Figure II-2 Artist's Concept of Receiver SRE--Exposed Configuration

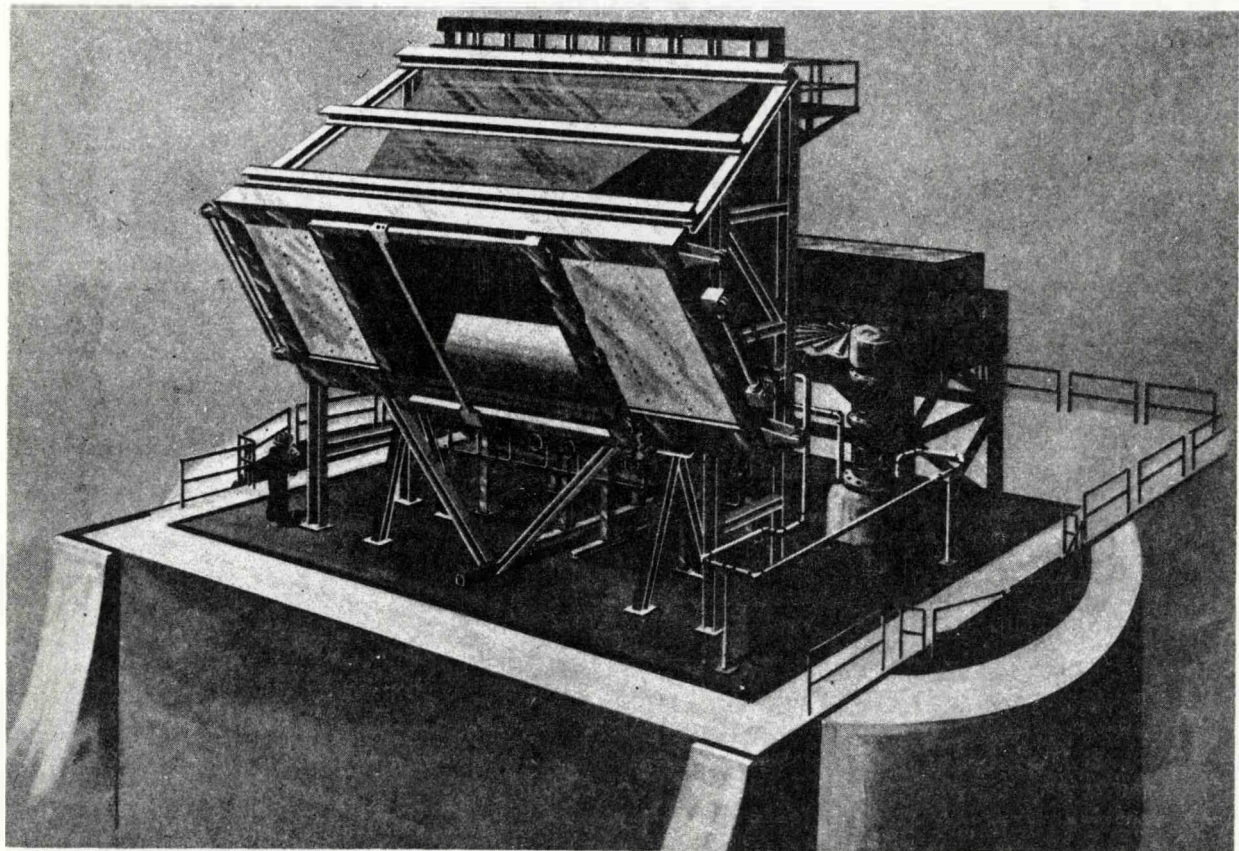


Figure II-3 Artist's Concept of Receiver SRE--Cavity Configuration

We have completed all of the receiver SRE components and plan to have the entire system shipped to the CRTF by mid-May, 1980. We will finish system assembly and checkouts in May and conduct solar testing from June through September.

We are also conducting a materials test program to obtain quantitative data on the salt and candidate construction materials in support of the commercial system design. The program comprises two major efforts: A long-term molten salt flow loop, and static salt and materials tests.

The molten salt flow loop duplicates the thermal and fluid flow characteristics of a full-scale central receiver power system to permit the study of material compatibility and salt stability in a dynamic system. Specifically, the loop simulates:

- 1) Fluid velocity--3.5 m/s (11 ft/s) in the vicinity of the materials samples,
- 2) Temperature profile--566°C (1050°F) at the hot end of the loop and 288°C (550°F) at the cold end, and
- 3) Materials--the loop is constructed of Incoloy 800 at the hot end and A516 carbon steel at the cold end.

Figure II-4 is a schematic of the molten salt loop. Molten salt is maintained at 288°C (550°F) in the sump. A vertical cantilever pump pumps the salt through the inside tube of the counterflow heat exchanger where it is heated to 482°C (900°F). The salt is heated to 566°C (1050°F) in a three-stage electrical resistance heater tube, then cooled to 371°C (700°F) as it passes through the outer tube of the counterflow heat exchanger. It then flows through a finned-tube forced-draft air cooler and is returned to the sump at 288°C (550°F).

Figure II-5 is a photograph of the assembled flow loop. The pump and sump are in the lower left. The three long legs of the counterflow heat exchanger as well as the line heaters can be seen up the left side of the photo. The air cooler is above and to the right of the sump, and the control console is in the lower right corner.

Seven sample ports are located at various temperatures throughout the loop (see Figure II-4). Ports 1-6 permit insertion and removal of metal sample coupons, and port 7 allows removal of salt samples from the sump. Every 1000 hours the coupons are examined visually for corrosion and checked for weight change, and the salt is chemically analyzed.

The test, which will run a minimum of 5000 hours, will permit investigation of:

- 1) Mass transport phenomena (if any) from the high to the low temperature end of the loop;

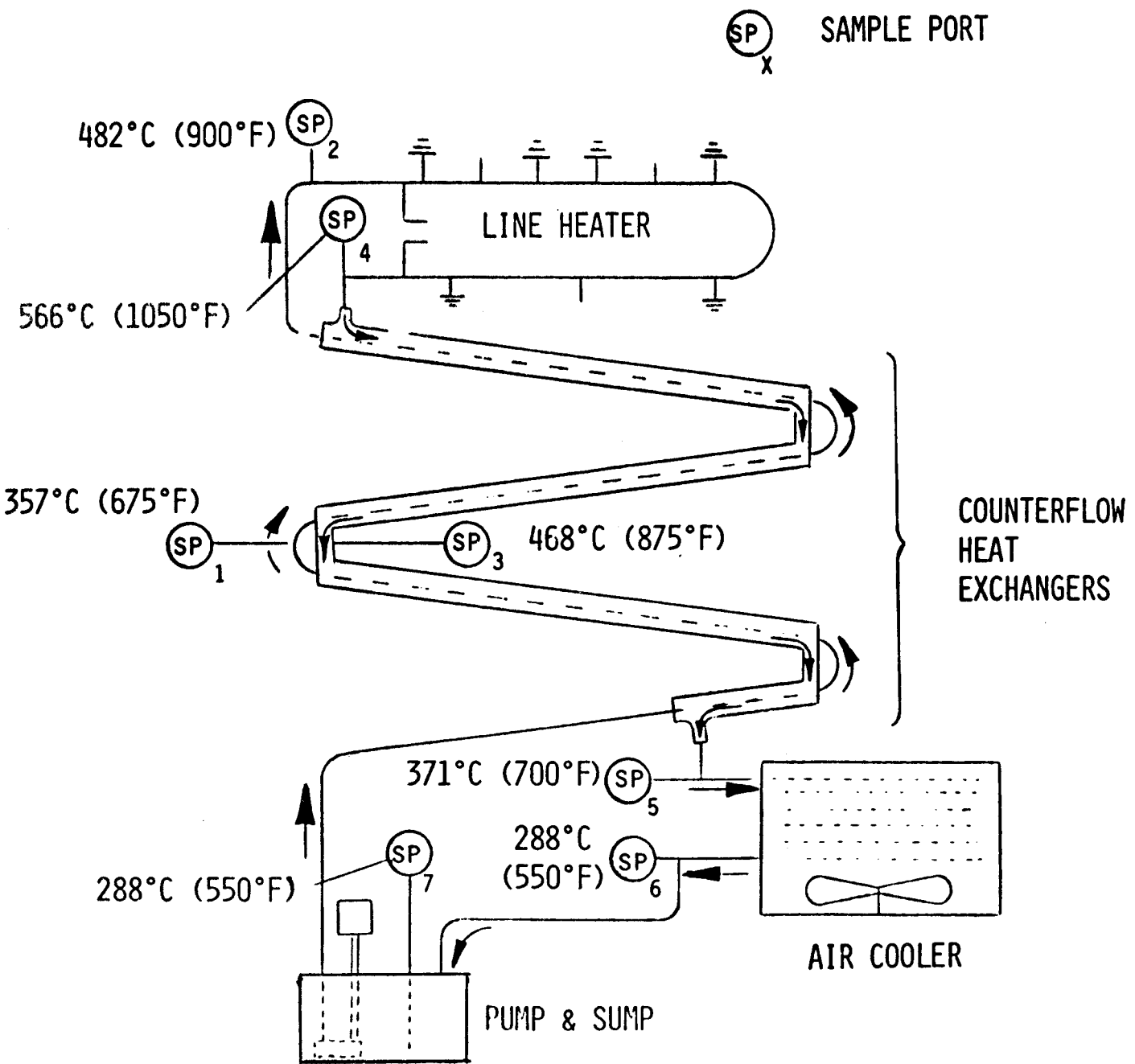


Figure II-4 Long-Term Molten Salt Flow Loop Schematic

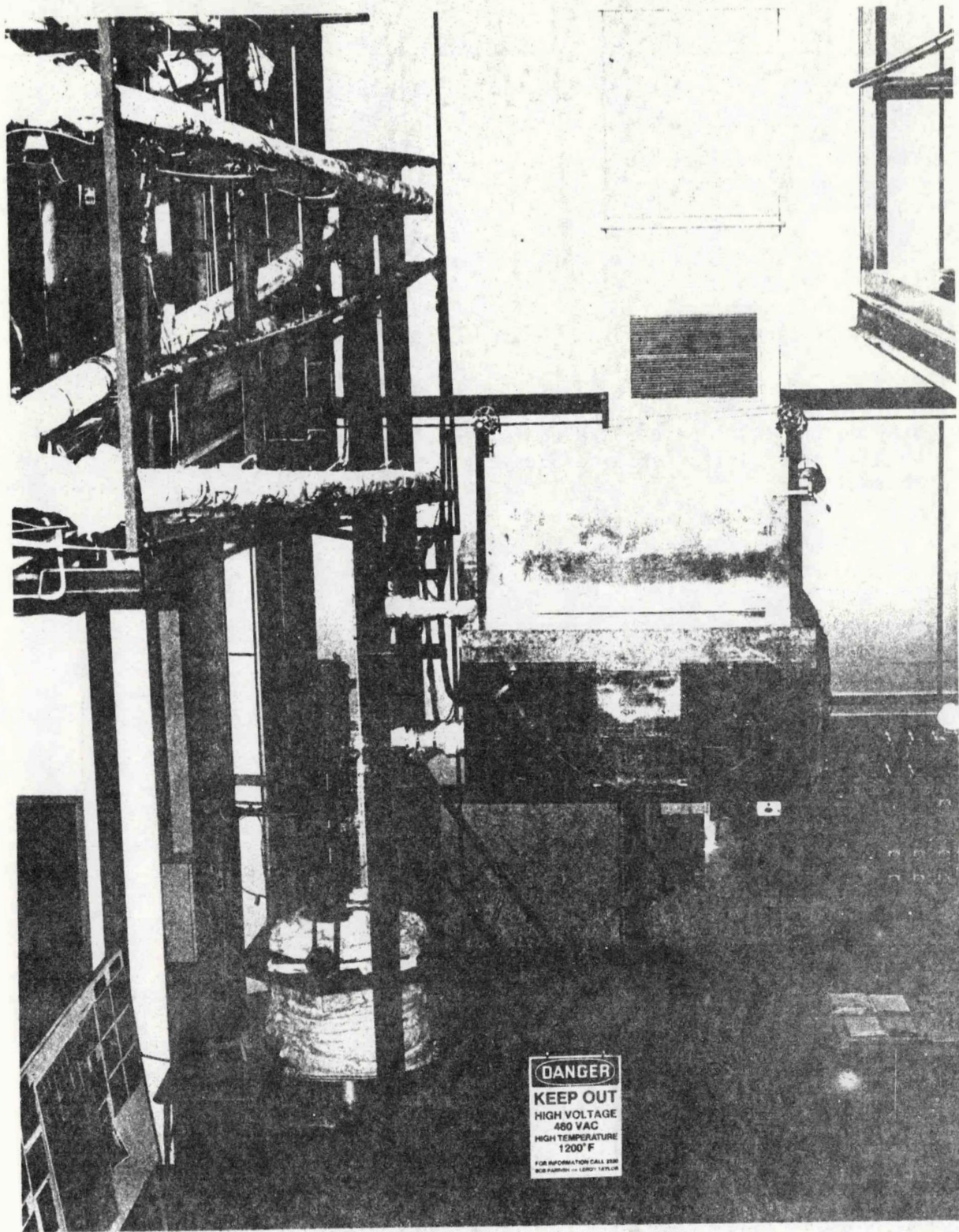


Figure II-5 Long-Term Molten Salt Flow Loop

- 2) Material compatibility and erosion in a flowing molten salt system;
- 3) Chemical stability of the molten salt in a flowing, thermally-cycled system; and
- 4) Electrolytic corrosion (if any) in a dynamic molten salt system.

Incoloy 800 and carbon steel materials samples examined after 1000 hours of testing showed no blistering, pitting, or flaking.

The static materials compatibility tests are an extension of materials tests conducted during Phase I of this program. The Phase II program continues the testing of Incoloy 800 and carbon steel (the selected construction materials) as well as testing other candidate materials such as 347, 316L, and RA330 stainless steels. The tests are designed to show the effects on materials and salt of specific conditions expected in a commercial molten salt central receiver system. Table II-1 summarizes the objectives and status of each test.

Near the end of the Phase II program we will update the commercial system design based on the results of the materials tests and data generated during the receiver SRE tests. We will revise performance and cost-of-electricity estimates for the commercial system recommended in Phase I.

Table II-1 Static Materials Tests and Status

<u>OBJECTIVES</u>	<u>STATUS</u>
TRACE CONTAMINANTS TEST --Evaluate effects of trace contaminants in the salt on the corrosion of construction materials	--Incoloy 800, 316L, and RA330 look good after 3000 hours exposure --Carbon steel shows some pitting and flaking at 399°C (750°F)
LONG-TERM TESTS --Continue Phase I materials tests to determine the long-term effects of salt exposure on construction materials	--Incoloy 800, RA330, and 347 show no visual signs of degradation --316 stainless and A516 carbon steels are blistering and flaking
STRESS CORROSION --Determine the susceptibility of parent metal and weld material to stress corrosion cracking	--Incoloy 800 stress corrosion samples are currently in test, with other materials to be tested shortly
CO₂/WATER VAPOR EFFECTS ON SALT --Evaluate the long-term effects of exposure of molten salt to the ambient atmosphere	--Both the carbonate and hydroxide/oxide concentrations seem to be approaching equilibrium levels below the solubility limits at test temperature
SALT TREATMENT TECHNIQUES --Investigate regenerating molten salt containing carbonates and hydroxides/oxides by exposure to nitrogen dioxide	--Test will be started after completion of the CO ₂ /water vapor tests
TENSILE/INTERGRANULAR CORROSION (IGC) --Assess the susceptibility of parent metal and weld material to IGC analysis	--Samples are in test, and 6-month results will be made in June, 1980
CORROSION FATIGUE TEST --Obtain fatigue data for candidate receiver metals immersed in molten salt	--Corrosion fatigue test is scheduled to start in mid-March, 1980
THERMAL CYCLING OF TEST COUPONS --Demonstrate the tenacity of the oxide passivation layer on test materials to thermal shock	--Thermal cycling test will start in April, 1980
NITRATE SALT DECOMPOSITION TEST --Determine the rate of nitrate salt decomposition to oxides in a closed system	--Salt sample is currently in test; no data available yet
SPECIAL PURPOSE MATERIALS TESTS --Determine the compatibility of limited-use materials such as gaskets and valve packing to molten salt	--Several materials tested show no degradation --New materials are being added to test as they become available

III. RECEIVER SUBSYSTEM RESEARCH EXPERIMENT (SRE)

A. REQUIREMENTS

Functional requirements of the receiver SRE are as follows:

- 1) Nominal thermal output - 5 MW;
- 2) Molten salt temperatures - 288°C (550°F) to 566°C (1050°F);
- 3) Heat fluxes (comparable to commercial receiver):
Average - 0.32 MW/m² (100,000 Btu/hr-ft²),
Peak - 0.66 MW/m² (210,000 Btu/hr-ft²).

The SRE was designed to be compatible with the Central Receiver Test Facility (CRTF) in Albuquerque, NM, which uses north-field heliostats and is designed to CTRF wind and seismic load requirements. It also accepts the Real Time Aperture Flux (RTAF) device for power input and flux measurement and interfaces with CRTF instrumentation and controls.

The receiver will be tested in both cavity and exposed configurations. To the extent possible, the receiver was designed and built using the same analytical and fabrication techniques as those expected on the commercial receiver. It was also designed to be easily transportable to the CRTF.

B. SRE CONFIGURATION SELECTION

1. Review of Commercial Receiver Selection

During Phase I, a trade-off study was done resulting in selection of a four-aperture, cavity-type receiver for the commercial system. Groundrules established for the study were:

- 1) Use a nominal commercial receiver size of 200 MWt,
- 2) Compare only those features exhibiting significant differences between cavity and exposed receivers.

Factors considered in the evaluation were:

- 1) System cost effectiveness,

- 2) Reliability,
- 3) Operational characteristics.

An estimate of the effects of receiver selection on system cost is given in Table III-1, which shows that the cavity approach is preferred. The primary reason for the cavity's cost effectiveness is that its efficiency is significantly better than that of the exposed receiver. Figure III-1 shows a loss comparison between the two types of receivers.

Among reliability factors considered was the effect of coating degradation on receiver efficiency. Figure III-2 shows receiver efficiency as a function of coating solar absorptivity. The cavity is much less sensitive to the coating absorptivity degradation.

Operational characteristics considered were ease of startup shutdown, and freeze protection. These are important considerations in a molten salt system since the freezing point of the salt is 221°C (430°F). Figure III-3 shows the temperature vs time of the coldest spot on the receiver tubes after power loss. A cavity configuration offers much greater protection against freezing. Also, the cavity receiver can be more easily preheated prior to start-up than an exposed receiver. In a cavity receiver, tubes could be kept hot during cloud interruptions by circulating the salt from storage through the receiver tubes. It may even be desirable to keep the receiver hot overnight to minimize thermal cycling and for ease of start-up.

Based on this study, a cavity receiver was selected as the preferred configuration for the commercial system.

2. Receiver SRE Selection

Specific receiver SRE objectives are as follows:

- 1) Demonstrate operation of a molten salt receiver including:
 - Performance at full load,
 - Performance at partial load,
 - "Cold" start-up,
 - Overnight shutdown and start-up,
 - Emergency shutdown, and
 - Ability of system to recover from cloud interruptions in a controlled manner.
- 2) Simulate commercial receiver characteristics such as:
 - Molten salt Reynolds, Nusselt, and Prandtl numbers;

Table III-1 Cavity vs Exposed Receiver Costs--Commercial System

Yearly Average Thermal Efficiency-%	Spillage-%	Number of Heliostats	Cost of Heliostats (2) (\$107.6/m ²) (\$10/ft ²) (4)	Cost of 9 Receivers	Cost of Heliostats Plus Receivers
Exposed 84.7	1.0	72,936	\$313.6M	\$9.3M	\$322.9M
Cavity 92.0	2.0	67,830	\$291.7M	\$11.9M	\$303.6M
Potential Savings (\$)					\$19.3M
Potential Savings (% of Total Plant Cost)					4.3% (5)

(1) Yearly energy leaving receiver/yearly energy incident on receiver, as calculated by STEAEC using 1976 Barstow insolation.

(2) Each heliostat 39.95 m² (430 ft²).

(3) Phase I Baseline - 300 MWe \approx 11 Hrs Storage

(4) For \$70/m² Heliostats the % difference in total plant cost is 3.7%.

(5) For 3 hours of storage and \$107.6/m² Heliostats the % difference in total plant cost is 3.9%.

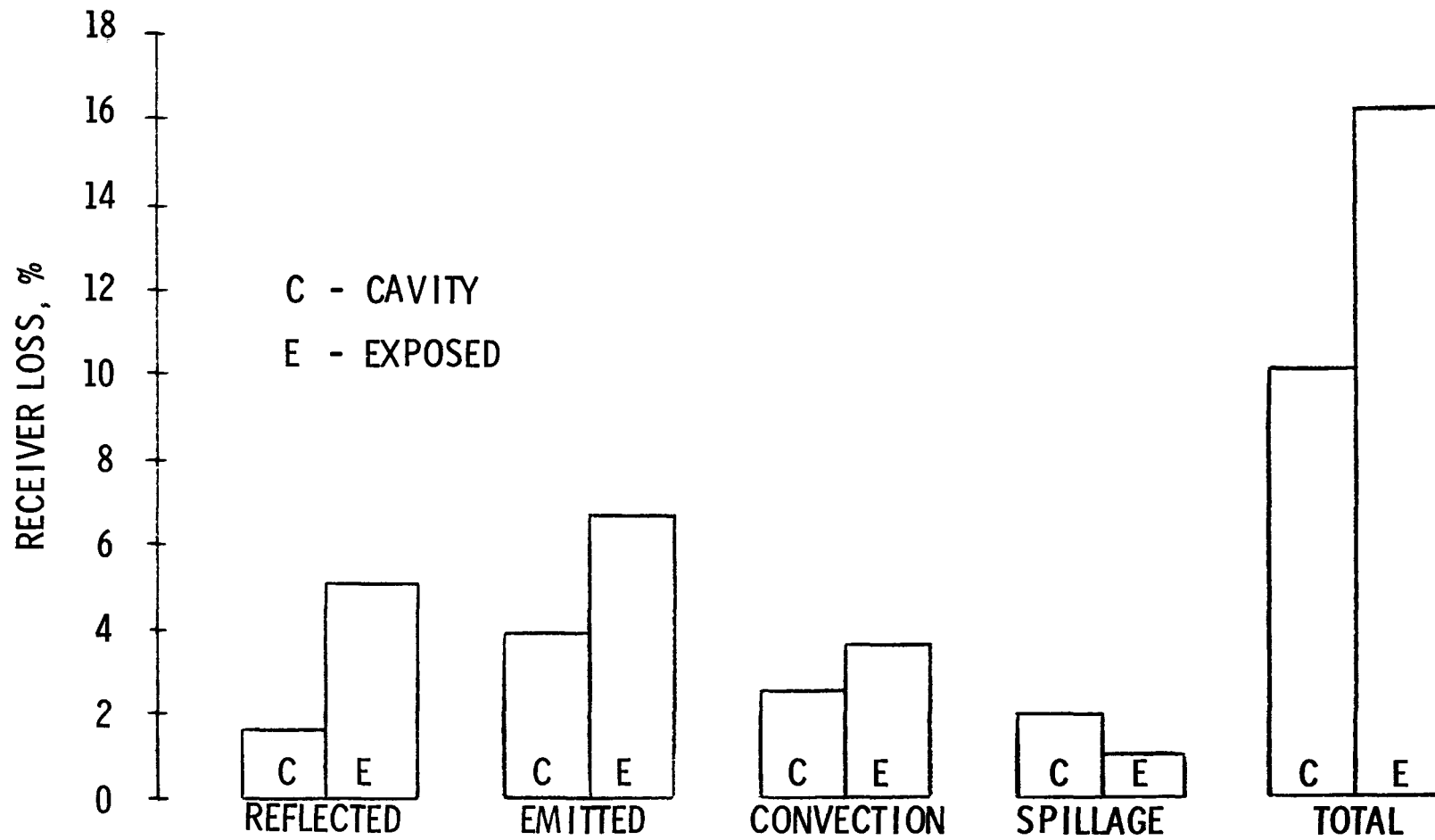
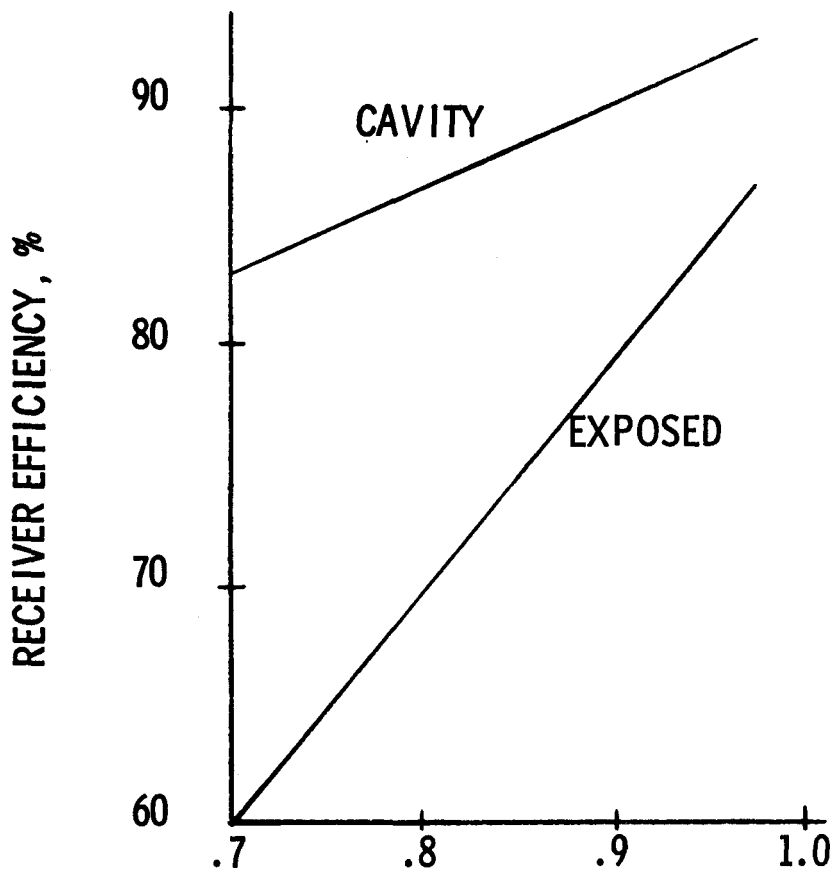


Figure III-1 Cavity vs Exposed Receiver Annual Losses--Commercial System



ABSORPTIVITY OF TUBE SURFACES

Figure III-2 Effect of Absorptivity Degradation on Receiver Performance

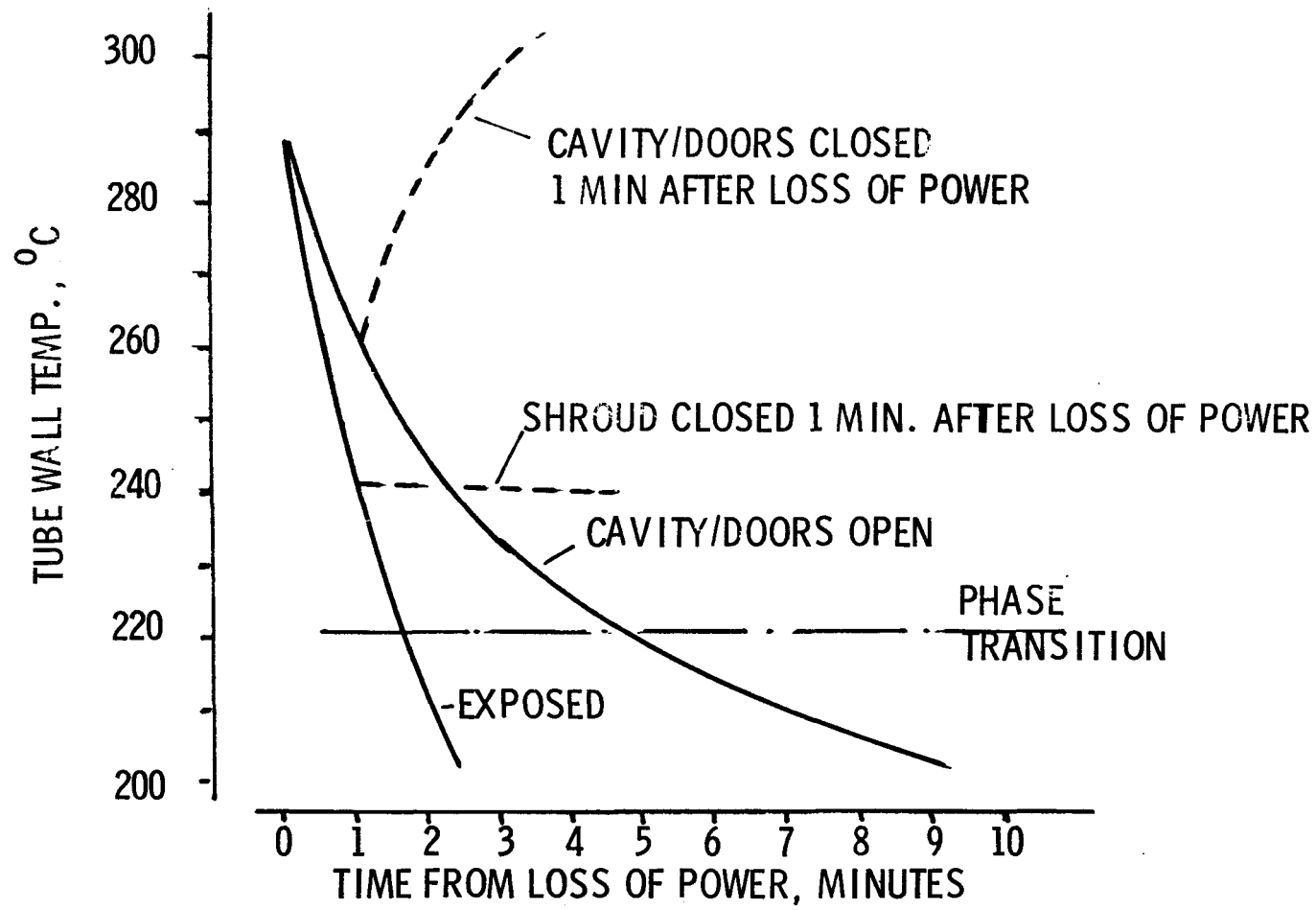


Figure III-3 Receiver Tube Cooldown after Power Loss

- Molten salt velocity;
- Peak fluxes; and
- Average fluxes.

3) Correlate analysis and test data for SRE:

- "Scale" analysis to commercial size,
- Receiver performance, and
- System control.

Criteria for selection of the receiver SRE configuration that we developed are:

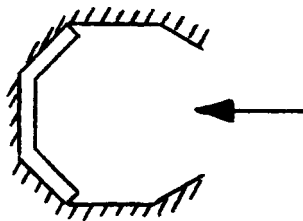
- 1) Ability to measure receiver performance,
- 2) Basic simplicity of tests,
- 3) Compatibility with CRTF,
- 4) Cost and schedule considerations,
- 5) Risk in extrapolating results from SRE to the commercial receiver, and
- 6) Ability to provide comparative data between cavity and exposed receivers.

The ability to measure receiver performance with confidence is particularly important. The major problem in measuring performance of a solar test is obtaining accurate input measurement. The best way to do this is to use the Real Time Aperture Flux (RTAF) device developed for the CRTF.

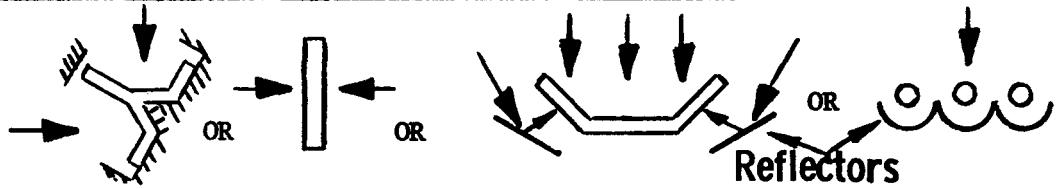
The SRE candidates considered are shown in Figure III-4. Of the alternatives considered, the cavity with two-sided heating is the most complex and difficult to measure.

A comparison of the candidates is given in Table III-2. Each candidate was rated using the criteria presented earlier. The candidate best meeting a particular criteria was given a rating of 10 and the other candidates were given a lower value. The cavity with one-sided heating was given the value of 10 for the ability to measure performance because the RTAF could be integrated into the cavity and provide an accurate measurement of the solar flux input at all times. The exposed "scaled" was considered the simplest. Several of the candidates were considered very compatible with the CRTF. The two-sided cavity was considered the least compatible. Cost and schedule considerations are strongly related to simplicity. Risk in extrapolating results is lowest in the exposed-modular configuration.

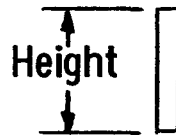
CAVITY - ONE SIDED
HEATING



CAVITY - TWO SIDED
HEATING

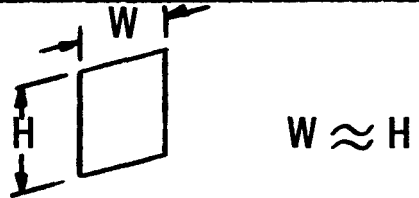


EXPOSED - MODULAR



Height of SRE \approx Height of Commercial
Receiver

EXPOSED - "SCALDED"



COMBINED CAVITY/EXPOSED

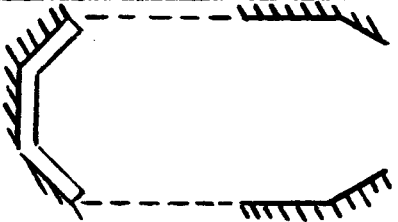


Figure III-4 Receiver SRE Candidate Configurations

Table III-2 Comparison of Receiver SRE Candidate Configurations

	Ability to Measure Performance	Simplicity	Compatibility with CRTF	Cost and Schedule	Risk in Extrapolating Results	Ability to Provide Comparative Data	Total
Cavity - one sided heating	10	9	10	9	8	5	51
Cavity - two sided heating	7	7	7	7	7	5	40
Exposed -- modular	6	9	8	9	10	5	47
Exposed - "Scaled"	8	10	10	10	9	5	52
Combined Cavity Exposed	9	9	10	8	8	10	54

Considering SRE factors alone (criteria 1-5), the exposed "scaled" configuration appears best. However, as discussed earlier, a cavity receiver is preferred for the commercial design. The next choice is the cavity with one-side heating followed closely by the combined cavity/exposed SRE. Since the latter can also provide comparative data for both receiver types (criterion 6), it was decided that this was the best approach for the SRE.

C. SRE SYSTEM DESIGN

1. Overall System Description

A simplified schematic of the system is shown in Figure III-5. The entire volume of salt for this experiment is contained in a sump. The salt is heated to 288°C (550°F) and is maintained at this temperature throughout the experiment. The pump circulates the molten salt through the receiver, which consists of Incoloy 800 tubes arranged in eighteen serpentine passes. As the salt passes through the receiver, the solar flux from the CRTF heliostats is directed onto this panel and increases the salt temperature to 566°C (1050°F). The salt flow then passes through an air-cooled, finned-tube heat exchanger. This reduces the salt temperature from 566°C (1050°F), to 288°C (550°F) and the salt is returned to the sump.

An artist's concept of the exposed configuration of the test setup as it would be assembled on top of the CRTF tower is shown in Figure III-6. The salt sump is shown to the center right of the elevating module with the vertical cantilevered shaft pump mounted on top. The molten salt is circulated through the interconnecting pipe and enters the receiver in the lower right header. A cutaway view of the receiver header insulation shows the individual header assemblies. The molten salt leaves the receiver at the lower left and is transported to the air cooler located in back of the elevating module (behind the receiver), protected from any stray solar insolation. The width of the elevating module parallel to the receiver surface is 9.1 m (30 ft) and the depth is 7.6 m (25 ft). The highest point of the receiver is approximately 8.2 m (27 ft) above the elevating module surface.

The cavity configuration of the molten salt solar receiver SRE is shown in Figure III-7. The cavity and support structure assembly is a freestanding unit not attached to the receiver support structure. The assembly in front of the cavity opening includes pneumatically operated doors, a water-cooled aperture lip, and the RTAF device supplied by the CRTF. This assembly is supported by a separate lower structure with minimum attachment to the cavity support structure.

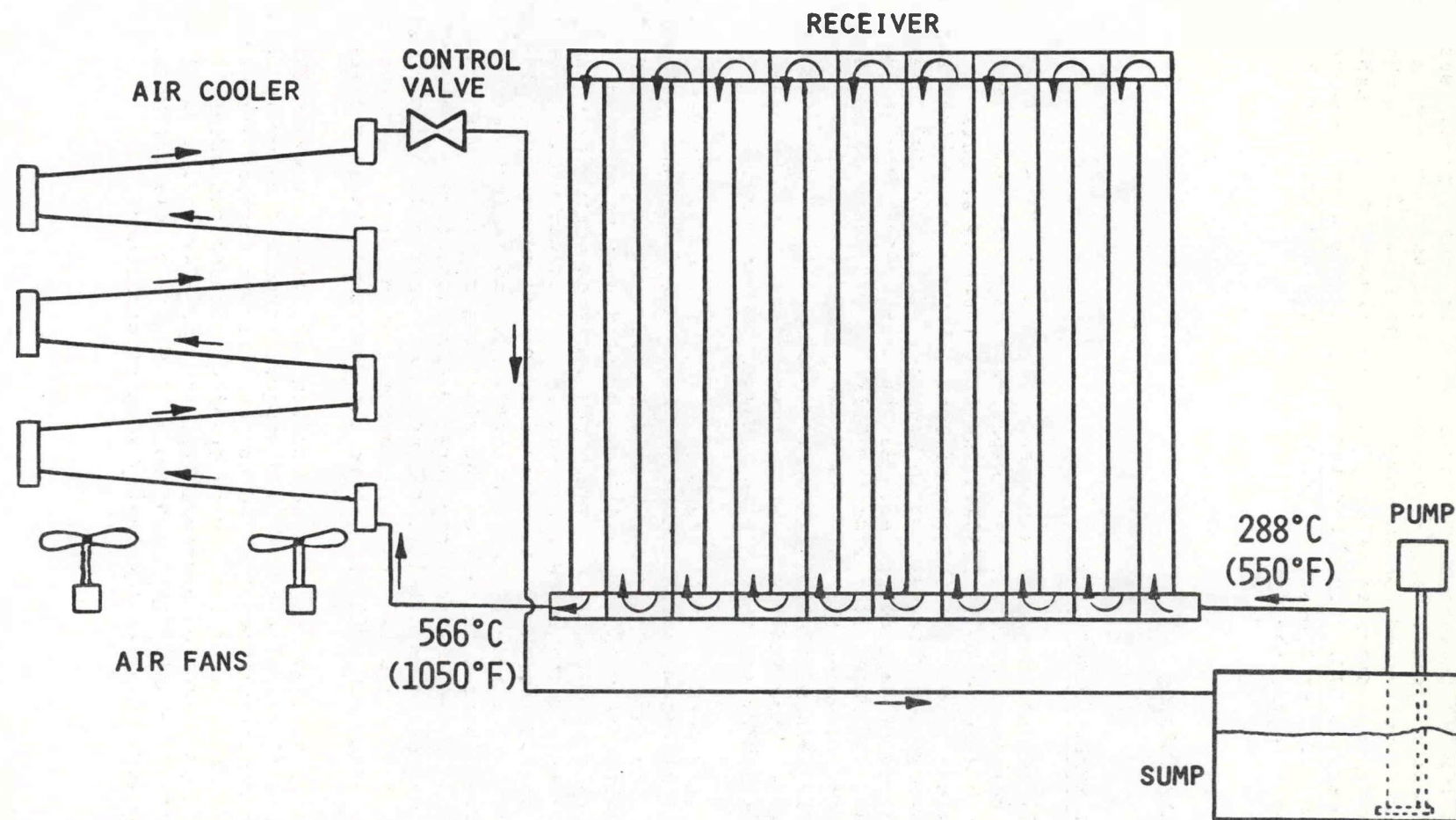


Figure III-5 Receiver SRE Schematic

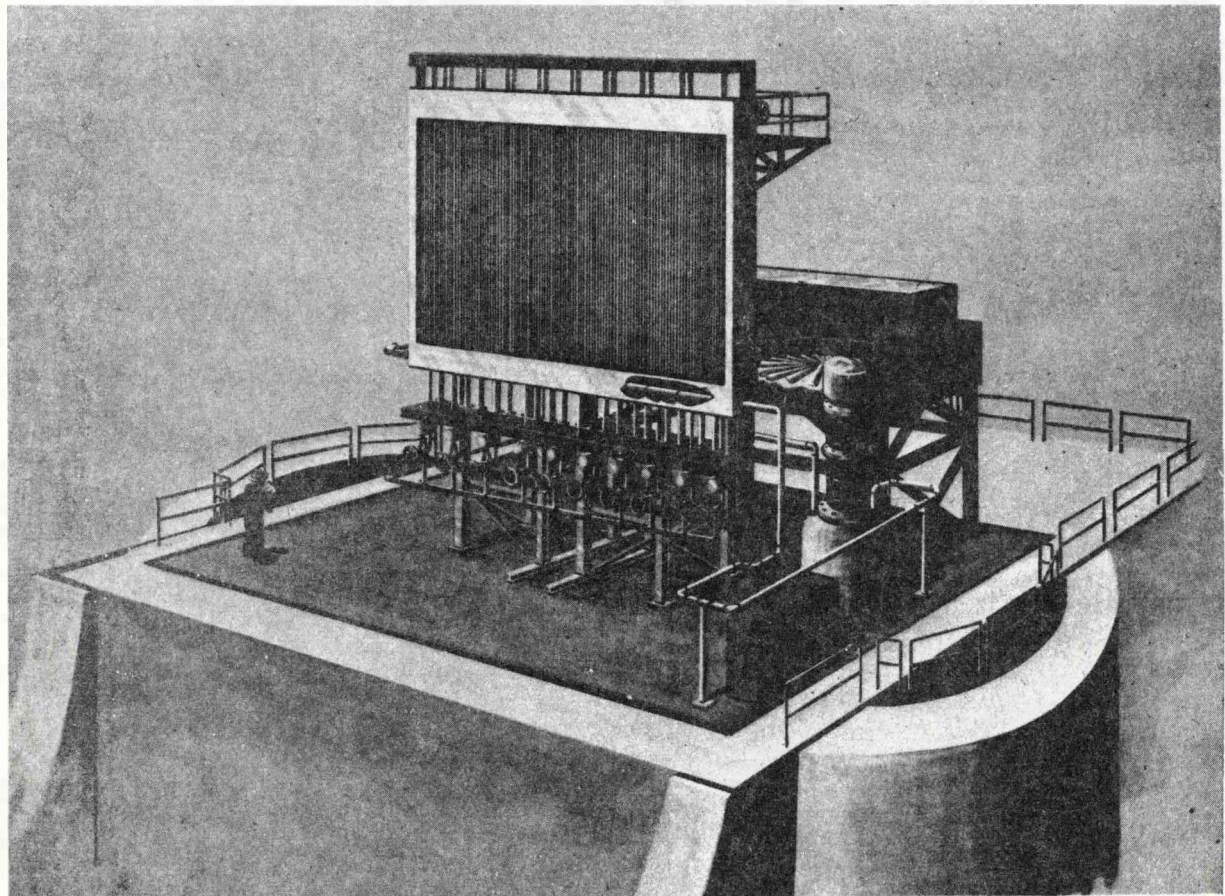


Figure III-6 Artist's Concept of Receiver SRE--Exposed Configuration

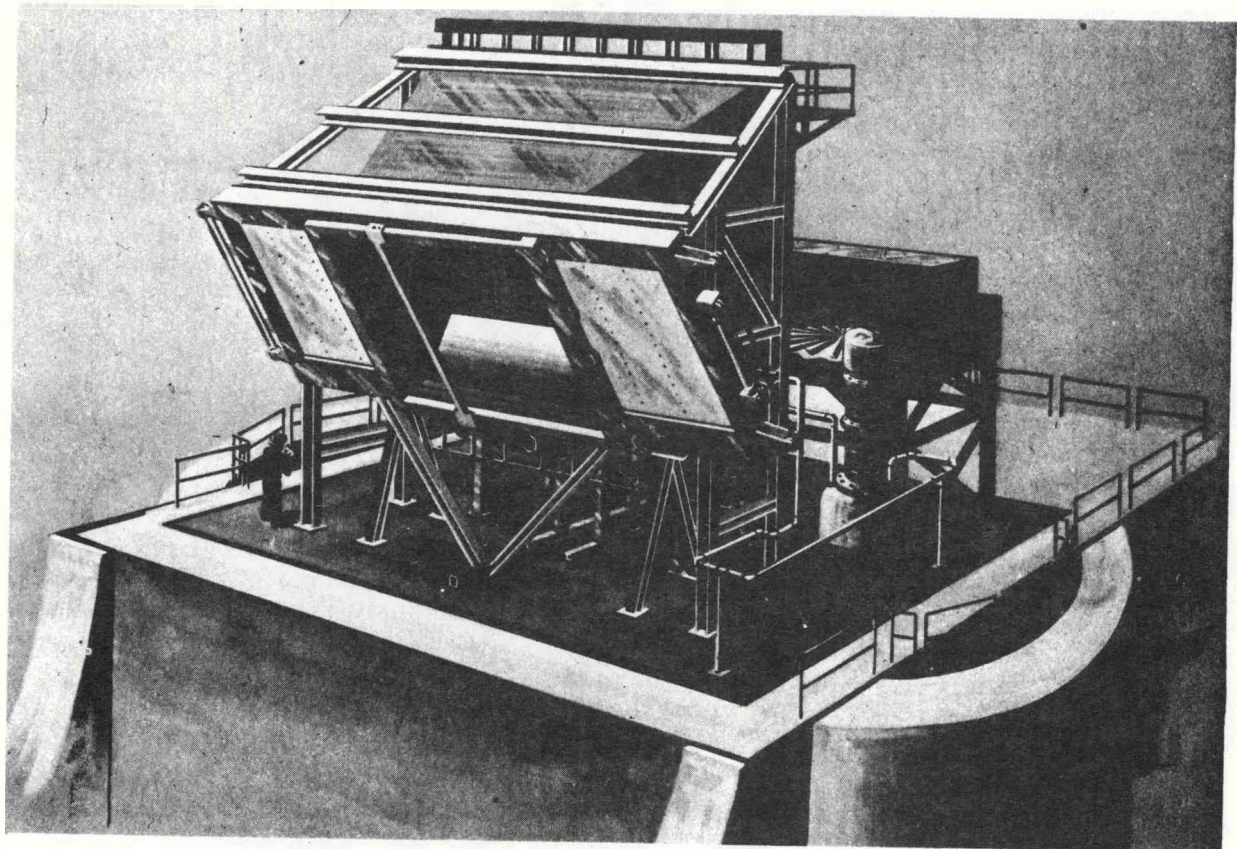


Figure III-7 Artist's Concept of Receiver SKE--Cavity Configuration

2. Detailed System Description

A more detailed system schematic is shown in Figure III-8. This shows a diagram of the receiver SRE as it will appear on the control console located in the elevating module. The entire experiment can be controlled and operated from this console. Once the SRE is started and in a steady-state flow condition, the system operation can be transferred to the CRTF main computer system(MCS).

The sump contains the entire volume of salt when the salt is drained from the system and stored during nonsolar portions of the day. There are thermocouples at various levels on the sump side wall. These temperatures are recorded on a data logger; one of the temperature readings is indicated on the control console, and a redundant temperature signal is sent to the MCS. The pump start and stop switches are located just above the diagram of the sump/pump. The pressure at the outlet of the pump (PT1) is also indicated on the control console. If this pressure drops below a set value, a signal will be sent to the annunciator panel shutting the system down.

The line between the sump and the receiver has an isolation valve (IV-1) that can be adjusted from the control console. The pressure at the inlet to the receiver (PT2) is sensed downstream of IV-1 and indicated on the control console. The temperature of the salt flow at the inlet to the receiver is sensed by dual temperatures signals (TT 2 and TT 3). Signal TT 3A is indicated on the control console and signal TT 2B is recorded on the strip chart recorder located in the upper right corner of the console. Signal TT 3B is sent to the MCS while signal TT 2A is a spare.

During normal SRE operation, the receiver drain valves (DV-1 through DV-10) as well as the receiver purge valves (PV-1 through PV-9, located above the diagram of the receiver) would be closed. This allows the molten salt to flow through the eighteen serpentine flow paths of the receiver to absorb the solar flux. The filling and draining sequence of the SRE will be discussed later.

The temperature of the salt flow leaving the receiver is measured by dual redundant thermocouples. Signal TT4A is indicated on the control console, signal TT4B is sent to a strip chart recorder located in the upper right section of the control console, signal TT5B is sent to the MCS, and signal TT5A is sent to the flow indicator controller and is used to adjust the flow control valve.

The salt then flows into the bottom of the air cooler, where two fans force ambient air over the series of finned tubes. The air cooler has a set of louvers between the fans and the finned tubes, which can be opened or closed by the valve positioner on the control console. Similarly, movable insulation panels are located on top of the finned-tube bundle and are activated by the on-off switch near the insulation diagram. There are indicating lights to verify that the panel is in the open or closed position. These insulation panels are used to keep the air cooler warm during initial start-up and during certain emergency situations.

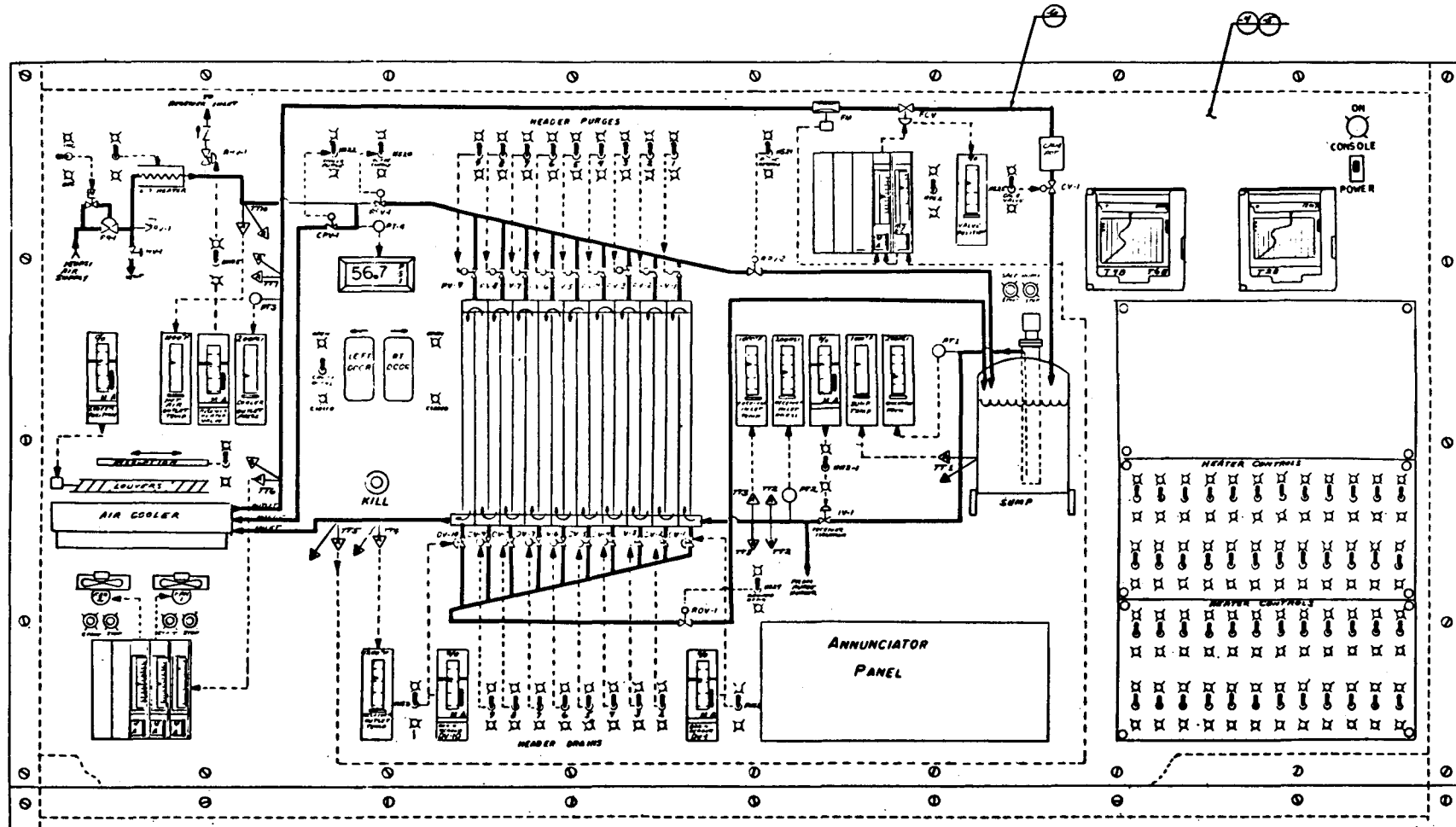


Figure III-8 Receiver SRE Control Console

Air cooler fans are controlled by sensing the outlet temperature of the air cooler. A signal is sent from TT 6A to the fan controller located in the lower left of the control console. This signal is converted to a control signal that varies the pitch on the fan blades and subsequently adjusts the air flow over the tube bundle. The signal from TT 6B is recorded on a strip recorder located in the upper right corner of the control console.

The pressure in the salt flow line from the air cooler to the pump/sump is sensed by a pressure sensor (PT 3) and is displayed on the control console. The temperature sensor (TT 7) has two signals that measure salt temperature in the piping between the air cooler and the sump. Signal TT 7B is sent to the MCS and signal TT 7A is a spare signal.

The flowmeter (FM) is a segmented orifice meter with silicone-filled capillary sensing tubes. This measurement is sent by a flow transmitter to the flow indicator/controller at the top center of the control console. A closed-loop control is provided that automatically sets the flow control valve (FCV) to maintain the desired flow rate. The flow indicator/controller also accepts a signal from the fluid temperature thermocouple at the outlet of the receiver (TT 5A), which automatically resets the flow rate to maintain the desired outlet temperature. The position of the FCV is indicated on the control console by the valve position indicator.

The calibration pot is downstream of the FCV as a check of the automatic flow meter. When the butterfly valve downstream of the calibration pot (CV-1) is closed, the salt will be retained in the calibration pot, which is suspended on a load cell. This load cell will record the weight of the salt retained for approximately 35 seconds. From a graph of weight vs time, an accurate flow rate can be determined. When CV-1 is opened the retained salt continues to the sump.

The kill button located to the left of the receiver panel sends a signal to the MCS to scramble the heliostats off the receiver surface in the event of an anomaly during system operation.

The switch located above the kill button opens and closes the cavity doors. Lights controlled by limit switches on the door assembly verify whether the doors have been opened or closed. The annunciator panel indicates by flashing lights and a horn the six alarm conditions to the operator. These are:

- 1) Low pressure at the outlet of the pump,
- 2) High/low salt temperature at the cooler outlet,
- 3) Low salt flowrate,
- 4) High salt temperature at the receiver outlet,

- 5) High receiver tube temperature, and
- 6) Power off.

Trace heating controls will be located on a separate panel. These switches turn the trace heaters on or off remotely. No variable controls are required since the heaters are sized for specific line requirements.

The top "insert" panel on the right side of the control will be used to verify signals sent to the MCS for operation by the CRTF computer and also to verify when these same signals are returned to the control console from the MCS.

3. Receiver Preheat, Fill, and Drain

Receiver tubes can be preheated without using solar insolation by passing compressed air through an air heater and introducing it at the inlet of the receiver. This system is shown schematically in the upper left corner of the control console. Air supplied by CRTF at 1034 kPa (150 psi) enters the system and is regulated to approximately 345 kPa (50 psi) by PR-1. This can be controlled by either increasing or decreasing the pressure on the regulator dome with the switch shown on the panel. The pressure is displayed on the digital indicator by a signal from PT 4 when valves RPV-1 and CPV-1 are both closed by hand switches HS20 and HS22.

Also in the air feed line is a hand valve (HV-1) to vent the system and a relief valve (RV-1) to protect the air heater. The air heater is an 81 kW capacity heater sized to heat the receiver tubes. The system valves must be set as follows to establish the correct flow path of the hot air to preheat the receiver tubes:

<u>Valve</u>	<u>Position</u>
IV-1	Closed
DV-1 through DV-10	Closed
PV-1 through PV-9	Closed
FCV	Open
CPV-1	Closed
RPV-1	Closed
RHV-1	Open
PR-1	345 kpa (50psi)

After the receiver tubes have been preheated and the heat tracing has heated all the salt lines and components to their proper warmup temperature, the system valves must be repositioned to allow proper filling of the receiver and the remainder of the system components. To fill the system, the valves must be positioned as follows:

<u>Valve</u>	<u>Position</u>
IV-1	Open
DV-1 through DV-10	Open
ROV-1	Closed
PV-1 through PV-9	Open
RPV-1	Open
CPV-1	Closed
FCV	Open 20%
CV-1	Open

The salt pump is then turned on to circulate the molten salt to the receiver. Instead of salt following the normal serpentine flow of the receiver, the salt will pass through DV-1 and fill that drain line since ROV-1 is closed. The salt will flow up through DV-2 through DV-10 and fill the receiver uniformly while purging the air in the system through purge valves PV-1 through PV-9, RPV-2, and through the vent in the sump.

Molten salt will also travel through DV-10 through the air cooler filling the finned tubes in the tube bundle and the return line to FCV, which is closed.

After salt flow to the sump has been verified by observation through a sight glass in the sump, PV-1 through PV-9 are closed and RPV-1 is opened. This allows heated air at 345 kPa (50 psi) to be introduced into this line ensuring that all remaining salt is purged back to the sump. Next, drain valves DV-1 through DV-10 are closed and ROV-1 opened to allow salt to drain back to the sump by gravity.

After this sequence, the system is set for normal operation and FCV can be opened manually at the desired flow rate. To drain the system of molten salt the pump will be turned off and the valves positioned as follows:

<u>Valve</u>	<u>Position</u>
IV-1	Closed
ROV-1	Open
DV-1 through DV-10	Open
PV-1 through PV-9	Open
RPV-2	Closed
RPV-1	Open
CPV-1	Open
FCV	Open
CV-1	Open

Heated purge air will enter the receiver through valve PV-1 through PV-9 and force molten salt through valves DV-1 through DV-10. This purge air will also enter the air cooler through CPV-1 and force the salt from the air cooler back through the drain valve DV-10 of the receiver. The lines from valve IV-1 to the sump and from the outlet of the air cooler to the sump are sloped to allow gravity draining of the molten salt.

4. Equipment Layout

The receiver SRE plan layout, Figure III-9, shows the location of major pieces of equipment on the tower elevating module. The receiver header and tubes are mounted to the receiver support structure. This structure was used as a fixture to fabricate the receiver and will also be used to transport the receiver from the Martin Marietta facility to the CRTF. The receiver support structure is attached to twin main-support towers located at the center of the elevating module. The receiver is located far back (south) on the elevating module to allow the cavity structure to be located in front of the receiver during a later test period without disturbing the system setup. The sump/pump assembly is located to the left (west) of the main support structures to allow direct pipeline flow routings, which assist in gravity-flow drainage of the system. The air cooler is located in the rear (south) of the elevating module away from any solar flux that may miss the receiver panel.

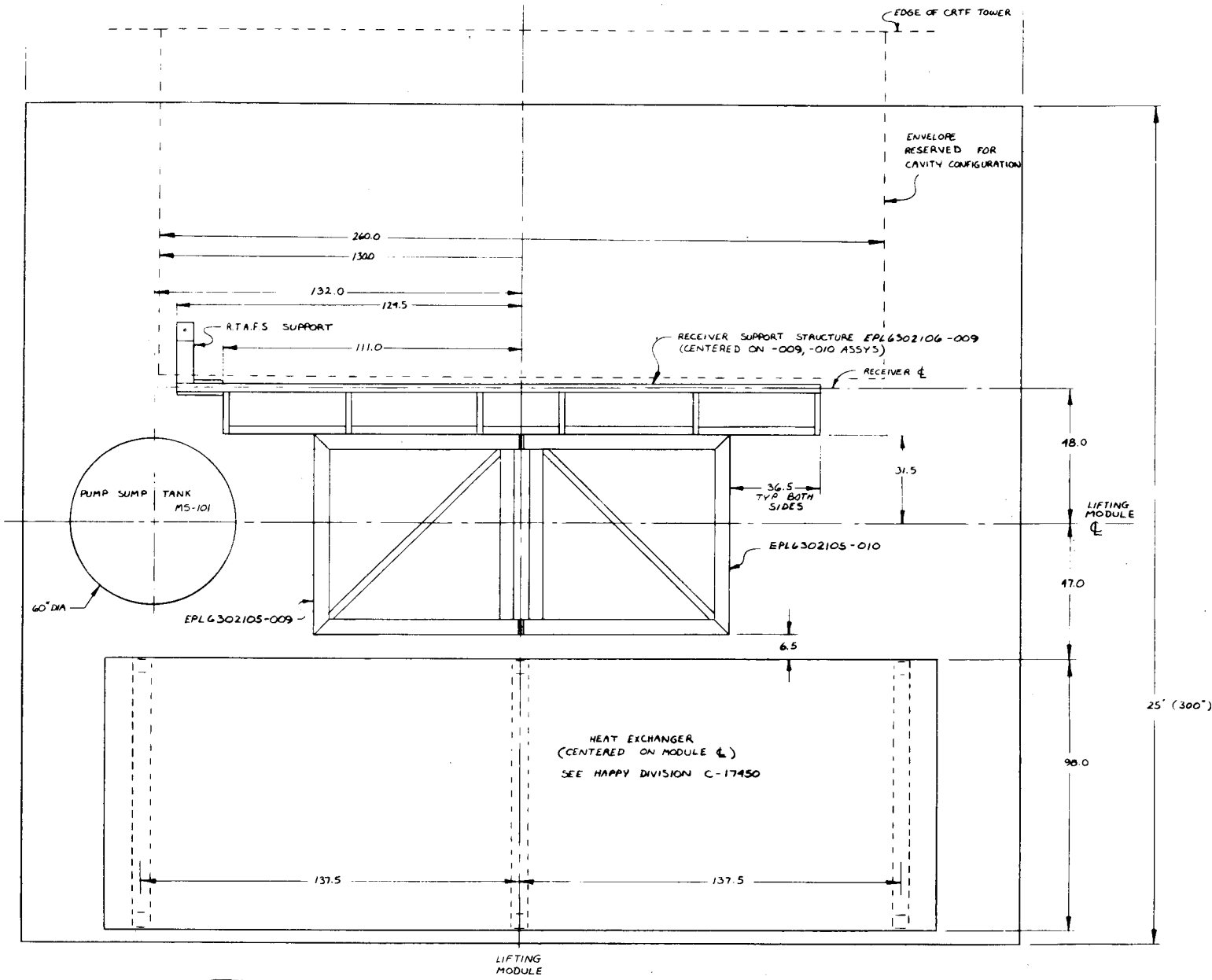


Figure III-9 Receiver SRE Equipment Layout--Plan View

The receiver elevation layout in Figure III-10 shows the relative equipment heights on the elevating module. The top of the receiver is approximately 8.2 m (27 ft) from the top of the elevating module.

Detailed plan and elevation views of the Receiver SRE are shown in Figures III-11 and III-12. These figures overlay the pipe routing interconnecting various system components. Additional pipe loops were used to minimize the forces and moments at the receiver connections. This eliminated the requirement for bellows in the piping system. Ten valves shown on the receiver marked HV-2, HV-3, and XV-2 through XV-9 are the drain valves identified earlier as DV-1 through DV-10. The valves shown in the "upper plan" marked XV-11 through XV-19 are the purge valves identified earlier as PV-1 through PV-9.

5. SRE Components

a. Receiver - Figure III-13 shows a detailed drawing of the back side of the receiver header tube assembly. The headers are marked in the same sequence of the salt flow with the molten salt entering header number 1 and exiting header number 19. The headers are 11-cm (4.5-in.) diameter schedule 40 Incoloy 800 pipe, 0.61-m (24-in.) long, which are capped at each end. The receiver tubes are 1.9-cm (0.75-in.) diameter tubes with 0.17-cm (0.065-in.) wall thickness, approximately 4.0-m (13-ft) long. Tube ends are bent to allow the tubes to be welded to the header and form a flat surface to accept solar heat input. There are 16 tubes per pass and a total of 18 passes in the serpentine flow through the receiver panel. The tubes are painted with a high-temperature flat black paint to increase the absorbtivity of the receiver panel.

At eighteen locations shown on the receiver (see flag note 6), receiver tubes have been indented to provide room for heat flux sensors. These sensors are attached to brackets mounted on the back of the receiver panel and shown in Figure III-14. The sensing foil surface is 0.16-cm (0.062-in.) in diameter and acts as a thermocouple producing a linear delta-temperature signal across the surface. The thermocouple is insulated with magnesium oxide and the body of the sensor housing is water-cooled. These sensors will be used to measure the direct solar insulation on the receiver panel throughout the experiment.

Each of the 288 receiver tubes are welded together using a Tungsten Inert Gas (TIG) process. Each tube is welded to the adjacent tube in nine places. the fabrication process will be detailed in Section III-H of this report.

Receiver headers are heat traced with a "built-in" spare. This eliminates the need to open up the header shroud and insulation in the event of a heat trace failure in this critical area. The receiver is insulated in the back and on the sides with approximately 0.2m(8 in) of flexwhite insulation.

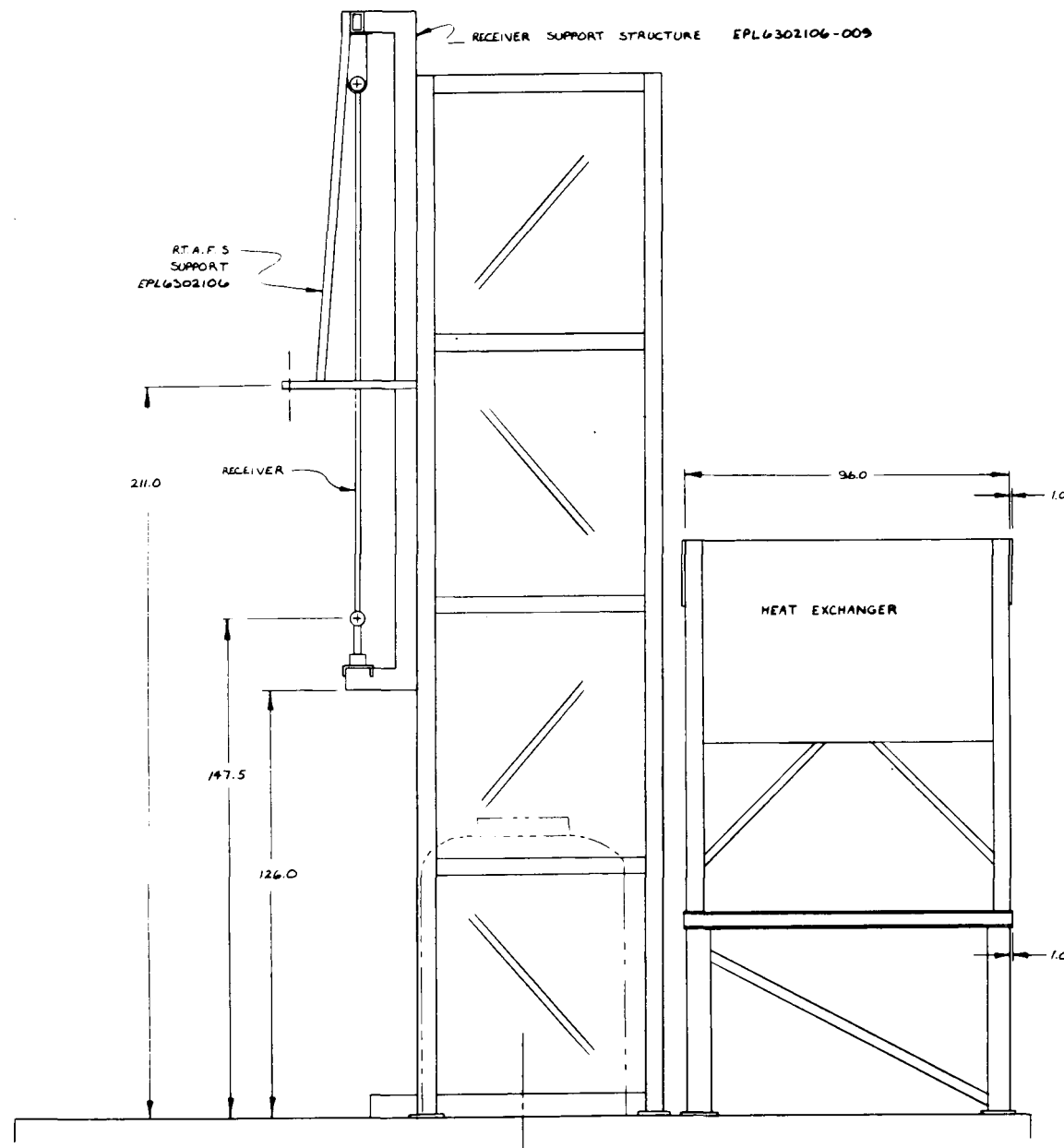


Figure III-10 Receiver SRE Equipment Layout--Elevation View

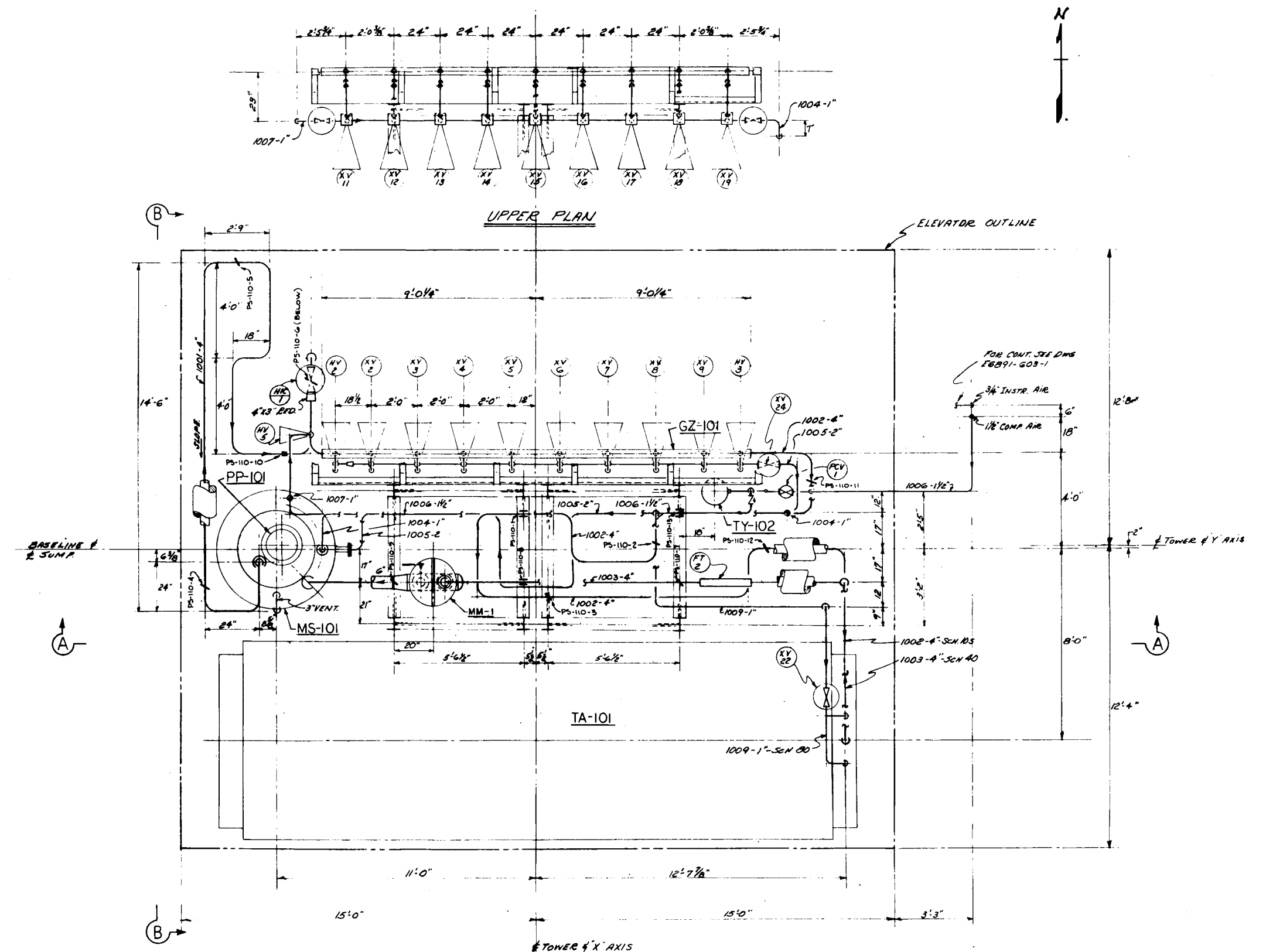


Figure III-11 Receiver SRE Piping Layout - Plan View

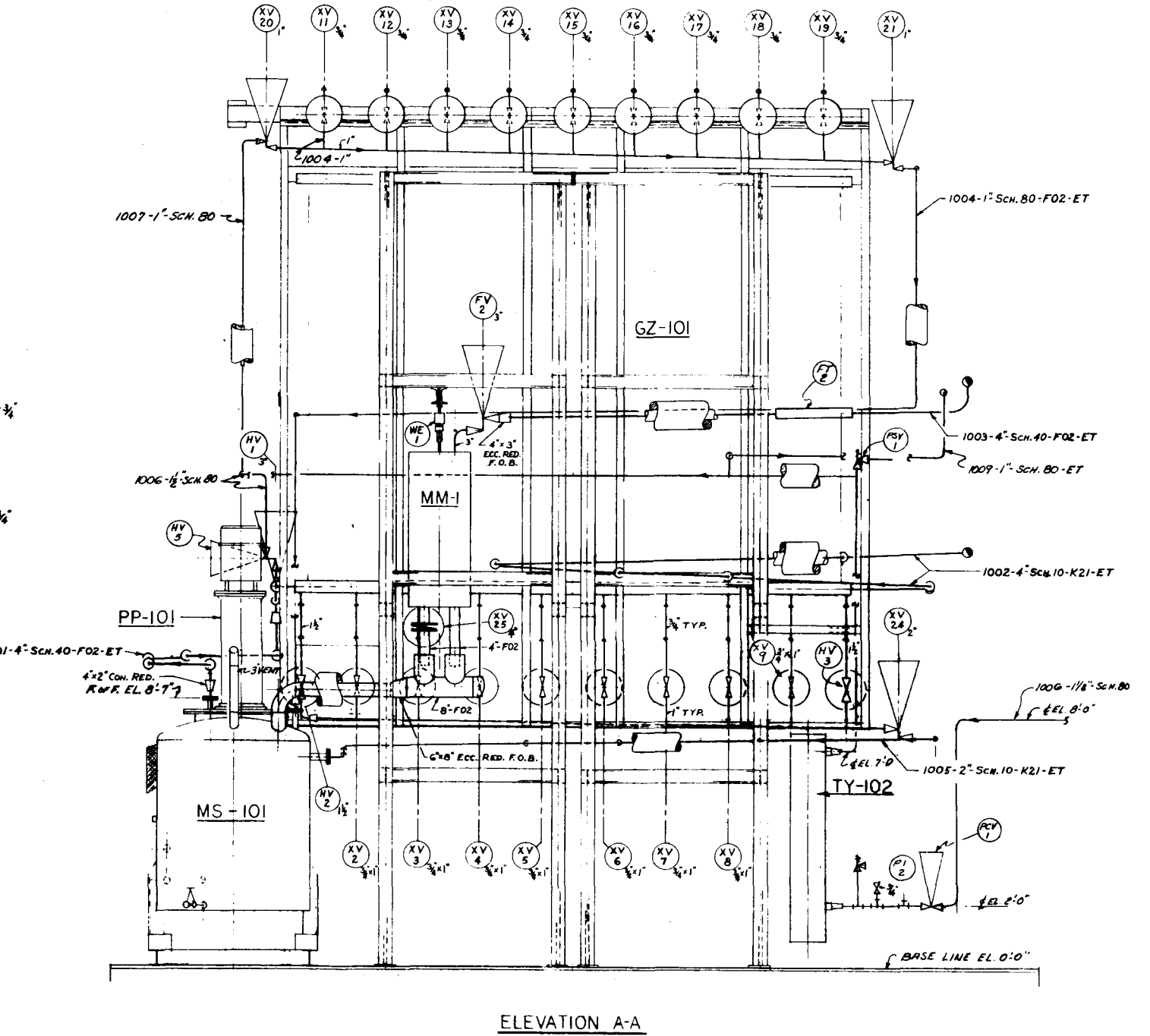
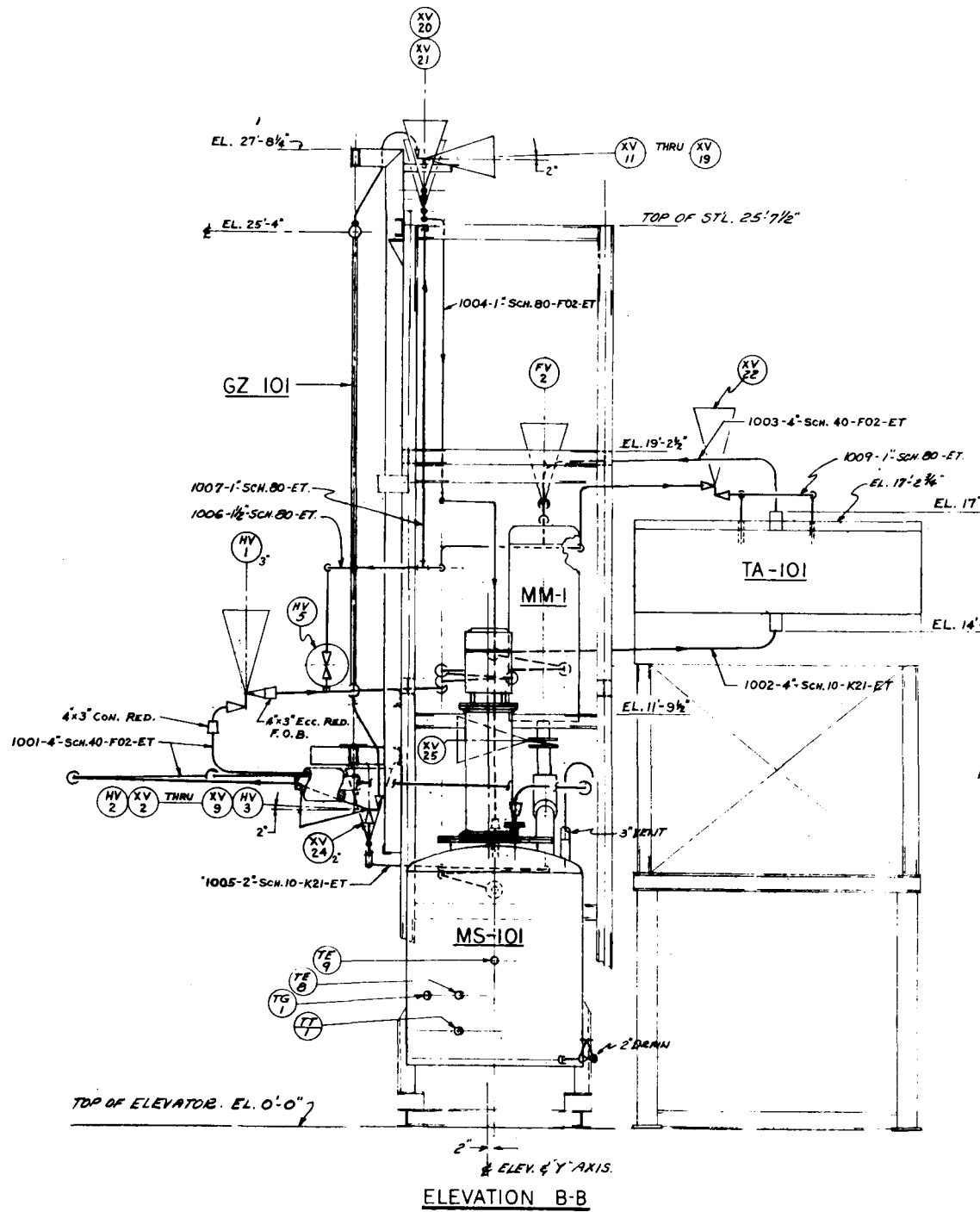


Figure III-12 Receiver SRE Piping Layout - Elevation View

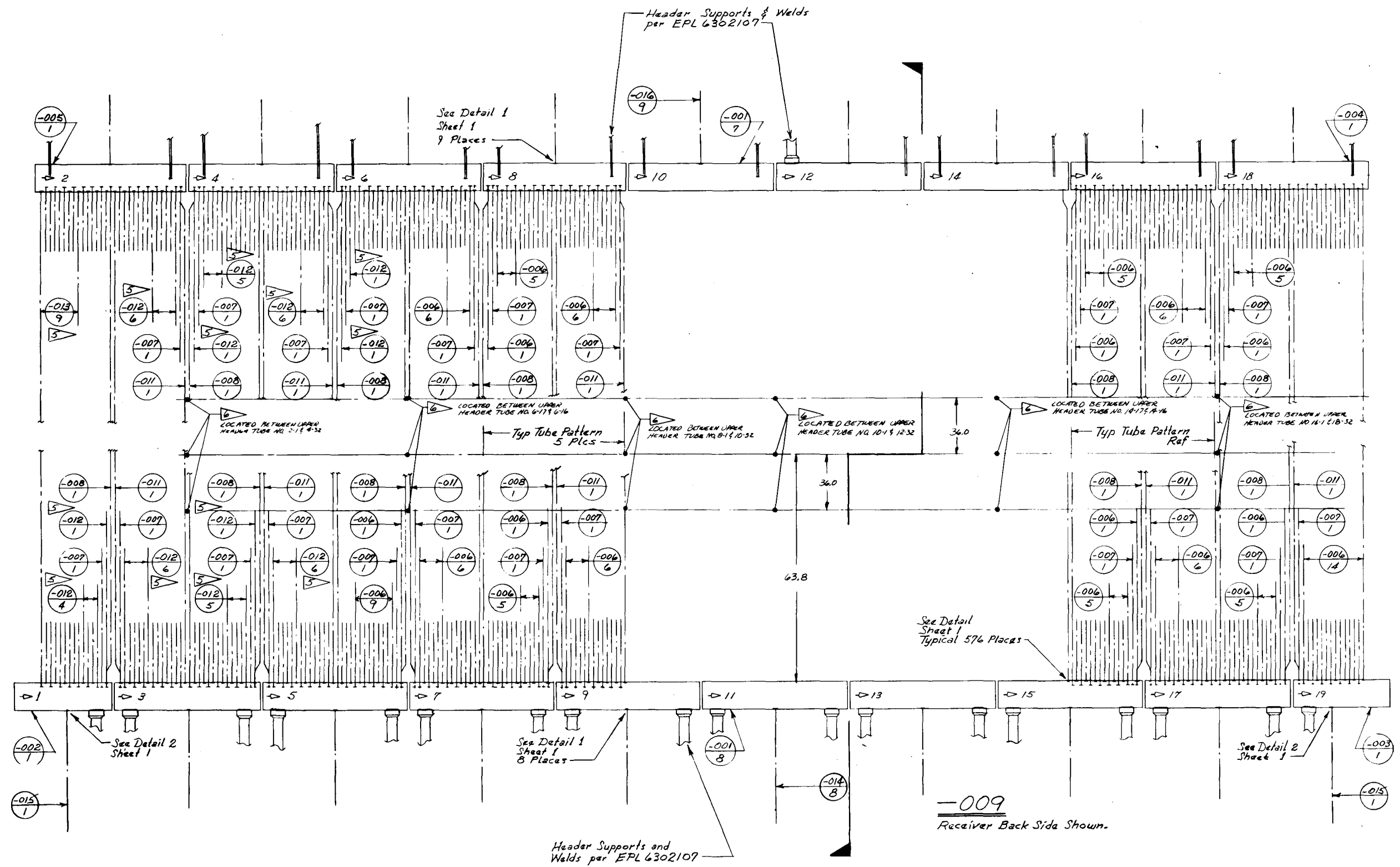


Figure III-13 Receiver Header Tube Assembly

III-28

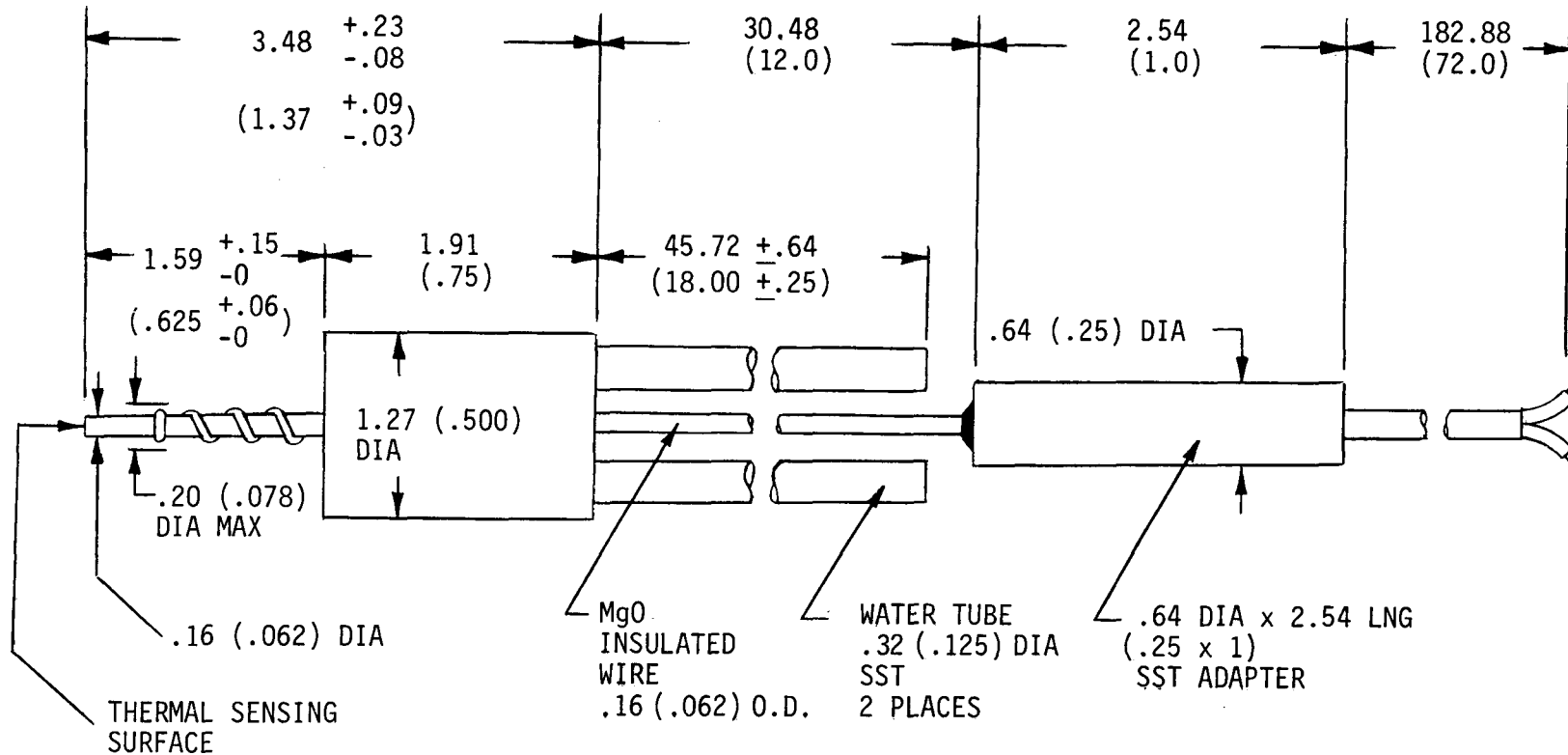


Figure III-14 Receiver Tube Heat Flux Sensor

Dimensions in cm (in.)

The receiver header assembly is suspended from the top and allowed to grow down vertically approximately 1.8 cm (0.71 in.) at the inlet and 3.7 cm (1.5 in.) at the outlet. Receiver header Number 12 is also rigidly attached to the receiver structure and is used to control lateral growth. The remaining upper headers are supported by thin plates that allow them to thermally expand laterally 1.9 cm (0.75 in.) at the hot end and 1.3 cm (0.5 in.) at the cold end. These displacements will be measured and recorded by linear variable displacement transducers (LVDT) mounted to the structure.

On the back of the receiver panel at the elevation center line, four targets are welded to the tubes. These targets are used by LVDTs to measure deflection of the tubes when they are heated. The estimated maximum displacement of these tubes is 6.1 cm (2.4 in.).

The header tube assembly was designed in accordance with Section I of the ASME boiler code. Although this code does not specifically outline design parameters for a solar boiler, it did provide basic design and quality control criteria. A summary of stress analysis is included in Section III F of this report.

b. Sump - The shell and heads of the sump (Figure III-15) are made from SA-285 grade C carbon steel and designed for atmospheric pressure. Line connections have flanged joints that will simplify installation at the CRTF. Throughout our experience during the Phase I portion of this contract, the salt was observed to "creep" through mechanical joints. To prevent salt from creeping out of the tank flanges and possibly contacting the heat tracing connections, a skirt of 3.2-cm (1/8-in.) thick carbon steel is welded to the perimeter of the barrel section of the sump. This is located between the flanges and the heaters and extends outside the insulation by approximately 5.1 cm (2 in.). If any salt does creep onto this skirt, it will freeze and solidify. The sump is electrically heat traced in five different zones with a total heat trace capacity of 12.1 kW. This is enough heat to initially melt the entire salt volume over a period of 2-3 days, maintain the salt temperature at 288°C(550°F) during the nonsolar portions of the test, and maintain the temperature of the remaining salt (partially filled sump) during the solar testing. The sump is insulated with 8.9 cm (3.5 in.) of insulation and protected from the weather by aluminum sheathing.

The sump is thermally isolated from the elevating module by castable insulation. A carbon steel dike will surround the sump to contain the entire volume of salt from the sump in case of tank rupture.

c. Pump - The vertical cantilever pump is manufactured by Lawrence Pumps and is similar to the one successfully used in the Phase I contract. The pump was specified by Badger and is an off-the-shelf item used in the commercial molten salt industry because the pump bearings and seals are not immersed in the molten salt. No new pump development or special user stamps were required for this application. The pump drive motor is 45 kW (60 hp) and the pump bearings are air cooled.

d. Structure - The main support structures for the receiver are shown in Figure III-16. There are two assemblies each approximately 1.8 m x 1.8 m (6 ft x 6 ft), by 7.9 m (26 ft) high constructed of 0.15-m (6-in.) wide flange structural steel members. They have been designed in accordance with the wind and seismic requirements outlined by the CRTF. There are two structural units to simplify the transportation and to minimize the amount of field welding.

The receiver support structure will be mounted to pads on the main support structure and match drilled after it is aligned.

e. Valves - Salt valves for the system, i.e., PV-1 through PV-9, and DV-1 through DV-10, are all carbon steel body valves with stainless steel internal bellows. Figure III-17 illustrates the location of the internal bellows and how it prevents the molten salt from leaking out of the valve body. Each of the PVs and DVs will be installed with a slope of 2° to ensure that all residual salt will drain from the valve body. Each valve will also have hand wheels mounted to the valve body, which can be used to manually force the valve poppet open or closed if it gets stuck. All valve ends will have socket weld connections to prevent any molten salt leakage.

f. Piping - The interconnecting piping for this system was designed in accordance with the ANSI B31.1 Power Piping Code. The pipe will be fabricated sectionally in Denver, allowing it to be shipped and assembled in the field. Because of the extreme wetting characteristics of the molten salt, especially at the higher temperatures, pipe connections are welded to the maximum extent practical.

The piping was also designed with an adequate slope to assist in gravity draining of the molten salt. This will prevent any salt from solidifying in the lines.

The piping will be heat traced for preheating before molten salt is circulated through the system. The piping will also be insulated and wrapped with a sheathing to protect it from the environment.

g. Air Cooler - We will use an existing fan assembly and lower support structure designed and built for Sandia Laboratories, Albuquerque, NM, on a previous contract by Thermatechnology, Inc., Tulsa, OK. We selected the same manufacturer to fabricate a finned tube bundle compatible with the existing fan assembly and designed for the temperature requirements of this experiment.

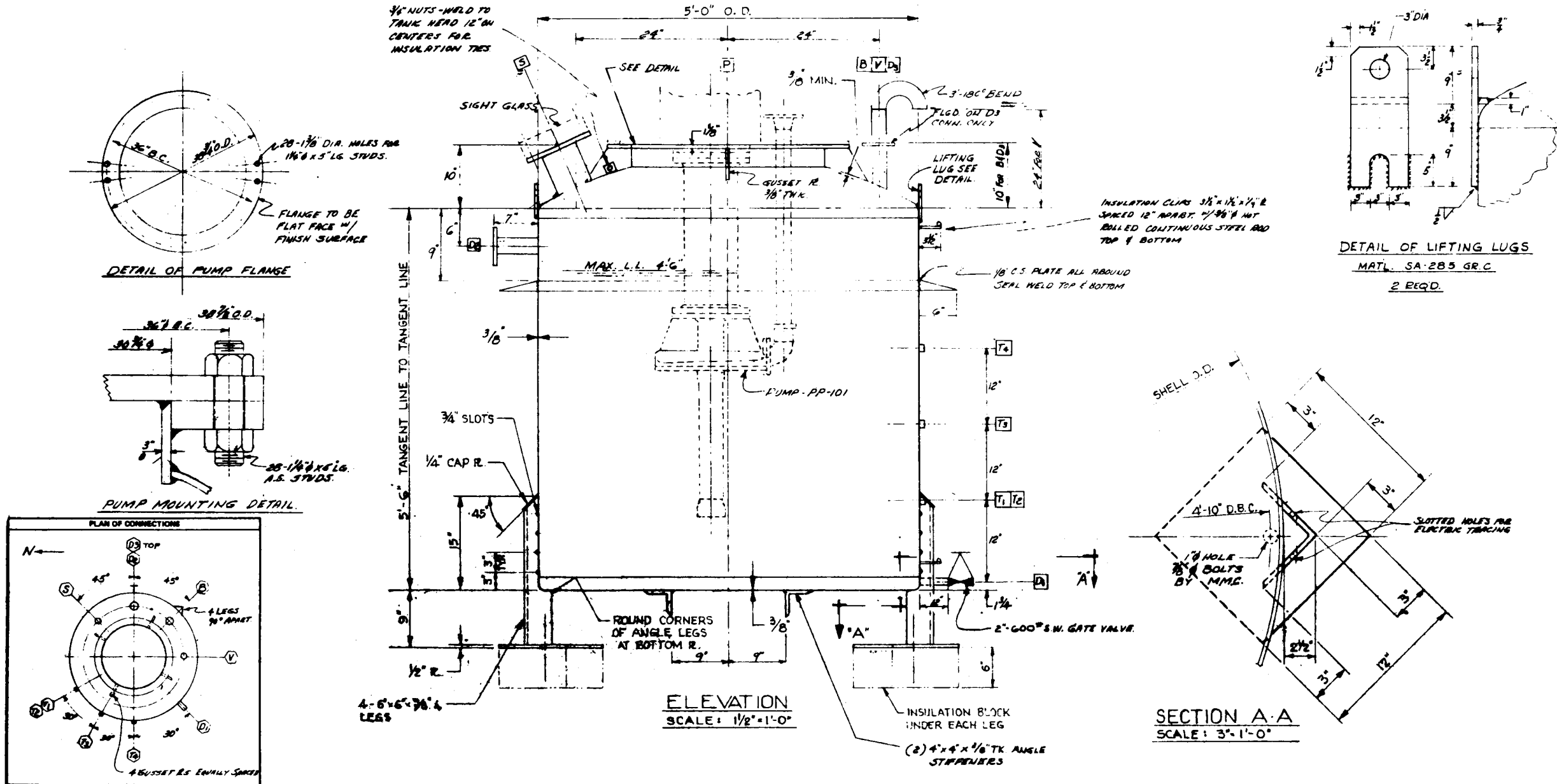


Figure III-15 Molten Salt Sump

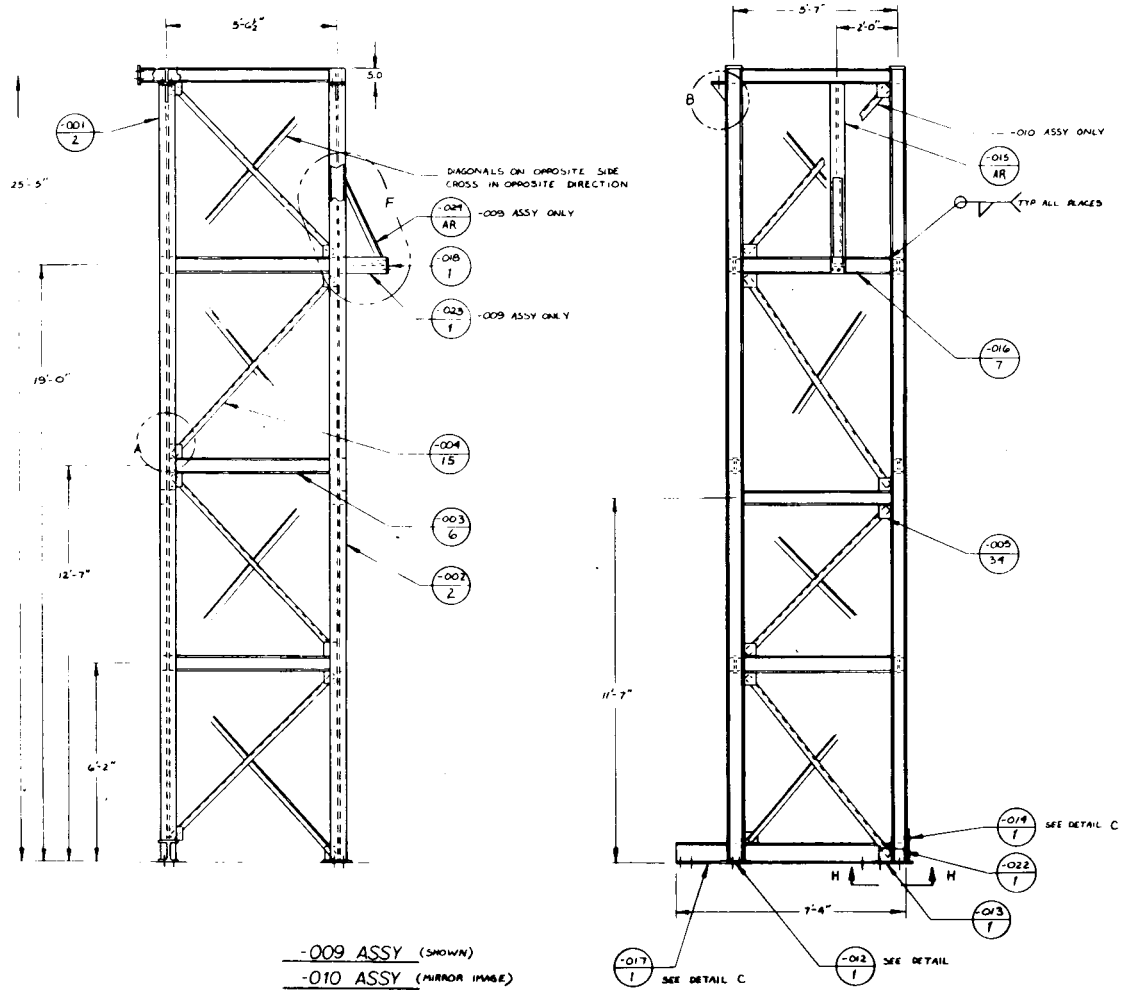


Figure III-16 Receiver Main Support Towers

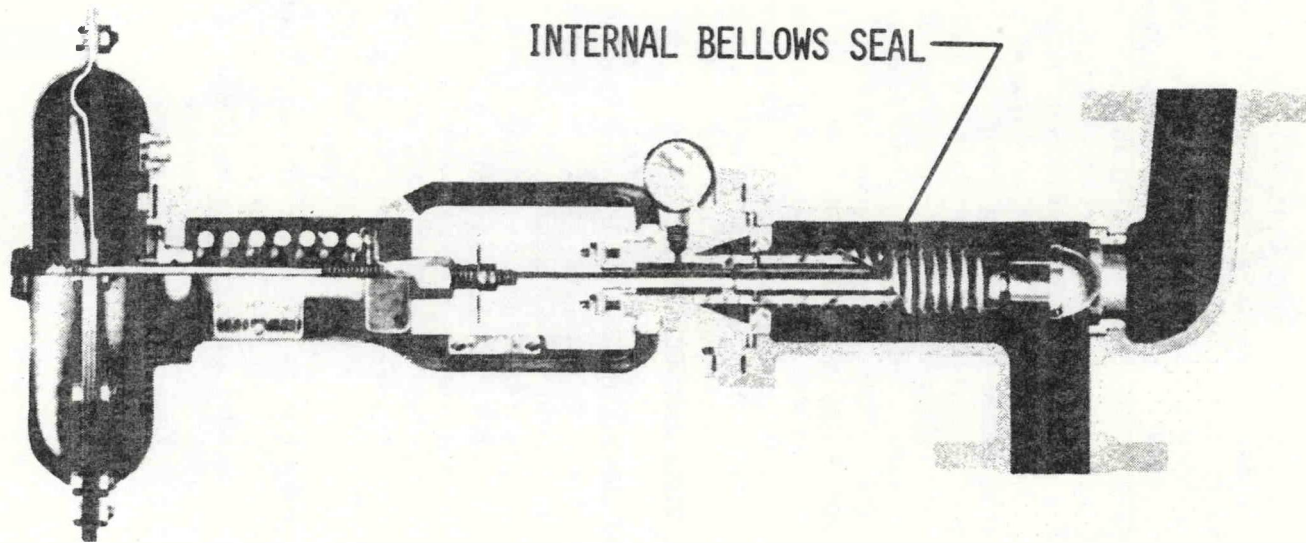


Figure III-17. Cross-Section of Molten Salt Valves

The tube bundle consists of 105 tubes 2.5 cm (1 in.) in diameter and 7.6 m (25 ft) long. The tubes have rectangular carbon steel fins 2.5 cm (1 in.) high welded to the tubes continuously around at a density of 394 fins per meter (10 fins per in.).

Rows of tubes will be staggered to provide better circulation from the two 2-m (7-ft) diameter fans.

Salt enters the lower header at 566°C (1050°F) and travels through the first pass of 18 finned tubes to a header at the opposite end. See Figure III-18. The salt flow returns through the second pass of 17 finned tubes just above the first pass and continues this serpentine flow through six passes and exits the top header. The air flow is supplied by the two fans located below the tube bundle. This salt-flow routing was selected because of two important design criteria. First, the molten salt leaving the air cooler could not be allowed to freeze. With the salt leaving the top header, the cooling air that starts at ambient conditions gets heated by passing over the first five rows of finned tubes and becomes quite hot and uniform in temperature as it passes over the last row of tubes. If the flow was from top down and the existing fans were used, the salt may cool down too much in the bottom passes and freeze in the cooler tubes.

The second design criterion was to provide a serpentine path with each pass sloped to allow it to gravity drain back to the sump. Under normal draining conditions, the tube bundle will be pressurized, forcing the molten salt to exit out the bottom header and through the drain valve DV-10 in the receiver.

To preheat the air cooler to a temperature acceptable for salt flow, the tube bundle is sealed from ambient air. Between the bottom portion of the tube bundle and the fans is a series of louvers positioned by pneumatic positioners. Its range can be varied for 0-100% open and it can be used to restrict air flow if required for control. Mounted on top of the tube bundle is a movable insulation panel. This panel seals off the top portion and minimizes heat flow during preheating of the cooler. The insulation panels are remotely operated by pneumatic cylinders and can be manually overridden in an emergency.

The two sides of the tube bundle are heat traced, insulated, and covered with thin metal to protect the insulation from the environment. The seven headers are individually heat traced, insulated, and covered with thin metal to ensure proper header temperatures prior to start up.

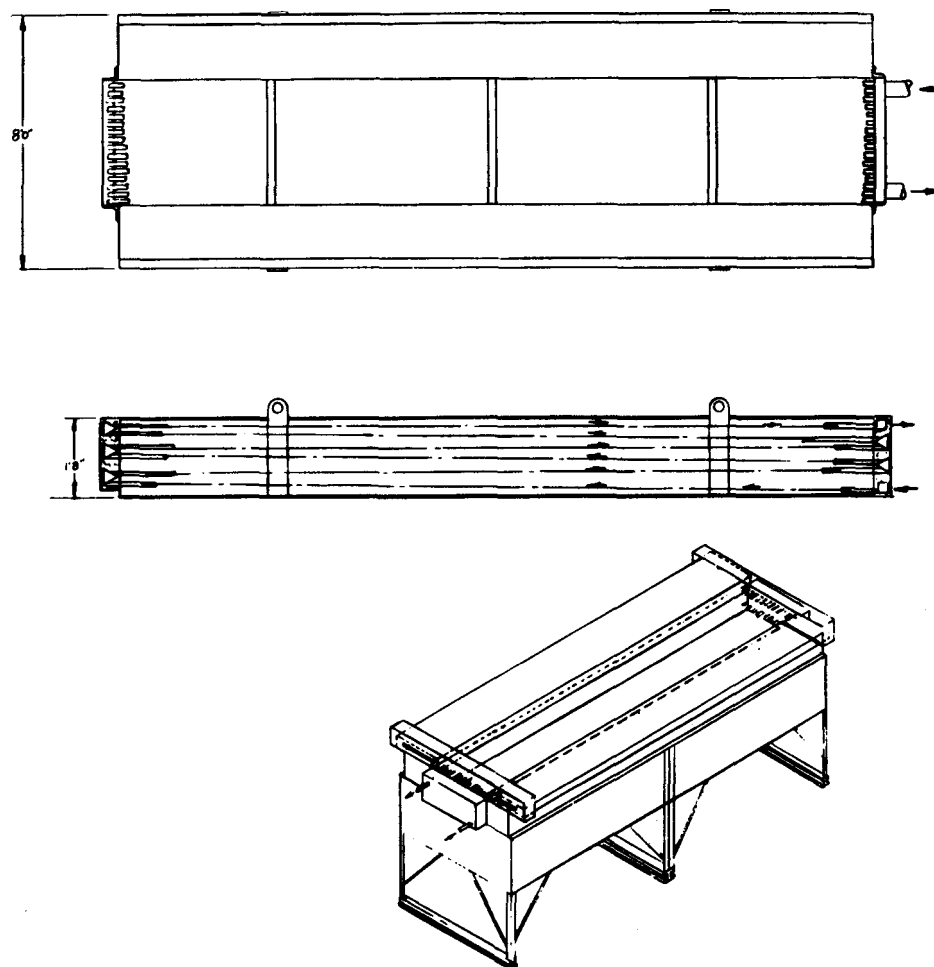


Figure III-18 Air Cooler Tube Bundle

h. Calibration Flowmeter - In addition to the segmented wedge flowmeter discussed earlier, there is an additional flow-measuring device, designed to improve accuracy. It is shown conceptually in Figure III-19. The tank is made from a 0.61-m (24-in.) diameter pipe 1.52-m (5-ft) long. The normal flow of molten salt enters the calibration pot through a 0.10-m (4-in.) pipe at the top and exits through the butterfly valve into a 0.21-m (8-in.) header at the bottom. When a flow measurement must be taken, the butterfly valve is closed remotely and molten salt accumulates for about 35-seconds in the calibration pot. The calibration pot is suspended from a load cell and the weight of this device is recorded as it fills with salt. This curve of weight vs time will give an accurate salt flowrate for a portion of the 35 second fill time and can be compared to the reading from the segmented wedge flowmeter. The system can then be drained by opening the butterfly valves and returned to normal flow operation. There is an overflow line in the pot to prevent the salt from overflowing. The calibration pot is completely heat traced to prevent any salt from freezing on the interior surface.

i. Cavity Assembly - As part of the SRE, we install a cavity assembly in front of the receiver surface. This cavity is shown in Figure III-20 and is a completely independent structure not attached to the main support structure. The back of the cavity is open to the full active surface of the receiver and tapers to an opening approximately 2.7 m x 2.7 m (9 ft x 9 ft) in the front. The top and bottom panels are made from 0.32-cm (1/8-in.) thick carbon steel. The internal surfaces of the cavity are lined with 0.152 m (6 in.) of a high-temperature insulation. An access door is located in the bottom panel of the cavity to allow inspection of the enclosure.

A front assembly consisting of two pneumatically-operated doors, a water-cooled aperture, and the RTAF device will be located in front of the cavity assembly, shown in Figure III-21. A separate support structure independent of the cavity structure will be used to hold the front assembly in place.

This hardware has been designed to clear the front edge of the elevating module by approximately 7.6 cm (3 in.) and will be installed with the elevating module at ground level.

The door assembly is shown in Figure III-22. It consists of two doors approximately 15 m (5 ft) wide by 30 m (10 ft) high and 7.6 cm (3 in.) thick. The doors are filled with high-temperature insulation and covered with a thin stainless steel plate. The cable arrangement for opening the doors is shown in the insert above the assembly. The doors are operated by two pneumatic actuators and guided inside a narrow channel track. These doors are activated from the control console and can be manually operated in an emergency.

ZONES

- I STEADY STATE FLOW LEVEL
- II CALIBRATION HOLDUP (35 SECONDS)
- III STEADY STATE FLOW LEVEL FOR OVERFLOW LINE
- IV SAFETY MARGIN

- A) 4" SCH 40
- B) 24" SCH 40
- C) 8" SCH 40
- D) 6" SCH 40

ALL CARBON STEEL

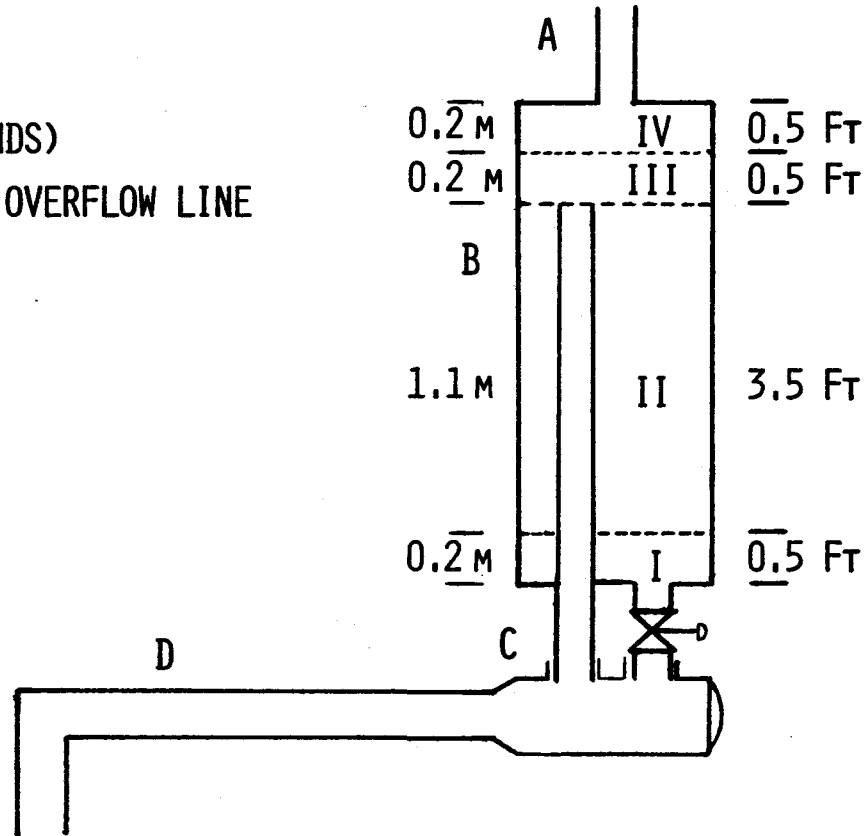


Figure III-19 Calibration Pot Flowmeter Concept

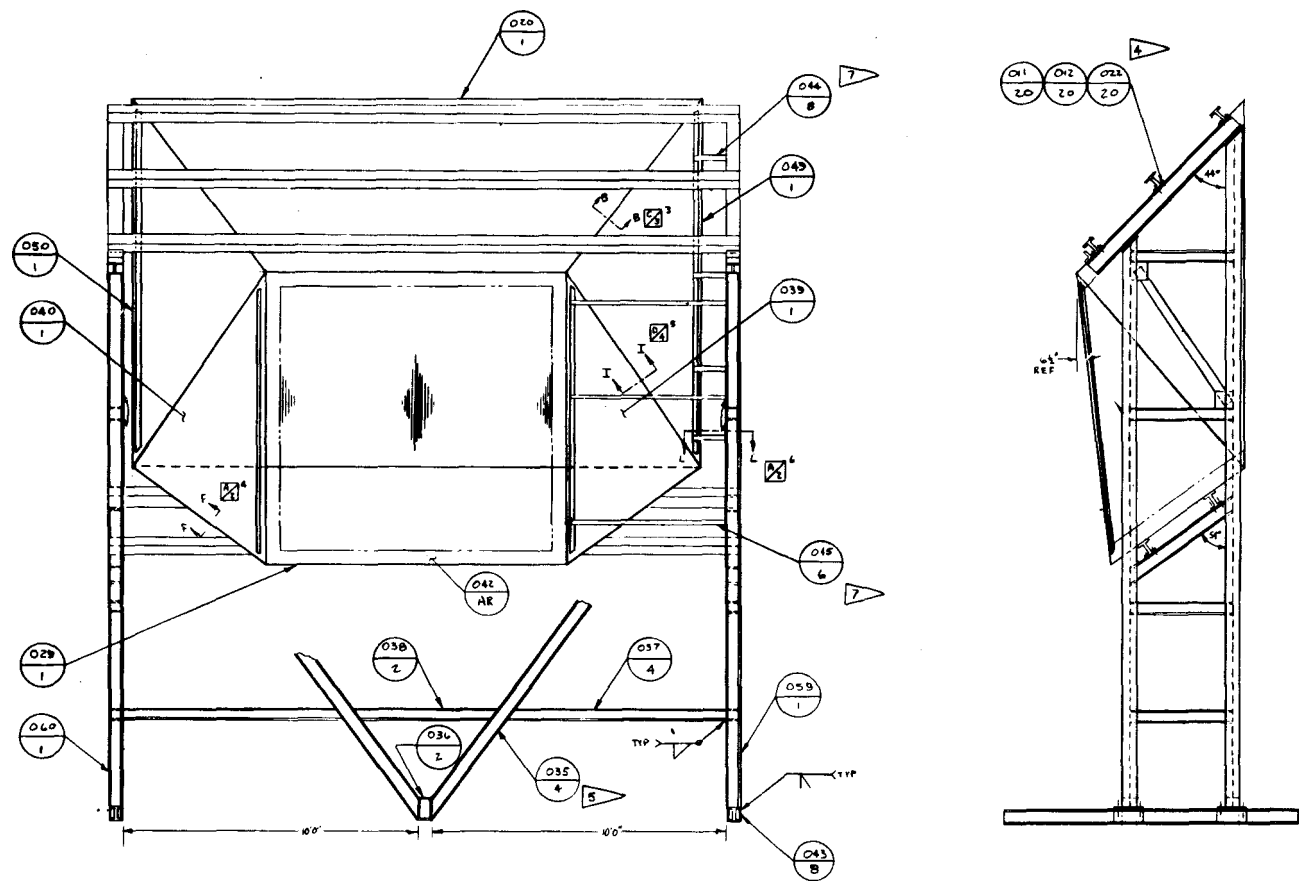


Figure III-20. Cavity Assembly

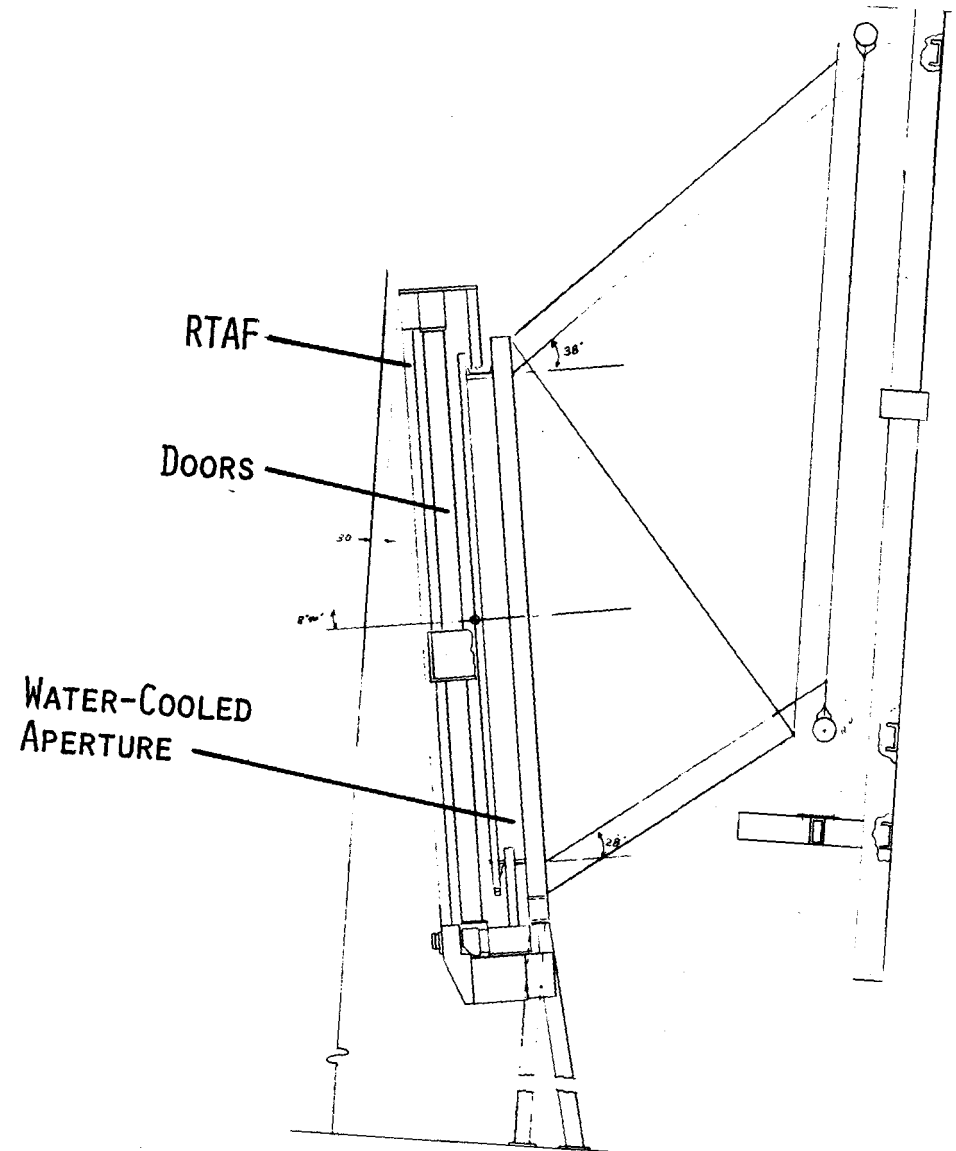


Figure III-21 Cavity Front Assembly

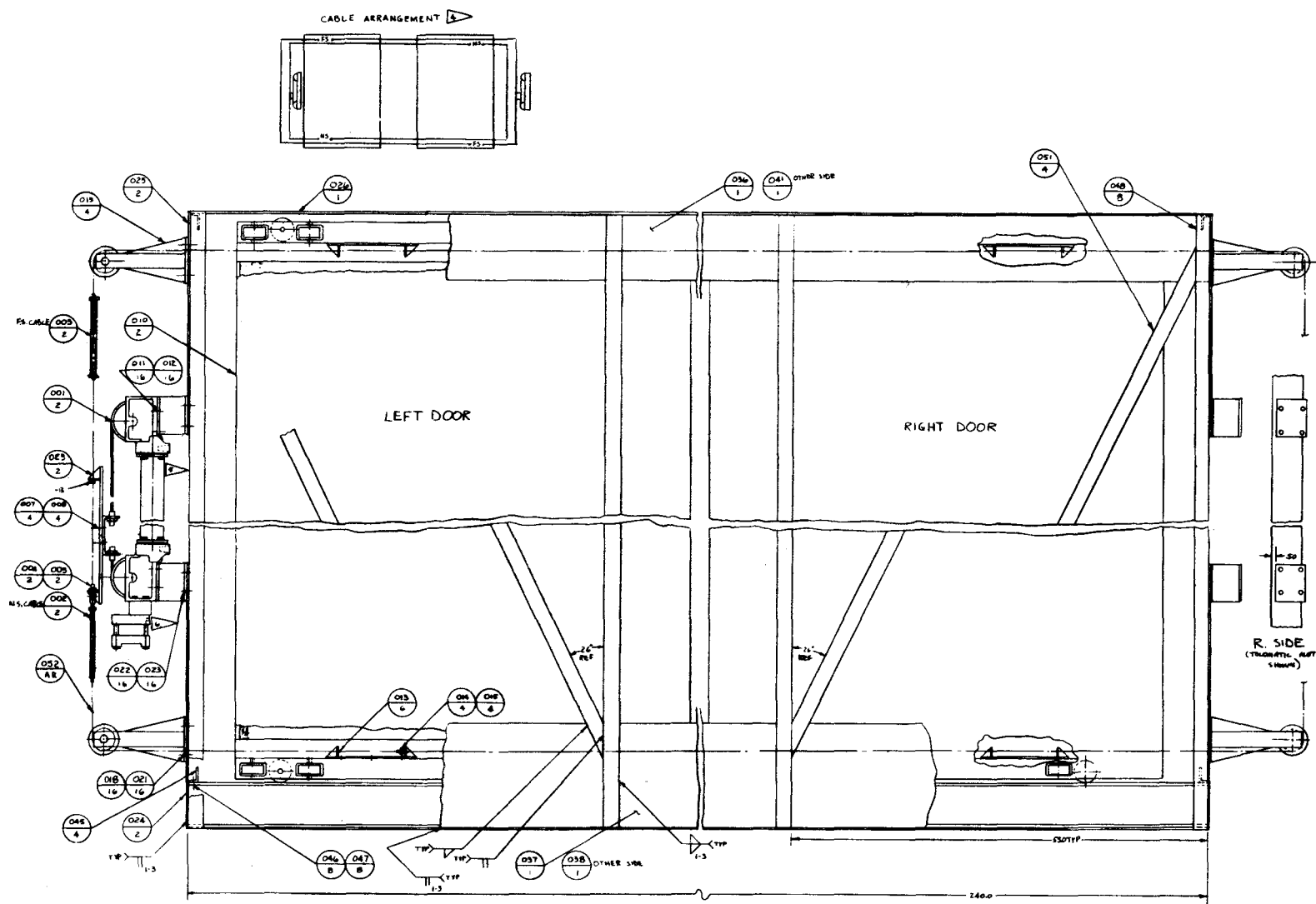


Figure III-22 Cavity Door Assembly

Attached to the door assembly is a water-cooled aperture (Figure III-23). This aperture is made from a carbon steel box section and has a 2.7-m (9-ft) square opening which has water circulating through it in series with the RTAF device.

D. FAILURE MODES AND EFFECTS ANALYSIS

Martin Marietta has identified the possible single failure modes of the receiver SRE. This analysis includes all of the SRE hardware and the CRTF support equipment. The results of this analysis is integrated into the test procedures.

A summary of the analysis is shown in Table III-3. This summary examines the potential impact of each failure mode on personnel and equipment safety, and identifies the corrective measures relative to the design and operational features of the test system to ensure that failure probabilities are minimized.

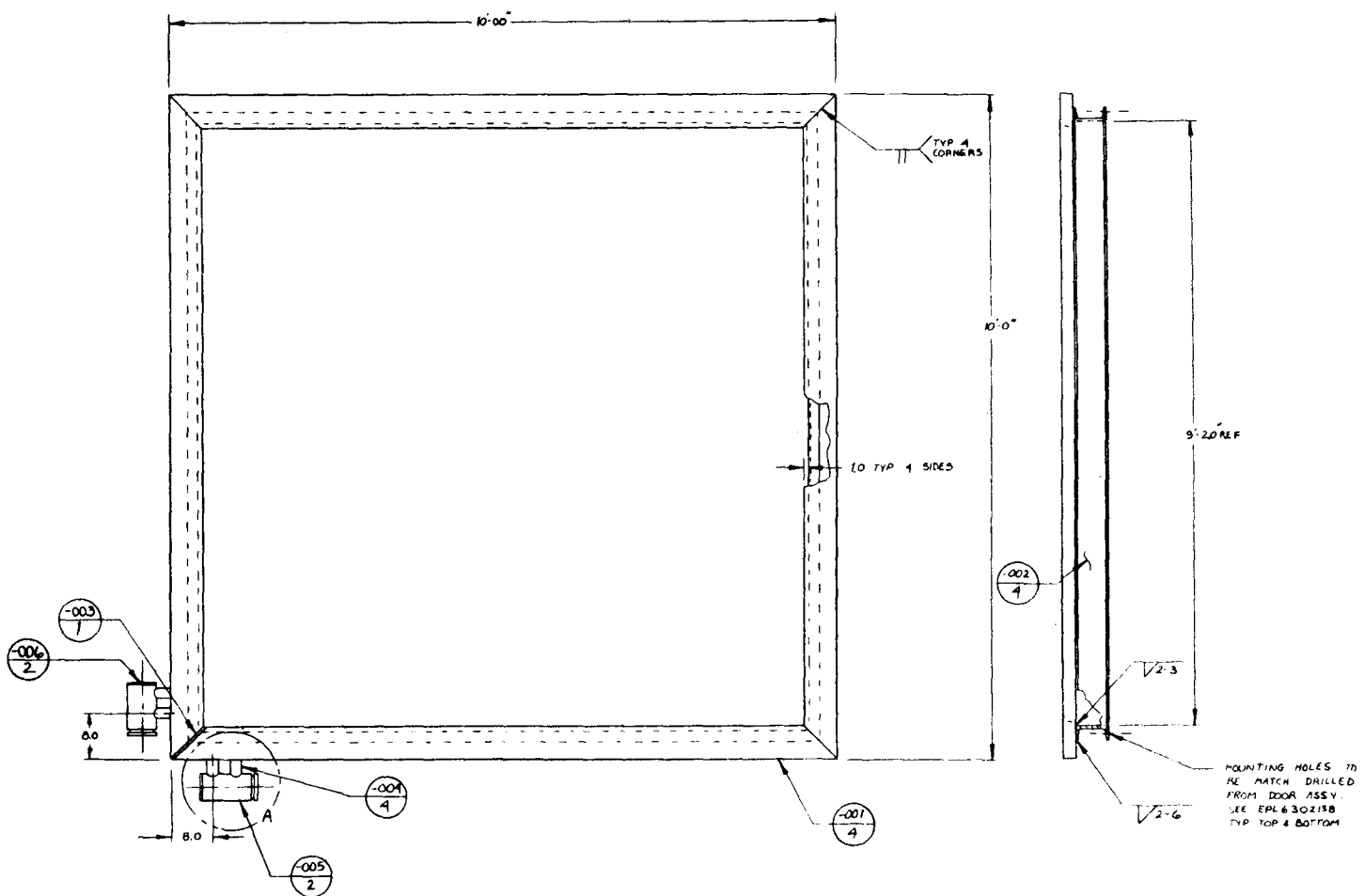


Figure III-23 Water-Cooled Aperture

Table III-3 Failure Modes and Effects Analysis

Subsystem/Component	Failure Mode	Effects		Detection	Preventive Measures or Corrective Action	Comments
		Ops Sequence	Consequences			
<u>SRE Receiver</u> <u>Tubes/Headers</u>	Leakage	All Sequences Involving Flow	Damaged Coatings and/or Insulation	Downtime Inspection	Design to Code Requirements Q/C Program	
		Sun-On	Could Cause Local Hot Spots or Cold Spots Large Leakage Could Lead to Reduction in Tube Flow and Receiver Overheating	Temperature Measurements Flow Measurements Temperature Measurements	Proof and Leak Testing Automatic and Manual Kill Parameters Include Over-temperatures	
	TIG Weld Joints Failures	Sun-On	Nonuniform Thermal Deformation of Disjointed Tubes may Cause "Opening" in Wet Wall and Possible Overheating of Structure/Equipment Behind Wet Wall	Downtime Inspection	Joint Safety Margin Demonstrated by Sample Tests Weld Integrity Verified by Metallurgical Inspection of Sample Joints Stress Requirements Established by Standard Stress Analyses	
			Uneven Flux Distribution on Disjointed Tubes may Result in Overheating	Temperature Measurements	Structure/Equipment Behind Wet Wall Thermally Protected	
	Burst Due to Volumetric Change of Salt during Thawing	Warmup Transient	System Inoperable due to Excessive Leakage	Visual Inspection Pressure/Flow Measurements Following Startup	Probability of Inadvertently Locking in Molten Salt Between Closed Valves Minimized by Procedure Checklist Safe Thawing Procedure Included in ITP	

Table III-3 Failure Modes and Effects Analysis (cont)

Subsystem/Component	Failure Mode	Effects		Detection	Preventive Measures or Corrective Action	Comments
		Ops Sequence	Consequences			
SRE Receiver <u>Flow Control Valves</u>	FCV	Sun-On	Excessive Flow and Reduced Salt Exit Temperature	Instrumentation (Temps. and Flow) Emergency Shutdown (Loss of Power or Pneumatics will Cause Automatic Shutdown)	Pretest C/O	This valve is of a "Fail Open" Design
	Valve Stuck in a Semiopen Position	Transients	Loss of Flow Control May Result in Excessive Metal or Salt Temps.	Valve Position Indicator and Temperature/Flow Monitoring	Shut Down and Repair	
	Fail Closed	Sun-On	Loss of Flow Could Result in Rapid Overheating and Tube Failure	Flow/Temp/Valve Position Indicators	Loss of Flow will Cause Automatic Heliostat Scram and Emergency Shutdown	
CV-1	Fail Open, Fail Closed, or Struck in an Intermediate Position	All Sequences Involving Salt Flow	Calibration Pot Inoperable	Via Monitoring Load Cell Output	Manual Override (Sun-Off) Overflow Capability Incorporated in Design	Valve of "Fail Open" Design
IV-1	Fail Open	Hot Air - Rec. Warmup (Exposed Config.)	Pump not Isolated During Warmup - Reduced Air Flow - Possible Violent Bubbling thru Pump	Valve Position Indicator	Abort Warmup Sequence	"Fail-Open" Design
	Fail Closed or Struck in Intermediate Position	Startup	Valve Prevents Filling of Receiver Tubes with Salt	Valve Position Indicator Excessive Pump Pressure	Abort Startup	This Failure Mode not likely during Normal Sun-On Operation

Table III-3 Failure Modes and Effects Analysis (cont)

Subsystem/Component	Failure Mode	Effects		Detection	Preventive Measure or Corrective Action	Comments
		Ops Sequence	Consequences			
<u>SRE Purge and Vent System</u>						
<u>Air Heater</u>	Loss of Power	Prefill Warmup	Unheated Tubes May Cause Local Freezing of Salt during Fill	Temperature Measurements	Abort Filling Sequence	
<u>Purge Control Valves</u> PV-1 Thru PV-9 (Any One)	Fail Closed	Drain	Inverted U-Tube Effect Prevents Draining of Pass with Potential Freezing	Valve Position Indicator	Maintain Flow to Prevent Freezing Pretest C/O Manual Override Handwheels Provided Pretest C/O Manual Override Handwheels Provided	"Fail Closed" Design
	Stuck in Semiopen Position, or Fail Open, or Leak	Fill Sequences with Salt Flow	Filling of Pass Prevented Leakage of Molten Salt into the Purge System and Subsequent Plugging of the Lines	Valve Position Indicator		This Failure Mode not Likely during Normal Sun-On Operation
RPV-1	Fail Closed	Drain	Drain Process Impaired or Prevented with Possible Freezing in Receiver	Valve Position Indicator Receiver Pressure (PT2) too Low	Manual Override Handwheels Provided Gravity Drain Option by Venting thru RPV-2	"Fail Closed" Design
	Stuck in Semiopen Position of Fail Open	Fill and Recirculation	Salt May Get into Purge and Vent System Up-Stream of RPV-1 with Potential Plugging of the Purge System	Valve Position Indicator	Manual Override	
RPV-2	Fail Closed	Fill and Recirculation	Impairs, Filling Process, Prevents Recirculation	Valve Position Indicator	Manual Override	"Fail Closed" Design
	Stuck in Semiopen Position or Fail Open	Purge/Drain	Inadequate Purge Pressure	Valve Position Indicator Receiver Pressure too Low	Manual Override	

Table III-3 Failure Modes and Effects Analysis (cont)

Subsystem/Component	Failure Mode	Effects		Detection	Preventive Measures or Corrective Action	Comments
		Ops Sequence	Consequences			
<u>SRE Receiver</u> <u>Drain System</u> <u>Control Valves</u> DV-1 Thru DV-10 (Any One)	Fail Closed	Draining	Draining of Pass Prevented	Valve Position Indicator Monitoring Cooling Transient of Pass	Manual Override	"Fail Closed" Designs
		Fill/Recirculation	Filling of/or Recirculation Thru Pass Prevented	Valve Position Indicator Temperature Monitoring	Manual Override	
ROV-1	Fail Closed	Fill, Drain	Prevents Filling or Draining Operation	Valve Position Indicator Tube Temperature Monitoring	Manual Override Fail-Open Design	"Fail-Open" Designs

Table III-3 Failure Modes and Effect Analysis (cont)

Subsystem/Component	Failure Mode	Effects		Detection	Preventive Measure or Corrective Action	Comments
		Ops Sequence	Consequences			
<u>SRE Air Cooler</u> Top Insulation Cover	Stuck in Closed Position	Sun-On	Salt Over-Temperature	Temperature Sensor	Receiver Outlet Overtemperature Included in Automatic Kill Parameters Manual Override	
	Stuck in Open Position	Prefill Warmup	Cold Spots Below Freezing Point of Salt May Impair Filling Operation	By Inspection Prior to Start of Filling Ops	Shutdown and Repair	
Tubes/Headers	Leakage	All Sequences Involving Flow	Salt Leakage may Create Frozen Salt Stalactites or Stalagmites which may Impair Louver or Fan Performance Large Leakage may Cause Excessive Loss of Salt from System	Pre/Posttest Inspection	Pretest/Posttest C/O and Maintenance	
Louvers	Fail Closed	Sun-On	Cooler Outlet Over-temperature	Temperature Sensor Pretest Inspection	Cooler Outlet Overtemperature Included in Automatic Kill Parameters	"Fail Close" Design
	Fail Open	Sun-On	Cooler Outlet Temperature Control Range Minimized	Temperature Monitoring	Pretest/Posttest C/O and Maintenance	
Fans	Loss of Power	Sun-On	Cooler Outlet Temperature	Temperature Sensor	Automatic Kill	

Table III-3 Failure Modes and Effects Analysis (cont)

Subsystem/Component	Failure Mode	Effects		Detection	Preventive Measures or Corrective Action	Comments
		Ops Sequence	Consequences			
<u>SRE Sump/Pump Subsystem</u> Pump	Loss of Power	Sun-On	Loss of Flow Resulting in Tube Overheating	Flow and Temperature Instrumentation	Automatic Kill	
	Loss of Air Cooling to Bearing	All Sequences Involving Flow	Bearing Overheating and Eventual Failure	Air Supply Pressure Indicator	Verification of Pneumatic Valve Positions during Pre-test C/O (Routine Checklist)	

Table III-3 Failure Modes and Effects Analysis (cont)

Subsystem/Component	Failure Mode	Effects		Detection	Preventive Measures or Corrective Action	Comments
		Ops Sequence	Consequences			
<u>SRE - Receiver</u> <u>Aperture Subsystem</u> Aperture Cooling System	Loss of Coolant Flow	Sun-On	Aperture Overheating and Failure	RTAFS Flow Monitoring	Loss of RTAFS Coolant Initiates Automatic Shutdown	Aperture Cooling Loop is Hooked Up in Series with the RTAFS Cooling Loop
	Coolant Leak	Sun-On	Small Leak--Vapor Cloud may Partially Obstruct Solar Radiation thru Aperture Causing Uncertainties in Test Data Large Leak--Reduction in Coolant Flow may Cause Local Overheating and Failure of RTAFS or Aperture	TV Monitoring of Aperture Area Cooling Water Flow Instrumentation	Periodic Visual (TV) Monitoring of the Structural Integrity of the Aperture System Loss of Coolant Flow Will Initiate Automatic Shutdown	
Aperture Doors	Stuck in Partially Opened Position	Sun-On	Those Surface of the Doors Exposed to Aperture Fluxes will Overheat or Burn Up	TV Monitoring Relay Switches	Test Procedure will Require Verification of Full Opening of the Doors Before Activating Heliostats	

Table III-3 Failure Modes and Effects Analysis (cont)

Subsystem/Component	Failure Mode	Effects		Detection	Preventive Measures or Corrective Action	Comments
		Ops Sequence	Consequences			
<u>SRE - Auxiliary Systems</u> <u>Power Supply</u>	Loss of Power	Sun-Off and Standby	Loss of Heat Tracing	Inspection of Control Panel	Standby Power Automatically Activated	
		All Sequences	Loss of Console Functions Loss of STTF Computer Functions Loss of Pump and Salt Flow All Remote or Automatic Controlled Valves Assume Their "Fail-Safe" (Open or Closed) Positions Flux Patterns will Drift to the East		Emergency Shutdown Using Standby Power Including Automatic Heliostat Scram	
<u>Pneumatic System</u> <u>Air Supply</u>	Loss of Pressure (Compressor Fails)	All Sequences	Loss of Remote and Automatic Control Functions (Valves Assume "Fail-Safe" Positions)	Inspection of Control Panel	Emergency Shutdown, Including Automatic Heliostat Scram	
Pressure Regulator(s)	Pressure(s) out Range	All Sequences	Possible Loss of Remote and Automatic Control Functions	Inspection of Control Panel	Use of Manual Override or Initiate Emergency Shutdown (Depending on Test Sequence)	

Table III-3 Failure Modes and Effects Analysis (concl)

Subsystem/Component	Failure Mode	Effects		Detection	Preventive Measures or Corrective Action	Comments
		Ops Sequence	Consequences			
<u>Trace Heaters and Controls</u>	Loss of Power (Individual Circuits)	Sun-Off Sequences	Flow Passages may be Plugged Up due to Local Freezing of Salt	Inspection of Console Indicator Lights Temperature Instrumentation	Test Procedure Requires Verification of Above-Freezing Temperatures Prior to Start of Fill and Drain Sequences	
<u>Instrumentation Subsystem</u> Temperature Sensors	Fail Open (Zero MV Indication)	Sun-On	Possible Loss of Feedback to Computer Control Loss of Data Impaired Test Monitoring Capability	Inspection of Control Console	Redundancy in Critical Measurements, Including Receiver Inlet and Outlet, and Cooler Outlet Fail-Safe Feature in Computer Software Prevents Over-Reaction of Automatic Control Redundant Control Modes (Console vs Computer)	

E. THERMAL/HYDRAULIC ANALYSIS

Before describing the analysis, it is important to define terms relating to the physical layout of central receivers. Two such terms are receiver control zones and receiver fluid passes. A receiver control zone is that portion of a receiver associated with a single fluid inlet and single fluid outlet. A receiver with two control zones would have two distinct outlets and two central systems regulating the temperatures of each outlet stream. Fluid passes describes the number of times the fluid is directed across the receiver's absorbing surface within a control zone. A single control zone, single pass receiver, for example, is a design having one upper and one lower manifold. The working fluid flows into the lower manifold, which distributes the fluid to a series of parallel tubes. These tubes carry the fluid to the upper manifold and from this manifold to the receiver outlet. For a single-pass receiver, any given fluid particle travels only once across the receiver's absorbing surface. For a six-pass receiver, any given fluid particle makes six passes across the receiver's absorbing surface.

The receiver designed for this program is an 18-pass receiver with a single control zone and 16 parallel tubes per pass. The receiver will be tested in three different configurations: fully exposed, partially exposed, and cavity. In the fully exposed configuration, the entire receiver surface is exposed to the solar flux. For the partially exposed configuration, the RTAF (a device for measuring the receiver's input power) is positioned directly in front of the receiver. The aperture of the RTAF is smaller than the receiver's absorbing surface, therefore receiver tubes outside the RTAF aperture are covered with thermal insulation. Receiver tubes inside the RTAF aperture are exposed to the solar flux. For this partially exposed configuration, there are eleven active receiver passes. The cavity configuration is similar to the fully exposed arrangement except that a cavity is positioned in front of the receiver tubes.

1. Receiver Sizing

It was established early in this program that our molten salt receiver would have a single control zone to minimize the need for receiver outlet temperature regulation hardware and to simplify receiver operation. Incoloy 800 tubing with an outside diameter of 1.9 cm (0.75 in.) was selected as the receiver tubing. It was decided to design the receiver output to be consistent with the CRTF capability of approximately 5 MW. To keep the peak input fluxes below approximately 0.63 MW/m² (200,000 Btu/ hr-ft²), the overall receiver size was set at 3.35-m high by 5.49-m long (11 x 18 ft). With these items defined, it was then possible to perform an analysis relating receiver pressure drop and inside convection film coefficient to the number of fluid passes through the receiver. The results of this analysis are given in Figure III-24. It is important to have as high a film coefficient as practical to limit tube wall temperatures. However, the film coefficient is a strong function of the receiver pressure drop. Based on available pump sizes and a practical compromise between film coefficient and pressure drop, it was decided to design the receiver with 18 fluid passes.

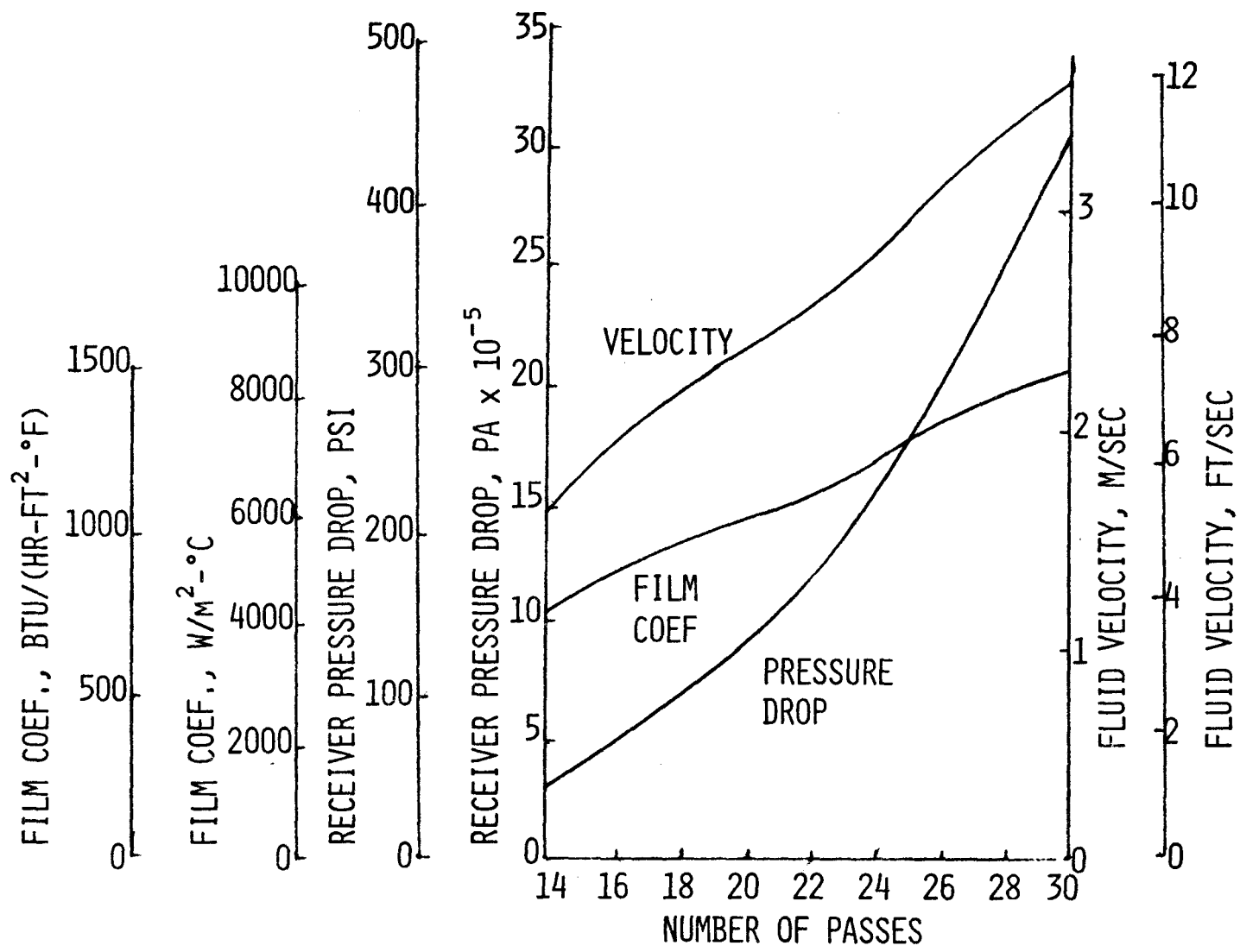


Figure III-24 Receiver Tube Layout Analysis

A preliminary evaluation of receiver performance with regard to heat balance, pumping requirements, and tube metal temperatures, was done using a simplified thermal-hydraulic analytical model of the receiver, programmed on an HP 9815A minicomputer. The principal features of the model are:

- a) 236 nodes, including 198 heated fluid pass sections, 37 unheated sections, and a single node representing the average cavity radiation environment.
- b) Provisions for inputting incident solar radiation fluxes on each of the 198 heated nodes. These fluxes are determined separately for various receiver and heliostat configurations using the TRASYS program (to be described later) and are recorded on a tape cartridge for minicomputer use.
- c) Convective, conductive, and radiative heat transfer modes through the fluid, tube metal, and on the outer surfaces of the tubes, respectively.
- d) Variable properties for both molten salt and tube metal. These are updated in a step-wise fashion from node to node in the direction of the flow.

With flow rate, salt inlet temperature, incident solar fluxes, and an estimated cavity radiation level as inputs, the program calculates pressure drops (including entrance and exit losses through headers), flow velocities, Reynolds, Prandtl, and Nusselt numbers, heat transfer coefficients, fluid temperatures, and inside/outside/local peak tube temperatures for each heated node.

Typical results of such calculations are depicted in Figures III-25 through III-29. Figures III-25, 26, and 27 show the maximum tube metal temperatures in each flow pass plotted against the corresponding salt temperatures at those locations, for maximum load conditions and the three test configurations shown. The upper curves represent peak local metal temperatures, whereas the lower curves depict the maxima of the external tube metal temperatures averaged over the heated semi-circumference. The peak local temperatures are significant because of the thermal-stress behavior of the tubes. Semi-circumferential averages are used in heat transfer calculations. The maximum internal tube temperatures are also plotted on Figure III-25. These are the temperature environments of the molten salt.

Figure III-28 and III-29 show performance maps for the cavity and partially exposed receiver configurations, respectively. The calculated salt exit temperature is plotted against flow rate, with an assumed 288°C (550°F) inlet temperature, and absorbed heat (in percent of full load) as a parameter. Also shown on the figures is the pressure drop through the receiver as a function of flow rate. The turbulent-to-laminar transition region shown by the shaded area corresponds to a Reynolds number range of 2000 to 4000 at salt inlet conditions 288°C (550°F).

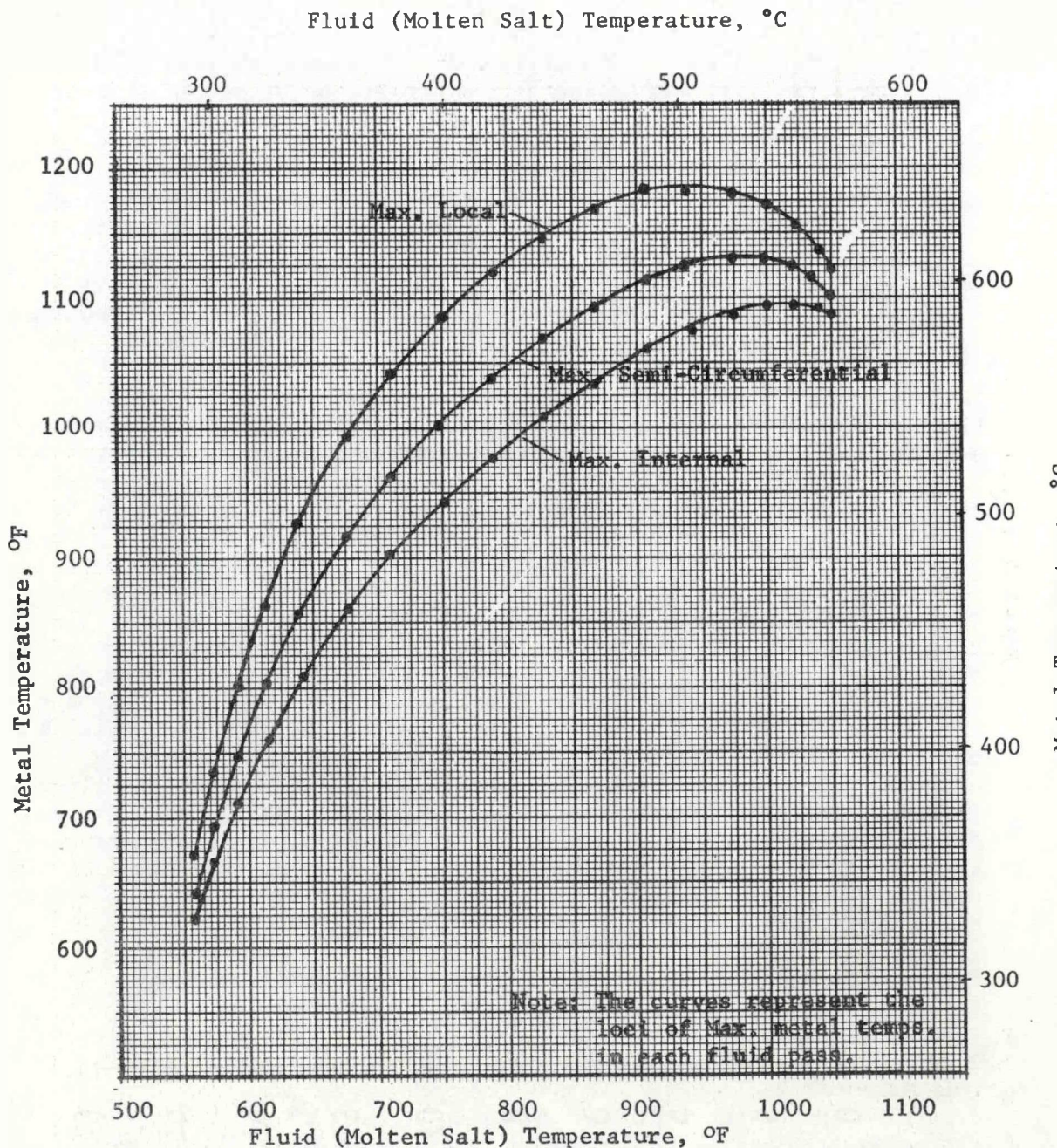


Figure III-25
Tube Metal Temperature vs Fluid Temperature — Cavity
Configuration @ 100% Load

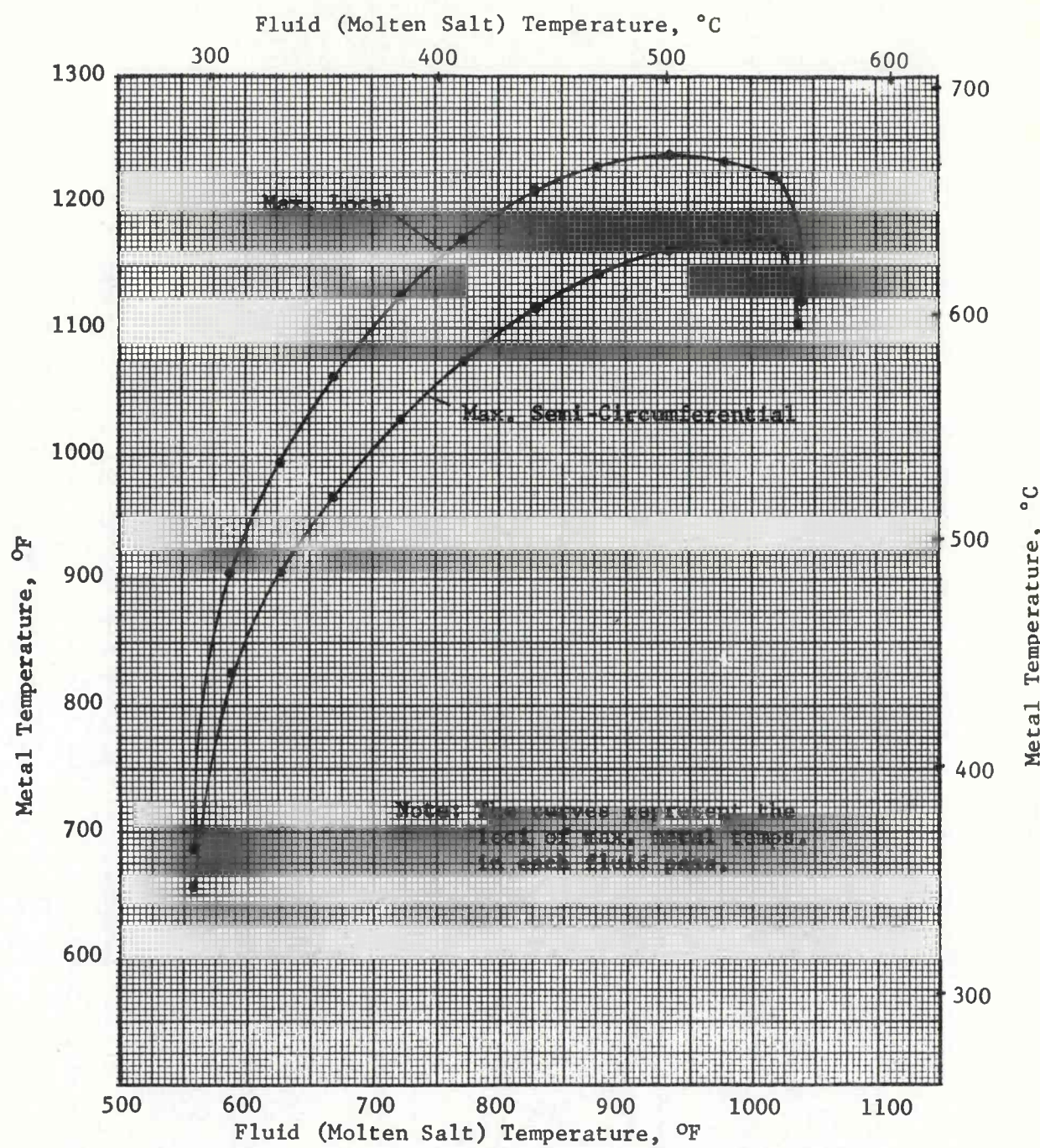


Figure III-26
Tube Metal Temperature vs Fluid Temperature — Partially Exposed Configuration @ 100% Load

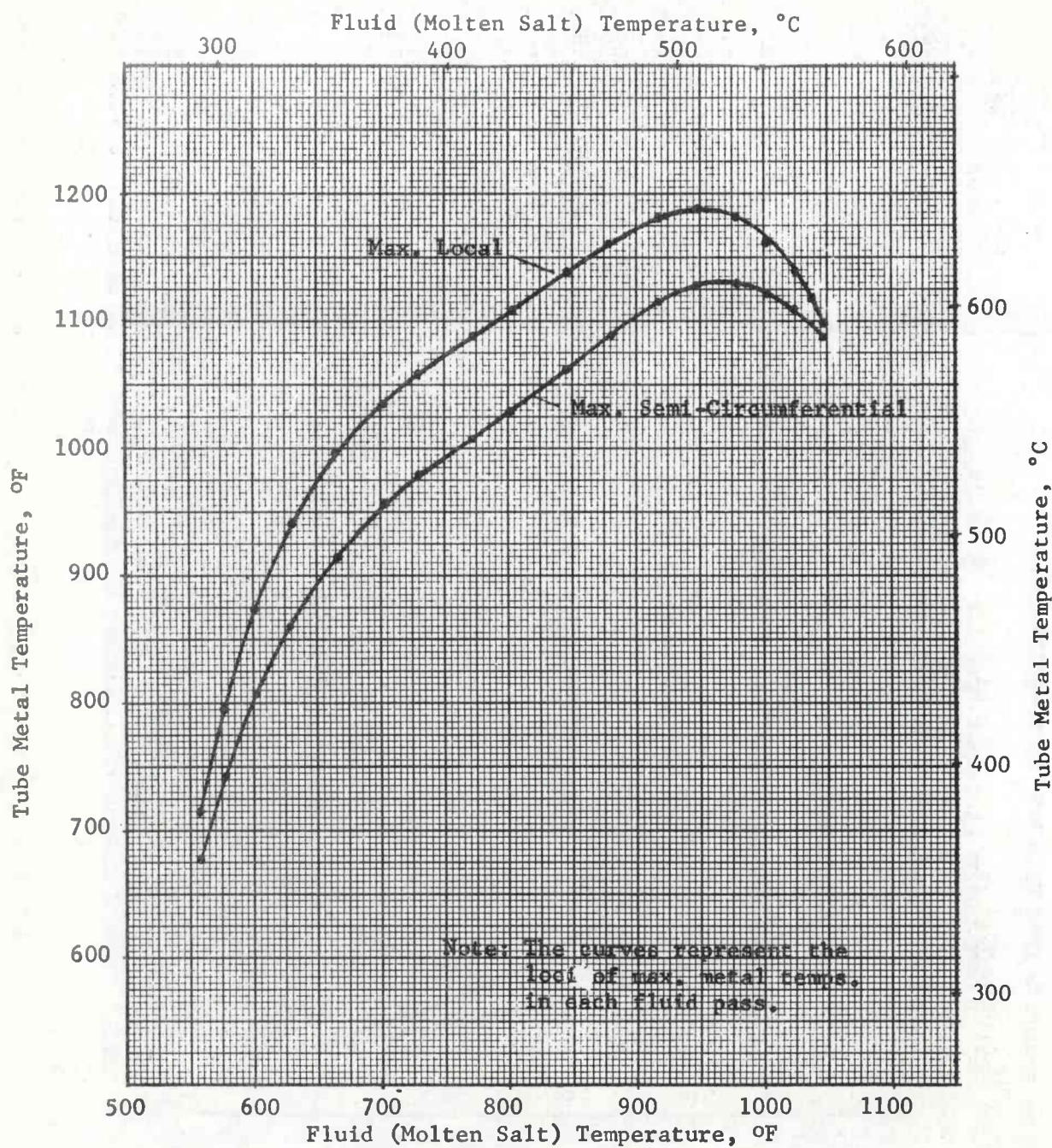


Figure III-27

Tube Metal Temperature vs Fluid Temperature — Fully Exposed Configuration @ 100% Load

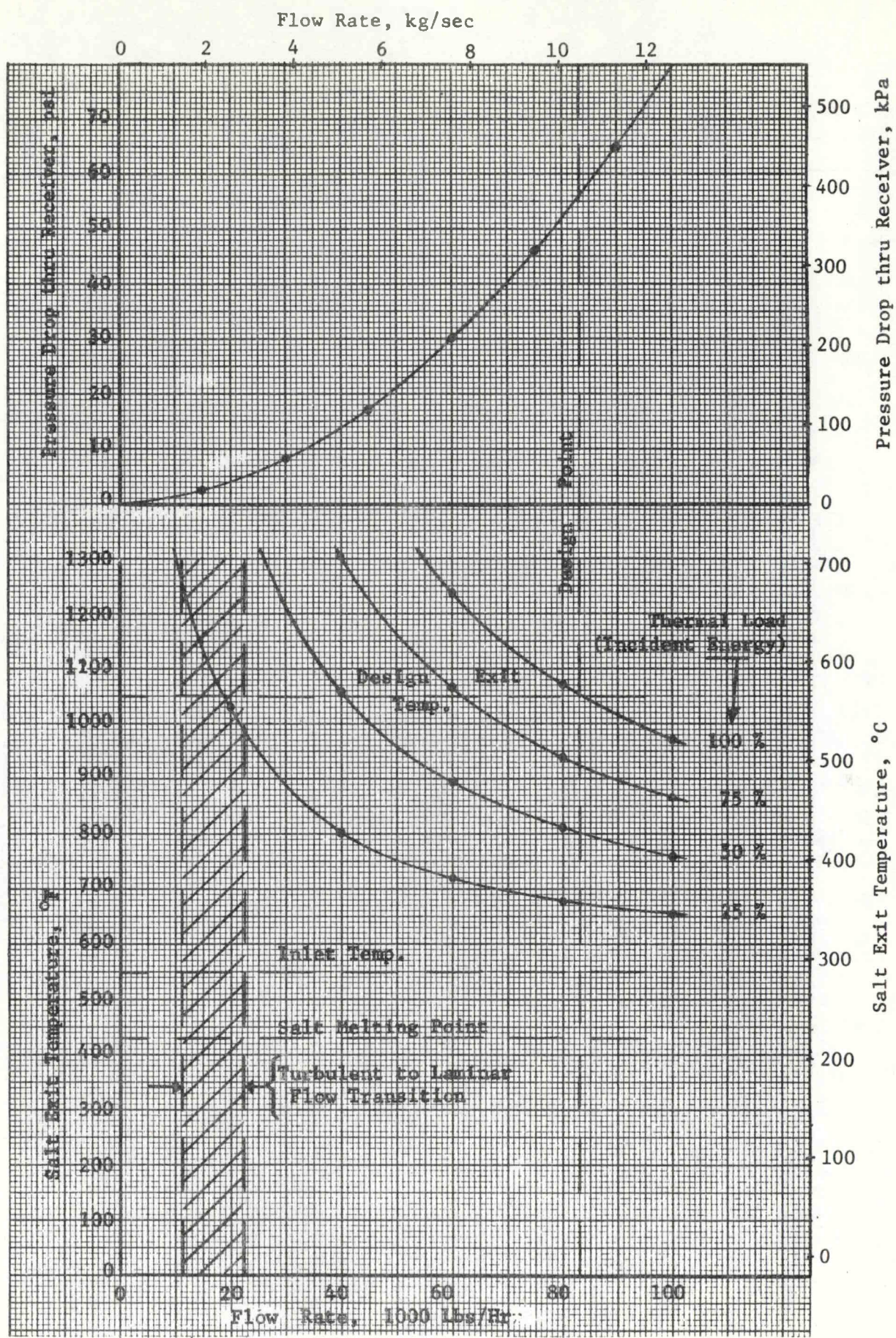


Figure III-28 Performance Map--Cavity Configuration

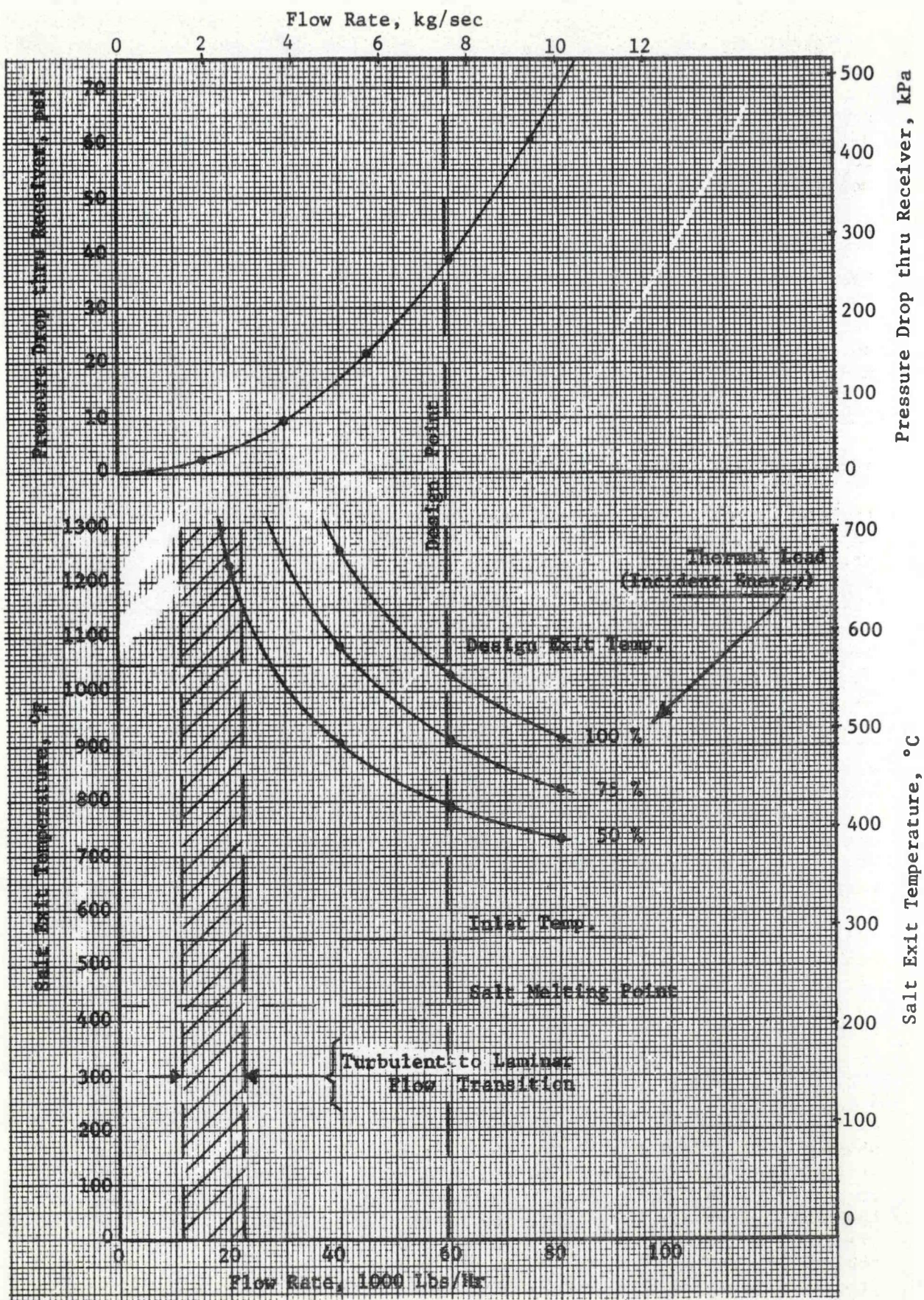


Figure III-29 Performance Map--Partially Exposed Configuration

The intent of performance maps is to indicate the relative sensitivity of performance to changes in flow rate and/or absorbed heat, as well as the overall range of these parameters to be considered for test-planing purposes (normally, one would not want to exceed the 566°C (1050°F) design exit temperature level by any significant amount, would not want to go below the 25% heating level during steady-state operation, and would stay safely to the right of the transition zone).

2. Flux Analysis

The calculation of incident solar fluxes on receiver surfaces as a function of heliostat radiation field parameters is essential to receiver design, performance prediction, and operational planning. The analytical tool used for this purpose is the Martin Marietta Thermal Radiation Analyzer System (TRASYS) - a computer program originally developed to support thermal analyses of space systems. Over several years, the program was expanded to handle radiation problems associated with heliostat fields by the addition of a "Mirror Field (MF) Library" of subroutines.

The basic element in the heliostat radiation model used by TRASYS is a beam of circular cross section with an area at the origin equal to the effective (cosine-modified) area of the heliostat that produces it. In the most general case, the beam is convergent-divergent along its axis; its minimum area occurs at the focal length and is equal to the subtended angle of the sun - also an input. The radial distribution of the solar flux within the beam is assumed to be Gaussian. The exact shape for the curve is specified by a single constant ("GAUSS") which is an input. The program accounts for atmospheric attenuation of reflected solar energy as well as effective heliostat reflectivity, and it takes into account the shadowing of the heliostat field by the tower. With insolation, atmospheric attenuation, and receiver and heliostat field geometry as inputs, the program calculates the incident radiation flux distribution on the target, which is divided into isothermal nodes. The target type may be exposed or cavity, the latter being distinguished by the inclusion of an "aperture" in the definition of target geometry. The aperture has the unique property of transmitting all radiation impinging inside its boundaries, while blocking all that falls on its plane external to the boundaries. A special block of node numbers is set aside by the program to permit calculation of incident fluxes on hardware in the front of the aperture plane, such as the RTAF in the case of the SRE. Aim-point coordinates can be specified for each heliostat in the field.

The program does not account for shadowing or blocking by adjacent heliostats, effects of guidance errors, mirror imperfections, optical aberations due to mirror curvature at large incidence angles, or "sun-shapes" different from the Gaussian. Fortunately, the combined errors in the predicted flux distributions due to these effects are expected to be relatively small during the "high noon" hours, which determine the peak design fluxes on the receiver surfaces. Comparisons of TRASYS predictions with actual test data indicate that a good match can be achieved by proper adjustments of the beam-defining constants in the program. Examples are shown in Figures III-30 through III-35, which compare those fluxes calculated by TRASYS against those measured by

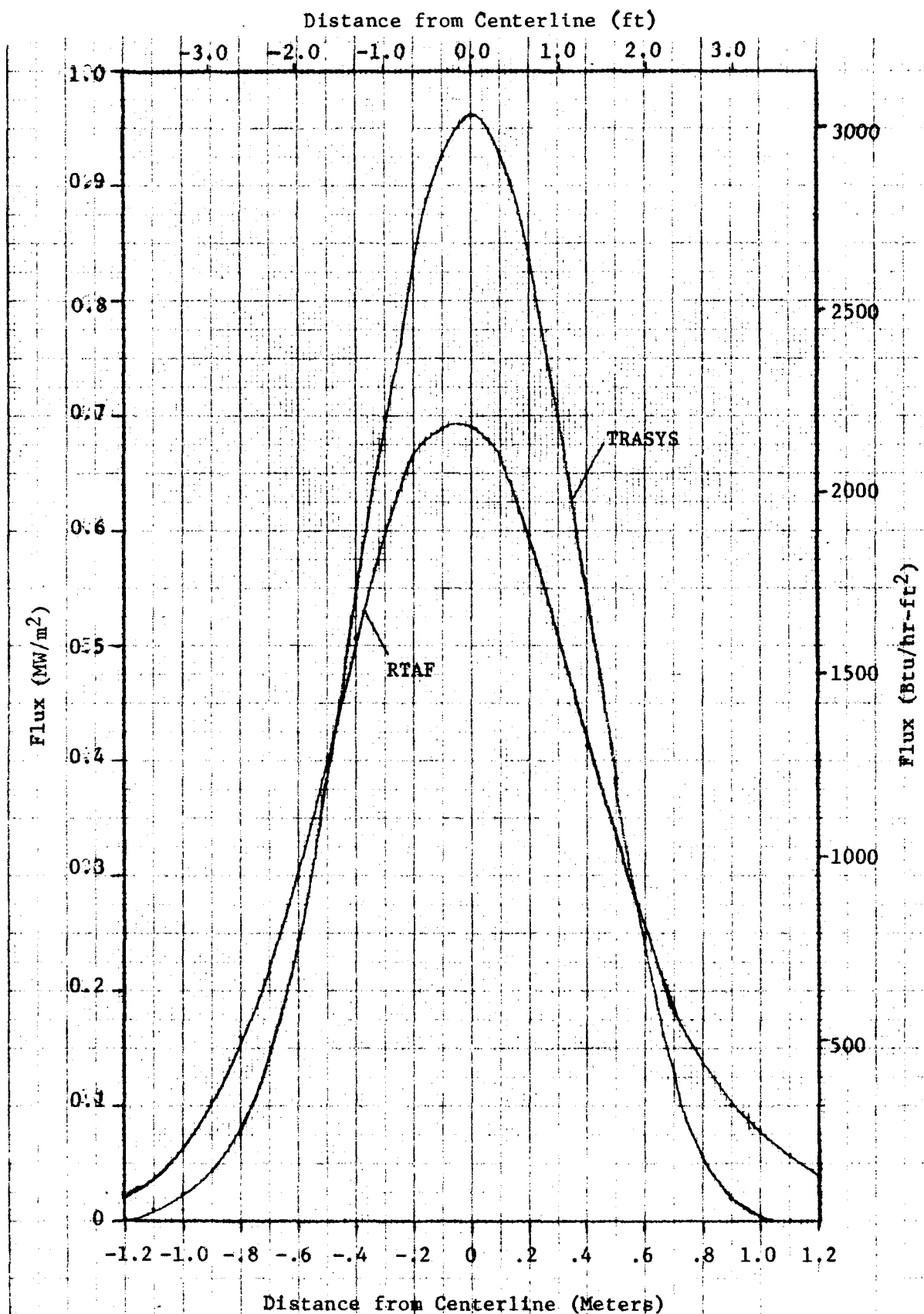


Figure III-30
 Flux Distribution-Horizontal Slice 40 cm above TRASYS Aim Point,
 30 cm above Aim Point per RTAF Run F02007

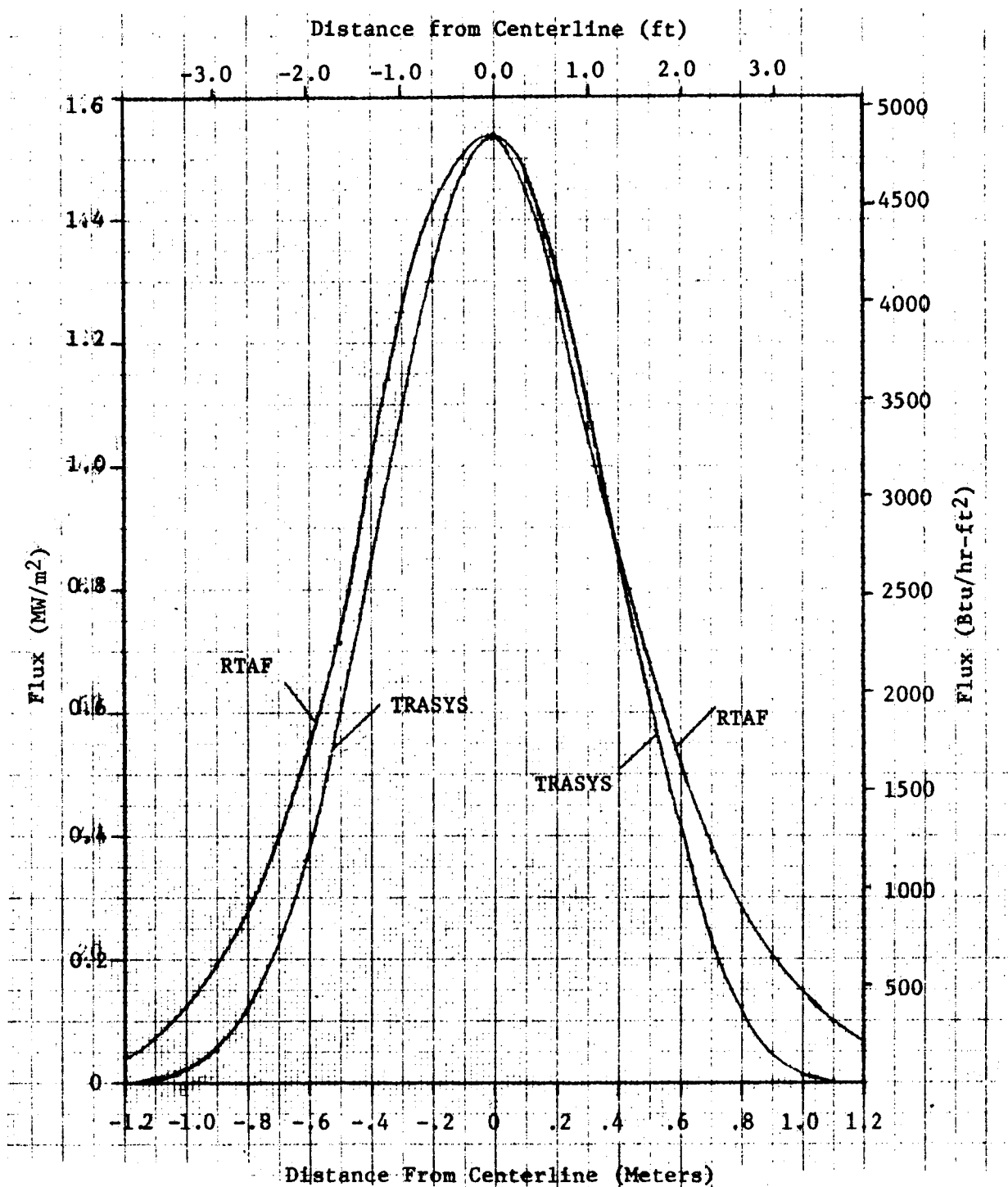


Figure III-31

Flux Distribution-Horizontal Slice 20 cm Above TRASYS Aim Point,
10 cm Above Aim Point per RTAF Run F02007

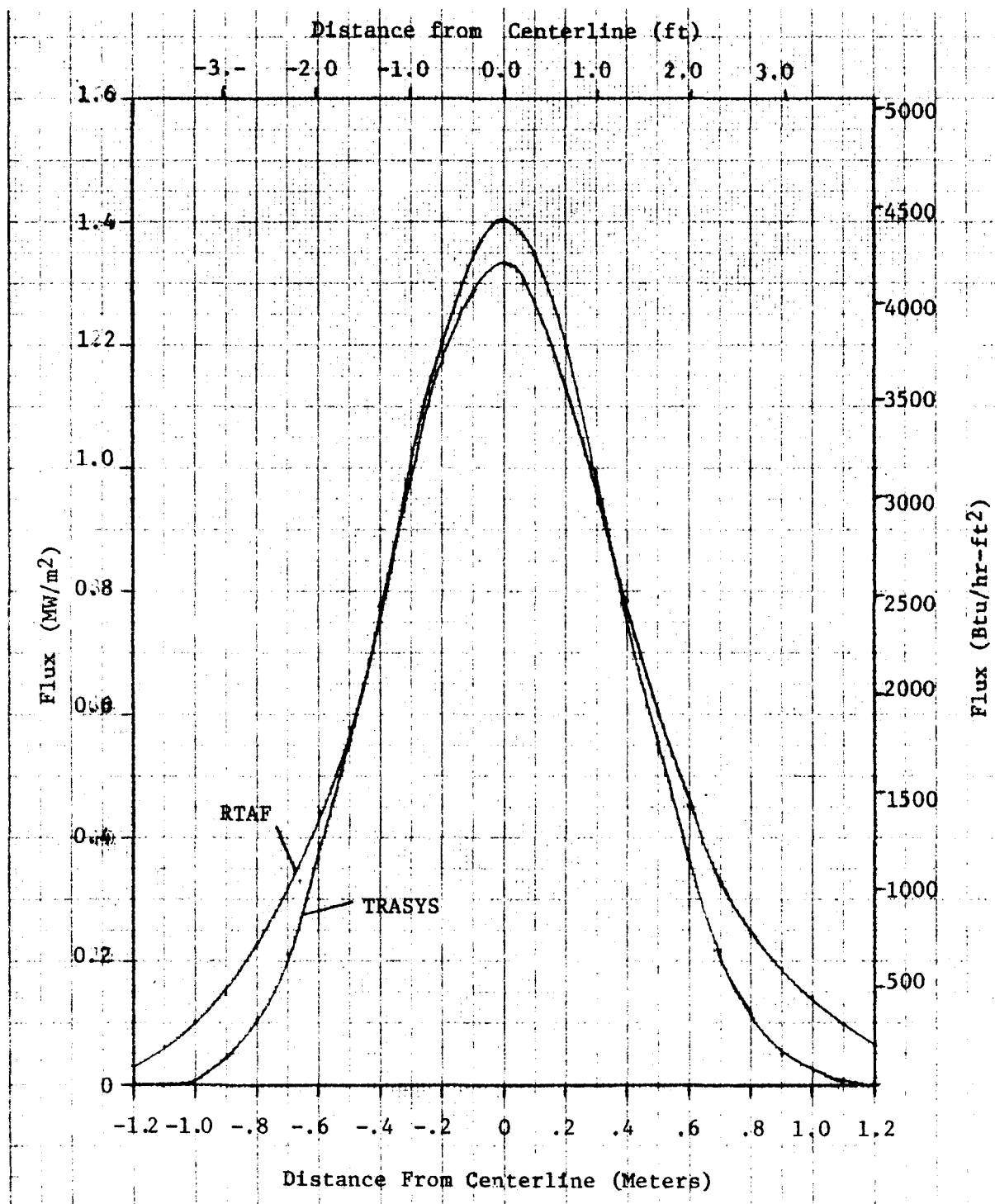


Figure III-32
 Flux Distribution-Horizontal Slice 20 cm below TRASYS Aim Point,
 30 cm below Aim Point per RTAF Run F02007

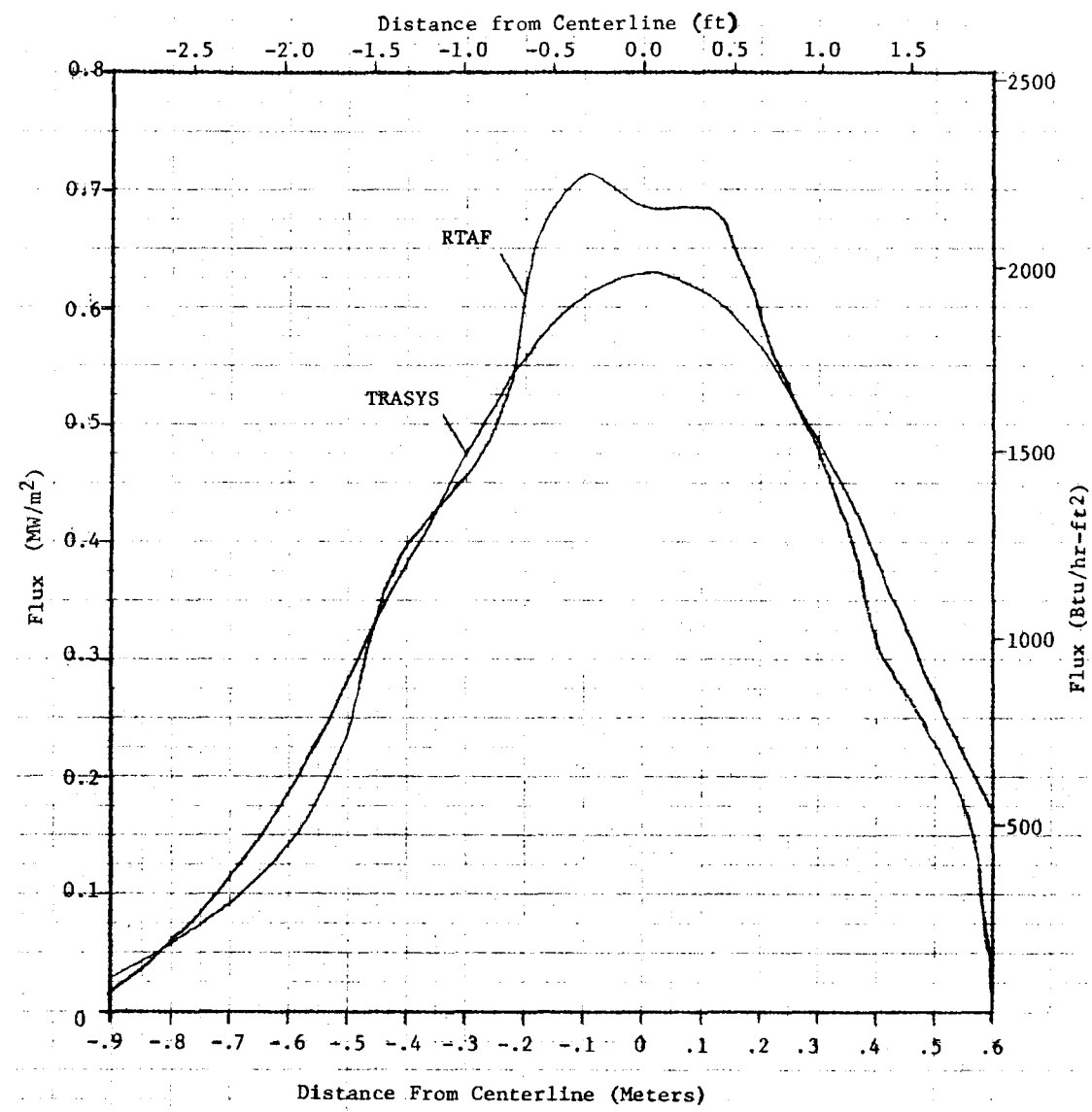


Figure III-33 Flux Distribution-Vertical Slice 50 cm East of Aim Point

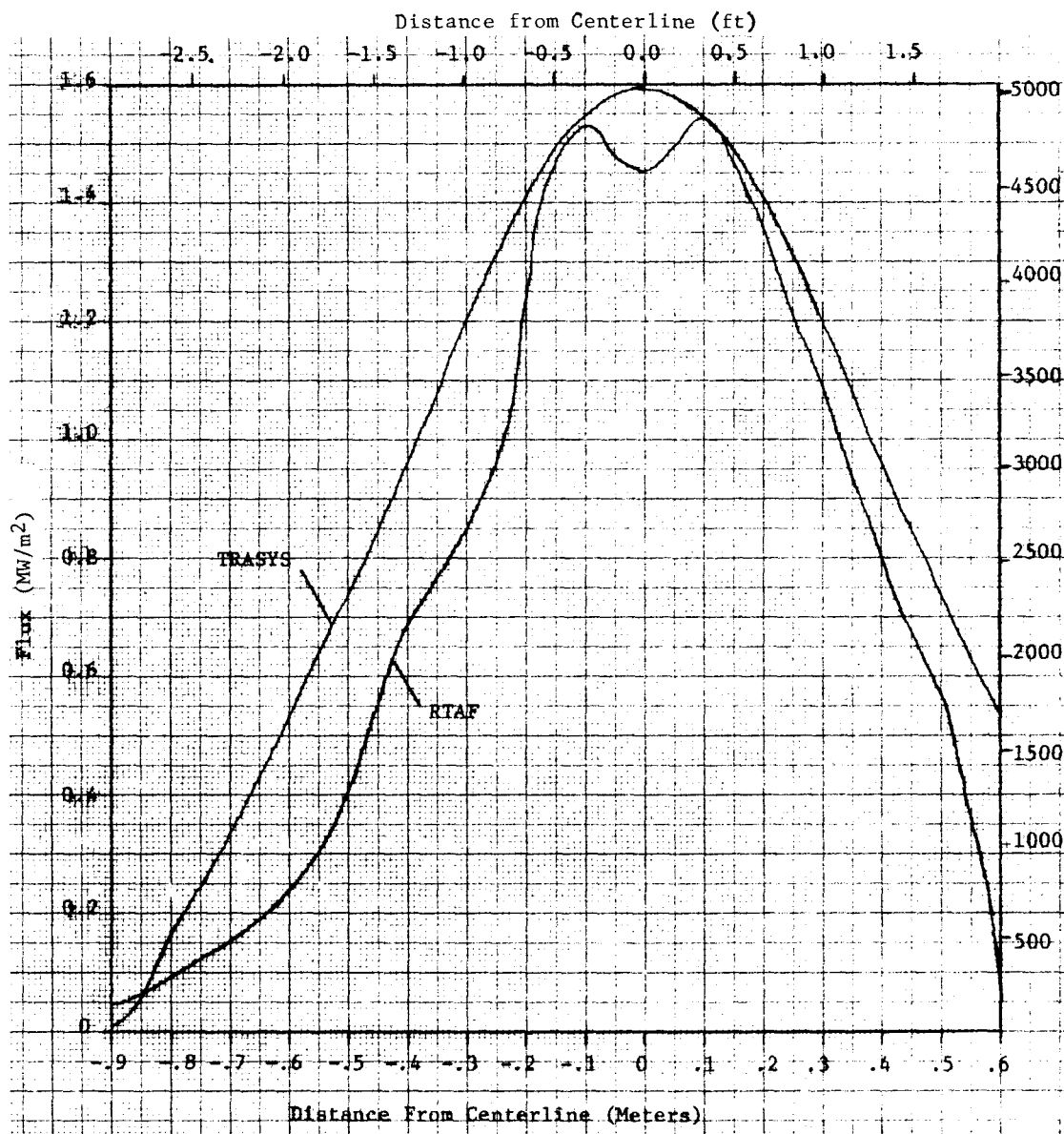


Figure III-34 Flux Distribution-Vertical Slice through Aim Point

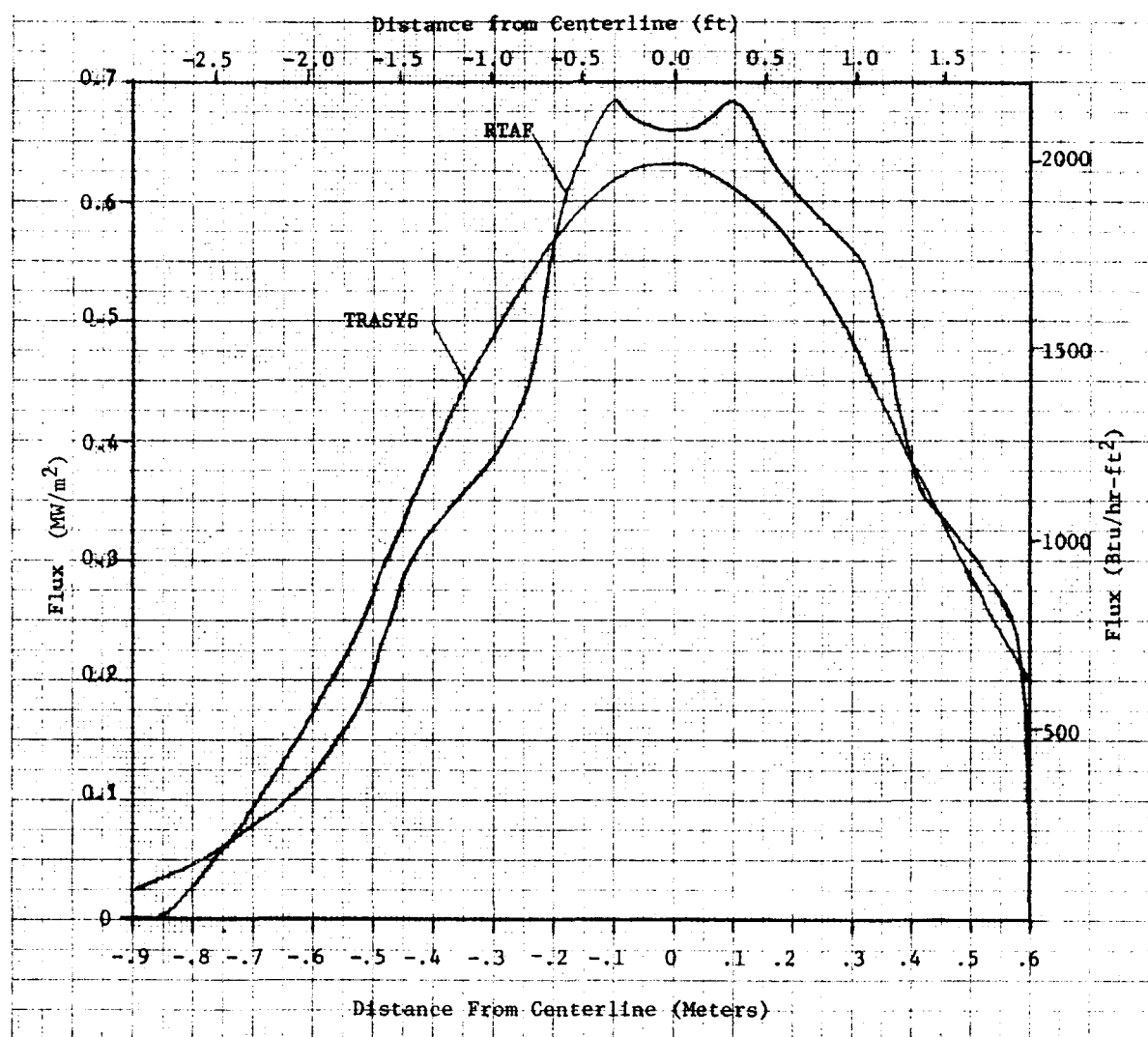


Figure III-35 Flux Distribution-Vertical Slice 50 cm West of Aim Point

RTAF Run F02007 on Jan. 20, 1979 (courtesy L. Matthews, CRTF). It was found that the best match was achieved if the aim point was assumed to be 10 cm (4 in.) off that reported by the RTAF. It is possible that this was caused by a faulty flux sensor at the center of the RTAF; this hypothesis is supported by the "dip" in the flux level at the center of the aperture in Figures III-33 to 35.

Flux analyses completed to-date or currently in progress may be divided into four categories: 1) Analyses in support of receiver design, 2) determination of heliostat field configurations for various test operational modes with the given receiver designs, 3) correlation of flux levels at calorimeter locations (RTAF and receiver calorimeters) with those in the aperture plane and on the active surfaces of the receiver, and 4) studies related to partial coverage of the heliostat field by cloud shadows. These are discussed in more detail below.

a. Receiver Thermal Design - When designing an experimental receiver that is physically much smaller than a typical commercial unit, it is important to consider experiment scaling. For a solar receiver, there are three major areas where scaling is important: Thermal and fluid flow conditions at the absorber surface, heliostat radiation field geometry relative to the tower height, and heliostat field geometry relative to the receiver target size. For the first scaling consideration, we have designed the experiment so that absorbed flux levels, Reynolds Numbers, heat transfer coefficients, and tube temperatures are representative of proposed commercial receivers.

The other two areas of scaling are geometric concerns. To investigate the field geometry relative to tower height and receiver target size, the nondimensional curves shown in Figure III-36 were developed. These curves are nondimensionalized by dividing by the applicable tower height. The information given in this figure addresses both tower height and receiver target size and secondary effects such as atmospheric attenuation. The CRTF heliostat field nondimensionalized layouts are shown with respect to the experiment at the various test levels at the CRTF. If these layouts are compared to nondimensional layouts for the commercial designs, it is readily seen that the 36.6-m (120-ft) or 42.7-m (140-ft) test locations at the CRTF are appropriate. Due to space limitations, though, it is only possible to install the experiment at the 61-m (200-ft) level. This means that incoming solar flux will be, on the average, at smaller incidence angles for the experiment than for a commercial system.

The circular shaped isolines represent the loci of points on the heliostat field from which elemental flat mirrors would produce solar images of equal major diameter on a vertical target plane at the receiver. The major axes represent minimum theoretical target dimensions required for zero spillage of reflected radiation originating from that portion of the heliostat field enclosed by the given isoline and the 45° field boundaries. Although highly idealized, this representation is believed to be adequate for comparative purposes. For the experiment, the appropriate isoline value is 0.045, and for the full-scale (commercial) molten salt receiver the value is 0.059. If isoline location is compared to heliostat field layouts, the theoretical spillage for the two cases is equivalent.

Nomenclature:

X, Y : Heliostat Field Coordinates

H : Tower Height

$2a$: Major Axis of Sun Image Ellipse
on Vertical Plane at $X=Y=0$
and normal parallel to Y

III
69

CONCEPTUAL
FULL SCALE
WATER/STEAM
CAVITY RECEIVER
(255 m TOWER)
NORTH FIELD

CONCEPTUAL
FULL SCALE
MOLTEN SALT
CAVITY RECEIVER
(155 m TOWER)
NORTH FIELD

$2a/H$

.08

.07

.06

.05

.04

.03

.02

.01

Y/H

7

6

5

4

3

2

1

0

X/H

-3

-2

-1

0

1

2

3

4

Figure III-36 Nondimensionalized Heliostat Field Map — SRE vs Full Scale Radiation Geometries

The location of the tube wall on the tower top was determined by an iterative process, involving the generation of flux maps in several planes parallel to the X-Z axes and with several aim points. From these, the plane and elevation of the tube wall was selected so that the average incident flux level on the wall would be about 0.315 MW/m² (100,000 Btu/hr-ft²), with corresponding local peaks of about 0.631 MW/m² (200,000 Btu/hr-ft²), at a (arbitrarily selected) maximum insolation of 1.08 kW/m² (342 Btu/hr-ft²). The aperture location and tilt was then determined from geometrical considerations, and the geometry of the cavity completed by connecting the tube wall with the aperture by a set of plane geometrical surfaces. The next step was to build a complete TRASYS model of the cavity so that the incident fluxes on active and inactive surfaces could be determined and the design adequacy verified. The complete flux map for maximum thermal load or design conditions and for internal and external surfaces of the cavity configuration is shown in Figures III-37, 38, and 39. The heliostat configuration associated with this run is depicted in Figure III-40, which also shows aperture and RTAF flux distributions.

Conversion to the fully exposed test configuration is achieved by removal of the passive cavity walls. The full-load heliostat configuration for this arrangement is shown in Figure III-41, together with the resulting flux distribution on the tube wall (there is no aperture or RTAF associated with this test configuration). The purpose of dual aiming is to bias the flux distribution towards the colder, receiver inlet side.

The full-load heliostat configuration and associated incident flux distributions on the RTAF and the tube wall for the partially exposed configuration are shown in Figure III-42.

b. Partial Load Studies - The objective of these analyses is to define heliostat configurations for performance tests at partial loads and for receiver warmup prior to filling the tubes with molten salt.

Results from the partial load analyses are shown in Figures III-43 through III-47 representing 75%, 50%, and 25% load for the cavity configuration, and 75% and 50% load for the partially exposed configuration. In establishing these heliostat configurations, an attempt was made to maintain similarity between the partial and full-load flux distributions.

Examples of heliostat warmup configurations for different input flux levels are depicted on Figures III-48 through III-53. The criteria used for determining these heliostat patterns was to maintain the radiation equilibrium temperature of the tube wall between 288°C (550°F) and 593°C (1100°F) without salt flow. The number and location of heliostats required to achieve this depends on intensity of insolation, time of day, and the test configuration of the receiver. Accordingly, a number of "warmup modes" (labeled A,B,C,...etc.) were established to suit each anticipated situation.

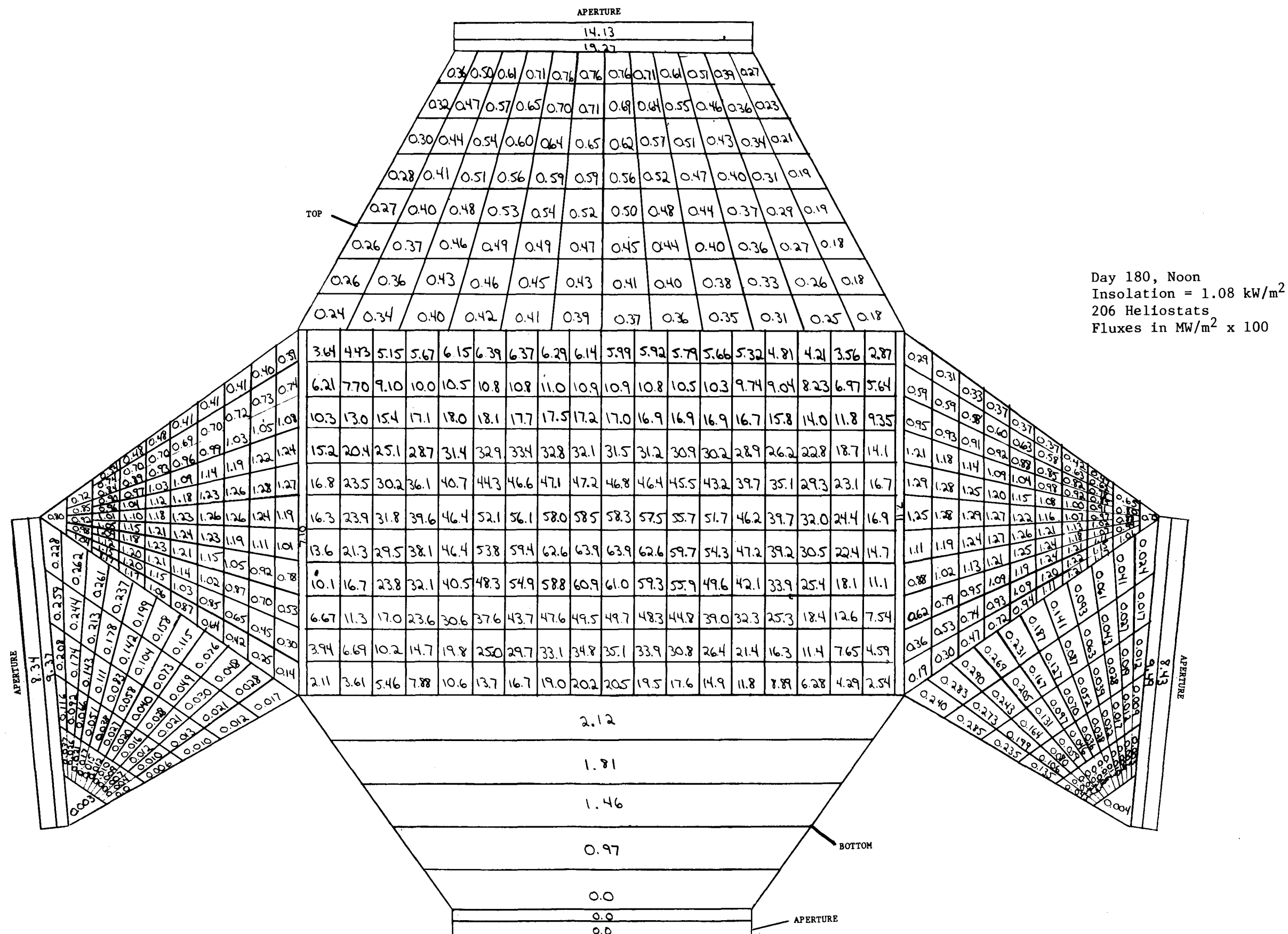


Figure III-37a Incident Fluxes Inside Cavity

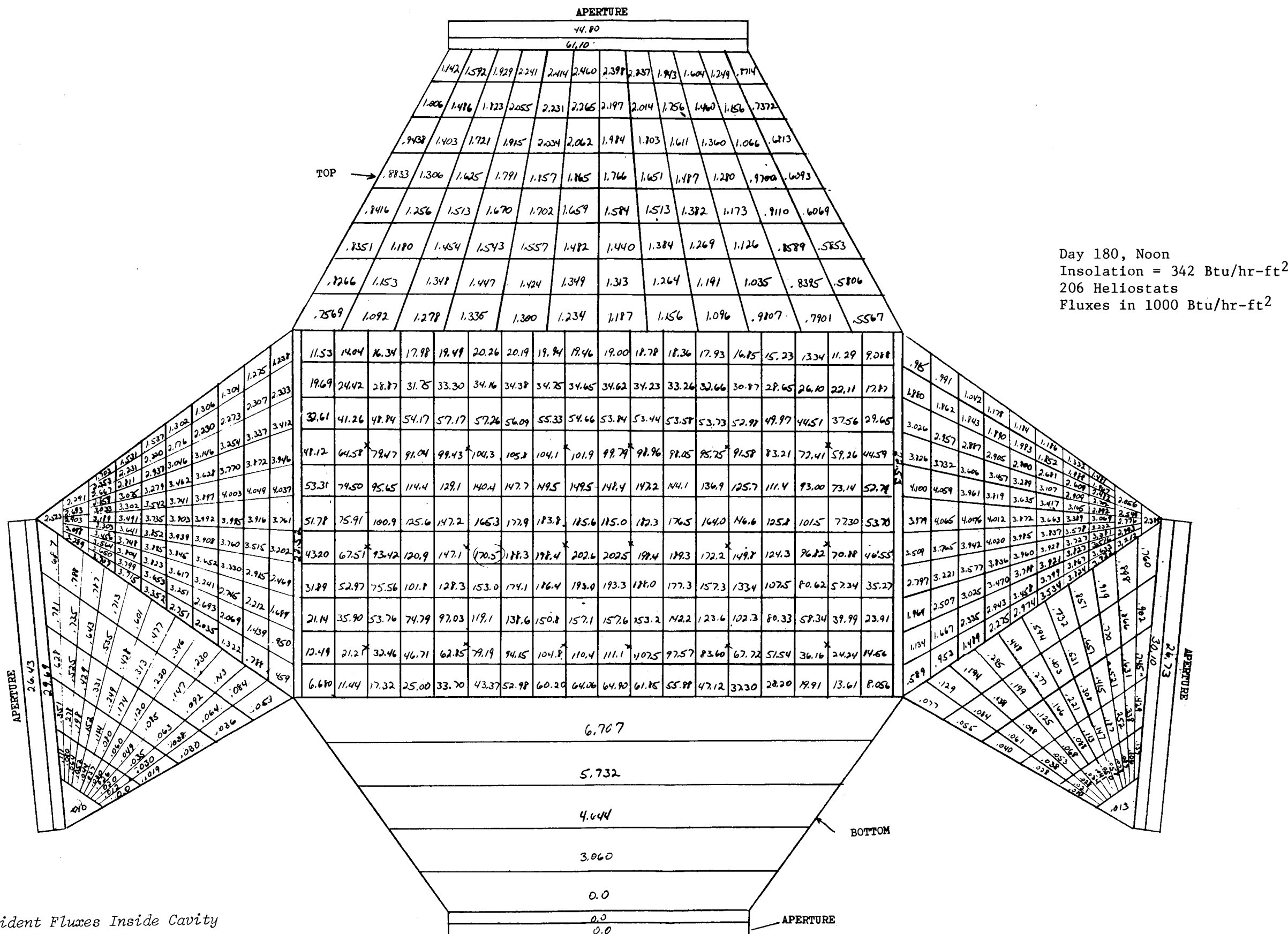


Figure III-37b Incident Fluxes Inside Cavity

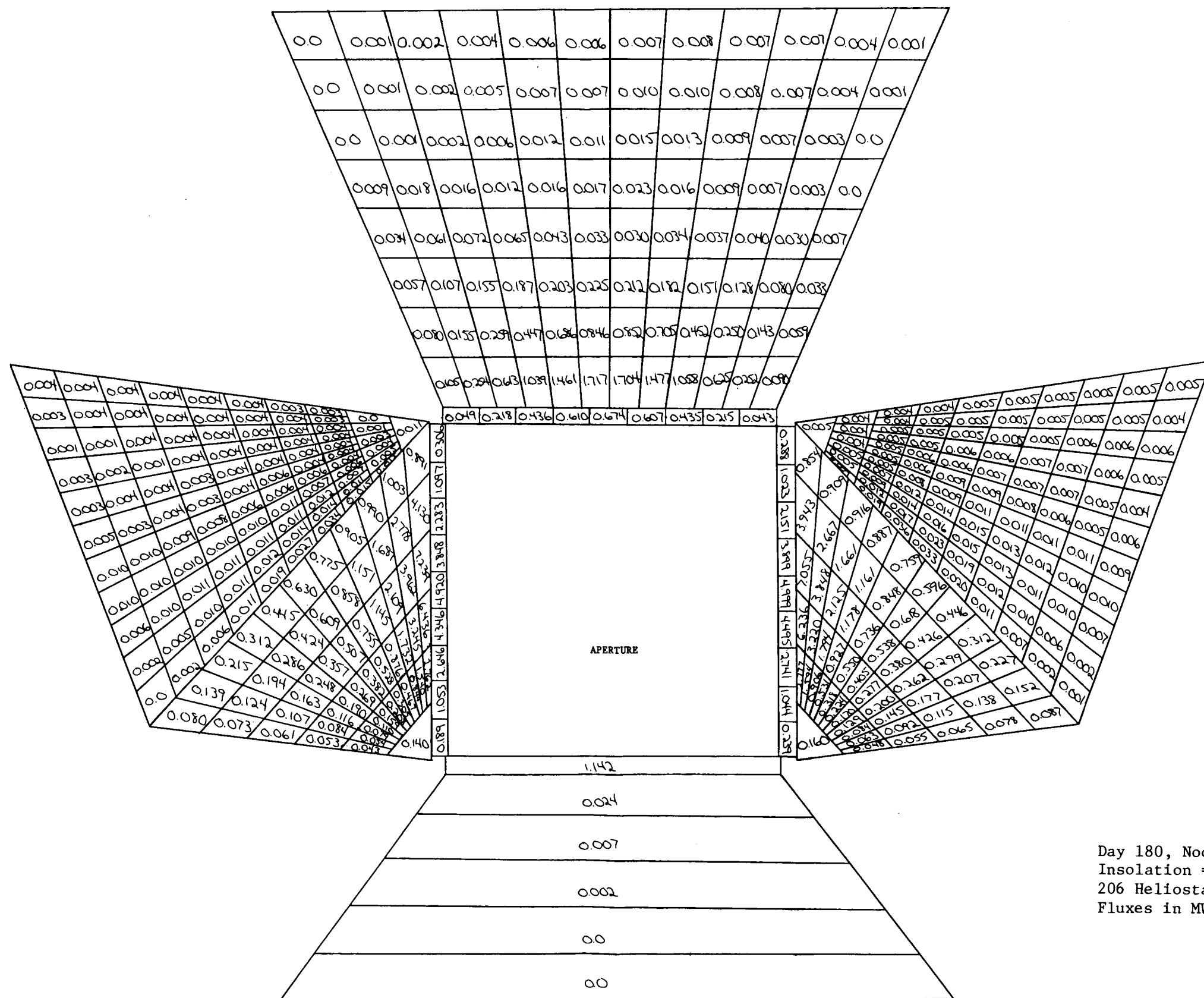


Figure III-38a Incident Fluxes Outside of Cavity

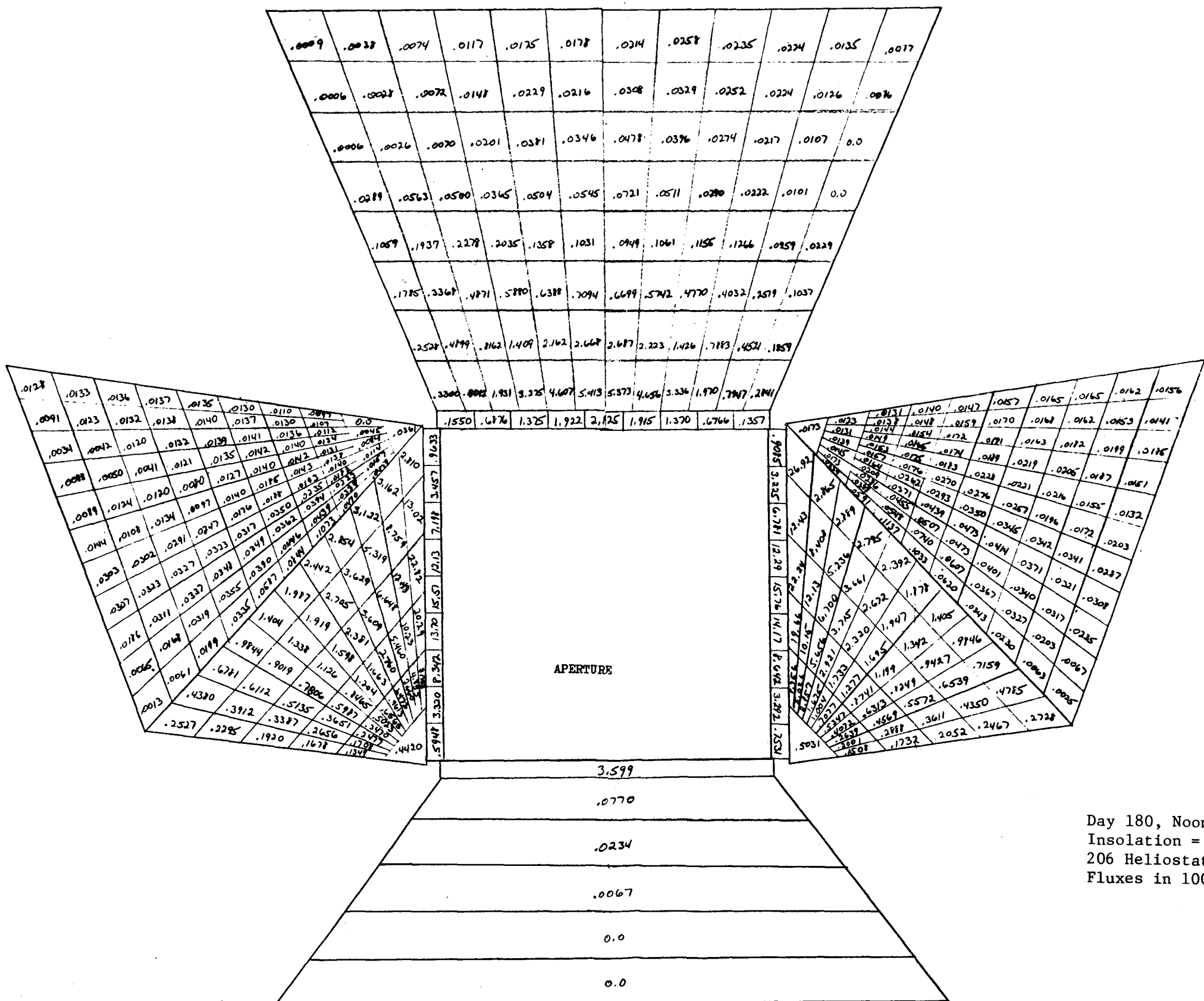


Figure III-38b Incident Fluxes Outside of Cavity

III-74

00	00	00	00	00	00	0.0
00	00	00	00	00	00	0.06
0.0	00	00	001	0.14	1.11	
0.0	00	00	012	0.93	4.31	
0.0	0.0	0.03	042	230	9.32	
0.0	00	0.11	073	357	13.6	
0.0	00	0.16	0.86	3.81	14.8	
00	00	0.13	073	2.96	11.8	
00	00	006	045	1.72	6.65	
00	00	00	017	0.75	2.73	
0.0	00	00	0.002	0.18	0.82	

EAST DOOR

0.0	0.0	0.0	0.0	0.0	0.0	0.0
0.07	0.0	0.0	0.0	0.0	0.0	0.0
0.98	0.12	0.0	0.0	0.0	0.0	0.0
4.05	0.87	0.08	0.0	0.0	0.0	0.0
8.97	2.23	0.38	0.02	0.0	0.0	0.0
13.4	3.54	0.72	0.10	0.0	0.0	0.0
14.7	3.91	0.88	0.15	0.0	0.0	0.0
11.9	3.15	0.76	0.13	0.0	0.0	0.0
6.92	1.92	0.48	0.07	0.0	0.0	0.0
2.98	0.83	0.19	0.01	0.0	0.0	0.0
0.76	0.20	0.02	0.0	0.0	0.0	0.0

WEST DOOR

0.34	1.51	3.80	6.18	7.27	6.06	3.65	1.44	0.31	0.25
0.23									1.99
1.66									6.30
5.27									11.8
10.2									14.6
14.1									11.8
13.9									6.22
9.65									RTAF FRAME
4.72									
1.45									
0.19	0.29	1.31	3.32	5.59	6.67	5.62	3.40	1.36	0.27

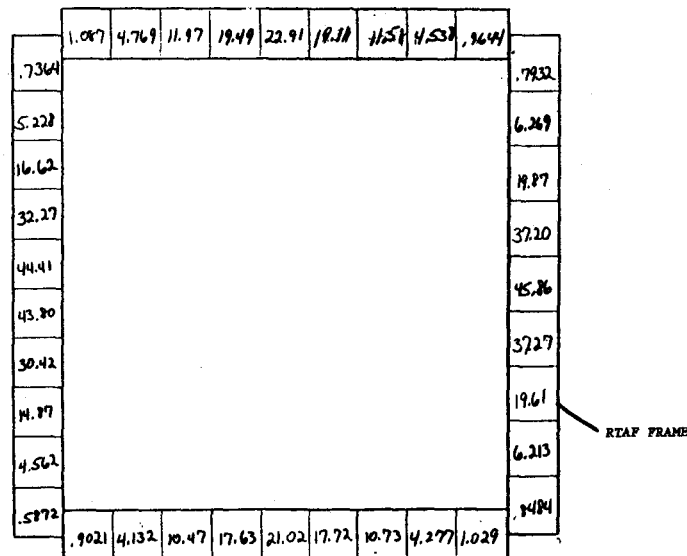
Day 180, Noon
 Insolation = 1.08 kW/m^2
 206 Heliostats
 Fluxes in $\text{MW/m}^2 \times 100$

Figure III-39a Incident Fluxes on Aperture Doors and RTAF Frame

0.0	0.0	0.0	0.0	0.0	0.0		0.0	0.0	0.0	0.0	0.0	0.0
0.0	0.0	0.0	0.0	0.0	0.0	.1868						
0.0	0.0	0.0	.0257	.4577	3.501							
0.0	0.0	0.0	.3644	2.933	13.59							
0.0	0.0	.1009	1.335	7.256	29.37							
0.0	0.0	.3530	2.292	11.25	42.87							
0.0	0.0	.4894	2.696	12.00	46.84							
0.0	0.0	.3966	2.304	9.333	37.24							
0.0	0.0	.1843	1.418	5.408	20.97							
0.0	0.0	.0090	.5801	2.371	8.599							
0.0	0.0	0.0	.0598	.5704	2.144							

EAST DOOR

WEST DOOR



Day 180, Noon
 Insolation = 342 Btu/hr-ft²
 206 Heliostats
 Fluxes in 1000 Btu/hr-ft²

Figure III-39b Incident Fluxes on Aperture Doors and RTAF

18	16	14	12	10	8	6	4	2
3.64	4.43	5.15	5.67	6.15	6.39	6.37	6.29	6.14
6.21	7.70	9.10	10.0	10.5	10.3	10.8	11.0	10.9
10.3	13.0	15.4	17.1	18.0	18.1	17.7	17.5	17.2
15.2	20.4	25.1	28.7	31.4	32.9	33.4	32.8	32.1
16.8	23.5	30.2	36.1	40.7	44.3	46.6	47.1	47.2
16.3	23.9	31.8	39.6	46.4	52.1	56.1	58.0	58.5
13.6	21.3	29.5	38.1	46.4	53.8	59.4	62.6	63.9
10.1	16.7	23.8	32.1	40.5	48.3	54.9	58.8	60.9
6.67	11.3	17.0	23.6	30.6	37.6	43.7	47.6	49.5
3.94	6.69	10.2	14.7	19.8	25.0	29.7	33.1	34.8
2.11	3.61	5.46	7.98	10.6	13.7	16.7	19.0	20.2
17	15	13	11	9	7	5	3	1

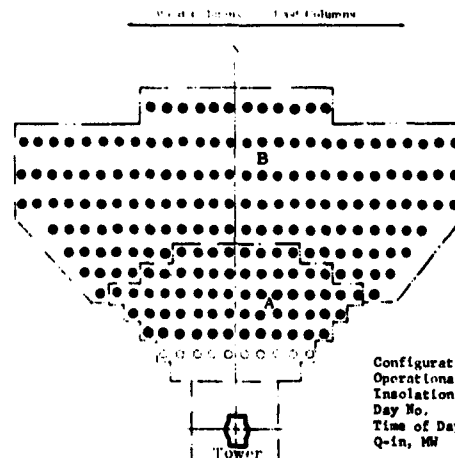
Tube Wall

NOTE: The Fluxes Shown are
in $\text{MW/m}^2 \times 100$

2.35	5.62	11.3	18.7	25.3	27.8	25.1	18.3	10.6	5.03	1.98
5.92	14.5	28.2	44.1	56.0	60.2	55.8	43.8	27.7	14.0	5.48
11.1	26.6	50.2	73.2	90.5	97.2	90.4	72.9	50.0	26.2	10.7
16.2	39.3	68.9	100.6	125.7	135.5	125.7	100.6	69.8	39.4	15.8
19.1	47.6	81.8	119.0	149.8	161.9	149.9	119.1	81.9	47.8	18.8
18.3	47.9	82.3	120.5	152.3	164.9	152.5	120.8	82.6	48.1	18.5
13.6	40.3	71.3	104.4	132.0	143.0	132.2	104.7	71.6	40.7	13.8
7.72	26.5	52.7	77.6	97.1	105.9	98.1	78.0	53.1	26.9	8.01
3.20	11.8	30.2	49.0	62.3	67.3	62.5	49.3	30.5	12.4	3.29
0.69	3.31	9.94	20.7	30.4	34.0	30.5	21.2	10.6	3.51	0.75
0.02	0.70	1.43	3.87	6.32	7.65	6.60	4.04	1.48	0.35	0.05

Aperture
(When Applicable)

RTAF



Configuration
Operational Mode : Single
Insolation, W/m^2 : 1000
Day No. : 120
Time of Day, Hr:Min : 12:00
Q-in, MM : 5.25

Figure III-40a Receiver Flux Levels-Cavity, 100% Load

18	16	14	12	10	8	6	4	2
11.5	14.0	16.3	18.0	19.5	20.3	20.2	19.9	19.5
19.7	24.4	28.9	31.8	33.3	34.2	34.4	34.8	34.7
32.6	41.3	48.8	54.2	57.2	57.3	56.1	55.3	54.7
48.1	64.6	79.5	91.0	99.4	104.3	105.8	104.1	101.9
53.3	74.5	95.7	114.4	129.1	140.4	147.7	149.5	149.5
51.8	75.9	100.9	125.6	147.2	165.3	177.9	183.8	185.6
43.2	67.5	93.4	120.9	147.1	170.5	188.3	198.4	202.6
31.9	53.0	75.6	101.8	128.3	153.0	174.1	186.4	193.0
21.1	35.9	53.8	74.8	97.0	119.1	138.6	150.8	157.1
12.5	21.2	32.5	46.7	62.9	79.2	94.2	104.8	110.4
6.68	11.4	17.3	25.0	33.7	43.4	53.0	60.2	64.1
17	15	13	11	9	7	5	3	1

Tube Wall

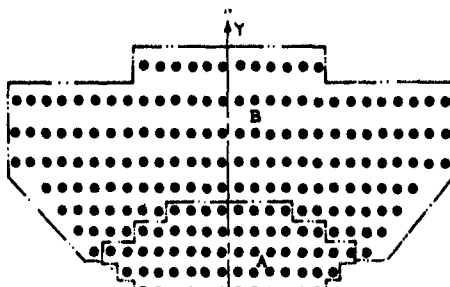
Note: Fluxes in 1000 BTU/HR-FT², Except as Noted

7.46	17.8	35.8	59.3	80.1	88.2	79.6	58.1	33.6	15.9	6.28
18.8	45.9	89.3	139.9	177.4	190.8	177.0	139.0	88.0	44.3	17.4
35.1	84.5	159.0	232.1	287.0	308.1	286.5	231.3	158.5	83.1	33.8
51.4	124.6	221.7	319.1	398.6	429.7	398.5	318.9	221.4	124.9	50.2
60.6	150.9	259.4	377.3	471.9	513.3	475.2	377.7	259.7	151.5	59.5
58.0	151.9	260.9	382.0	482.8	522.7	483.4	382.9	261.8	152.6	58.5
43.2	127.9	225.5	331.1	418.7	453.3	419.3	332.1	227.0	129.0	43.8
24.5	84.1	167.2	246.1	310.3	335.7	310.9	247.2	168.4	85.3	25.4
10.1	37.3	95.6	155.5	197.6	213.5	198.2	156.4	96.6	39.4	10.4
2.18	10.5	31.5	65.4	96.5	107.9	96.8	67.2	33.7	11.1	2.38
0.07	0.94	4.53	12.3	20.0	24.3	20.9	12.8	4.68	1.12	0.17

Aperture
(When Applicable)

RTAF

West Columns East Columns



Single Aim Point at X = 0.0 FT
Y = 12.5 FT
Z = 213.7 FT
206 Heliostats

Configuration : Cavity
Operational Mode : 100% Load
Insolation, W/m² : 1000
Day No. : 170
Time of Day, Hr:Min : 12:00
Q-in, MW : 5.35

Figure III-40b Receiver Flux Levels-Cavity, 100% Load

18	16	14	12	10	8	6	4	2
2.84	3.54	4.28	5.07	5.52	5.74	5.56	5.07	4.67
5.10	6.56	7.69	8.29	8.30	8.46	8.36	7.98	7.48
8.04	10.7	13.3	15.5	16.9	16.5	15.1	13.6	12.2
11.0	15.1	19.5	22.4	26.4	27.9	27.6	25.4	22.9
13.2	18.9	25.2	31.5	36.6	39.7	40.1	38.5	36.2
13.8	20.7	28.7	37.4	45.0	50.0	51.9	51.6	49.5
12.7	19.8	28.7	38.8	48.4	55.3	59.3	60.4	59.5
10.2	16.6	25.0	35.1	45.5	53.7	59.2	61.7	62.1
7.06	12.0	18.9	27.6	37.3	45.5	51.2	54.6	56.1
4.23	7.37	12.1	18.6	26.2	33.5	38.7	41.9	43.6
2.23	3.91	6.52	10.3	15.3	20.3	24.6	27.0	28.3
17	15	13	11	9	7	5	3	1

Tube Wall

NOTE: The Fluxes Shown are
in $\text{MW/m}^2 \times 100$

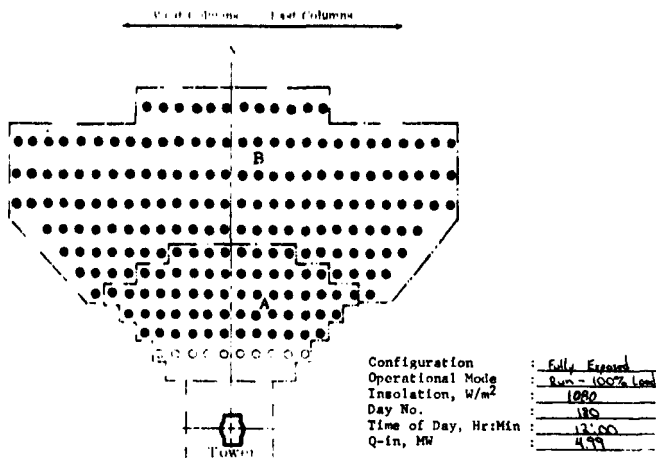
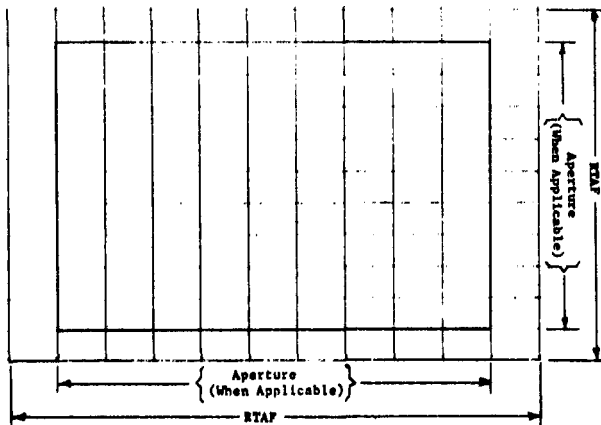


Figure III-41a Receiver Flux Levels-Fully Exposed, 100% Load

18	16	14	12	10	8	6	4	2
8.99	11.2	13.6	16.1	17.5	18.2	17.6	16.1	14.8
16.2	20.8	24.4	26.3	26.8	26.5	25.3	23.7	22.7
25.5	34.1	42.2	49.2	53.5	53.2	48.0	43.1	38.6
35.0	48.0	61.8	74.2	83.7	88.3	87.5	80.5	72.6
41.8	57.9	80.0	101.8	116.2	125.8	137.1	132.1	119.7
43.9	65.6	91.1	118.6	142.6	158.4	163.9	163.6	157.1
46.4	62.9	90.9	123.1	153.5	175.4	187.9	191.6	186.6
32.3	52.5	79.2	111.3	144.3	176.1	187.6	190.5	196.8
22.4	38.0	60.0	87.5	118.4	141.1	141.3	141.2	135.2
13.4	23.4	38.1	51.0	83.0	106.1	122.6	132.5	138.1
7.06	12.1	20.7	32.8	48.5	64.5	73.1	85.5	89.7
17	15	11	11	11	9	7	5	3

Tube Wall

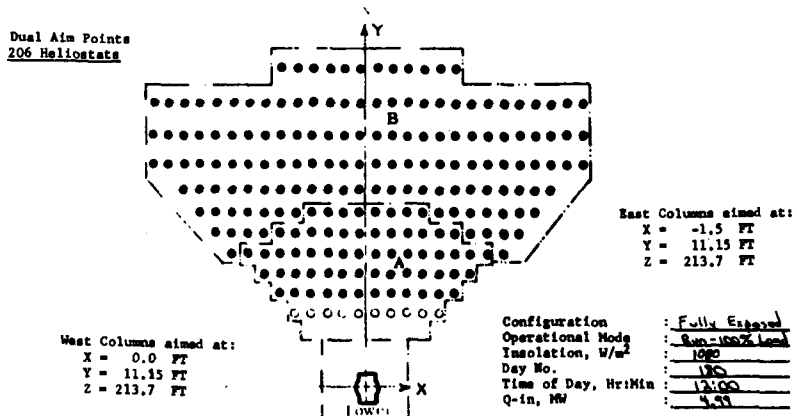
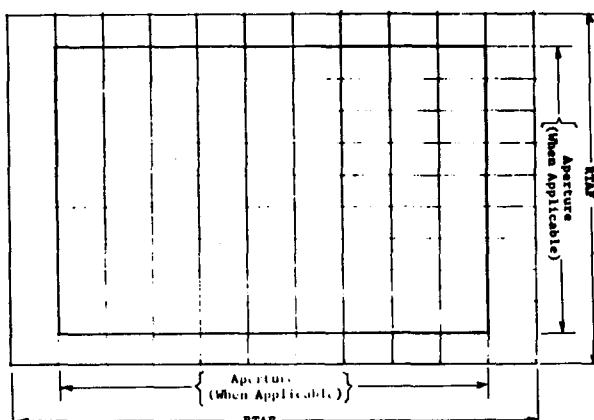
Note: Fluxes in 1000 BTU/Hr-FT², Except as Noted

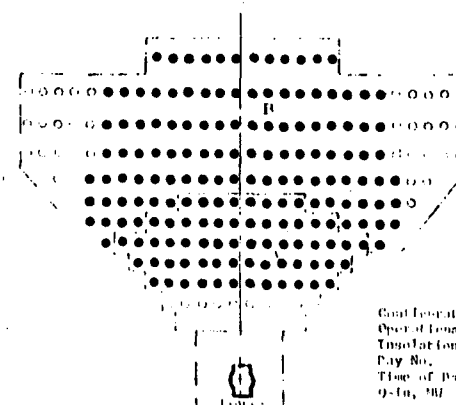
Figure III-41b Receiver Flux Levels-Fully Exposed, 100% Load

5.18	6.06	6.63	7.10	7.74	8.12	8.42	8.43	8.35	8.27	8.21	8.11	7.82	7.35	6.63	5.91	5.21	4.44
7.57	9.21	10.8	11.8	12.1	12.1	12.0	11.9	11.8	11.8	11.5	11.2	11.0	10.7	10.2	9.47	8.18	6.74
9.98	12.9	15.8	18.2	20.0	21.0	21.3	21.4	21.1	20.8	20.4	20.2	19.7	18.6	16.8	14.5	11.9	9.24
11.9	16.3	20.8	24.8	28.3	30.7	32.5	33.4	33.6	33.4	32.7	31.4	29.5	27.2	23.8	19.8	15.6	11.6
12.5	18.1	24.2	30.4	35.8	40.3	43.8	45.9	46.8	46.6	45.4	43.0	39.5	35.2	29.9	23.9	18.0	12.7
11.2	17.4	24.6	32.4	40.0	46.8	52.3	56.1	57.8	57.7	55.8	52.1	46.8	40.2	32.9	25.3	18.0	11.9
8.62	14.4	21.8	30.2	39.1	47.7	54.8	60.0	62.6	62.7	60.2	55.4	48.4	40.1	31.4	23.1	15.5	9.60
5.52	10.1	16.5	24.3	33.2	42.1	50.0	55.9	59.1	59.2	56.5	51.0	43.3	34.6	25.9	17.9	11.3	6.42
2.70	5.81	10.6	16.7	24.0	32.1	39.4	45.0	48.2	48.3	45.8	40.6	33.4	25.6	18.2	11.7	6.72	3.28
0.88	2.49	5.26	9.32	14.6	20.4	26.0	30.7	33.5	33.7	31.5	26.9	21.5	15.7	10.3	5.98	3.02	1.21
0.11	0.70	1.96	4.02	6.74	10.2	13.9	17.1	19.0	19.2	17.4	14.6	11.1	7.51	4.54	2.36	0.97	0.19

4.96	5.33	5.51	5.60	5.43	5.32	5.31	5.24	5.07	4.88	4.49							
7.23	7.90	8.61	8.99	9.07	9.10	8.93	8.68	8.27	7.52	6.57							
13.0	14.3	14.7	14.8	14.6	14.6	14.3	13.8	13.4	12.7	11.6							
20.1	23.5	26.1	27.8	28.6	28.4	28.0	26.8	24.8	22.3	18.9							
27.5	33.3	38.5	42.3	44.6	45.1	44.1	41.6	37.4	32.4	26.7							
33.1	41.9	50.2	56.7	60.9	62.2	60.7	56.3	49.7	41.5	33.0							
34.7	46.2	57.4	66.8	73.1	75.4	73.1	66.9	57.6	46.6	35.4							
31.6	44.2	57.0	68.4	76.4	79.5	76.7	69.1	58.0	45.2	32.7							
24.6	36.5	49.1	60.8	69.2	72.5	69.7	61.7	50.3	37.8	25.9							
16.1	25.6	36.4	46.5	54.0	56.9	54.6	47.5	37.5	26.8	17.3							
8.22	14.5	22.2	29.9	35.5	37.6	35.9	30.7	23.0	15.4	8.96							

Ap 1100
(Other Aperture 100%)

RPM



Coil Excitation
Operational Mode
Excitation, A/m²
Pole No.
Time of Poles, Min
9-10, 90

Partially Exposed

100% Load

1000

100

10

1.00

.10

.10

.01

.01

.01

.01

.01

.01

.01

.01

.01

.01

.01

.01

.01

.01

.01

.01

.01

.01

.01

.01

.01

.01

.01

.01

.01

.01

.01

.01

.01

.01

.01

.01

.01

.01

.01

.01

.01

.01

.01

.01

.01

.01

.01

.01

.01

.01

.01

.01

.01

.01

.01

.01

.01

.01

.01

.01

.01

.01

.01

.01

.01

.01

.01

.01

.01

.01

.01

.01

.01

.01

.01

.01

.01

.01

.01

.01

.01

.01

.01

.01

.01

.01

.01

.01

.01

.01

.01

.01

.01

.01

.01

.01

.01

.01

.01

.01

.01

.01

.01

.01

.01

.01

.01

.01

.01

.01

.01

.01

.01

.01

.01

.01

.01

.01

.01

.01

.01

.01

.01

.01

.01

.01

.01

.01

.01

.01

.01

.01

.01

.01

.01

.01

.01

.01

.01

.01

.01

.01

.01

.01

.01

.01

.01

.01

.01

.01

.01

.01

.01

.01

.01

.01

.01

.01

.01

.01

.01

.01

.01

.01

.01

.01

.01

.01

.01

.01

.01

.01

.01

.01

.01

.01

.01

.01

.01

.01

.01

.01

.01

.01

.01

18	16	14	12	10	8	6	4	2
16.4	19.2	21.0	22.5	24.5	25.7	26.7	26.5	26.2
24.0	29.2	34.2	37.3	38.4	38.2	37.9	37.7	37.4
31.6	41.0	50.3	57.7	63.4	66.4	67.6	67.7	67.0
37.7	51.6	66.0	78.7	89.7	97.4	103.0	105.8	106.7
39.6	57.2	76.8	96.3	113.4	127.7	139.0	145.5	148.4
35.7	55.2	78.1	102.8	126.9	148.5	165.8	177.8	183.2
27.3	45.8	69.1	95.8	123.9	151.2	173.7	190.4	198.5
17.5	32.2	52.5	77.2	105.1	133.6	158.6	177.3	187.3
8.57	18.4	33.5	52.9	76.2	101.7	125.1	142.6	152.7
2.78	7.90	16.7	29.6	46.2	64.8	82.6	97.5	106.3
0.34	2.21	6.20	12.8	21.4	32.5	44.1	54.2	60.3
17	15	13	11	9	7	5	3	1

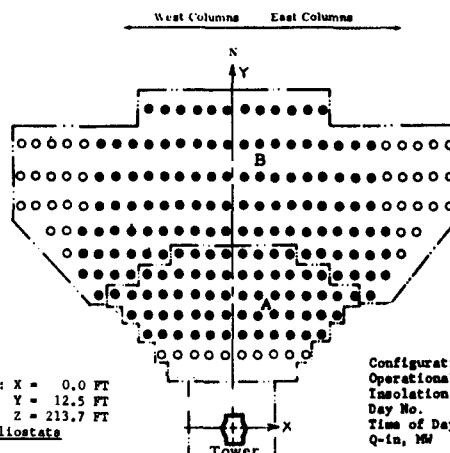
Tube Wall

Note: Fluxes in 1000 BTU/HR-FT², Except as Noted

15.7	16.9	17.5	17.8	17.2	16.9	16.8	16.6	16.1	15.5	14.3
22.9	25.1	27.3	28.5	28.8	28.8	28.3	27.5	26.2	23.8	20.8
41.1	45.3	46.7	47.0	46.4	46.4	45.3	43.8	42.4	40.1	36.7
63.8	74.5	82.8	88.1	90.6	90.1	88.7	84.9	78.7	70.6	60.0
87.2	105.6	122.1	134.2	141.2	142.9	139.8	135.8	118.7	102.6	84.5
104.9	132.9	159.2	179.7	193.2	197.3	192.3	178.5	157.4	131.6	104.5
110.2	146.5	181.9	211.7	231.7	239.0	231.7	212.1	182.7	147.7	112.2
100.1	140.0	180.8	217.0	242.2	252.0	243.2	219.1	184.0	143.3	103.8
78.0	115.6	155.7	192.9	219.3	229.9	221.0	195.6	157.6	119.7	82.1
51.1	81.3	115.5	147.5	171.3	180.4	173.1	150.5	119.0	85.1	54.8
26.1	45.8	70.4	95.0	112.6	119.3	113.8	97.3	73.0	48.8	28.4

Aperture
(When Applicable)

RTAF



Single Aim Point at: X = 0.0 FT
Y = 12.5 FT
Z = 213.7 FT
170 Heliostats

Configuration	Partially Exposed
Operational Mode	Beam - Localized
Insolation, W/FT ²	1080
Day No.	180
Time of Day, Hr:Min	12:00
Q-in, MW	3.76

Figure III-42b Receiver Flux Levels-Partially Exposed, 100% Load

18	16	14	12	10	8	6	4	2
2.49	3.18	3.83	4.20	4.52	4.59	4.42	4.17	3.95
4.56	5.68	6.83	7.50	7.77	7.71	7.45	7.29	7.19
7.67	9.56	11.6	12.8	13.3	13.1	12.3	12.0	11.7
11.5	15.2	19.0	21.7	23.5	24.2	23.9	23.1	22.4
12.7	17.6	22.8	27.4	30.6	32.7	33.6	33.7	33.2
12.3	17.9	24.0	30.1	34.9	38.4	40.7	41.6	41.5
10.4	16.0	22.2	29.0	34.9	39.7	43.3	45.0	45.5
1.70	12.5	18.0	24.5	30.5	35.7	40.0	42.3	43.4
5.09	8.56	12.8	18.0	23.2	27.8	31.8	34.2	35.3
3.01	5.11	7.82	11.2	15.1	18.7	21.6	23.9	24.9
1.65	2.76	4.22	6.07	8.21	10.4	12.4	13.7	14.5
17	15	13	11	9	7	5	3	1

Tube Wall

NOTE: The Fluxes Shown are
in $\text{MW/m}^2 \times 100$

1.77	4.20	8.29	13.5	18.2	20.0	18.2	13.3	7.62	3.69	1.50
4.42	10.8	20.5	32.1	40.7	43.8	40.6	31.9	20.3	10.3	4.03
8.40	19.6	36.7	53.5	66.1	70.9	66.0	53.3	36.5	19.3	7.96
12.2	28.7	51.3	73.7	92.0	99.1	91.9	73.6	51.1	28.9	11.8
14.3	34.9	60.0	87.2	109.7	118.5	109.7	87.2	60.1	35.1	13.9
13.6	35.1	60.3	88.3	111.5	120.7	111.6	88.4	60.5	35.3	13.7
10.2	29.6	52.2	76.5	96.6	104.6	96.8	76.7	52.5	29.9	10.3
5.86	19.4	38.6	56.8	71.5	72.4	71.7	57.0	38.9	19.7	6.05
2.48	8.72	22.0	35.8	45.5	49.1	45.6	36.0	22.2	9.19	2.58
0.52	2.54	7.26	15.0	22.1	24.7	22.1	15.4	7.90	2.72	0.58
0.02	0.23	1.13	2.93	4.61	5.56	4.89	3.04	1.17	0.27	0.04

RTAF

West Columns East Columns

N

B

A

Tower

Configuration : Cooling
 Operational Mode : Run - 75% Load
 Insolation, W/m^2 : 1000
 Day No. : 180
 Time of Day, Hr:Min : 12:00
 Q-in, MW : 3.84

Figure III-43a Receiver Flux Levels-Cavity, 75% Load

18	16	14	12	10	8	6	4	2
789	10.1	12.1	13.3	14.3	14.5	14.0	13.2	12.5
14.5	18.0	21.7	23.8	24.6	24.4	23.6	22.1	22.8
24.3	30.1	36.7	40.7	42.3	41.6	39.2	37.9	37.2
36.3	48.2	60.1	68.8	74.4	76.8	75.9	73.1	70.9
40.3	55.8	72.3	86.8	97.1	103.5	106.5	106.8	105.2
39.0	56.9	76.2	95.4	110.7	121.8	131.2	133.0	131.7
32.9	50.6	70.5	92.1	110.7	125.8	131.3	142.6	144.3
24.4	39.8	57.0	77.7	96.7	113.1	126.9	134.1	137.7
16.1	27.1	40.6	57.0	73.4	88.3	100.7	108.5	112.0
9.55	16.2	24.8	35.5	41.8	57.2	68.4	75.8	79.0
5.22	8.74	13.4	19.2	26.0	32.9	31.2	43.6	45.9
17	15	13	11	9	7	5	3	1

Tube Wall

Note: Fluxes in 1000 BTU/HR-FT², Except as Noted

5.60	13.3	26.3	42.9	57.6	63.5	57.6	42.0	24.2	11.7	4.76
14.0	34.1	65.0	101.8	129.1	138.8	128.7	101.2	64.3	32.7	12.8
26.6	61.0	116.3	169.6	209.5	224.8	209.1	168.9	115.9	61.1	25.2
38.6	91.1	162.5	233.6	291.6	314.2	291.4	233.4	162.1	91.7	37.5
45.2	110.8	196.1	274.9	317.7	375.7	317.8	276.6	190.4	111.2	44.3
43.1	111.1	171.2	277.9	353.6	381.7	353.9	280.4	191.9	112.0	43.4
32.3	93.8	165.6	212.4	306.4	339.7	306.8	243.1	166.3	94.7	32.7
18.6	61.6	122.4	180.0	226.8	245.3	227.2	180.7	123.2	62.5	19.2
7.85	27.1	69.9	113.4	144.2	155.8	144.6	114.1	70.3	29.1	8.17
1.65	8.07	23.0	47.6	70.0	78.4	70.2	48.7	25.0	8.62	1.85
0.06	0.72	3.58	9.28	14.6	17.6	15.5	9.64	3.70	0.85	0.14

Aperture
(When Applicable)

RTAF

When Applicable

RTAF

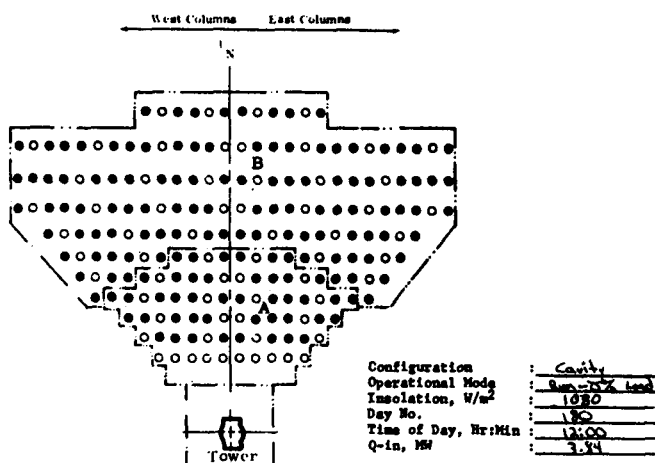


Figure III-43b Receiver Flux Levels-Cavity, 75% Load

18	16	14	12	10	8	6	4	2									
1.51	2.07	2.34	2.63	2.97	3.22	3.33	3.31	3.23	3.16	3.05	2.96	2.81	2.52	2.20	1.89	1.66	1.15
3.02	3.83	4.35	4.81	5.13	5.40	5.51	5.58	5.59	5.57	5.45	5.32	5.12	4.69	4.26	3.88	3.41	2.69
5.37	6.61	7.60	8.42	8.90	9.02	8.98	8.90	8.69	8.52	8.57	8.59	8.43	8.18	7.72	6.84	5.91	4.73
7.99	10.4	12.5	14.4	15.7	16.6	16.9	16.8	16.2	15.9	15.9	15.6	15.2	14.4	13.0	11.4	9.54	7.35
8.92	12.1	15.3	18.3	20.7	22.6	23.8	24.1	23.9	23.8	23.7	23.0	21.7	19.9	17.6	14.8	11.9	8.78
8.57	12.4	16.3	20.2	23.7	26.7	28.7	29.6	29.8	29.7	29.2	28.2	26.1	23.3	20.0	16.3	12.6	8.92
7.06	11.0	15.1	19.6	23.8	27.6	30.4	31.9	32.6	32.5	31.7	30.2	27.4	23.8	19.8	15.7	11.6	7.57
5.31	7.66	12.2	16.5	20.8	24.8	28.1	30.1	31.0	31.0	30.1	28.2	25.0	21.2	17.1	13.0	9.37	5.17
3.43	5.75	8.72	12.1	15.8	19.4	22.4	24.4	25.2	25.3	24.5	22.6	19.7	16.3	12.7	9.43	6.44	3.90
2.02	3.33	5.26	7.65	10.3	13.0	15.3	17.1	17.9	17.9	17.3	15.7	13.3	10.8	8.19	5.84	3.82	2.35
1.08	1.79	2.79	4.10	5.58	7.22	8.68	9.93	10.5	10.5	10.1	8.93	7.56	5.95	4.48	3.20	2.11	1.30

Tube Wall

NOTE: The Fluxes Shown are
in $\text{MW/m}^2 \times 100$

1.07	2.89	5.77	9.49	12.8	14.1	12.7	9.29	5.27	2.49	0.92							
3.04	7.40	14.4	22.4	28.4	30.5	28.3	22.2	14.1	7.07	2.77							
5.30	13.6	25.6	37.3	46.1	49.4	45.9	37.1	25.4	13.4	5.48							
8.43	20.1	35.7	51.3	64.0	69.0	64.0	51.2	35.5	20.1	8.20							
9.57	24.4	41.8	60.7	76.3	82.5	76.3	60.7	41.8	24.4	9.70							
9.47	24.5	42.0	61.5	77.6	84.0	77.7	61.5	42.1	24.6	9.47							
7.07	20.6	36.4	53.2	67.3	72.8	67.3	53.4	36.5	20.8	7.14							
4.07	13.6	26.9	39.5	49.8	53.9	49.9	39.7	27.1	13.8	4.13							
1.69	6.10	15.3	24.9	31.7	34.3	31.8	25.1	15.5	6.39	1.69							
0.34	1.73	5.11	10.6	15.4	17.3	15.5	10.8	5.50	1.77	0.35							
0.00	0.13	0.80	2.06	3.30	3.97	3.46	2.14	0.76	0.16	0.02							

Aperture
(When Applicable)

RTAF

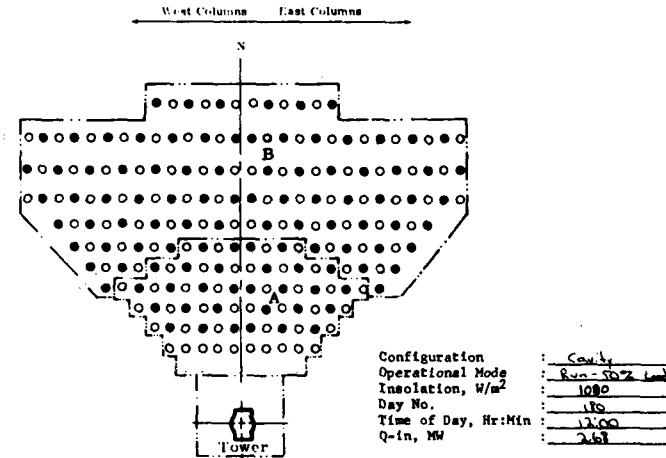


Figure III-44a Receiver Flux Levels-Cavity, 50% Load

18	16	14	12	10	8	6	4	2
4.79	6.55	7.42	8.34	9.42	10.2	10.6	10.5	10.2
9.57	12.1	13.8	15.3	16.3	17.1	17.5	17.7	17.7
17.0	20.9	24.1	26.7	28.2	28.6	28.5	28.2	27.5
25.3	33.1	39.7	45.6	49.9	52.7	53.5	53.1	51.5
28.3	38.4	48.4	57.9	65.7	71.7	75.4	76.5	75.9
27.2	39.3	51.6	64.1	75.2	84.6	91.1	93.8	94.5
22.4	35.0	48.0	62.0	75.5	87.6	96.4	101.3	103.4
16.8	27.4	38.7	52.3	66.0	78.8	89.2	95.3	98.4
10.9	18.2	27.6	38.3	50.1	61.5	71.0	77.4	79.9
6.40	10.6	16.7	24.2	32.6	41.1	48.6	54.2	56.6
3.41	5.66	8.83	13.0	17.7	22.9	27.5	31.5	33.3
1.7	1.5	1.3	1.1	0.9	0.7	0.5	0.3	0.1

Tube Wall

Note: Fluxes in 1000 BTU/HR-FT², Except as Noted

3.41	9.16	18.3	30.1	40.5	44.6	40.4	29.5	16.7	7.89	2.90
9.64	23.5	45.6	71.2	90.1	96.9	99.7	70.4	44.8	22.4	8.77
18.4	43.2	81.2	118.2	146.1	156.6	145.6	117.5	80.5	42.4	17.4
26.7	63.8	113.2	162.8	203.1	218.7	202.8	162.3	112.7	63.8	26.0
31.4	77.2	132.5	192.5	242.0	261.4	242.0	192.4	132.4	77.3	30.8
30.0	77.6	133.2	194.9	246.1	246.3	246.2	195.1	133.5	77.8	30.0
22.4	65.3	115.3	168.8	213.2	230.8	213.5	169.2	115.7	65.8	22.6
12.9	43.0	85.2	125.3	157.9	170.9	158.3	125.9	85.8	43.7	13.1
5.37	19.4	48.6	79.0	100.5	108.6	100.8	79.6	49.2	20.3	5.37
1.07	3.48	16.2	33.5	48.9	54.7	49.2	34.2	17.5	5.61	1.11
0.02	0.41	2.52	6.54	10.5	12.6	11.0	6.78	2.40	0.50	0.05

Aperture (When Applicable)

RZAP

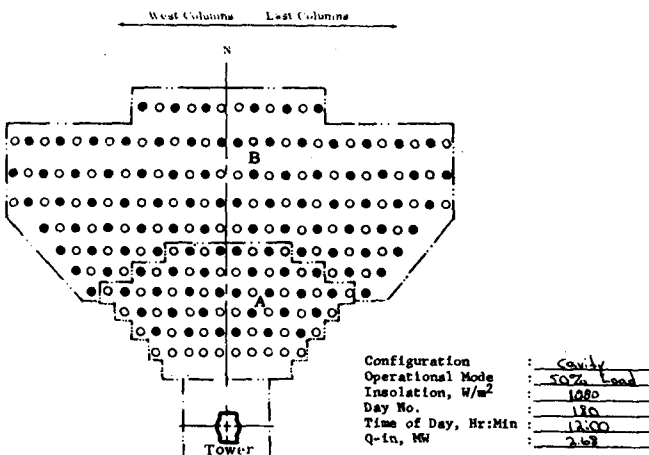


Figure III-44b Receiver Flux Levels-Cavity, 50% Load

18	16	14	12	10	8	6	4	2
1.15	1.25	1.32	1.47	1.63	1.80	1.95	2.12	2.19
1.65	2.02	2.27	2.51	2.74	3.07	3.39	3.67	3.73
2.61	3.16	3.84	4.76	4.69	4.93	5.34	5.44	5.50
3.72	5.15	6.10	7.10	8.04	8.89	9.60	10.0	10.0
4.09	5.90	7.37	8.92	10.5	12.2	13.5	14.1	14.6
4.03	6.01	7.78	9.80	12.1	14.4	16.2	17.2	17.9
3.24	5.32	7.24	9.44	12.1	14.9	17.1	18.7	19.5
2.36	4.17	5.86	7.97	10.7	13.5	16.0	17.7	18.6
1.58	2.76	4.15	5.75	8.12	10.6	12.9	14.5	15.3
0.93	1.58	2.41	3.81	5.32	7.04	9.04	10.2	10.9
0.46	0.85	1.24	2.03	2.86	3.92	5.05	6.03	6.48
17	15	13	11	9	7	5	3	1

Tube Wall

NOTE: The Fluxes Shown are
in $\text{MW/m}^2 \times 100$

0.59	1.47	3.20	5.47	7.41	9.11	7.23	5.30	3.08	1.34	0.48
1.54	3.93	8.03	12.5	15.8	17.0	15.8	12.3	7.77	3.32	1.45
2.85	7.43	14.0	20.4	25.2	27.1	25.2	20.3	13.9	7.24	2.79
4.30	11.0	19.3	27.8	34.8	37.5	34.7	27.8	19.3	10.8	4.18
5.15	13.2	22.6	32.1	41.3	44.6	41.3	32.8	22.5	13.1	5.09
5.01	13.3	22.7	33.2	42.0	45.4	42.0	33.3	22.7	13.2	5.02
3.72	11.2	19.7	28.9	36.5	39.5	36.5	28.9	19.8	11.3	3.76
2.05	7.44	14.7	21.6	27.2	29.4	27.3	21.7	14.8	7.56	2.12
0.79	3.31	8.30	13.8	17.5	18.9	17.5	13.8	8.67	3.48	0.79
0.17	0.84	2.91	6.04	8.74	9.74	9.82	6.16	2.98	0.87	0.17
0.00	0.07	0.35	1.05	1.91	2.32	1.91	1.16	0.34	0.09	0.01

Aperture
(When Applicable)

RTAF

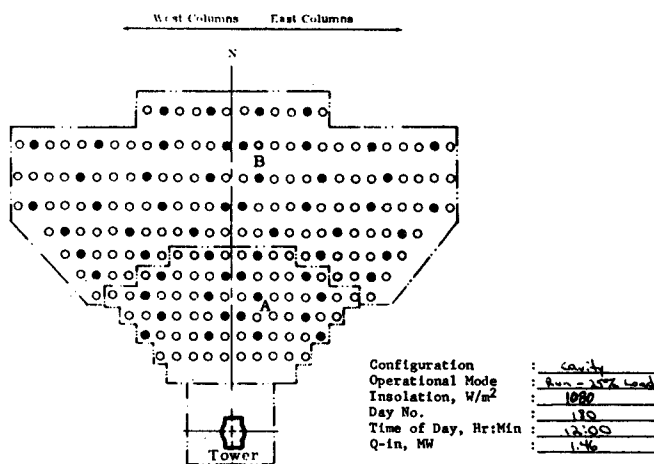


Figure III-45a Receiver Flux Levels-Cavity, 25% Load

18	16	16	12	10	8	6	4	2
3.65	3.97	4.20	4.67	5.18	5.72	6.18	6.72	6.93
5.22	6.42	7.20	7.96	8.48	9.72	10.8	11.6	11.8
8.23	11.0	12.2	13.5	14.9	15.6	16.9	17.3	17.4
11.8	16.3	19.3	22.5	25.5	28.2	30.4	31.7	31.8
13.0	18.7	23.4	28.3	33.4	38.6	42.9	44.7	46.4
12.8	19.0	24.7	31.1	38.3	45.6	51.5	54.6	56.7
10.3	16.9	23.0	30.0	38.5	47.3	54.3	59.2	61.7
7.48	13.2	18.6	25.3	33.8	42.9	50.7	56.0	59.0
5.62	8.76	13.2	18.9	25.7	33.8	41.0	46.1	48.7
2.94	5.01	7.66	12.1	16.9	22.5	28.7	32.2	34.6
1.46	2.70	3.95	6.45	9.06	12.4	16.0	19.1	20.6
17	15	13	11	9	7	5	3	1

Tube Wall

Note: Fluxes in 1000 BTU/HR-FT², Except as Noted

1.96	4.15	10.1	17.3	23.5	25.7	22.9	16.8	9.78	4.23	1.52
4.87	12.5	25.5	39.6	50.0	53.8	50.0	39.1	24.6	12.1	4.58
9.04	23.6	44.4	64.6	80.0	85.9	79.8	64.3	44.0	22.9	8.85
13.6	34.9	61.3	88.3	110.3	118.8	110.2	88.1	61.1	34.4	13.3
16.3	41.7	71.5	104.0	130.9	141.4	130.9	104.1	71.5	41.6	16.1
15.9	42.0	72.0	105.4	133.0	143.9	133.1	105.5	72.1	42.0	15.9
11.8	35.6	62.5	91.6	115.7	125.2	115.8	91.8	62.7	35.7	11.9
6.50	23.6	46.6	68.4	86.3	93.3	86.4	68.7	46.8	24.0	6.71
2.52	10.5	27.0	43.7	55.4	59.9	55.5	43.9	27.5	11.0	2.49
0.53	2.66	9.24	19.1	27.7	30.9	28.0	19.5	9.46	2.75	0.53
0.01	0.21	1.11	3.31	6.46	7.36	6.06	3.66	1.08	0.27	0.02

Aperture
(When Applicable)

RTAF

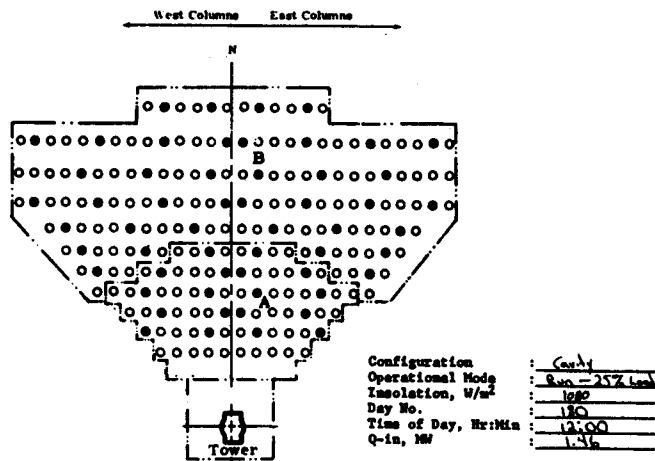


Figure III-45b Receiver Flux Levels-Cavity, 25% Load

10	10	14	12	10	8	6	4
3.7	4.41	4.96	5.13	5.56	5.77	5.79	5.42
5.75	7.05	8.32	8.84	8.91	8.64	8.21	7.94
7.80	9.2	12.3	13.9	15.1	15.5	15.1	14.8
9.45	13.07	16.4	19.3	21.6	22.7	23.5	23.6
9.98	14.4	19.2	23.7	27.3	30.0	32.0	33.1
9.98	13.9	19.7	25.6	30.7	35.1	38.5	40.9
6.94	11.6	17.5	24.0	30.1	36.0	40.6	44.2
4.50	7.22	13.4	19.5	25.8	32.1	37.4	41.5
2.27	4.79	8.58	13.6	19.0	24.6	29.8	33.5
0.82	2.23	4.32	7.64	11.7	15.9	19.9	23.1
0.11	0.70	1.86	3.41	5.66	8.19	10.8	13.1
17	13	11	9	7	5	3	1

Table III-11

NOTE: The Fluxes Shown are
in $\text{W/m}^2 \times 100$

0.93	2.74	6.35	11.1	15.4	17.1	15.3	10.8	5.96	2.43	0.73
2.61	8.17	17.0	27.7	35.8	38.8	35.8	27.6	16.7	7.79	2.31
5.60	15.5	31.3	47.0	58.8	63.3	58.7	46.9	31.3	15.3	5.32
8.40	23.5	44.2	65.1	92.3	99.1	82.3	65.1	44.3	23.6	8.19
9.93	28.9	51.9	77.3	98.4	106.8	98.5	77.4	52.1	29.1	9.71
9.27	29.2	52.2	78.2	100.0	108.7	100.2	78.4	52.4	29.3	9.34
6.31	24.2	44.9	67.4	86.3	93.8	86.4	67.6	45.1	24.4	6.38
2.84	15.1	32.9	49.6	63.4	68.8	63.5	49.8	33.1	15.3	2.96
0.64	5.66	17.9	30.8	39.8	43.1	39.8	30.9	18.0	6.02	0.67
0.01	0.99	4.86	11.9	18.5	21.0	18.5	12.1	5.31	1.08	0.0
0.0	0.01	0.43	1.64	2.98	3.79	3.17	1.75	0.38	0.0	0.0

Aperture
(when Applicable)

RTAF

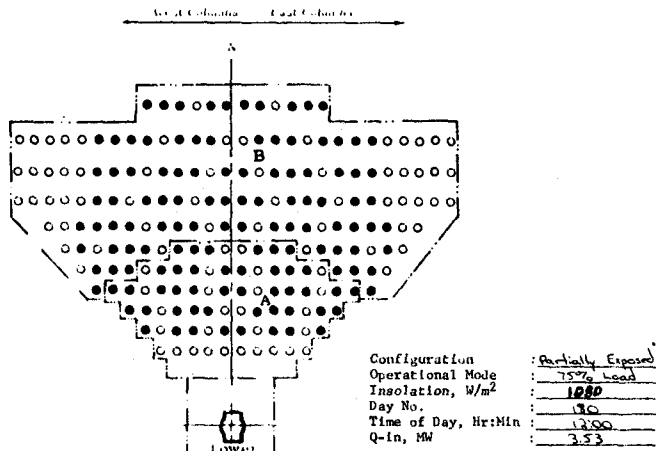


Figure III-46a Receiver Flux Levels-Partially Exposed, 75% Load

18	16	14	12	10	8	6	4	2
11.9	14.0	15.4	16.3	17.6	18.3	17.7	11.2	16.9
18.2	22.4	26.4	28.0	28.2	27.4	26.0	25.2	25.2
24.7	32.5	39.0	44.1	47.9	49.1	47.8	46.9	46.5
30.0	41.1	51.9	61.1	68.3	72.1	74.4	74.9	75.5
31.6	45.8	61.0	75.3	86.7	95.1	101.4	104.8	106.4
28.5	44.2	62.4	81.0	97.4	111.3	122.0	129.6	132.8
22.0	36.8	55.5	76.0	95.6	114.2	123.8	140.0	145.1
14.3	26.1	42.4	61.8	81.7	101.7	118.4	131.5	138.1
7.21	15.2	27.2	43.1	60.0	78.0	94.4	106.9	113.6
2.65	7.08	13.7	24.2	37.2	50.5	63.0	73.4	79.9
0.34	2.21	5.91	10.8	17.9	26.0	34.4	41.6	45.8
17	15	13	11	9	7	5	3	1

Notes: Fluxes in 1000 Btu/Hr- ft^2 , Except as noted.

2.913	8.69	26.1	35.2	48.9	54.2	48.5	34.4	18.6	7.69	2.64
8.227	25.91	53.9	87.9	113.6	122.9	113.6	97.5	53.1	24.7	7.52
17.7	49.1	99.1	148.9	186.4	160.8	186.2	148.6	99.1	48.4	16.9
26.6	74.4	140.2	206.4	266.9	282.3	261.0	206.5	140.3	74.9	26.0
31.5	91.6	164.6	214.9	312.0	338.6	312.4	245.4	165.1	92.2	30.8
28.4	92.4	163.4	247.9	317.1	344.6	317.5	248.5	166.0	92.8	29.6
7.0.0	76.8	147.4	213.7	273.6	297.4	274.0	214.3	143.0	77.5	20.2
9.00	47.8	104.2	157.3	200.9	218.2	201.2	157.8	104.8	48.4	9.37
2.04	18.0	56.8	97.6	126.0	136.7	126.3	98.1	57.2	19.1	2.13
0.03	3.15	15.4	37.6	58.7	66.6	58.8	39.5	16.8	3.44	0.0
0.0	0.04	1.55	5.21	9.45	12.0	10.1	5.56	1.22	0.0	0.0

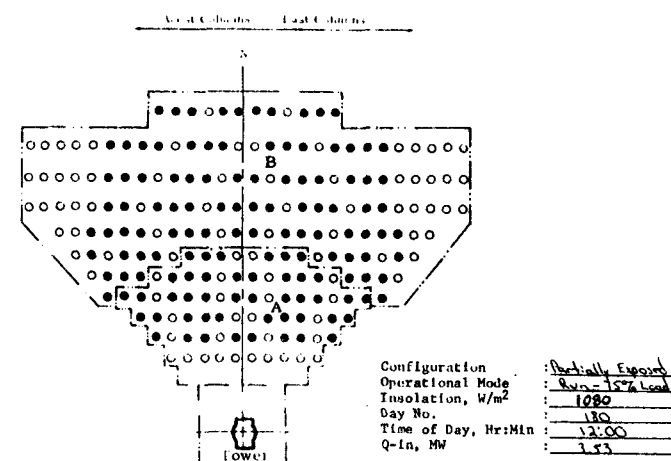


Figure III-46b Receiver Flux Levels-Partially Exposed, 75% Load

12	10	8	6	4	2
2.53	290	319	336	384	405
3.77	458	523	573	593	606
5.18	645	736	905	100	106
6.22	827	105	125	143	156
6.59	9.30	124	154	183	206
5.97	9.05	127	167	201	241
4.62	7.57	113	157	202	246
3.02	5.42	8.67	127	173	218
1.43	3.16	5.66	8.75	126	167
0.49	1.38	2.91	5.06	7.72	108
0.08	0.43	1.16	2.30	3.71	5.60
17	15	13	11	9	7

Tube Wall

NOTE: The Fluxes Shown are
in $\text{MW/m}^2 \times 100$

0.53	1.92	4.37	7.66	10.6	11.8	10.6	7.48	3.92	1.60	0.47
1.90	5.46	11.6	19.0	24.5	26.5	24.4	18.8	11.4	5.16	1.58
3.82	10.4	21.3	32.0	40.2	43.3	40.1	31.9	21.1	10.3	3.54
5.66	15.9	30.1	44.4	56.2	60.8	56.1	44.3	30.0	16.0	5.45
6.73	19.6	35.3	52.7	67.2	72.9	67.2	52.6	35.3	19.6	6.48
6.23	19.7	35.4	53.2	68.2	74.2	68.3	53.3	35.5	19.7	6.20
4.20	16.3	30.5	45.9	58.8	64.0	58.9	46.0	30.6	16.4	4.73
1.89	10.2	22.2	33.7	43.2	46.9	43.2	33.8	22.4	10.3	1.86
0.46	3.82	7.1	20.9	27.1	29.4	27.1	21.0	12.2	4.03	0.43
0.0	0.70	3.29	8.13	12.6	14.3	12.7	8.31	3.63	0.67	0.0
0.0	0.01	0.37	1.22	2.15	2.72	2.29	1.24	0.27	0.0	0.0

RTAF

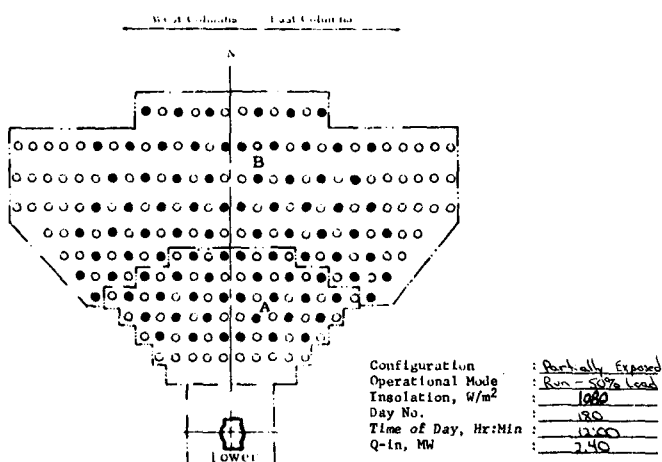


Figure III-47a Receiver Flux Levels-Partially Exposed, 50% Lead

18	16	14	12	10	8	6	4	2
8.03	9.19	10.1	10.7	12.2	12.8	13.5	13.7	13.5
12.0	14.5	16.6	18.2	19.2	19.3	19.3	19.2	18.6
16.4	20.5	24.9	28.7	31.8	33.7	34.6	34.7	33.9
19.7	26.2	33.2	39.7	45.4	49.6	52.5	54.2	54.3
20.9	29.5	39.2	49.0	57.9	65.4	71.2	74.5	75.6
18.9	28.7	40.4	52.8	65.3	76.4	85.4	91.0	93.5
14.6	24.0	36.0	49.6	64.1	78.1	89.7	97.7	101.6
9.58	17.2	27.5	40.3	54.7	69.3	82.0	91.3	95.9
4.55	10.0	17.9	27.7	39.9	53.0	64.8	73.8	78.2
1.56	4.36	9.24	16.1	24.5	34.1	43.2	50.6	54.7
0.26	1.36	3.67	7.30	11.8	17.8	23.6	28.6	31.4
17	15	13	11	9	7	5	3	1

Tube Wall

Note: Fluxes in 1000 BTU/HR-FT², Except as Noted

1.69	6.07	13.8	24.3	33.6	37.4	33.6	23.7	12.4	5.09	1.50
5.69	17.3	36.7	60.1	77.7	84.0	77.4	59.5	36.1	16.3	5.02
12.1	33.1	67.5	101.5	127.3	137.2	127.0	101.0	67.0	32.5	11.2
18.0	50.4	95.3	140.7	178.2	192.8	177.9	140.4	95.0	50.6	17.3
21.3	62.0	111.9	166.9	212.9	231.1	212.9	166.9	111.9	62.1	20.6
19.7	62.3	112.4	168.8	216.3	235.1	216.4	169.0	112.6	62.5	19.7
13.3	51.7	96.7	145.4	186.5	202.8	186.7	145.7	97.0	52.1	13.4
5.98	32.3	70.5	106.9	136.8	148.7	137.1	107.3	70.9	32.8	5.91
1.46	12.1	38.4	66.3	95.8	93.2	86.1	66.6	38.8	12.8	1.36
0.01	2.21	10.4	25.8	40.0	45.3	40.2	26.3	11.5	2.11	0.0
0.0	0.04	1.16	3.87	6.81	8.62	7.27	3.94	0.86	0.0	0.0
RTAF										
Aperture (When Applicable)										

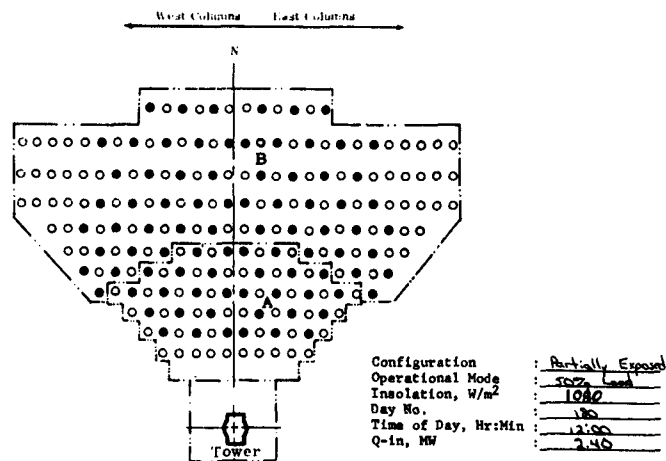


Figure III-47b Receiver Flux Levels-Partially Exposed, 50% Load

18	16	14	12	10	8	6	4	2
0.98	1.02	1.14	1.31	1.30	1.24	1.20	1.11	1.15
1.05	1.22	1.35	1.53	1.48	1.42	1.42	1.34	1.34
1.26	1.45	1.57	1.74	1.70	1.55	1.57	1.49	1.47
1.93	2.18	2.30	2.48	2.37	2.17	2.03	1.95	1.91
2.07	2.27	2.52	2.78	2.70	2.50	2.44	2.18	1.96
2.06	2.38	2.58	2.89	2.83	2.63	2.63	2.30	1.98
1.99	2.21	2.40	2.78	2.77	2.61	2.62	2.33	1.97
1.54	1.76	2.03	2.34	2.46	2.37	2.38	2.19	1.86
1.17	1.42	1.61	1.90	1.92	1.90	1.95	1.76	1.47
0.93	1.04	1.15	1.40	1.44	1.40	1.41	1.30	1.06
0.59	0.65	0.76	0.97	1.02	0.99	1.07	1.05	0.85
17	15	13	11	9	7	5	3	1

Tube Wall

NOTE: The Fluxes Shown are
in $\text{MW/m}^2 \times 100$

0.46	1.11	1.35	2.47	2.91	3.11	2.38	2.42	1.75	1.57	0.66
1.16	2.11	3.13	4.19	4.90	5.13	4.85	4.10	3.03	2.04	1.14
1.77	2.99	4.61	6.04	7.08	7.45	7.02	5.95	4.51	2.99	1.73
2.14	3.85	5.81	7.69	9.12	9.61	9.07	7.61	5.73	3.80	2.10
2.33	4.35	6.50	8.72	10.4	11.1	10.4	8.67	6.45	4.33	2.27
2.27	4.30	6.47	8.76	10.5	11.2	10.5	8.75	6.47	4.31	2.26
1.96	3.79	5.74	7.78	9.38	10.0	9.40	7.81	5.77	3.82	1.98
1.29	2.73	4.52	6.11	7.36	7.85	7.40	6.17	4.58	2.92	1.26
0.77	1.70	3.04	4.25	5.10	5.43	5.13	4.31	3.12	1.78	0.76
0.34	0.87	1.53	2.38	3.04	3.29	3.07	2.46	1.61	0.91	0.36
0.02	0.19	0.57	0.76	1.11	1.25	1.16	0.87	0.47	0.21	0.03
RTAF										
Aperture (When Applicable)										

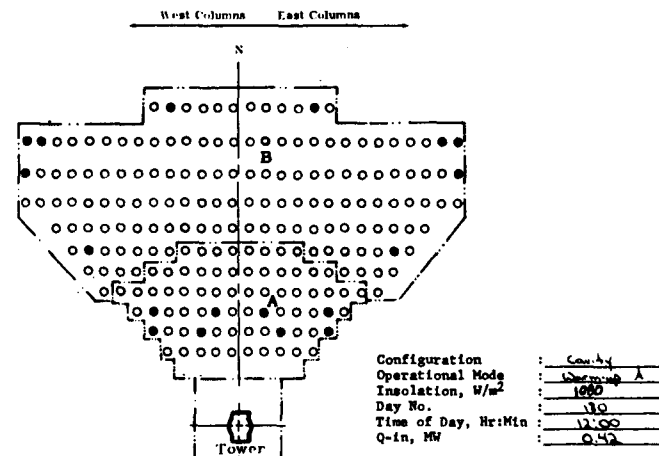


Figure III-48a Receiver Flux Levels-Cavity, Warmup A

18	16	16	12	10	8	6	4	2
2.80	3.23	3.62	4.15	4.13	3.95	3.79	3.53	3.63
3.33	3.86	4.27	4.85	4.71	4.51	4.50	4.26	4.26
3.99	4.60	4.99	5.51	5.38	4.90	4.97	4.72	4.65
6.13	6.92	7.31	7.85	7.52	6.89	6.43	5.88	5.36
6.57	7.52	7.98	8.82	8.56	7.94	7.74	6.93	6.20
6.55	7.55	8.16	9.16	8.96	8.35	8.33	7.30	6.28
6.00	7.00	7.61	8.81	8.79	8.28	8.32	7.40	6.23
4.87	5.91	6.43	7.43	7.81	7.50	7.55	6.94	5.71
3.71	4.50	5.09	6.02	6.10	6.04	6.18	5.57	4.65
2.61	3.29	3.66	4.45	4.57	4.43	4.48	4.13	3.37
1.71	2.06	2.40	3.09	3.24	3.15	3.39	3.32	2.70
17	15	13	11	9	7	5	3	1

Tube Wall

Note: Fluxes in 1000 BTU/HR-FT², Except as Noted

2.08	3.52	5.86	7.82	9.24	9.85	9.14	7.46	5.86	3.39	2.10
3.66	6.69	9.91	13.3	15.5	16.3	15.4	13.0	9.62	6.48	3.63
5.61	9.47	14.6	19.1	22.4	23.6	22.3	18.9	14.3	9.17	5.49
6.77	12.2	18.4	24.4	28.9	30.6	28.8	24.1	18.2	12.1	6.65
7.37	13.8	20.6	27.6	33.1	35.1	33.0	27.5	20.5	13.7	7.21
7.19	13.6	20.5	27.8	33.4	35.6	33.4	27.7	20.5	13.7	7.15
5.90	12.0	18.2	24.7	29.7	31.7	29.8	24.8	18.3	12.1	5.95
4.07	8.96	14.3	19.4	23.3	24.9	23.5	19.6	14.5	9.25	4.00
2.44	5.39	9.65	13.5	16.2	17.2	16.3	13.7	9.90	5.64	2.42
1.08	2.75	4.84	7.54	9.65	10.4	9.73	7.79	5.12	2.56	1.14
0.07	0.59	1.80	2.74	3.52	3.95	3.68	2.76	1.50	0.65	0.10

Aperture
(When Applicable)

RTAF

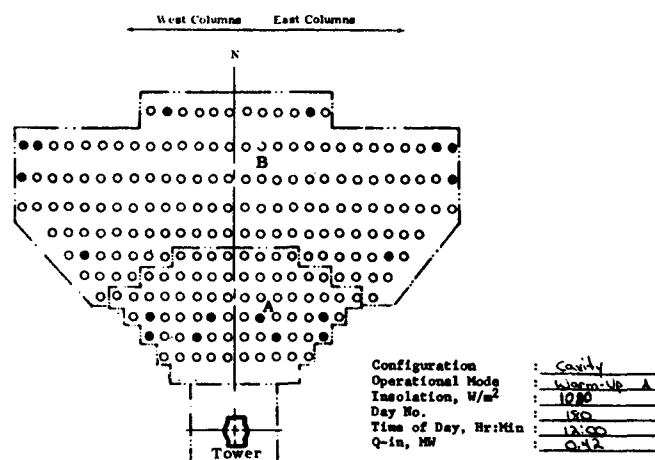


Figure III-48b Receiver Flux Levels-Cavity, Warmup A

18	16	14	12	10	8	6	4	2
0.66	0.77	0.86	0.98	0.98	0.93	0.90	0.94	0.96
0.79	0.92	1.01	1.15	1.11	1.07	1.07	1.01	1.00
0.95	1.09	1.18	1.30	1.27	1.16	1.18	1.12	1.10
1.64	1.83	1.95	2.13	2.06	1.91	1.78	1.61	1.47
1.80	2.04	2.23	2.61	2.61	2.50	2.47	2.28	2.02
1.84	2.10	2.36	2.84	2.89	2.80	2.84	2.61	2.24
1.72	2.00	2.28	2.87	2.98	2.94	3.01	2.83	2.41
1.44	1.73	2.01	2.57	2.80	2.82	2.92	2.83	2.43
1.12	1.35	1.64	2.18	2.34	2.43	2.56	2.48	2.12
0.81	1.00	1.22	1.68	1.84	1.91	2.02	2.01	1.72
0.53	0.64	0.82	1.19	1.34	1.40	1.55	1.60	1.39
17	15	13	11	9	7	5	3	1

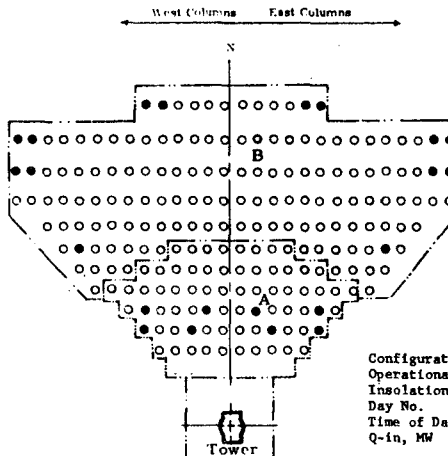
Tube Wall

NOTE: The Fluxes Shown are
in $\text{MW/m}^2 \times 100$

0.56	0.98	1.72	2.33	2.74	2.90	2.70	2.27	1.61	0.92	0.55
1.03	2.01	2.97	3.93	4.57	4.78	4.52	3.83	2.87	1.92	1.00
1.71	2.89	4.35	5.66	6.61	6.94	6.54	5.56	4.24	2.78	1.63
2.14	3.71	5.51	7.23	8.52	8.98	8.46	7.13	5.41	3.64	2.07
2.36	4.70	6.18	8.21	9.74	10.3	9.70	8.14	6.12	4.15	2.29
2.32	4.18	6.19	8.27	9.87	10.5	9.85	8.24	6.16	4.16	2.29
1.95	3.71	5.51	7.38	8.93	9.38	8.84	7.40	5.53	3.72	1.96
1.40	2.82	4.37	5.84	6.98	7.42	7.00	5.88	4.41	2.88	1.38
0.81	1.78	2.99	4.10	4.88	5.18	4.90	4.14	3.05	1.84	0.81
0.29	0.89	1.60	2.37	2.96	3.19	2.98	2.43	1.67	0.85	0.32
0.02	0.15	0.54	0.92	1.22	1.35	1.26	0.93	0.50	0.18	0.03

Aperture (When Applicable)

RTAF



Configuration : Cavity
Operational Mode : Warmup B
Insolation, W/m^2 : 810
Day No. : 190
Time of Day, Hr:Min : 12:00
Q-in, MW : 0.40

Figure III-49a Receiver Flux Levels-Cavity, Warmup B

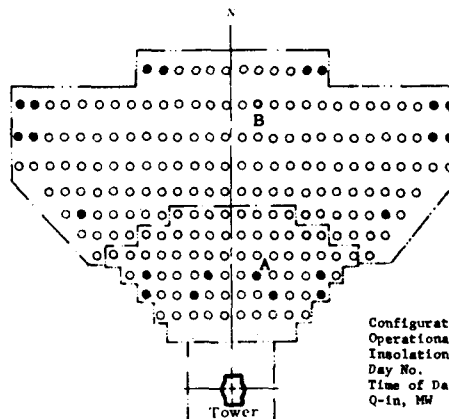
18	16	14	12	10	8	6	4	2
2.10	3.43	2.72	3.11	3.10	2.96	2.85	2.65	2.73
2.50	2.90	3.20	3.64	3.53	3.39	3.38	3.19	3.19
3.00	3.45	3.71	4.14	4.03	3.68	3.73	3.54	3.48
5.18	5.80	6.17	6.77	6.54	6.05	5.64	5.11	4.46
5.70	6.46	7.07	8.29	8.28	7.92	7.92	7.24	6.49
5.82	6.66	7.48	9.02	9.16	8.87	8.59	8.27	7.11
5.47	6.33	7.23	9.09	9.15	9.32	9.56	8.48	7.64
4.51	5.48	6.36	8.14	8.87	8.41	9.26	8.97	7.70
3.56	4.29	5.20	6.90	7.42	7.70	8.12	7.88	6.72
2.58	3.18	3.86	5.32	5.83	6.04	6.39	6.36	5.44
1.69	2.04	2.61	3.79	4.24	4.45	4.91	5.06	4.41
17	15	13	11	9	7	5	3	1

Tube Wall

Note: Fluxes in 1000 BTU/HR-FT², Except as Noted

1.77	3.11	5.46	7.39	8.68	9.20	8.57	7.21	5.09	2.92	1.75
3.27	6.39	9.42	12.5	14.5	15.1	14.2	12.1	9.09	6.09	3.16
5.43	9.16	13.8	18.0	21.0	22.0	20.7	17.6	13.4	8.82	5.17
6.79	11.8	17.5	22.9	27.0	28.5	26.8	22.6	17.2	11.5	6.58
7.47	13.3	19.6	26.0	30.9	32.7	30.8	25.8	19.4	13.2	7.38
7.35	13.2	19.6	26.2	31.3	33.2	31.2	26.1	19.5	13.2	7.27
6.19	11.7	17.5	23.4	28.0	29.7	28.0	23.5	17.5	11.8	6.20
4.44	8.93	13.9	18.5	22.1	23.5	22.2	18.6	14.0	9.13	4.37
2.56	5.63	9.48	13.0	15.5	16.4	15.5	13.1	9.68	5.83	2.56
0.94	2.81	5.07	7.51	9.39	10.1	9.46	7.71	5.30	2.70	1.02
0.05	0.48	1.71	2.91	3.85	4.27	3.98	2.95	1.57	0.56	0.11

West Columns East Columns



Configuration
Operational Mode
Insolation, W/m²
Day No.
Time of Day, Hr:Min
Q-in, MW

Figure III-49b Receiver Flux Levels-Cavity, Warmup B

18	16	14	12	10	8	6	4	2
0.95	0.94	1.15	1.31	1.32	1.28	1.20	1.16	1.15
1.02	1.13	1.35	1.52	1.50	1.46	1.42	1.38	1.34
1.37	1.39	1.60	1.74	1.71	1.57	1.55	1.51	1.45
1.94	2.11	2.32	2.48	2.41	2.23	2.03	1.99	1.71
2.10	2.33	2.57	2.85	2.81	2.65	2.51	2.36	2.07
2.12	2.38	2.61	3.00	2.98	2.83	2.73	2.46	2.16
1.94	2.24	2.50	2.92	2.97	2.85	2.79	2.50	2.15
1.60	1.79	2.13	2.53	2.67	2.62	2.57	2.32	2.04
1.21	1.46	1.71	2.06	2.15	2.14	1.87	1.61	1.55
0.95	1.04	1.22	1.53	1.61	1.61	1.59	1.45	1.23
0.51	0.65	0.80	1.06	1.15	1.21	1.17	1.01	1.00
17	15	13	11	9	7	5	3	1

Tube Wall

NOTE: The Fluxes Shown are
in $\text{MW/m}^2 \times 100$

0.64	1.14	1.87	2.53	3.01	3.19	2.99	2.47	1.78	1.06	0.62
1.15	2.15	3.21	4.32	5.05	5.29	5.00	4.23	3.11	2.08	1.11
1.81	3.07	4.75	6.22	7.31	7.69	7.25	6.14	4.66	2.98	1.73
2.22	3.98	6.00	7.93	9.42	9.97	9.38	7.87	5.92	3.93	2.16
2.42	4.50	6.72	9.01	10.8	11.4	10.8	8.97	6.68	4.47	2.37
2.37	4.45	6.70	9.06	10.9	11.6	10.9	9.05	6.70	4.46	2.35
1.95	3.92	5.94	8.06	9.71	10.3	9.72	8.08	5.97	3.95	1.97
1.36	2.93	4.68	6.33	7.62	8.12	7.64	6.37	4.72	3.01	1.37
0.80	1.75	3.15	4.39	5.27	5.61	5.30	4.44	3.21	1.83	0.79
0.27	0.85	1.59	2.46	3.15	3.40	3.17	2.53	1.67	0.82	0.29
0.01	0.13	0.48	0.85	1.15	1.29	1.19	0.87	0.44	0.15	0.03

Aperture
(When Applicable)

RTAP

RTAP Aperture (When Applicable)

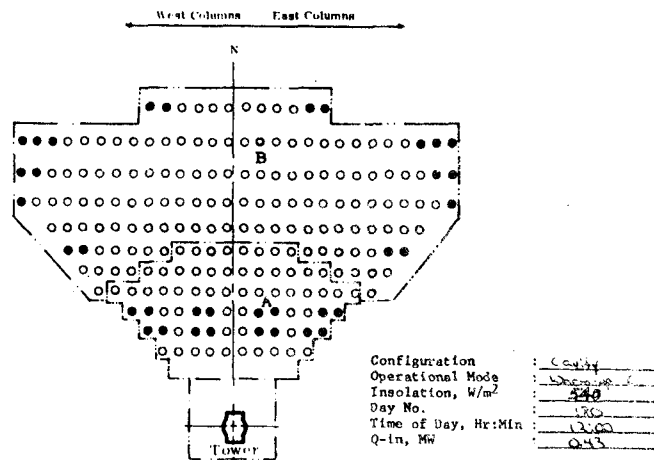


Figure III-50a. Receiver Flux Levels-Cavity, Warmup C

18	16	14	12	10	8	6	4	2
270	298	365	417	421	405	3.81	367	3.66
3.22	3.57	4.28	4.81	4.76	4.62	4.19	4.37	4.23
4.04	4.42	5.06	5.51	5.41	4.98	4.92	4.79	4.58
6.15	6.70	7.35	7.87	7.64	7.06	6.43	5.98	5.42
6.67	7.39	8.16	9.05	8.92	8.41	7.95	7.30	6.56
6.71	7.55	8.37	9.51	9.46	8.97	8.67	7.79	6.83
6.14	7.10	7.92	9.26	9.41	9.02	8.84	7.94	6.82
5.08	5.99	6.76	8.03	8.45	8.29	8.16	7.37	6.45
3.84	4.64	5.41	6.53	6.82	6.83	6.80	5.94	5.09
270	3.30	3.87	4.86	5.12	5.09	5.04	4.61	3.91
1.63	2.06	2.54	3.37	3.64	3.65	3.82	3.71	3.21
17	15	13	11	9	7	5	3	1

Tube Wall

Note: Fluxes in 1000 BTU/HR-FT², Except as Noted

203	360	592	803	9.55	101	9.48	784	565	338	1.96
3.65	6.83	10.2	13.7	16.0	16.8	15.9	13.4	9.87	6.59	3.53
5.73	9.74	15.1	19.7	23.2	24.4	23.0	19.5	14.8	9.46	5.50
7.04	12.6	19.0	25.2	21.9	31.6	29.7	24.9	18.8	12.5	6.84
7.69	14.3	21.3	28.6	34.2	36.3	34.1	28.4	21.2	14.2	7.52
7.50	14.1	21.3	28.7	34.6	36.8	34.5	28.7	21.2	14.1	7.45
6.18	12.4	18.8	25.5	30.8	32.8	30.8	25.6	18.9	12.5	6.23
4.33	9.28	14.8	20.1	24.2	25.7	24.2	20.2	15.0	9.53	4.35
2.54	5.56	9.98	13.9	16.7	17.8	16.8	14.1	10.2	5.81	2.50
0.87	2.69	5.05	7.79	9.99	10.8	10.0	8.04	5.29	2.60	0.92
0.03	0.41	1.51	2.69	3.64	4.07	3.78	2.75	1.41	0.49	0.08
Aperture (When Applicable)										
RTAF										

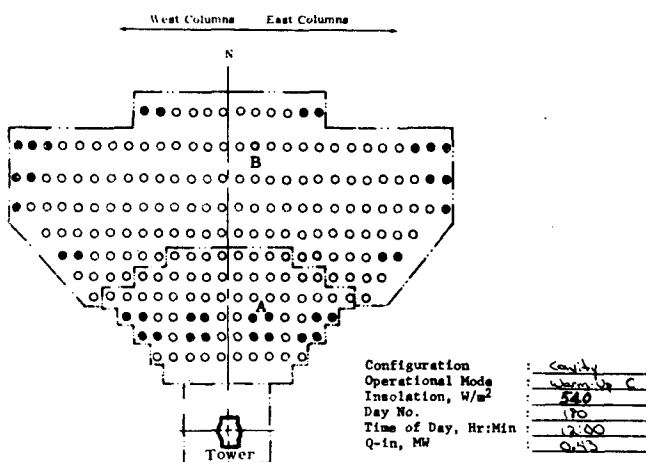


Figure III-50b Receiver Flux Levels-Cavity, Warmup C

10	10	14	12	10	0	0	2
0.13	0.22	0.44	0.63	0.80	0.92	1.05	1.14
0.11	0.22	0.47	0.68	0.91	1.07	1.25	1.33
0.12	0.27	0.53	0.81	1.09	1.30	1.52	1.61
0.15	0.30	0.63	0.91	1.18	1.43	1.66	1.82
0.15	0.36	0.67	0.98	1.26	1.51	1.81	1.99
0.19	0.40	0.69	1.02	1.31	1.55	1.89	2.09
0.21	0.42	0.65	1.02	1.31	1.57	1.95	2.11
0.21	0.42	0.62	0.97	1.23	1.49	1.70	1.98
0.17	0.37	0.56	0.76	0.96	1.27	1.47	1.66
0.13	0.28	0.45	0.62	0.78	0.94	1.10	1.26
0.06	0.16	0.33	0.46	0.58	0.69	0.82	0.91
17	5	13	11	9	7	5	3

NOTE: The Fluxes Shown are
in $\text{MW/m}^2 \times 100$

0.07	0.33	0.84	1.34	1.63	1.73	1.61	1.32	0.77	0.32	0.12
0.25	0.81	1.51	2.09	2.53	2.68	2.50	2.05	1.47	0.75	0.27
0.53	1.28	2.10	2.91	3.53	3.76	3.50	2.86	2.06	1.22	0.50
0.75	1.62	2.61	3.63	4.44	4.74	4.41	3.59	2.57	1.60	0.72
0.95	1.83	2.91	4.08	5.00	5.35	4.98	4.05	2.88	1.91	0.81
0.80	1.82	2.90	4.09	5.03	5.39	5.02	4.08	2.89	1.91	0.79
0.65	1.61	2.59	3.66	4.51	4.84	4.51	3.46	2.60	1.61	0.65
0.49	1.17	2.06	2.91	3.59	3.86	3.61	2.93	2.08	1.21	0.46
0.19	0.69	1.42	2.06	2.54	2.74	2.56	2.08	1.45	0.70	0.18
0.0	0.28	0.70	1.23	1.60	1.72	1.61	1.26	0.74	0.22	0.0
0.0	0.001	0.17	0.40	0.64	0.77	0.67	0.39	0.11	0.0	0.0

Aperture
(When Applicable)

RTAF

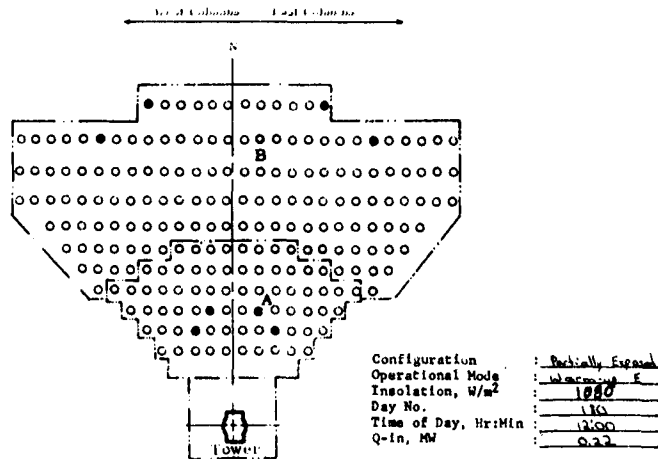


Figure III-51a Receiver Flux Levels-Partially Exposed, Warmup E

18	16	14	12	10	8	6	4	2
0.40	0.71	1.39	1.79	2.54	2.91	3.34	3.62	3.63
0.36	0.69	1.48	2.19	2.87	3.40	3.97	4.23	4.26
0.39	0.87	1.68	2.58	3.44	4.14	4.83	5.10	5.05
0.48	0.94	1.98	2.88	3.74	4.53	5.28	5.79	5.99
0.48	1.16	2.12	3.09	3.99	4.80	5.73	6.31	6.61
0.59	1.26	2.18	3.25	4.16	4.92	5.98	6.63	6.98
0.68	1.33	2.05	3.22	4.16	4.99	5.86	6.70	6.97
0.66	1.32	1.95	2.77	3.89	4.72	5.40	6.27	6.59
0.54	1.18	1.77	2.41	3.05	4.03	4.65	5.27	5.66
0.40	0.89	1.43	1.98	2.48	2.99	3.50	3.98	4.14
0.19	0.52	1.03	1.45	1.84	2.19	2.59	2.90	3.05
17	15	13	11	9	7	5	3	1

Tube Wall

Note: Fluxes in 1000 BTU/HR-Ft²

0.23	1.05	2.66	4.25	5.18	5.48	5.12	4.18	2.45	1.03	0.38
0.80	2.56	4.78	6.63	8.01	8.51	7.93	6.51	4.65	2.38	0.85
1.68	4.04	6.65	9.21	11.2	11.9	11.1	9.07	6.52	3.86	1.59
2.39	5.15	8.26	11.5	14.1	15.0	14.0	11.4	8.14	5.06	2.27
2.69	5.79	9.22	12.9	15.9	17.0	15.8	12.8	9.13	5.74	2.58
2.54	5.76	9.21	13.0	15.9	17.1	15.9	12.9	9.18	5.74	2.52
2.07	5.10	8.22	11.6	14.3	15.3	14.3	11.6	8.23	5.11	2.06
1.56	3.70	6.54	9.23	11.4	12.2	11.4	9.29	6.59	3.83	1.44
0.61	2.20	4.52	6.54	8.07	8.67	8.11	6.60	4.60	2.21	0.56
0.0	0.89	2.21	3.91	5.07	5.44	5.09	3.99	2.36	0.68	0.0
0.0	0.02	0.52	1.27	2.03	2.43	2.13	1.23	0.35	0.0	0.0

RTAF

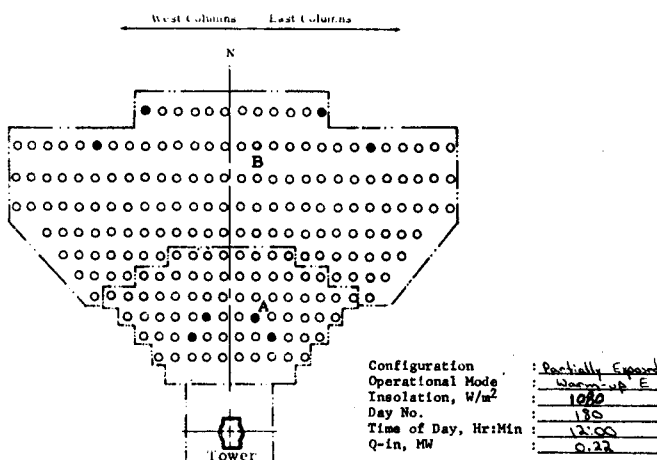


Figure III-51b Receiver Flux Levels-Partially Exposed, Warmup E

19	18	17	16	15	14	13	12	11	10	9	8	7	6	5	4	3	2	1
0.10	0.27	0.51	0.76	1.01	1.20	1.46	1.55	1.55	1.48	1.35	1.15	0.86	0.65	0.45	0.28	0.10	0.0	
0.08	0.25	0.52	0.80	1.10	1.36	1.66	1.75	1.73	1.66	1.53	1.28	0.97	0.70	0.48	0.28	0.08	0.0	
0.09	0.26	0.55	0.92	1.32	1.68	2.00	2.11	2.10	1.98	1.90	1.55	1.23	0.99	0.58	0.34	0.10	0.01	
0.11	0.24	0.67	1.08	1.46	1.83	2.19	2.41	2.46	2.36	2.12	1.71	1.35	1.02	0.73	0.42	0.12	0.07	
0.11	0.30	0.75	1.17	1.57	1.95	2.42	2.66	2.74	2.64	2.37	1.95	1.45	1.13	0.83	0.51	0.19	0.11	
0.14	0.39	0.77	1.25	1.67	2.06	2.59	2.84	2.93	2.82	2.54	2.14	1.57	1.23	0.92	0.54	0.30	0.13	
0.17	0.44	0.75	1.23	1.70	2.15	2.60	2.93	3.00	2.89	2.61	2.17	1.68	1.28	0.91	0.58	0.36	0.16	
0.16	0.44	0.74	1.09	1.60	2.10	2.46	2.82	2.90	2.79	2.51	2.07	1.68	1.21	0.85	0.60	0.37	0.16	
0.13	0.31	0.67	0.98	1.30	1.81	2.18	2.45	2.55	2.45	2.20	1.85	1.47	1.02	0.71	0.55	0.33	0.13	
0.09	0.27	0.55	0.91	1.08	1.41	1.69	1.99	1.95	1.89	1.73	1.46	1.16	0.86	0.66	0.46	0.24	0.10	
0.04	0.15	0.39	0.60	0.81	1.04	1.28	1.43	1.48	1.44	1.31	1.12	0.84	0.65	0.49	0.33	0.13	0.05	

NOTE: The Fluxes Shown are
in $\text{MW/m}^2 \times 100$

19	18	17	16	15	14	13	12	11	10	9	8	7	6	5	4	3	2	1
0.08	0.45	1.08	1.70	2.05	2.15	1.98	1.58	0.90	0.28	0.02								
0.30	1.04	1.90	2.62	3.15	3.32	3.06	2.47	1.73	0.85	0.17								
0.66	1.58	2.61	3.61	4.37	4.63	4.28	3.45	2.44	1.42	0.48								
0.94	2.01	3.22	4.49	5.47	5.82	5.38	4.34	3.06	1.88	0.77								
1.03	2.24	3.57	5.01	6.14	6.56	6.08	4.91	3.46	2.14	0.91								
0.97	2.22	3.55	5.01	6.17	6.61	6.14	4.96	3.50	2.16	0.91								
0.77	1.95	3.16	4.48	5.53	5.94	5.54	4.48	3.16	1.95	0.75								
0.54	1.42	2.50	3.56	4.42	4.76	4.44	3.60	2.55	1.49	0.56								
0.19	0.79	1.73	2.52	3.13	3.38	3.17	2.58	1.30	0.87	0.19								
0.0	0.24	0.83	1.52	1.97	2.13	2.01	1.59	0.95	0.27	0.0								
0.0	0.0	0.12	0.43	0.82	1.01	0.88	0.52	0.14	0.0	0.0								

Aperture
(When Applicable)

RTAF

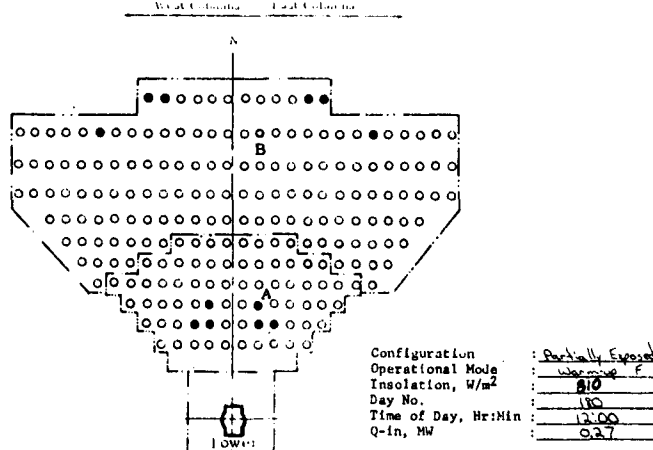


Figure III-52a Receiver Flux Levels-Partially Exposed, Warmup F

18	16	14	12	10	8	6	4	2
0.30	0.76	1.63	2.41	3.19	3.81	4.63	4.90	4.70
0.27	0.78	1.66	2.53	3.48	4.33	5.27	5.56	5.30
0.29	0.81	1.76	2.90	4.20	5.31	6.35	6.68	6.67
0.36	0.77	2.11	3.43	4.61	5.79	6.94	7.63	7.81
0.36	0.96	2.39	3.71	4.99	6.17	7.66	8.43	8.68
0.45	1.23	2.43	3.95	5.29	6.54	8.22	9.01	9.29
0.53	1.39	2.37	3.90	5.39	6.83	9.25	9.29	9.51
0.52	1.41	2.33	3.45	5.06	6.64	7.80	8.93	9.21
0.42	1.23	2.14	3.10	4.14	5.72	6.91	7.76	8.09
0.30	0.76	1.75	2.57	3.43	4.46	5.36	6.01	6.17
0.14	0.48	1.23	1.91	2.58	3.29	4.07	4.54	4.70
17	15	13	11	9	7	5	3	1

Tube Wall

Notes: Fluxes in 1000 BTU/HR-FT², Except as Noted

0.25	14.2	3.43	5.40	6.51	6.82	6.27	5.01	2.84	0.99	0.05
0.95	3.29	6.02	9.30	9.99	10.5	9.70	7.87	5.49	2.70	0.55
2.10	5.02	8.27	11.4	13.9	14.7	13.6	10.9	7.73	4.51	1.51
2.97	6.38	10.2	14.2	17.4	18.4	17.1	13.8	9.71	5.96	2.43
3.28	7.10	11.3	15.9	19.5	20.8	19.3	15.6	11.0	6.79	2.90
3.07	7.02	11.3	15.9	19.6	21.0	19.5	15.7	11.1	6.86	2.89
2.43	6.19	10.0	14.2	17.5	18.8	17.6	14.2	10.0	6.18	2.38
6.71	4.50	7.94	11.3	14.0	15.1	14.1	11.4	8.07	4.74	1.78
0.60	2.50	5.49	7.98	9.92	10.7	10.1	8.17	5.69	2.77	0.62
0.0	0.76	2.64	4.73	6.24	6.76	6.36	5.03	3.02	0.84	0.0
0.0	0.0	0.37	1.36	2.60	3.19	2.79	1.64	0.45	0.0	0.0

Aperture
(When Applicable)

RTAP

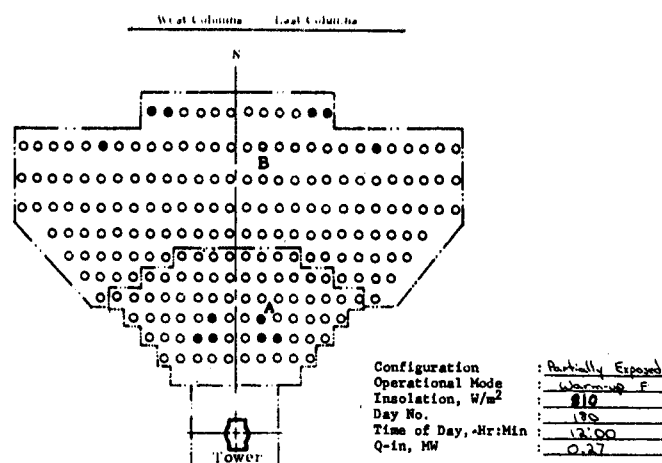
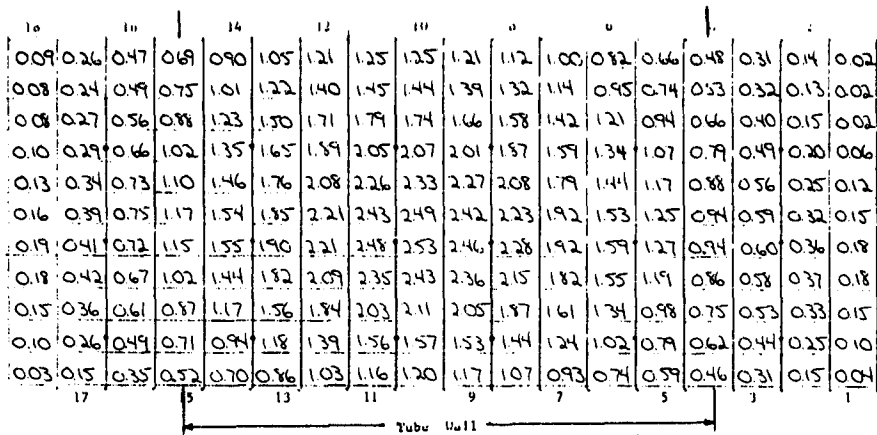


Figure III-52b Receiver Flux Levels-Partially Exposed, Warmup F



NOTE: The Fluxes Shown are
in $\text{MW/m}^2 \times 100$

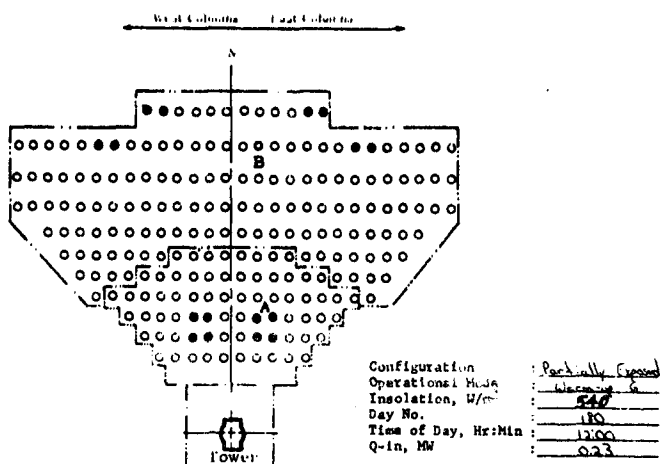
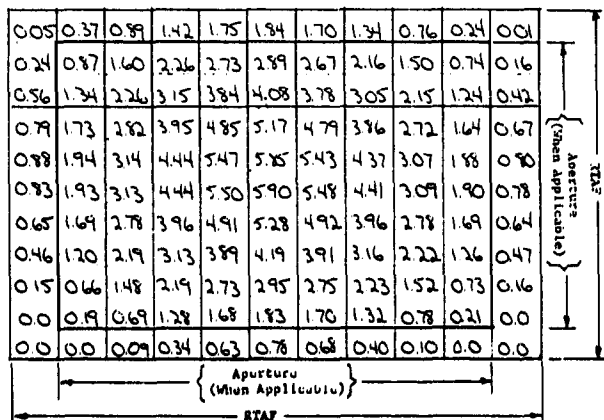


Figure III-53a Receiver Flux Levels-Partially Exposed, Warmup G

18	16	14	12	10	8	6	4	2
0.28	0.42	1.49	2.18	3.34	3.33	3.93	3.95	3.84
0.26	0.78	1.55	2.37	3.21	3.36	4.43	4.61	4.56
0.24	0.85	1.77	2.80	3.39	4.76	5.43	5.67	5.52
0.32	0.93	2.08	3.24	4.29	5.23	5.99	6.50	6.57
0.41	1.07	2.32	3.50	4.63	5.58	6.60	7.17	7.40
0.51	1.22	2.37	3.69	4.87	5.87	7.00	7.70	7.90
0.59	1.31	2.28	3.64	4.90	6.02	7.00	7.88	8.04
0.58	1.32	2.13	3.22	4.37	5.77	6.61	7.45	7.72
0.47	1.15	1.93	2.76	3.71	4.95	5.92	6.43	6.68
0.33	0.83	1.56	2.27	2.97	3.74	4.42	4.94	4.99
0.10	0.48	1.10	1.66	2.20	2.74	3.26	3.67	3.79
17	15	13	11	9	7	5	3	1
Tube Wall								

Note: Fluxes in 1000 BTU/HR-FT², Except as Noted

0.17	1.16	2.81	4.49	5.55	5.84	5.37	4.25	2.40	0.77	0.03
0.77	2.77	5.08	7.15	8.65	9.15	8.46	6.84	4.75	2.35	0.51
1.76	4.25	7.17	9.99	12.2	12.9	12.0	9.66	6.82	3.92	1.33
2.51	5.47	8.93	12.5	15.4	16.4	15.2	12.2	8.61	5.21	2.11
2.79	6.15	9.96	14.1	17.3	18.6	17.2	13.9	9.73	5.98	2.52
2.62	6.11	9.92	14.1	17.4	18.7	17.4	14.0	9.81	6.03	2.47
2.06	5.35	8.80	12.5	15.6	16.8	15.6	12.6	8.81	5.37	2.03
1.45	3.82	6.94	9.91	12.3	13.3	12.4	10.0	7.03	3.99	1.50
0.99	2.09	4.70	6.94	8.65	9.34	8.73	7.07	4.83	2.31	0.51
0.0	0.61	2.20	4.05	5.34	5.80	5.40	4.19	2.46	0.68	0.0
0.0	0.0	2.78	1.06	2.00	2.47	2.17	1.26	0.33	0.0	0.0
RTAF										
Aperture (When Applicable)										

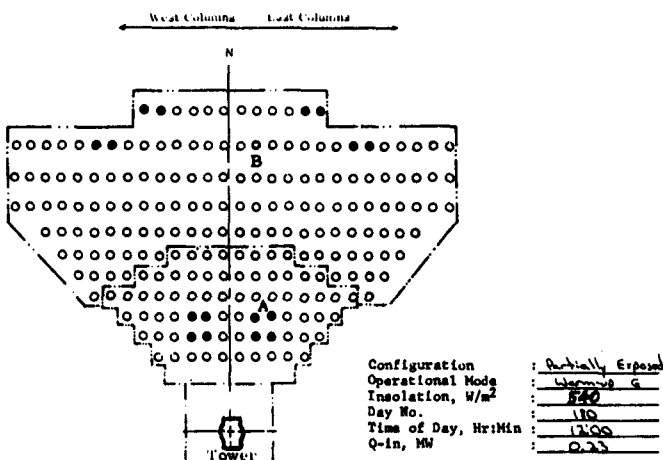


Figure III-53b. Receiver Flux Levels-Partially Exposed, Warmup G

c. Flux Gage Correlations - A series of TRASYS models of the RTAF and the cavity aperture were constructed to obtain information needed to develop a transfer function that would allow determination of radiant fluxes passing through the aperture from those measured at the RTAF plane. To account for various cloud shadowing situations, the heliostat field was divided into ten regions as shown on Figure III-55, and a partial transfer function determined for each. The summation of the individual contributions from these regions is accomplished as follows:

Q_{RTAF}/Q_{Aperture} Transfer Functions for Noon, Day 180

All functions are of the form: $Q_{\text{Aperture}} = \phi(\psi_i, q_i) \times Q_{\text{RTAF}}$

Where: $\phi = \frac{\sum_{i=1}^n \psi_i}{\sum_{i=1}^n q_i}$ = transfer function

$$\psi_i = \frac{Q_{A,i}}{10} \quad q_i = \frac{Q_{R,i}}{10}$$

$$\sum_{j=1}^n Q_{R,j} \quad \sum_{j=1}^n Q_{R,j}$$

n = number of active heliostat regions,
 $Q_{A,i}$ = flux through aperture with only the ith heliostat region on,
 $Q_{R,i}$ = flux through central region (same size and shape as aperture) of RTAF with only the ith heliostat region on.

The values of ψ_i and q_i are listed in the following table*:

Region	$Q_{R,i}$	$Q_{A,i}$	ψ_i	q_i	
1	5.348	5.337	.071208	.071355	
2	5.314	5.316	.070928	.070902	
3	7.283	7.290	.097266	.097173	
4	7.225	7.242	.096626	.096399	
5	8.344	8.329	.111129	.111329	
6	8.304	8.296	.110689	.110795	
7	9.869	9.863	.131596	.131676	
8	9.829	9.825	.131089	.131143	(Fluxes in W/cm^2)
9	6.731	6.724	.089714	.089808	
10	6.702	6.696	.089341	.089421	
Full Field	74.949	74.918	.999586	1.0	

* The values of ψ_i and q_i listed in the table only apply to noon, day 180. Further analyses will be required to verify their validity for other dates and times.

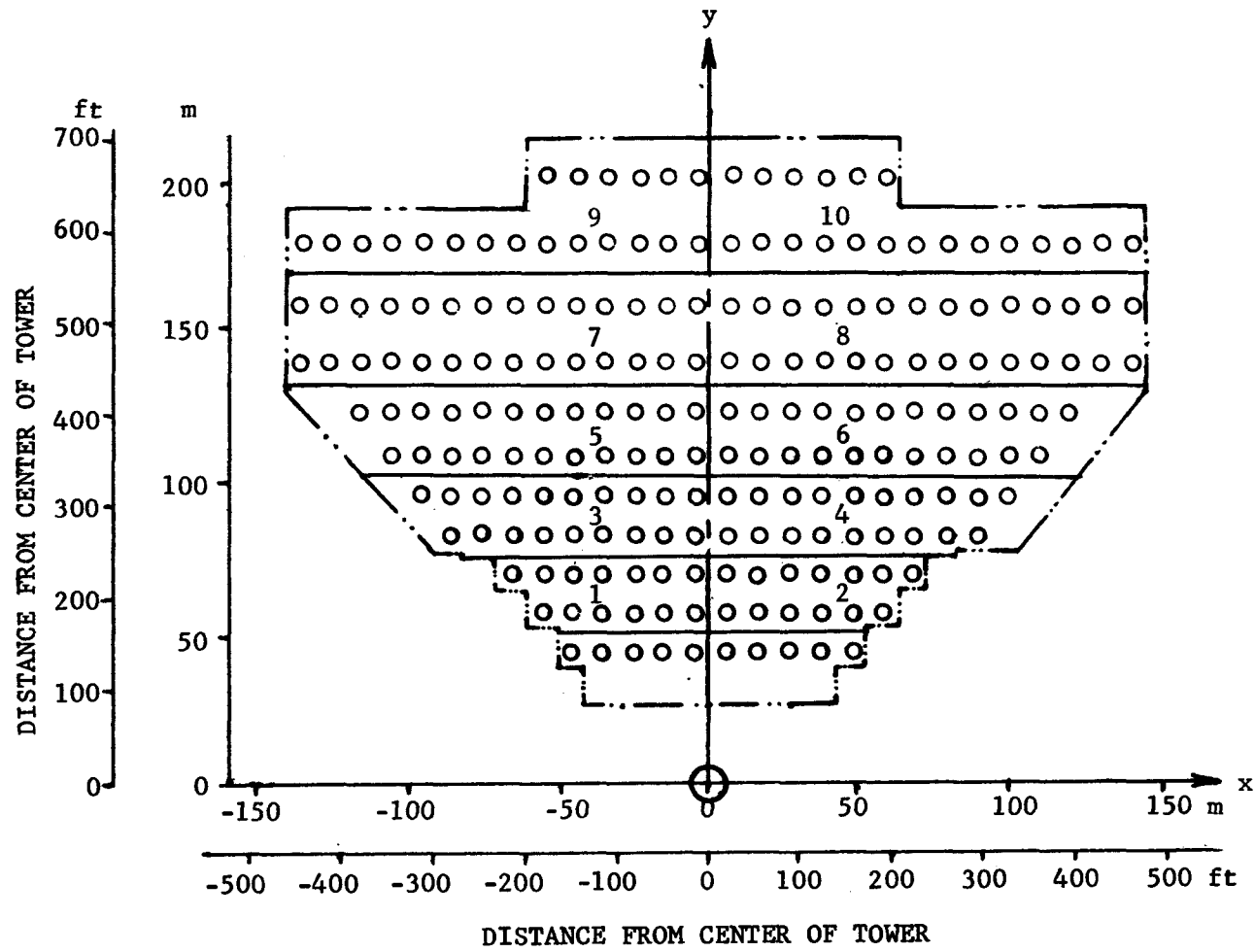


Figure III-55 Heliostat Field Regions for Transfer Function Calculations

Example: Suppose a flux of 33.0 W/cm² is measured by the RTAF at noon on day 180 with heliostat regions 6 through 10 shaded by clouds. One may expect a flux through the aperture of:

$$\begin{aligned} Q_{\text{Aperture}} &= \phi(\psi_i, q_i) \times Q_{\text{RTAF}} \\ &= \frac{(.071208 + .070928 + .097266 + .096626 + .111129) \times 33.0}{(.071355 + .070902 + .097173 + .096399 + .111329)} \\ &= 33.0 \end{aligned}$$

Possible correlations between the flux distribution on the tube wall and the fluxes measured by the 18 calorimeters installed on this wall are currently being investigated. Figures III-56, 57, and 58 show predicted flux levels at the calorimeter locations for 100% load conditions for the three test configurations. These can be used to check the measured flux distribution as determined at these locations against those calculated by the TRASYS models.

d. Partial Cloud Cover - To provide checkout data for an algorithm currently being developed for computer control of the receiver, several cloud passage situations were simulated by TRASYS models. For these analyses, the heliostat field was divided into four regions, and the receiver tube wall into six nodes. The field was analysed twice: Once divided vertically simulating East to West (or West to East) cloud passage, and once horizontally simulating North to South or South to North passage. The incident flux on each of the six nodes was calculated for four progressive fractions of cloud cover as shown on Figure III-59.

3. Detailed Receiver Analyses

Areas of detailed analysis of the receiver include receiver tube warmup with the hot air system, thermal analysis of welded tubes, salt cool-down transients, receiver tube temperature after sudden flow stoppage, calorimeter cooling system, and two-dimensional tube temperature. A description of these analyses' results are included here.

a. Receiver Tube Warmup with Hot Air - Heating up the receiver with heated system air has been analyzed. Trace heaters are used on everything except the receiver tubes. The receiver was analyzed as 16 tubes 71.3-m (234-ft) long (18 passes x 5.49 m (13 ft) per pass). Since all the tubes are the same, only one tube was analyzed with 1/16th of the proposed flow rate. Analysis was further simplified by noting that during startup, the receiver front and back will be insulated equally well and heat loss will be the same in either direction. A thermal model was developed to simulate heat loss from the front of one receiver tube using MITAS (for Martin Marietta Integrated Thermal Analyzer System, a generalized thermal modeling computer program). The 71.3-m (234-ft) tube was divided into 23 3.1-m (10-ft) sections. Each tube node required three insulation nodes (with capacitance), two arithmetic nodes (no capacitance), and one air node for a total of 164 nodes in network (3 additional boundary nodes). The system model with temperatures (at time = 0.5 hr) are presented in Figure III-60. The final design required 0.20 m (8 in.) of insulation.

Fluxes in MW/m^2 x 100
Lengths in meters

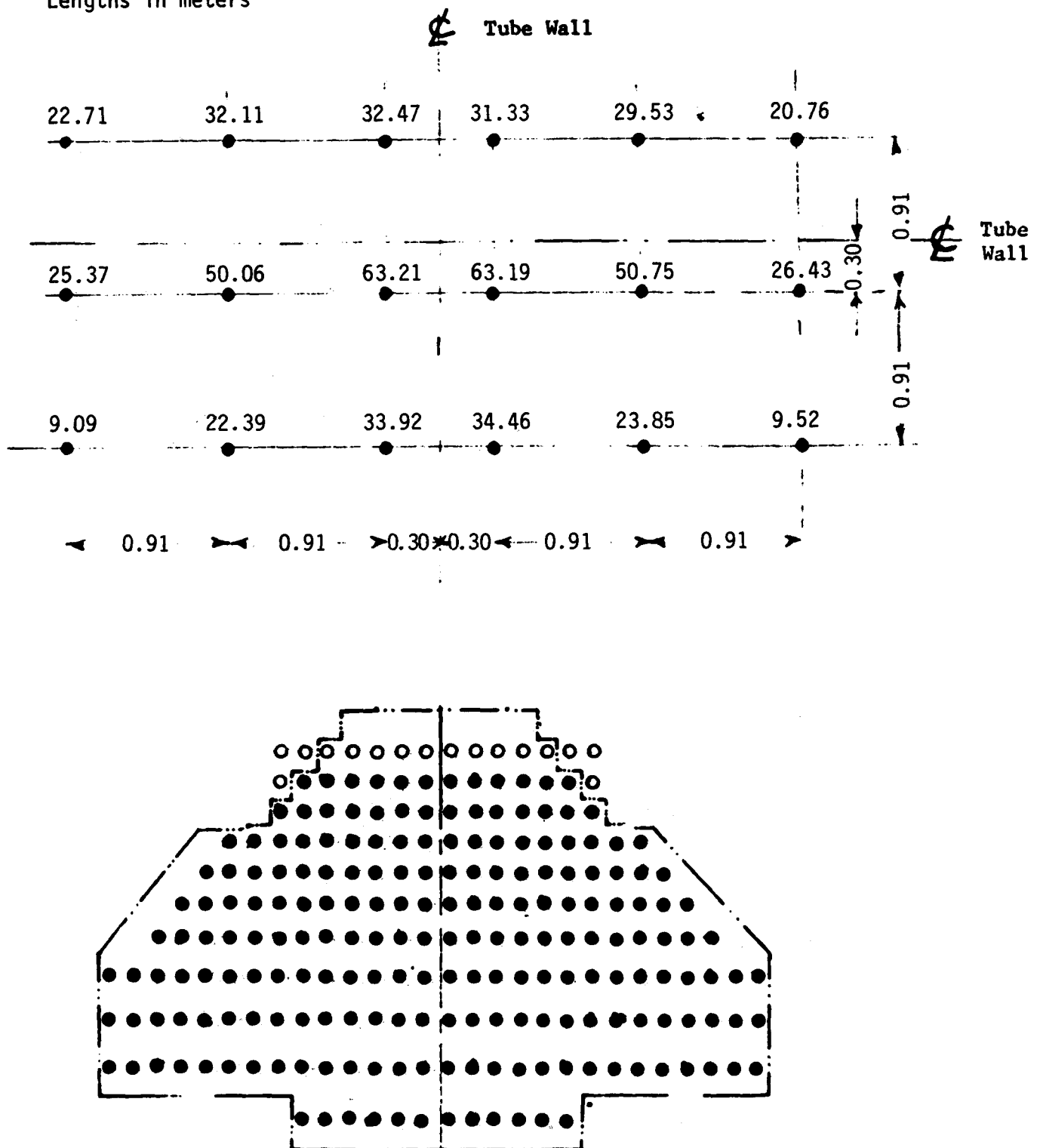
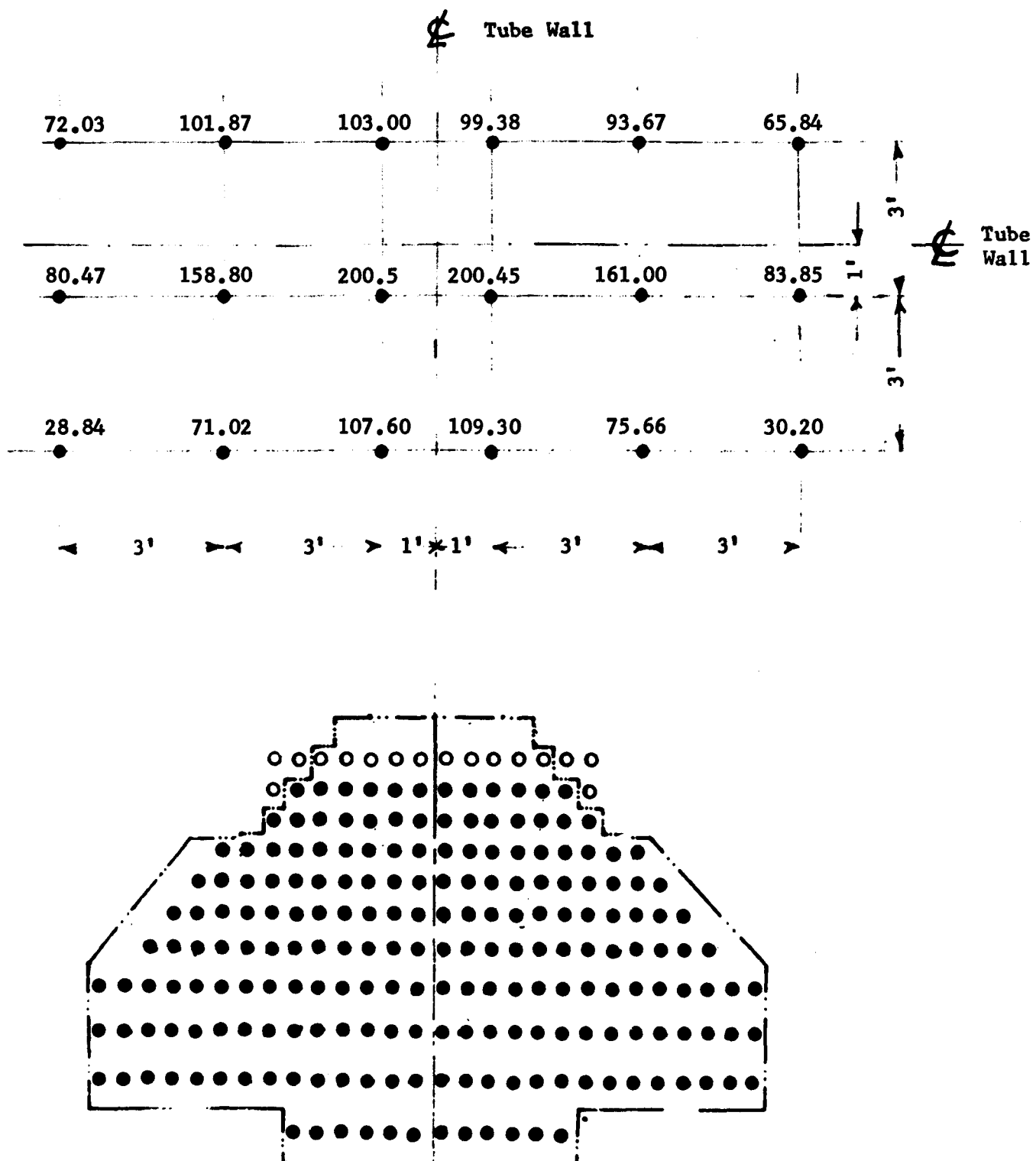


Figure III-56a
Flux Levels @ Flux Gage Locations, Cavity Configuration, Maximum Input

Note: Fluxes in 1000 BTU/Hr-Ft²



Fluxes in $\text{MW/m}^2 \times 100$
Lengths in meters

Tube Wall

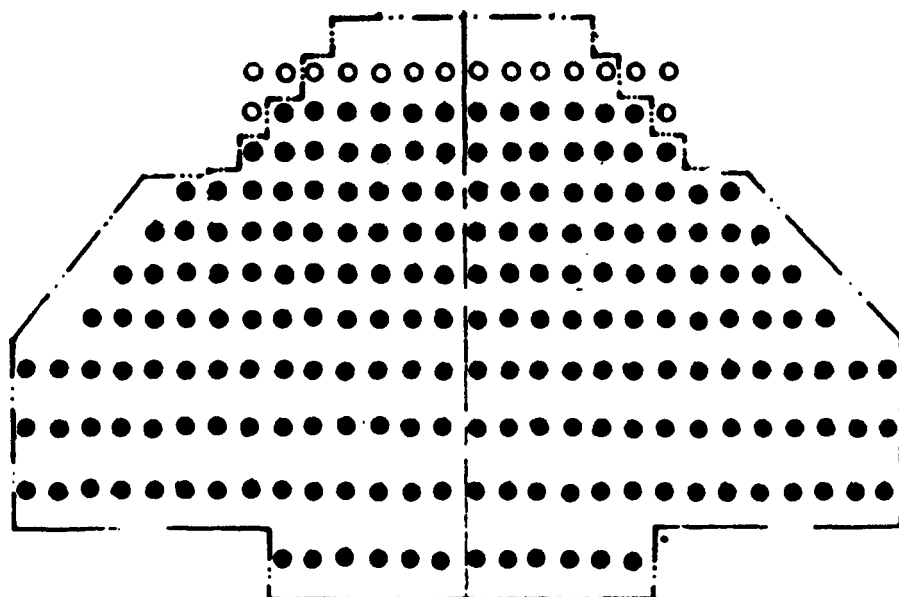
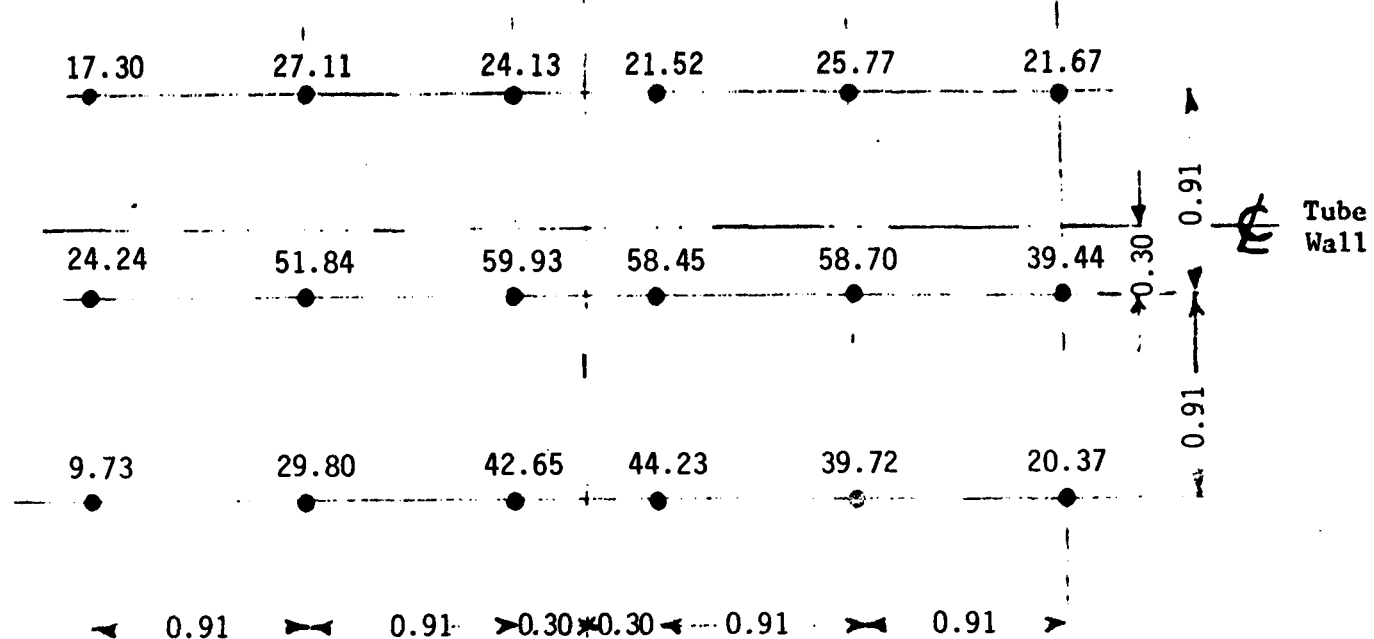


Figure III-57a
Flux Levels @ Flux Gage Locations, Fully Exposed Configuration, Maximum Input
(Dual Aim)

Note: Fluxes in 1000 BTU/Hr-Ft²

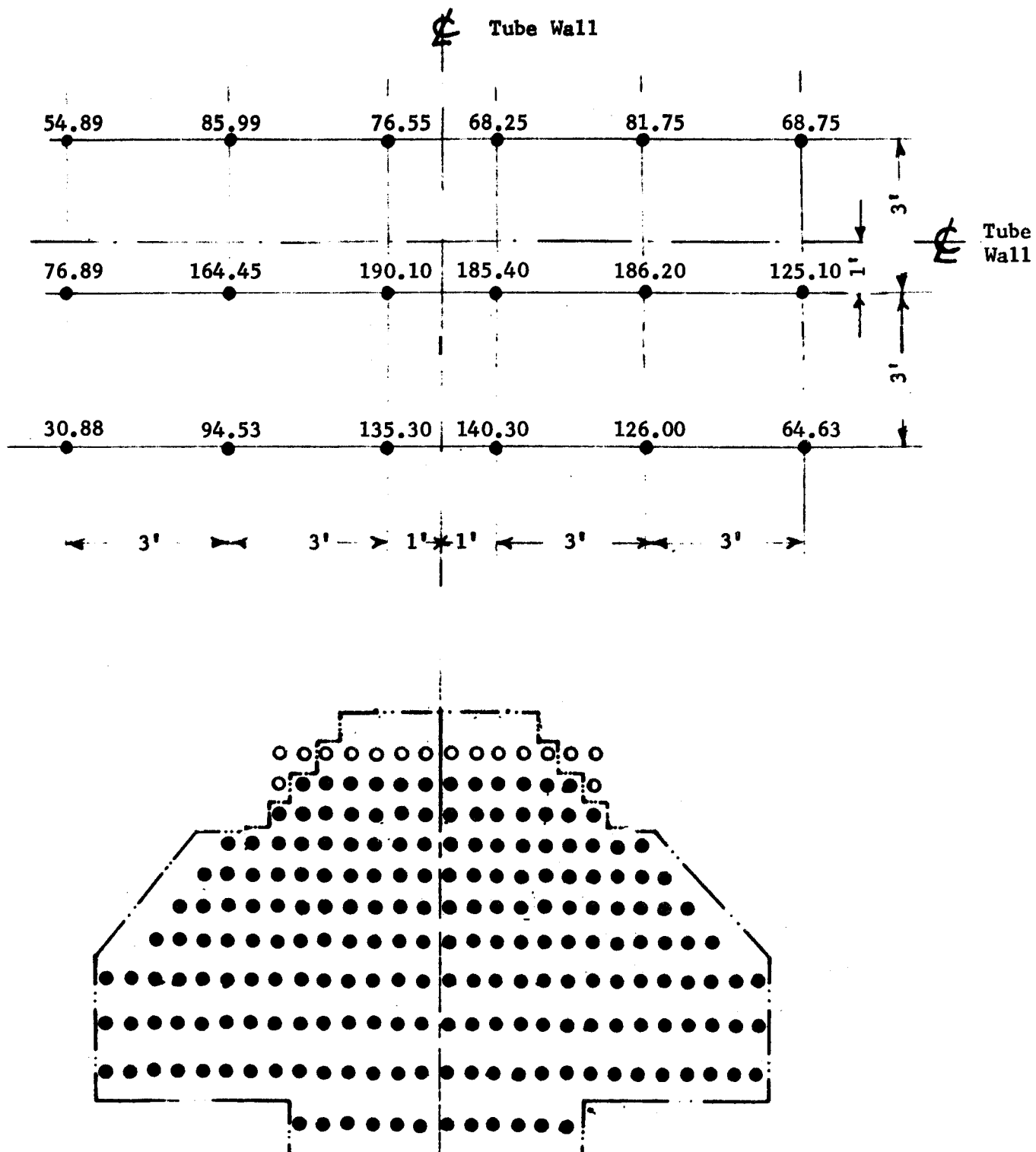


Figure III-57b
Flux Levels @ Flux Gage Locations, Fully Exposed Configuration,
Maximum Input (Dual Aim)

Fluxes in $\text{MW/m}^2 \times 100$
Lengths in meters

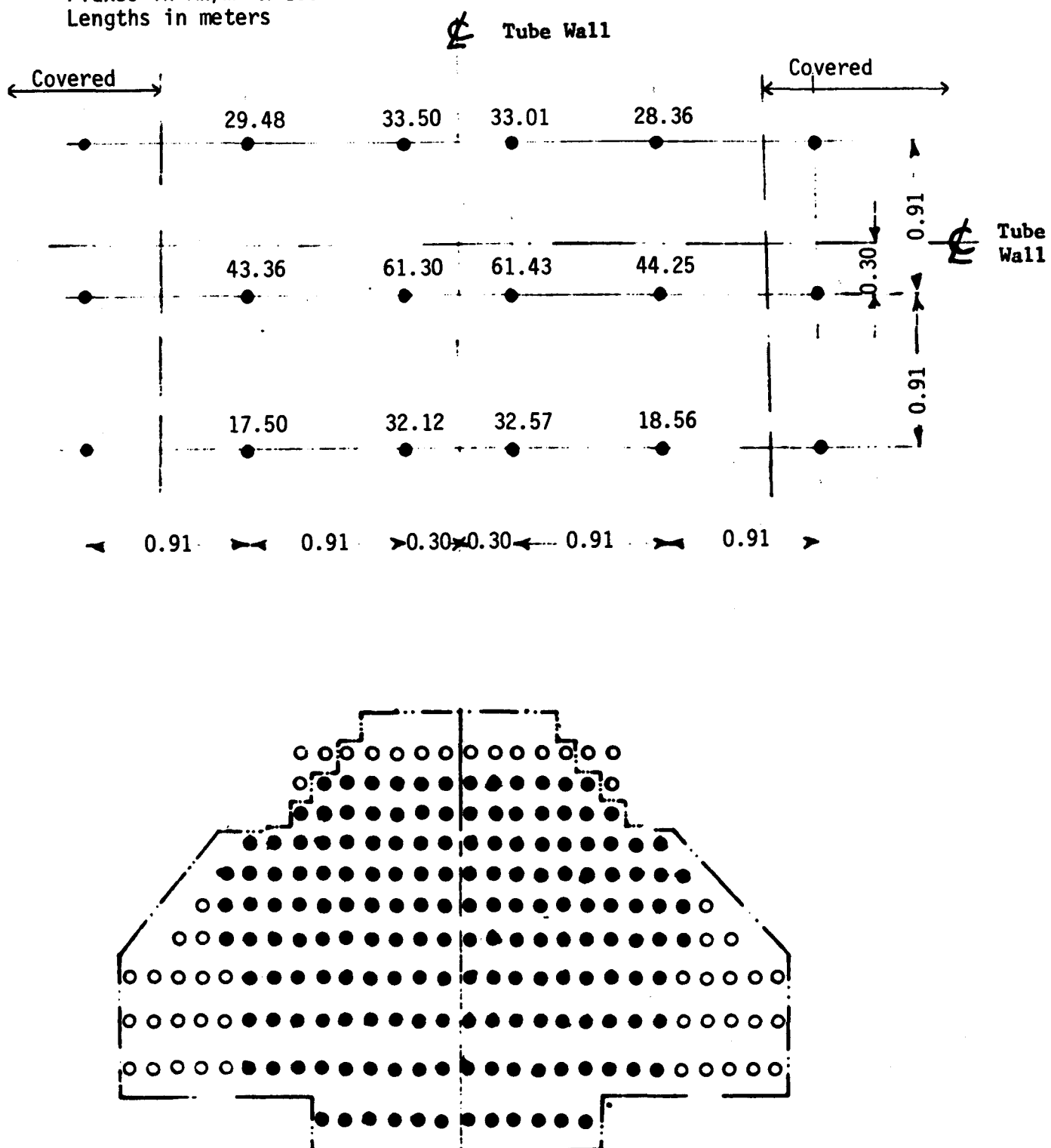


Figure III-58a
Flux Levels @ Flux Gage Locations, Partially Exposed Configuration, Maximum Input

Note: Fluxes in 1000 BTU/Hr-Ft²

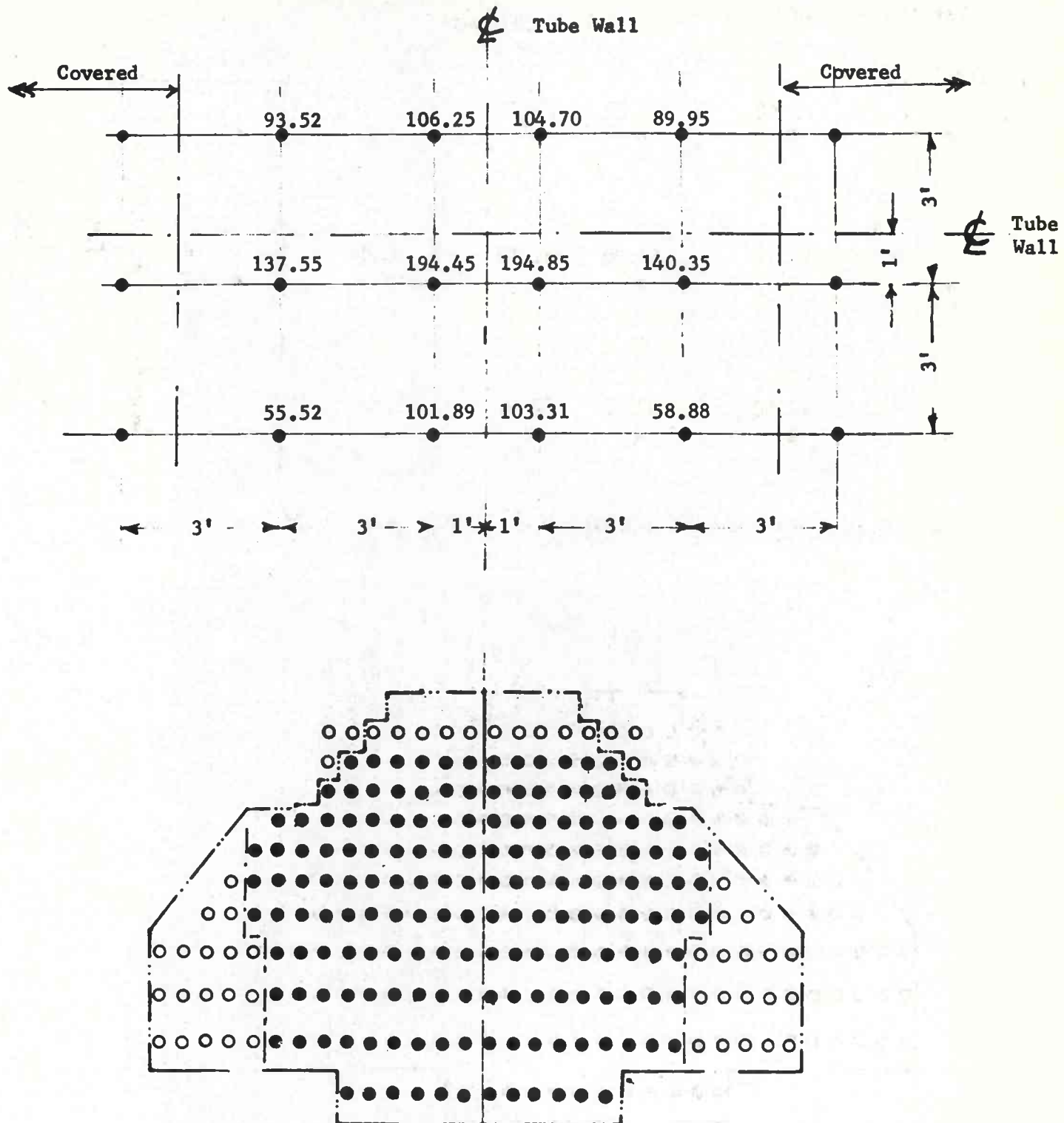


Figure III-58b
Flux Levels @ Flux Gage Locations, Partially Exposed
Configuration, Maximum Input

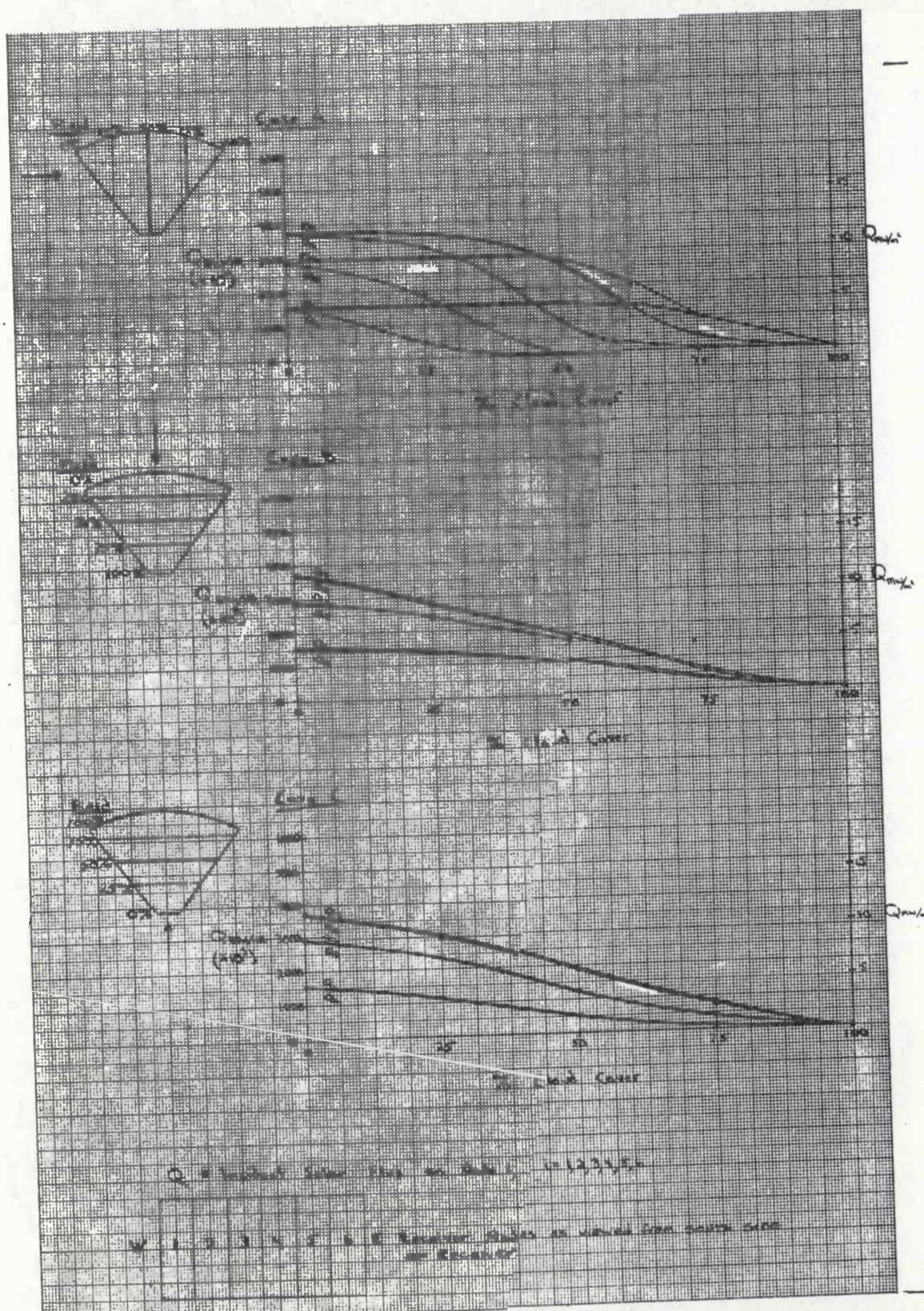
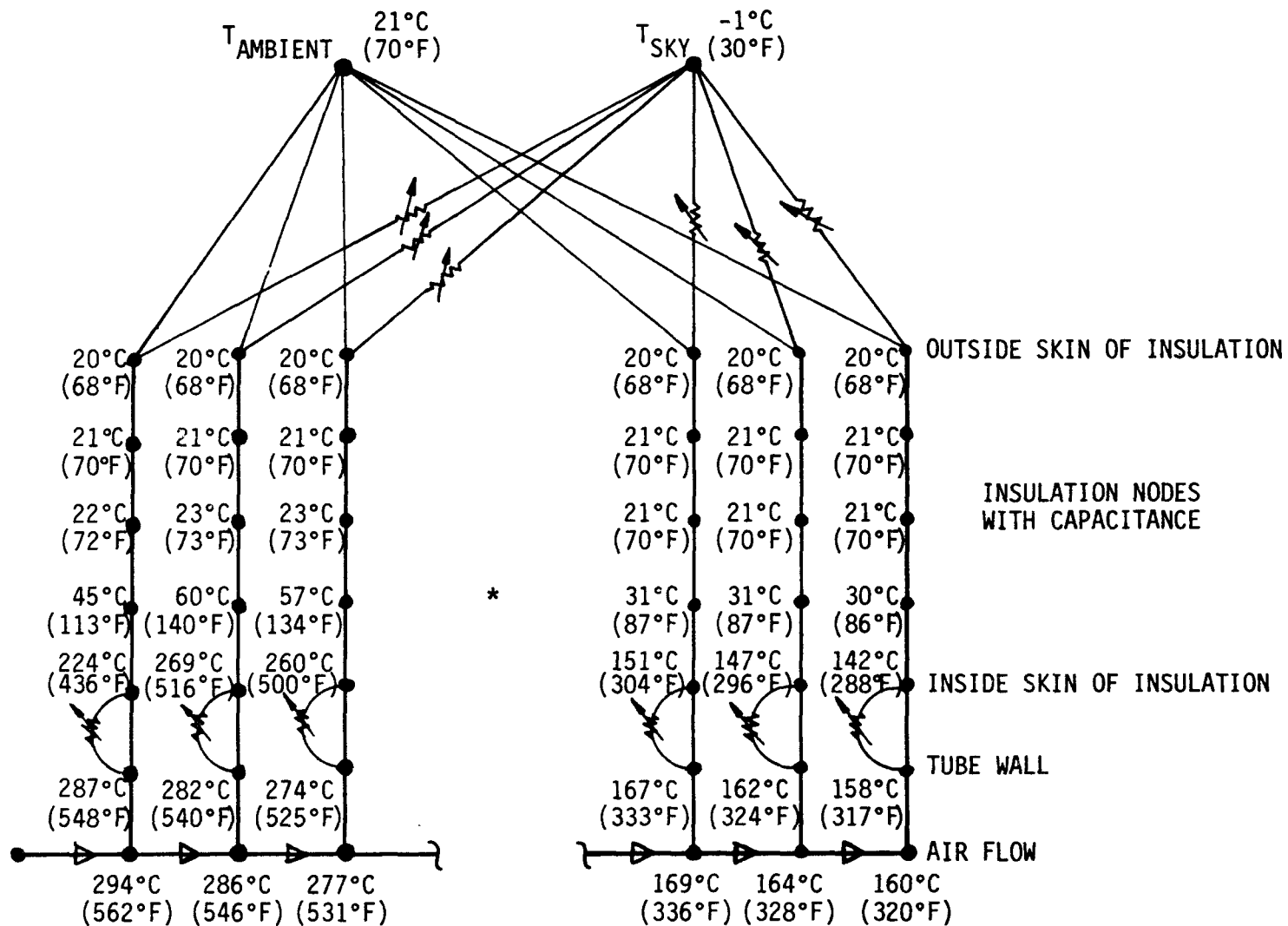


Figure III-59
Effect of Partial Cloud Coverage of Heliostat Field on Receiver Fluxes



* 17 SIMILAR BRANCHES LEFT OFF

Figure III-60 Thermal Model for Receiver Tube Air Heating

The MITAS model was developed with variable inputs. The final design inputs are described below.

- 1) Insulation Density = 256 kg/m³ (16 lbm/ft³)
- 2) Insulation Conductivity = 0.072 W/m-°C (0.042 Btu/hr-ft-°F)
- 3) Insulation Heat Capacity = 921 J/kg-°C (0.22 Btu/lbm-°F)
- 4) Insulation Thickness = 0.20m (8 in.)
- 5) Insulation Emissivity = 0.9

Simulation results are presented in Figure III-61. Under these conditions, the receiver would reach operating conditions in approximately 1 hour in the fully-insulated mode and 25 minutes in the partially-insulated mode (Albuquerque test with RTAF in place). During this heat-up, the insulation must also be warmed up. Presented in Figure III-62 are the temperature of insulation nodes on the twelfth node of the receiver (midway through). These insulation nodes are still being heated even through the receiver tube wall has reached operating temperature.

b. Thermal Analysis of Welded Tubes - The weld joints on the receiver tubes have been analyzed using the MITAS thermal analyzer program. The 30-node, 56-conductor MITAS network was used to analyze three situations. Worst-case results are included here at the point on the receiver with the hottest tube wall temperature. This point is defined by both the fluid temperature (504°C (940°F)) and the solar flux (0.536 MW/m² (170,000 Btu/hr-ft²)). Two additional parametric studies were performed, one at maximum solar flux, and another at a lower flux with a higher fluid temperature. The worst-case weld material analyzed was Inconel 82 weld rod with a thermal conductivity of 11.2 W/m-°C (6.5 Btu/hr-ft-°F). The Incoloy tube conductivity at 510°C (950°F) is 22.0 W/m-°C (12.7 Btu/hr-ft-°F), and the heat transfer coefficient based on actual conditions is 5718W/m²-°C (1007 Btu/hr-ft²-°F). The weld dimensions as analyzed are height 6.0 mm (0.235 in.) and width 4.3 mm (0.17 in.). Results of the analysis are presented in Figure III-63 and indicate that no problems exist with the system as designed because the maximum temperature in the worst-case situation is 638°C (1180°F).

c. Salt Cooldown Transients - Worst-case cooldown transients for salt-filled receiver tubes without flow were calculated using a small thermal model programmed on the HP 9815A minicomputer for the following cases: 1) exposed receiver; 2) cavity receiver with the door open; and 3) cavity receiver with the door closed one minute after loss of insulation. The tube metal and the salt were assumed to be at 288°C (550°F) at the beginning of the cooldown transient. In the case of the cavity, that location on the tube wall having the largest view factor to the aperture opening was selected for analysis. Results are shown on Figure III-64.

d. Sudden Flow Stoppage Analysis - Analysis was performed to determine the maximum receiver tube wall temperature achieved after a sudden flow stoppage. A worst-case example was analyzed using MITAS. A conserva-

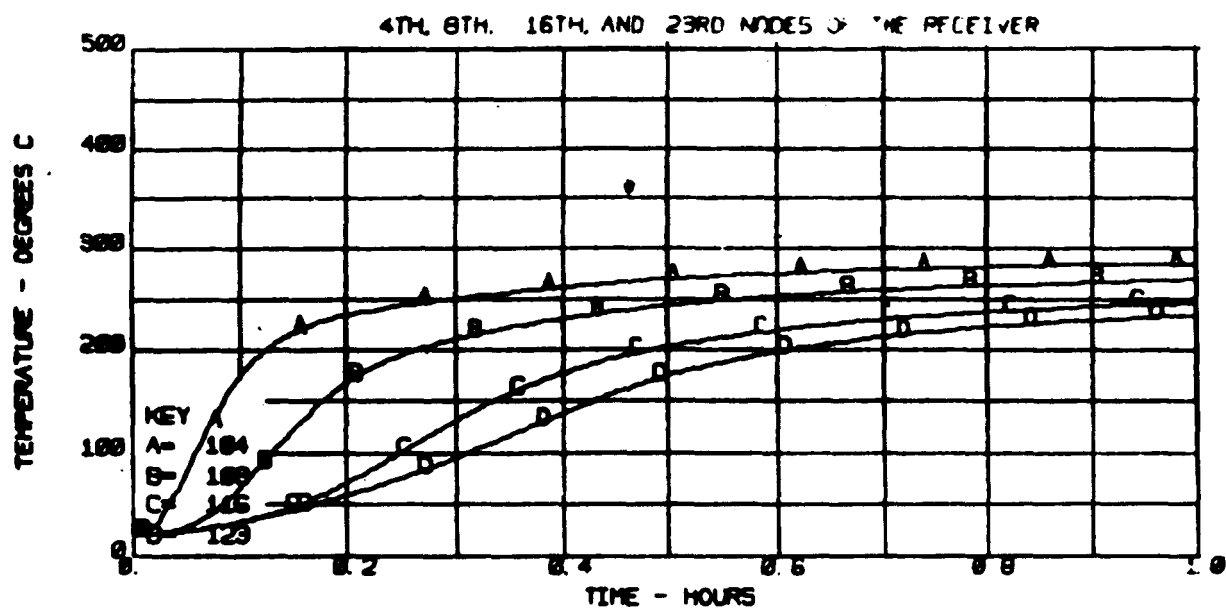


Figure III-61
Receiver Tube Air Heating System Performance - Temperatures Across Tube Wall

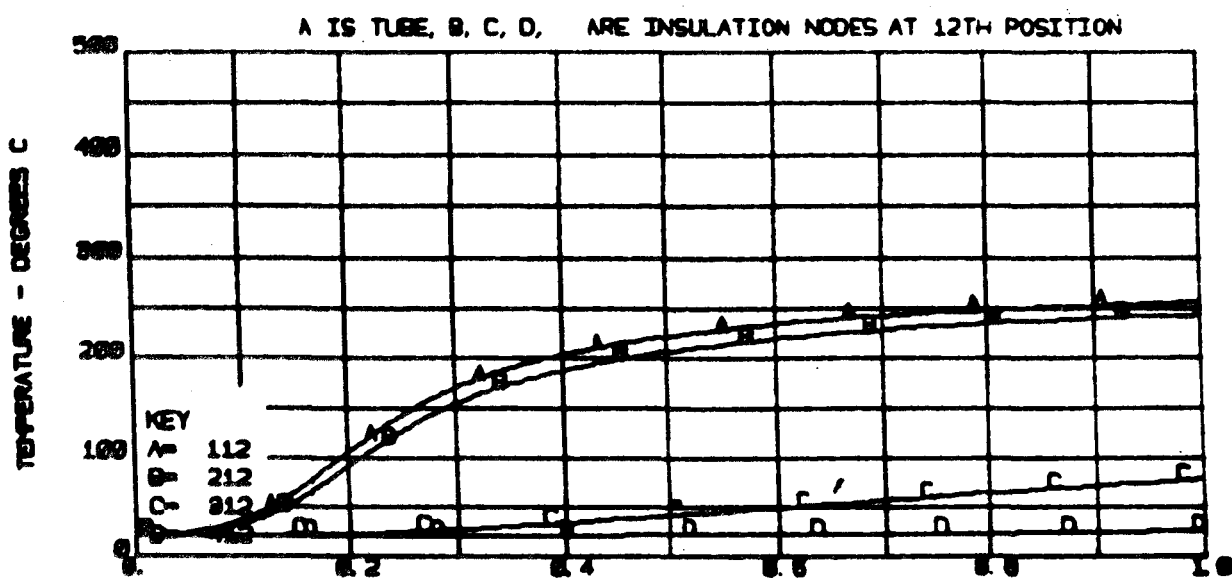


Figure III-62
Receiver Tube Air Heating System Performance--Insulation Temperatures

III-119

$$T_{SALT} = 504 \text{ C}$$

$$Q_{SOLAR} = 536 \text{ KW/m}^2$$

$$K_{WELD} = 11.25 \text{ W/m C}$$

$$K_{TUBE} = 21.97 \text{ W/m C}$$

$$h = 5.72 \text{ KW/m}^2 \text{ C}$$

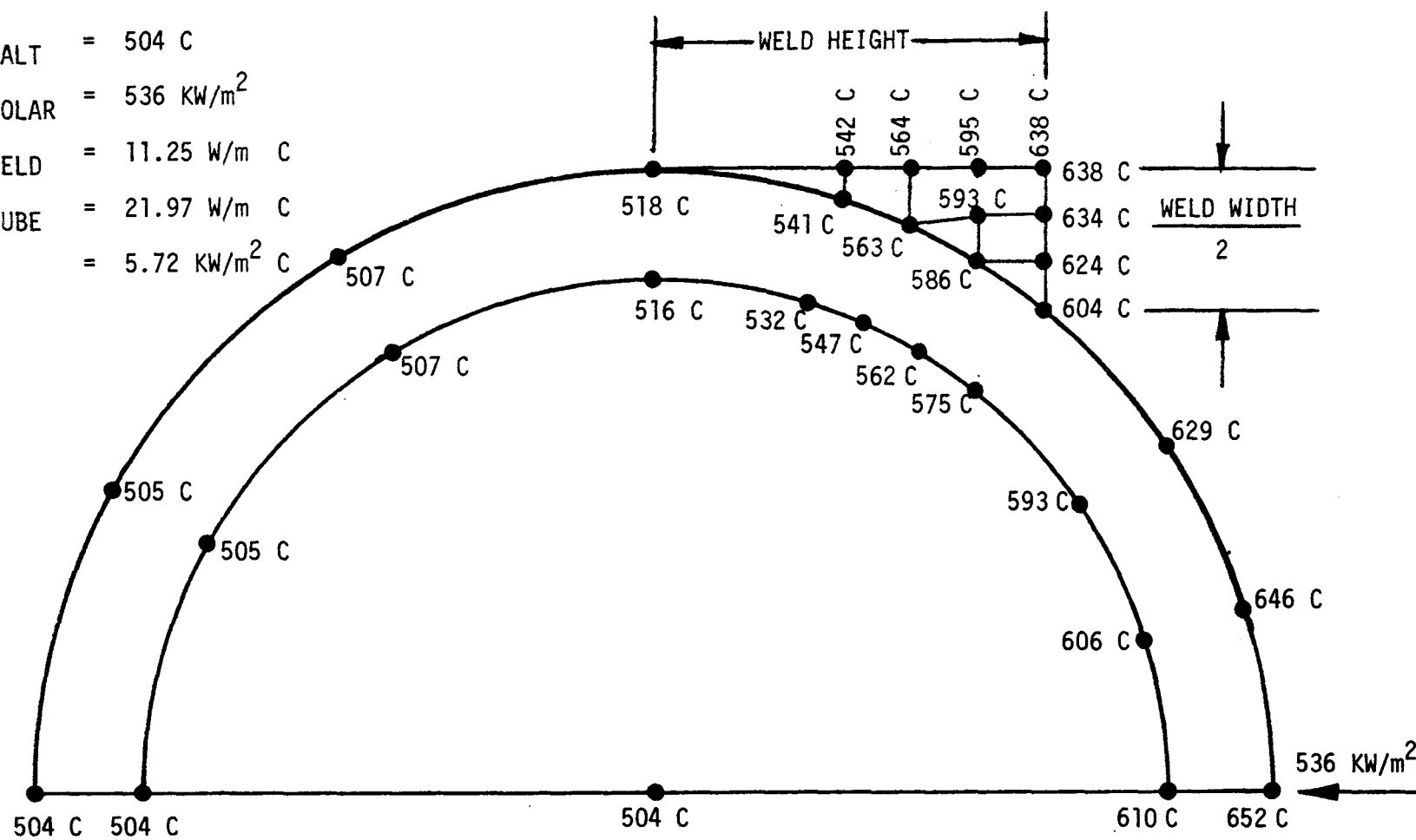


Figure III-63a Weld Temperature Analysis - Worst Case

III-120

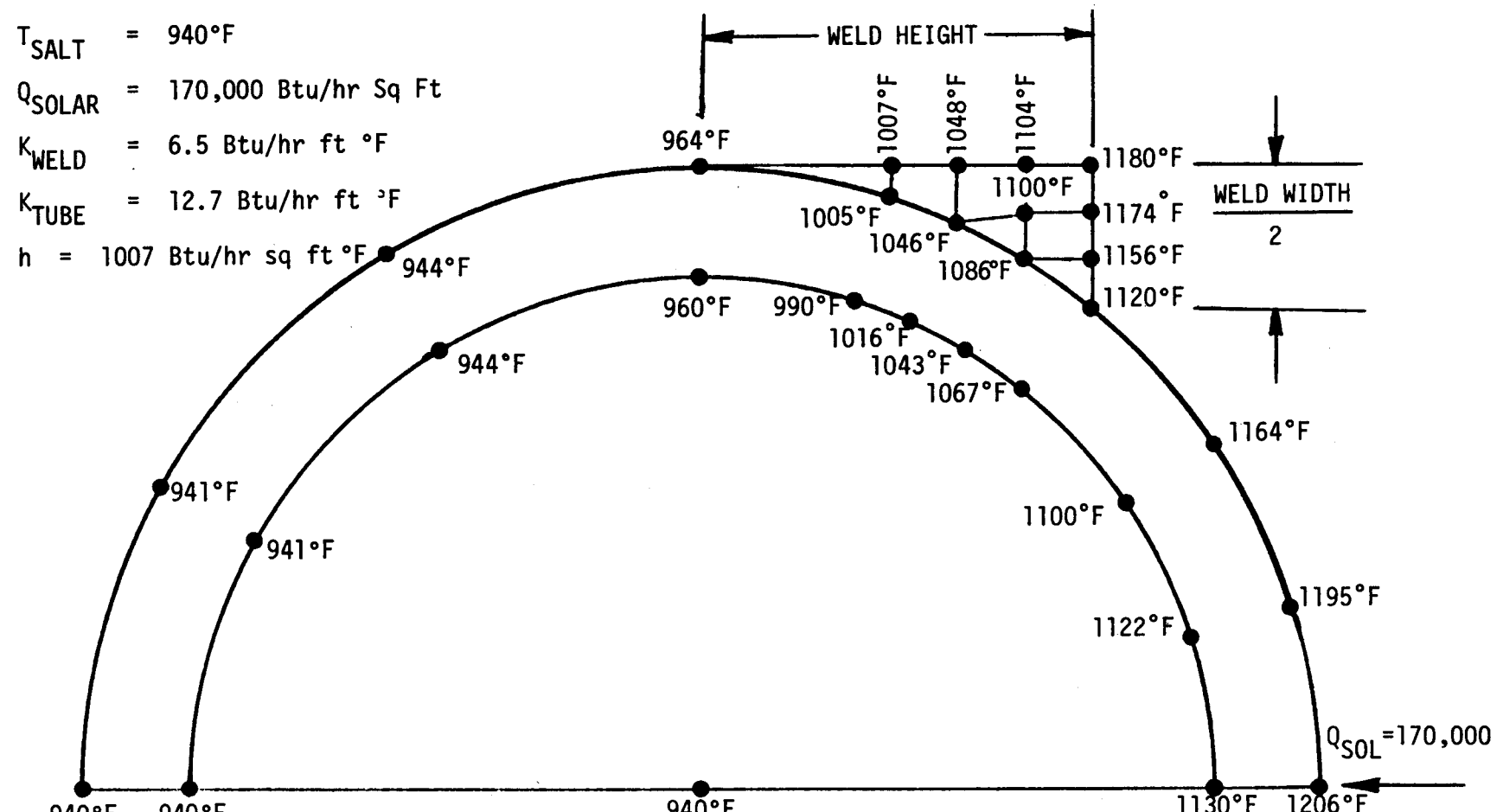


Figure III-63b Weld Temperature Analysis - Worst Case

III-121

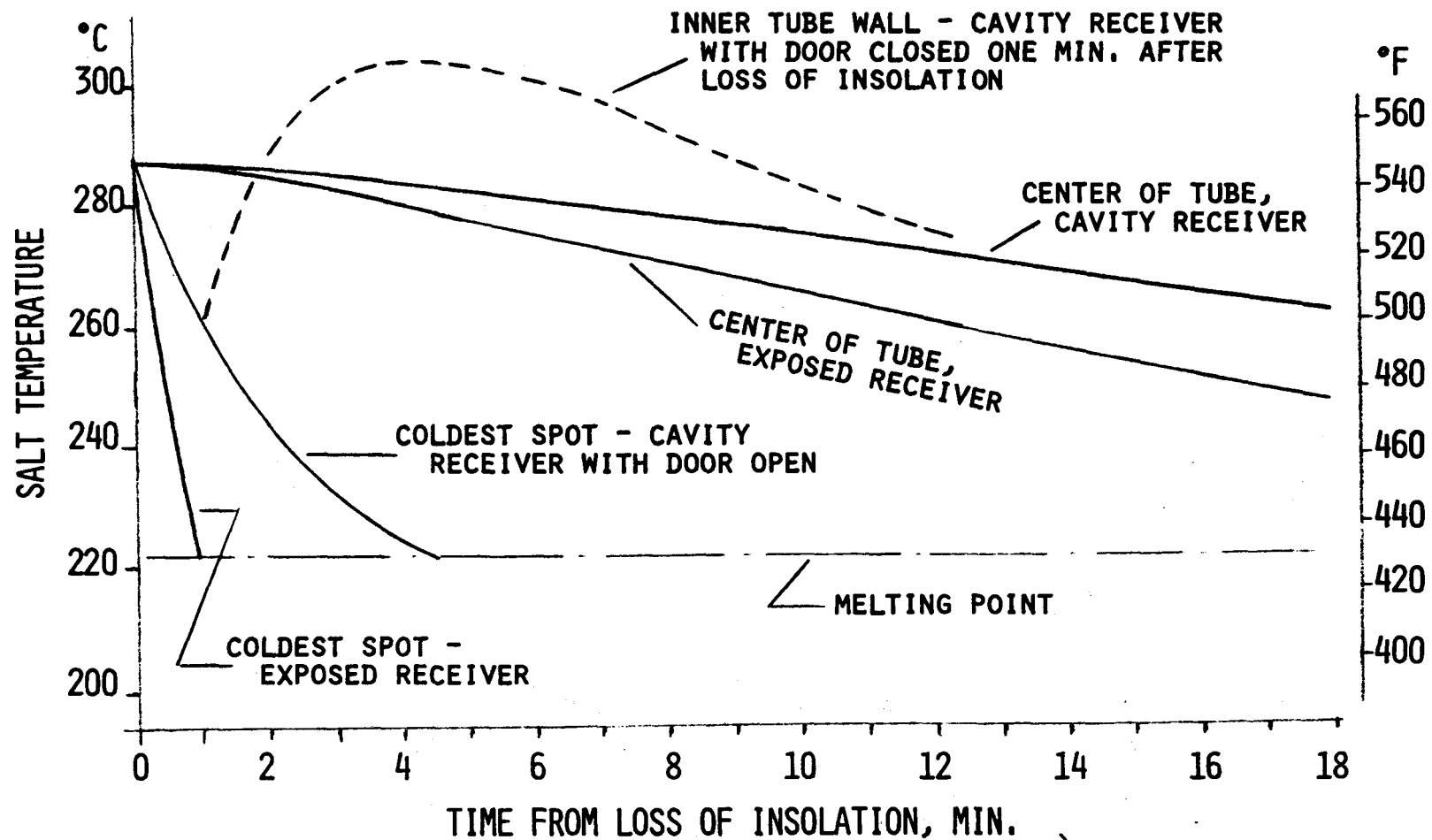


Figure III-64 Receiver Salt Cooldown Transients

tive assumption was that the solar flux was constant at 0.694 MW/m^2 ($220,000 \text{ Btu/hr-ft}^2$) for 5 seconds then instantaneously reduced to zero for the remainder of the transient analysis. Other assumptions were: salt temperature was 566°C (1050°F), heat transfer path from tube wall to salt was by conduction only, and solar flux distribution was constant across the tube wall.

The system model is described in Figure III-65, which includes the temperatures 5 seconds after flow stoppage. The maximum temperature achieved in this transient condition is 769°C (1417°F). Comparison of the maximum tube temperature and average salt temperature vs time is graphed in Figure III-66. Further studies will be performed to determine a more realistic maximum temperature through less conservative, more accurate analyses.

e. Receiver Calorimeter Cooling System - Eighteen calorimeters on the receiver surface will require active cooling to prevent overheating. Analysis was on the thermal and hydraulic performance of the cooling system. Conservative assumptions were: a surrounding air temperature of 566°C (1050°F), a cooling water temperature of 24°C (75°F), an incident solar flux of 0.694 MW/m^2 ($220,000 \text{ Btu/hr ft}^2$), and thermal losses neglected. Results of the analysis are presented in Figure III-67 with pressure drops of 62.1 kPa (9 psi) per calorimeter at $8.6 \text{ cm}^3/\text{s}$ (0.13 gpm) and a 3.3°C (6.0°F) temperature rise. Cooling system lines are sized at 3.2 mm (1/8 in.) between calorimeters and a minimum of 1.3 cm (1/2 in.) I.D. for the two headers.

The calorimeter cooling system supplied by CRTF is a 10.6-kW (3-ton) chiller providing $0.0063 \text{ m}^3/\text{s}$ (100 gpm) at 345 kPa (50 psig). It will be located under the heat exchanger on the tower elevator, and will travel up and down with the receiver, so it can be easily connected. The cooling fluid is a solution of 30-40% ethylene glycol.

f. Two-dimensional Steady-State Tube Thermal Model - To support the receiver tube creep/fatigue studies, a two-dimensional, steady-state thermal model of the tube was developed. The model network used is shown in Figure III-68. The network contains 86 nodes and 165 conductors, and the thermal conductivity of the tube material is varied as a function of temperature. This analysis was carried out using MITAS and 41 cases were analyzed.

4. Air Cooler Thermal Analysis

Thermal energy absorbed by the receiver is dissipated to the atmosphere via the air cooler. For nominal operating conditions, the molten salt is cooled from 566°C (1050°F) to 288°C (550°F). This is accomplished by forcing ambient air over the 105 air cooler tubes.

The thermal analysis used to size the air cooler was performed on a Texas Instruments TI 59 programmable calculator. Two programs were developed for this analysis: the first determines the overall thermal conductance between the molten salt and the air, and the second computes the molten salt and air temperatures throughout the air cooler. Overall thermal conductance calculations are based on a method provided by the finned tube manufacturer (ESCOA) and are based on empirical cor-

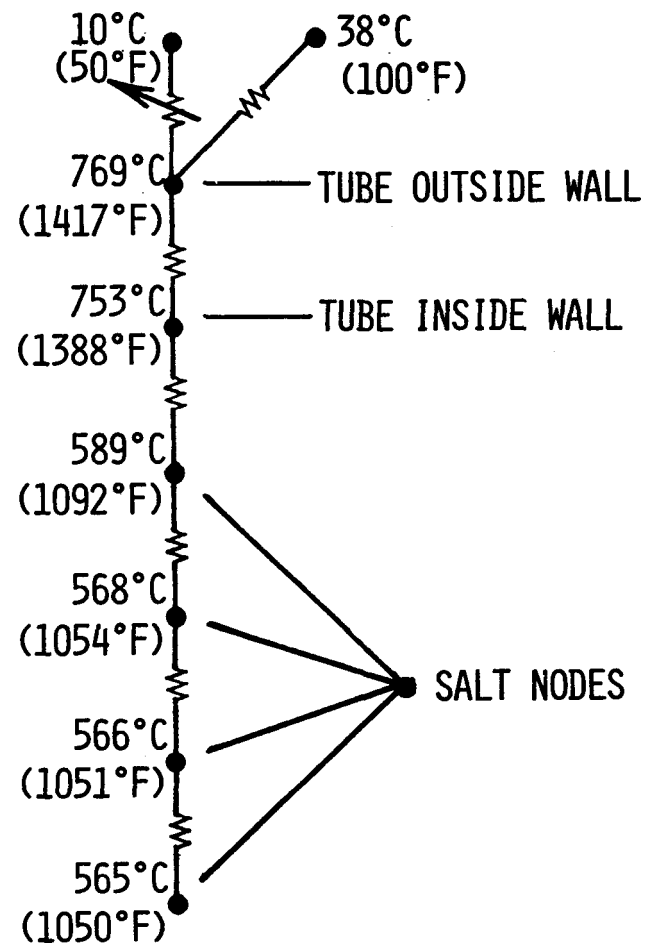
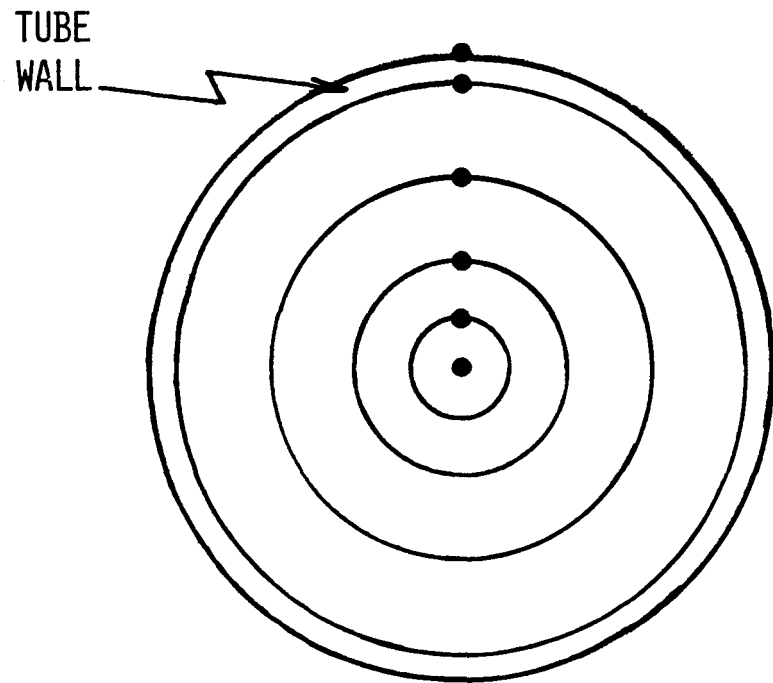


Figure III-65 Receiver Tube Thermal Model for Sudden Flow Stoppage

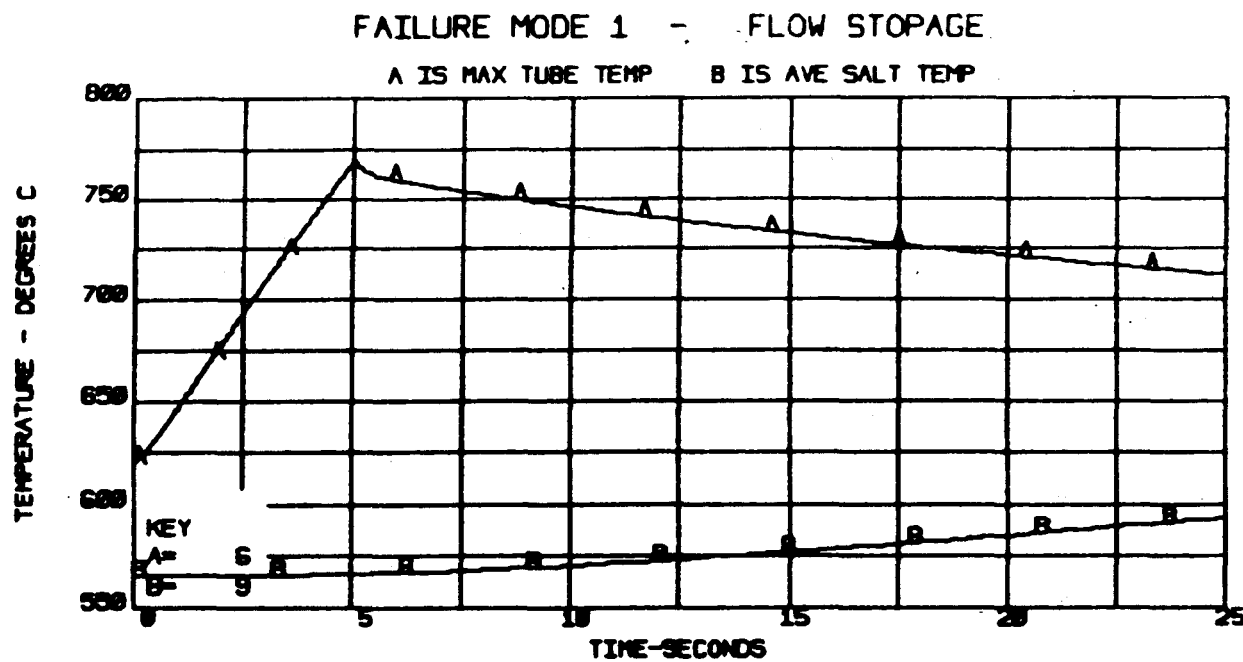


Figure III-66 Receiver Tube Temperature after Sudden Flow Stoppage

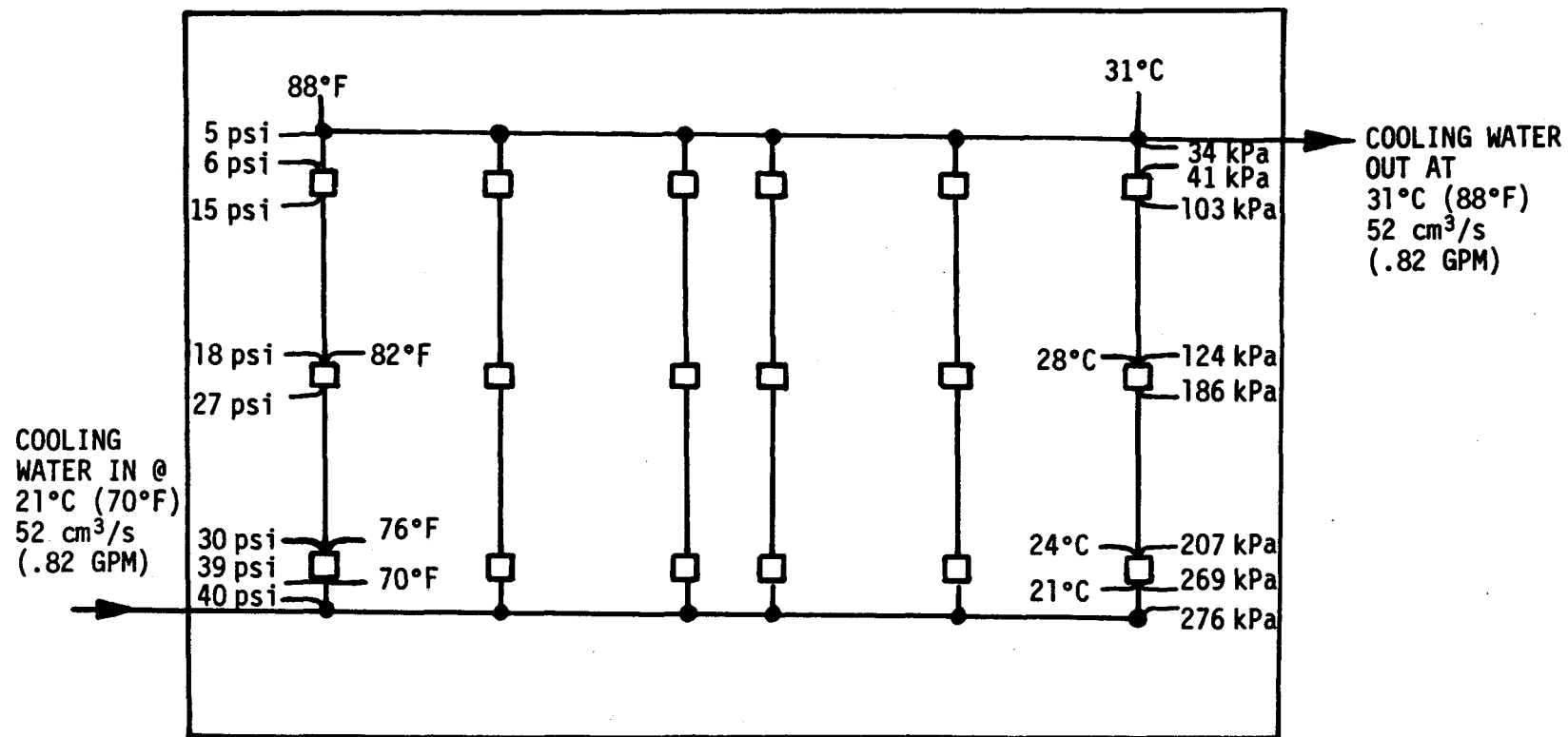


Figure III-67 Calorimeter Cooling System--Temperatures and Pressures

- ANALYSIS PERFORMED USING MITAS
- 86 NODES, 165 CONDUCTORS
- CONDUCTIVITY OF THE TUBE IS A FUNCTION OF TEMPERATURE
- 41 CASES ANALYZED

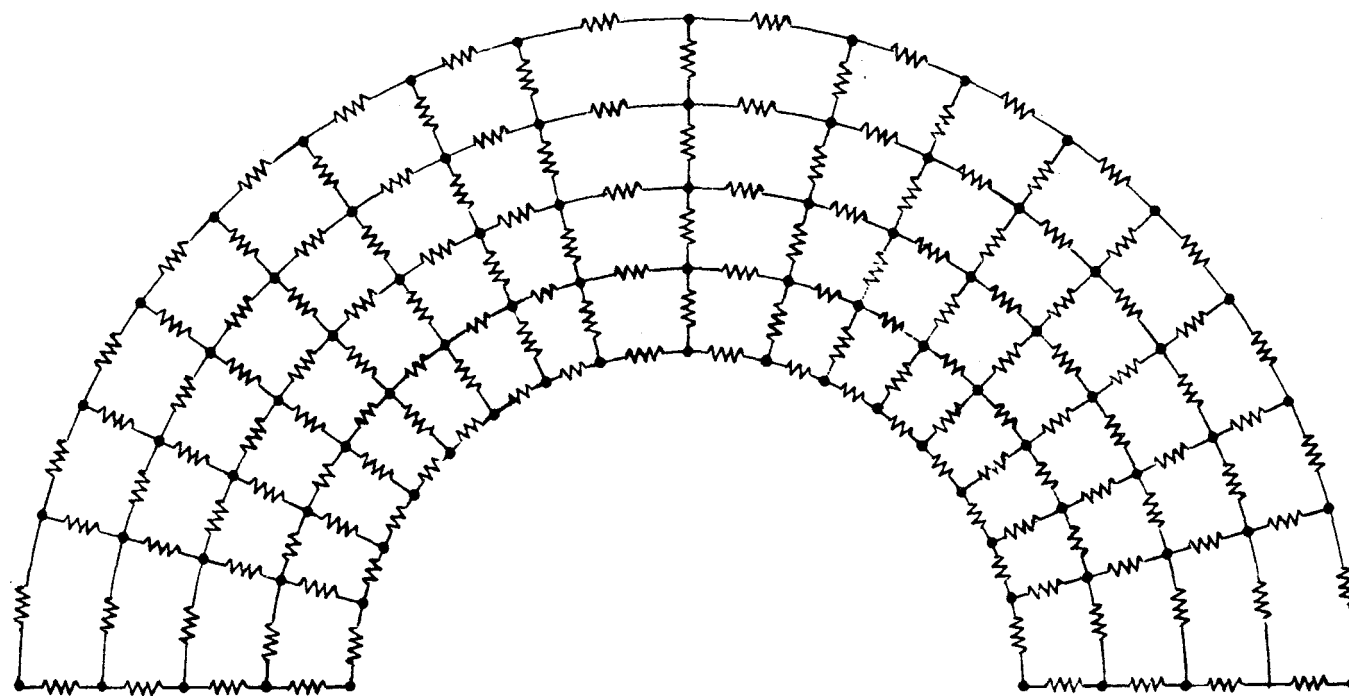


Figure III-68 Two-Dimensional Receiver Tube Temperature Thermal Model

relations. The thermal model used to predict temperatures is a 25-node model. Results of this model for the design point are given in Figure III-69. Note that there are two important conditions that must be met by the air cooler: molten salt must be cooled from 566°C (1050°F) to 288°C (550°F) at the maximum design point, and the tube wall temperature at the outlet must be significantly above the salt freezing temperature of 221°C (430°F). This second requirement drove the design to the 6-pass configuration. As noted on Figure III-69, the present design meets all the requirements with the outlet tube wall temperature well above the salt freezing point for all operational conditions.

During shutdown periods, the cooler will be closed by shutting the louvers (on bottom) and cooler doors (on top). The cooler will be kept hot by the heat tracing on the cooler side walls. Analysis of the steady-state heat loss was performed to estimate power requirements. Assumptions of the analysis were ambient insulation temperatures of 10°C (50°F) around the cooler, aluminum louvers ($\epsilon = 0.1$), and cooler steady-state temperatures of 371°C (700°F) (conservative). The MITAS model, temperatures, and heat flows are presented in Figure III-70. The heat-loss rate from the cooler for this condition is 19 kW (65,000 Btu/hr). Therefore, heat tracing was sized at 23.7 kW (80,900 Btu/hr), with an additional 5.5 kW (18,800 Btu/hr) on the cooler headers (located outside of the enclosed unit).

5. System Drain Time Analysis

The system (receiver and cooler) will be drained to prevent salt freezing during shutdown periods. The draining will be accomplished by applying air pressure to the purge side. Analysis has been performed on the hydraulic performance of the receiver and cooler. Pressure distribution along the receiver drain lines (at the bottom) was assumed constant at 345 kPa (50 psig). The salt properties were taken at receiver drain temperatures of 288°C (550°F). The pressure drops and salt flow rates of the drain system are presented in Figure III-71. The actual drain procedure will be determined experimentally during the checkout tests, but based on present analysis, the receiver will drain in 20 to 40 seconds and the cooler will drain in an additional 30 seconds. These drain times are all within calculated safety limits. Based on the salt cooldown transient analysis, the exposed receiver's coldest spot will not begin to freeze for 1 minute (when the system is closed up, not draining).

Further analysis was performed on the air purge system. The air purge pressure drop was conservatively calculated to be 13.8 kPa (2.0 psig), and approximately 3.91 scm (138 scf) was required to purge the system. To insure purge capability, an auxiliary purge system of three H bottles will be part of the SRE.

6. System Level Analysis

To gain an understanding of the receiver system transient behavior and to develop the control strategy for the receiver and air cooler outlet temperatures, a thermal model of the system was developed. An existing generalized thermal analyzer computer program, MITAS, was used for this

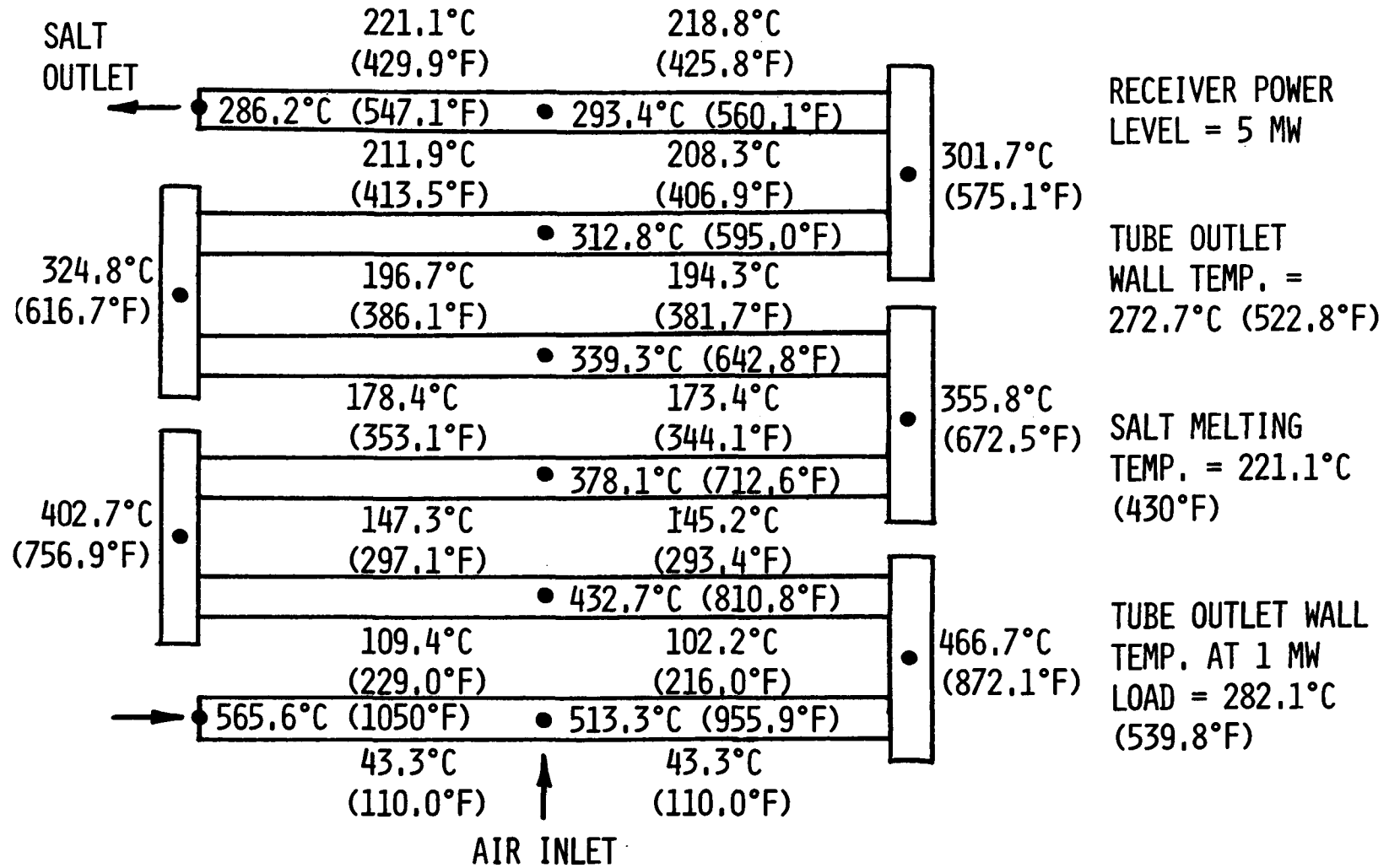


Figure III-69 Air Cooler Performance

III-129

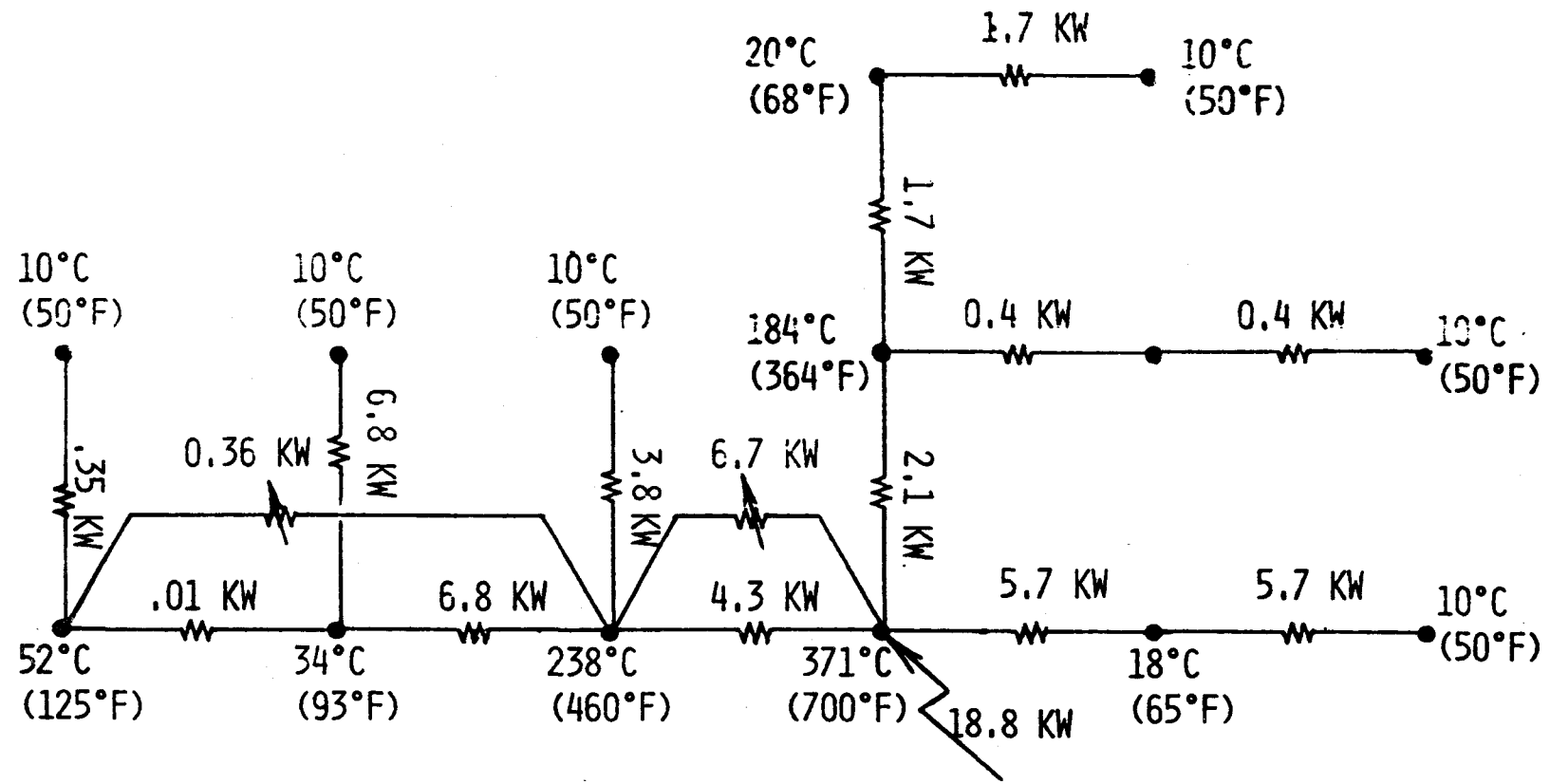


Figure III-70 Air Cooler Preheat Power Requirements

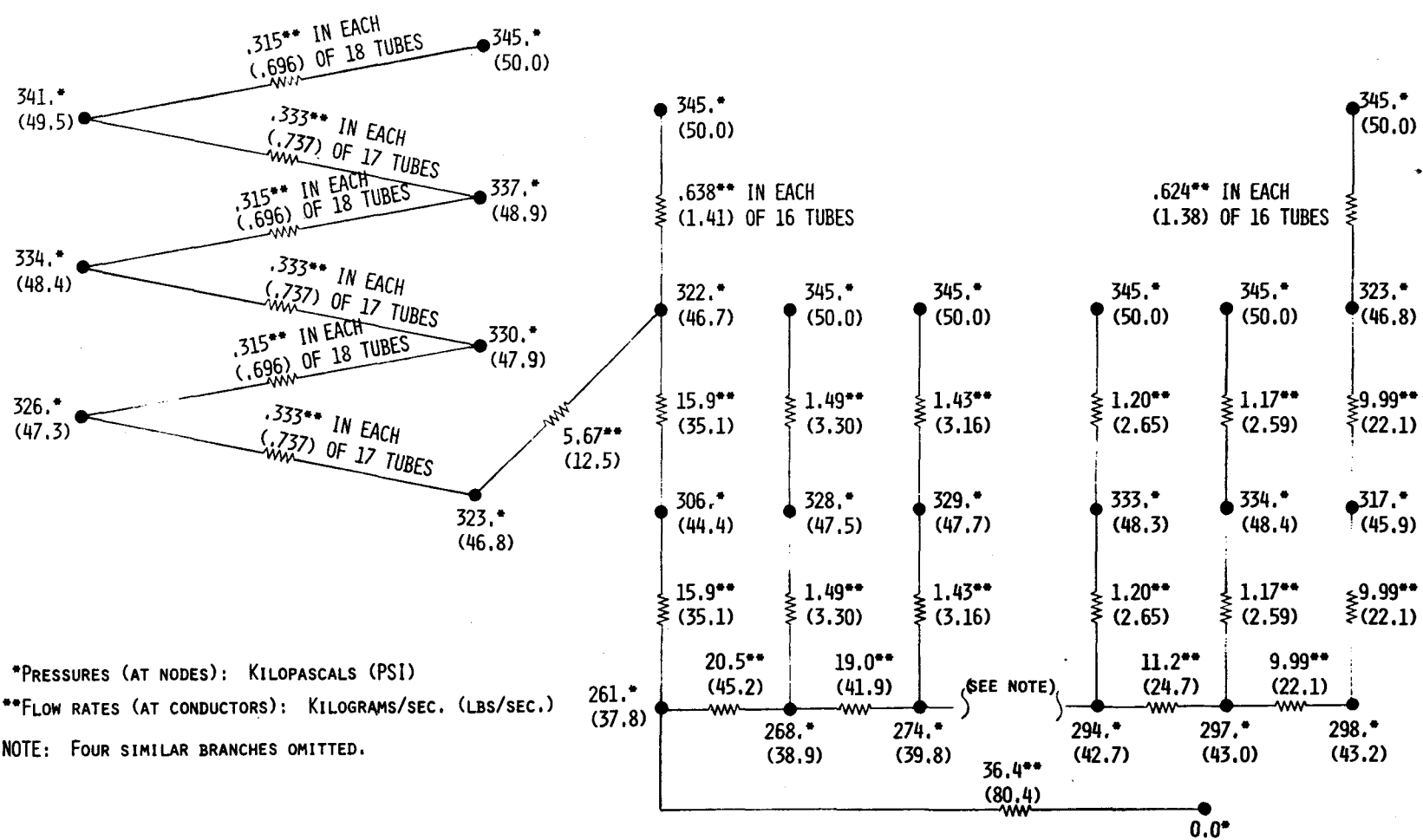


Figure III-71 Receiver SRE System Drain Time Thermal Model

analysis. The numerical technique employed by this program is the finite difference type with forward differencing, backward differencing, or control differencing algorithms available at the discretion of the analyst.

The nodal network describing the receiver system is given in Figure III-72. The model contains 71 nodes and 106 thermal conductors. All system components are modeled including the receiver, air cooler, pump, and interconnecting piping. The program checks at each time step to determine if the flow is laminar or turbulent. It then applies the forced convection film coefficient consistent with the flow regime. For this calculation, salt thermal physical properties are treated as functions of temperature. Three different types of thermal insulations are used throughout the system and their thermal conductivities are handled as temperature-dependent properties. Both forced and free convection losses are accounted for at the receiver and for these calculations, the air properties are varied with the film temperatures. Radiation losses from the receiver are made up of emission and reflection and the model is constructed so that sensitivity studies can be readily conducted relative to the influence of surface emissivity and absorptivity on these losses.

A finite time is required to accelerate and decelerate the flow after resetting the flow control valve. An example of this hydraulic transient is given in Figure III-73. Both the time lag to reset the valve and the "settling" time of the salt flow are accounted for in the model. Control strategies are easily programmed into the program logic and several approaches will be studied. Both the receiver outlet temperature control and the air cooler outlet temperature control will be investigated. An example of receiver transient performance, based on a preliminary model of the same basic approach as the MITAS model, is given in Figure III-74. This figure illustrates the receiver outlet temperature recovery to its nominal value of 566°C (1050°F) after a simulated cloud passage over a portion of the heliostat field, which reduces the insolation on the outlet third of the receiver by 25%.

7. Experimental Uncertainties

Two system uncertainty analyses were performed. One was on receiver efficiency uncertainties and the other on receiver convection experiment uncertainties.

Receiver efficiency is described as the output divided by the input, or:

$$\eta = \frac{\dot{m} C_p (t_o - t_i)}{Q_i}$$

The uncertainty of η is a function of the uncertainties of all of the parameters. C_p and Q_i are assumed to have fixed uncertainties of 2% and 5%, respectively, while \dot{m} and ΔT have varying uncertainties from 0% to 4% and 2°C to 8°C (3.6°F to 14.4°F). The uncertainty of η , the receiver efficiency, varied from 4.8% to 6.6% (Figure III-75 shows uncertainty of η for varying conditions). Thus, reasonably accurate calculation of receiver efficiency can be expected.

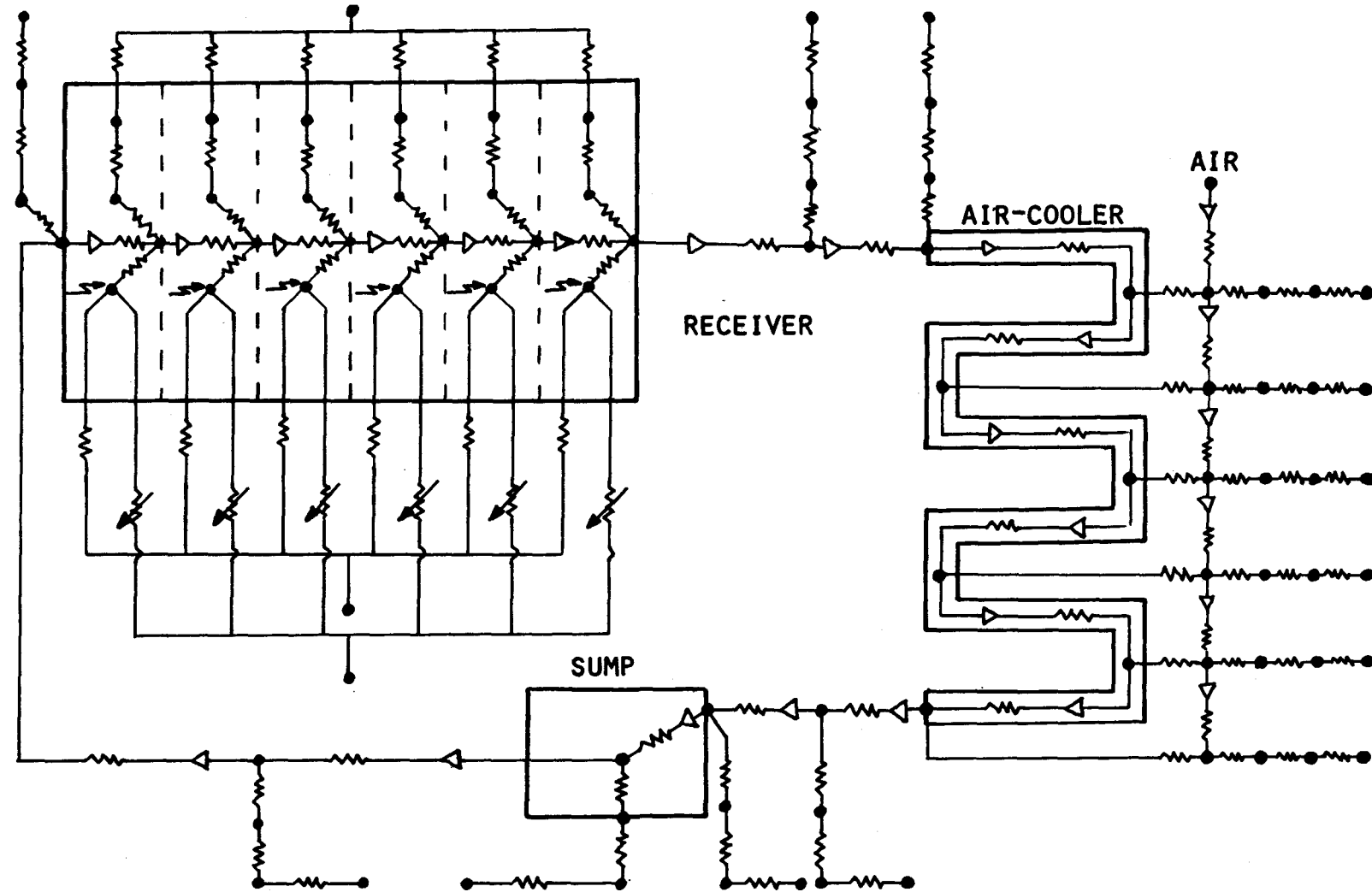
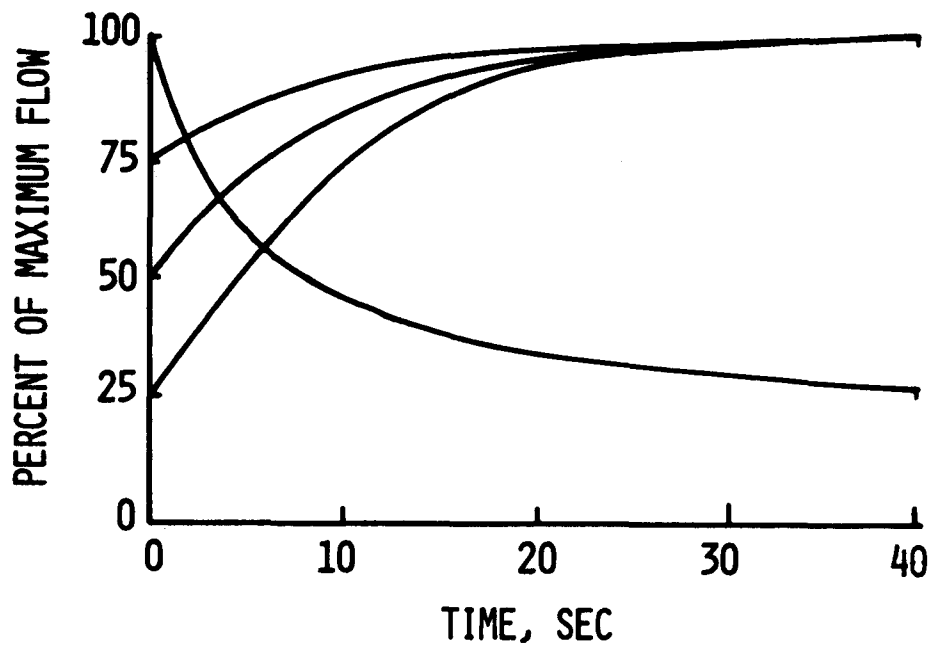


Figure III-72 Receiver SRE System Thermal Model



NOTE:

THE FLOW IS STEADY AT
TIMES LESS THAN ZERO;
AT TIME ZERO THE FLOW
CONTROL VALVE IS RESET.

Figure III-73. Receiver SRE System Hydraulic Flow Transients

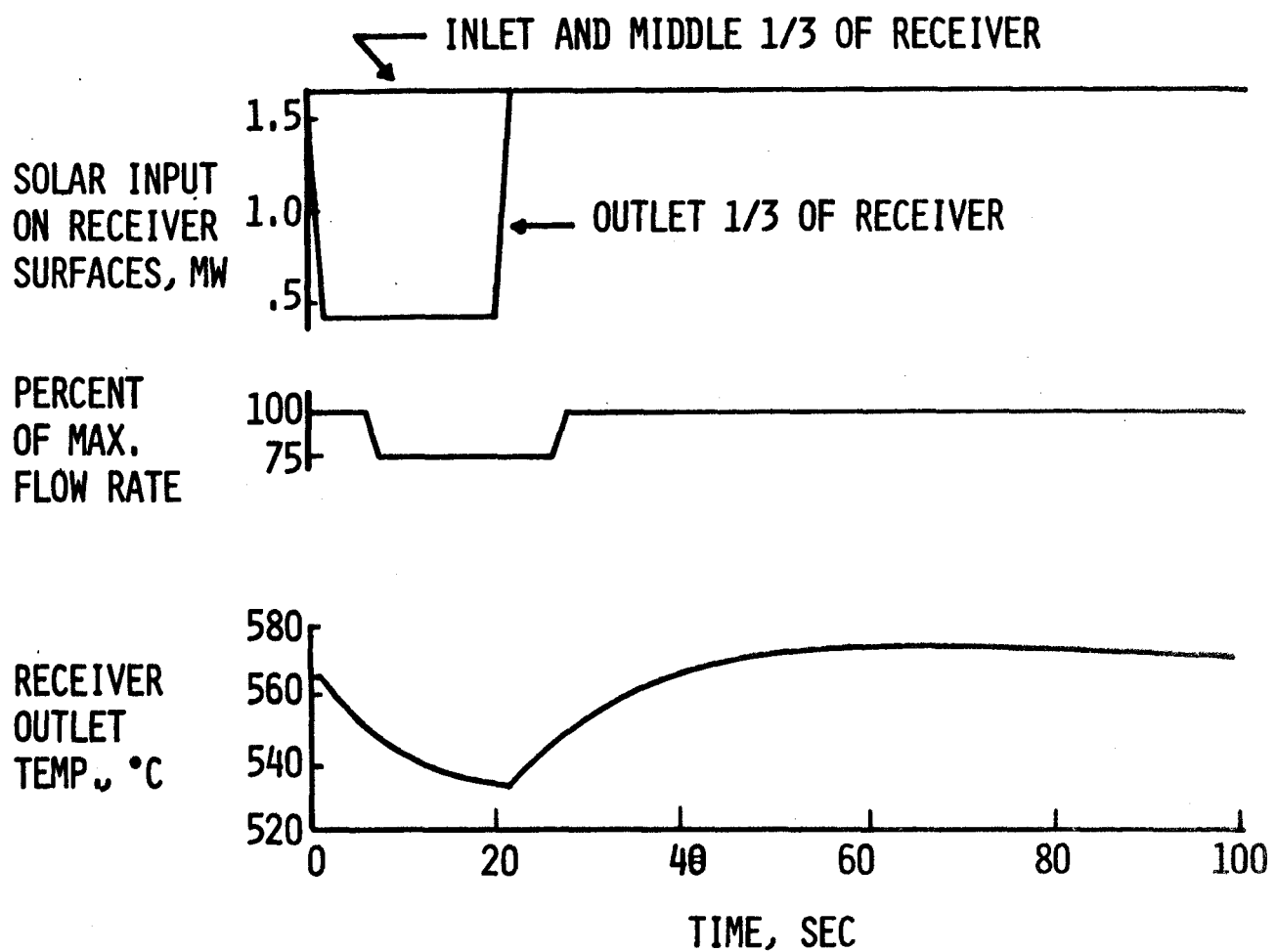


Figure III-74 Receiver Transient Performance during Cloud Passage

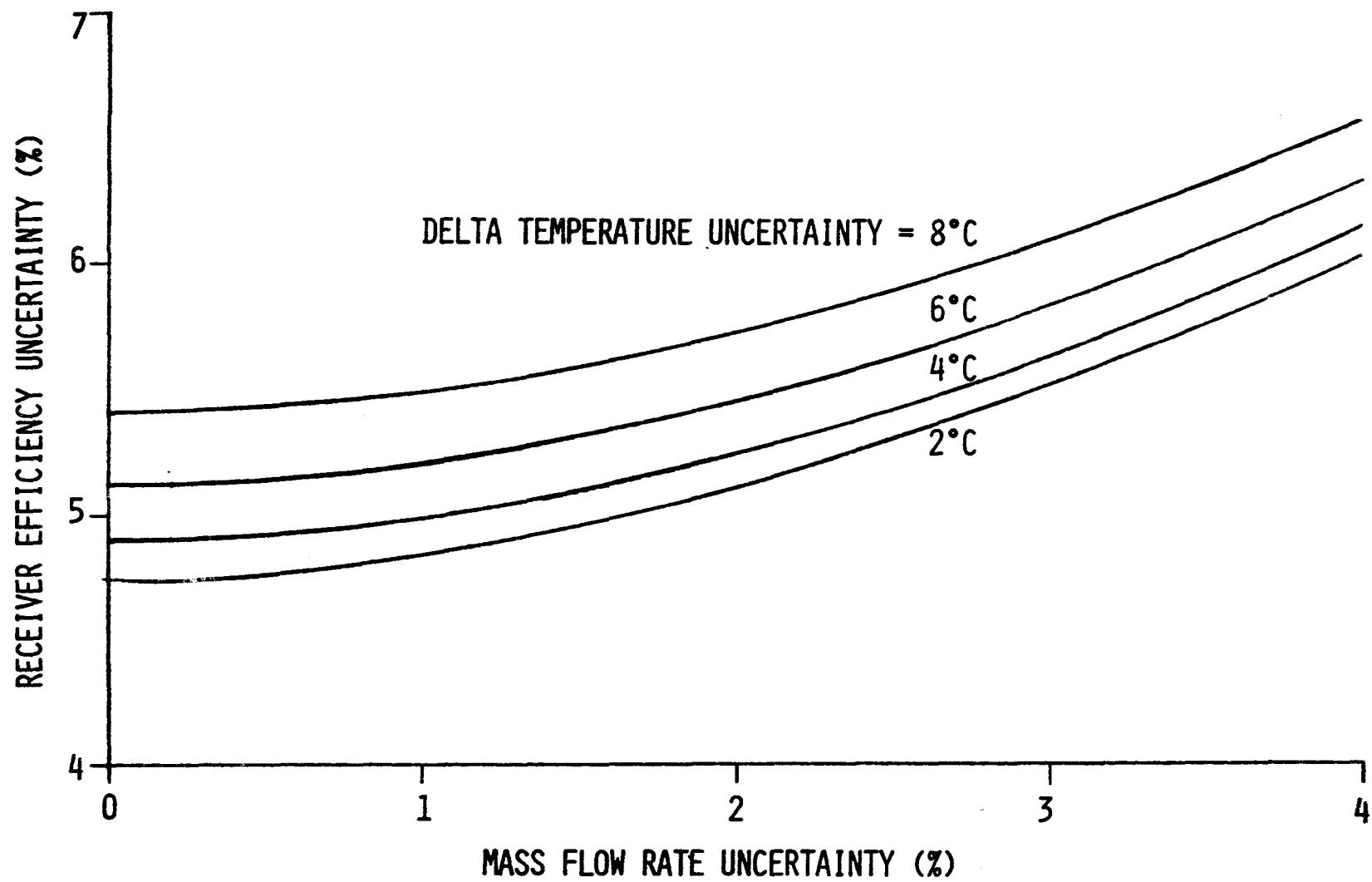


Figure III-75 Receiver Efficiency Uncertainty Analysis

The convection experiment was analyzed for uncertainty of h , the convective film coefficient. During this test, the receiver will be operated with no solar flux. By measuring the steady-state temperature drop of the salt flowing through the receiver, it is possible to calculate the convective heat transfer film coefficient, h . The steady-state energy equation is:

$$\dot{m} C_p (t_i - t_o) = hA (\bar{t}_r - t_a) + \frac{kA}{\Delta X} (\bar{t}_r - t_a) + \sigma \epsilon A (\bar{t}_r^4 - t_s^4)$$

The following parameters were assumed to have fixed uncertainties.

C_p , heat capacity of the salt = $1.55 \text{ kJ/kg} \cdot ^\circ\text{C}$ ($0.371 \text{ Btu/lbm} \cdot ^\circ\text{F}$) $\pm 2\%$

\bar{t}_r , average receiver temperature = $273.90^\circ\text{C} \pm 1.1^\circ\text{C}$ ($525^\circ\text{F} \pm 2^\circ\text{F}$)

t_a , ambient temperature = $10^\circ\text{C} \pm 2.78^\circ\text{C}$ ($50^\circ\text{F} \pm 5.0^\circ\text{F}$)

t_s , sky temperature = $1.1^\circ\text{C} \pm 11.1^\circ\text{C}$ ($30^\circ\text{F} \pm 20^\circ\text{F}$)

ϵ , receiver emissivity = 0.9 ± 0.05

The remaining parameters had variable uncertainties:

\dot{m} , mass flow rate = $2.52 - 8.82 \text{ kg/s}$ ($20,000 - 70,000 \text{ lbm/hr}$) ± 0 to 3%

$(t_i - t_o)$, temperature differential between inlet and outlet = $11.1 - 38.90^\circ\text{C} \pm 0$ to 11.1°C ($20 - 70^\circ\text{F} \pm 0$ to 2°F)

The operating range of the experiment is described in Figure III-76. Based on these curves of varying film coefficients, three design points were chosen to cover the possible range of operations. Presented in Figures III-77, 78, and 79 are the results of the uncertainty analysis at the three design points. Uncertainty of the film coefficient varied from 10% to 17% for the more common design points (below 5 kg/s (40,000 lbm/hr) and only increased to 27% for the worst-case situation. Expected uncertainties range from 11% to 13%, thus yielding excellent results.

8. Additional Thermal/Hydraulic Analyses

Additional analyses that have been done in support of the receiver SRE are listed below.

- 1) Heat tracing thermal analysis,
- 2) Auxiliary purge air requirements,
- 3) Auxiliary control air requirements,
- 4) Purge air and receiver tube air heating system pressure drops,
- 5) Transient insulation heating due to heliostat "scram",

- 6) Cavity insulation sizing,
- 7) Receiver back insulation sizing,
- 8) Heat transfer and pressure drop analysis of water-cooled aperture,
- 9) Updated analysis of receiver tube temperatures,
- 10) Software identification, and
- 11) Electrical power requirements.

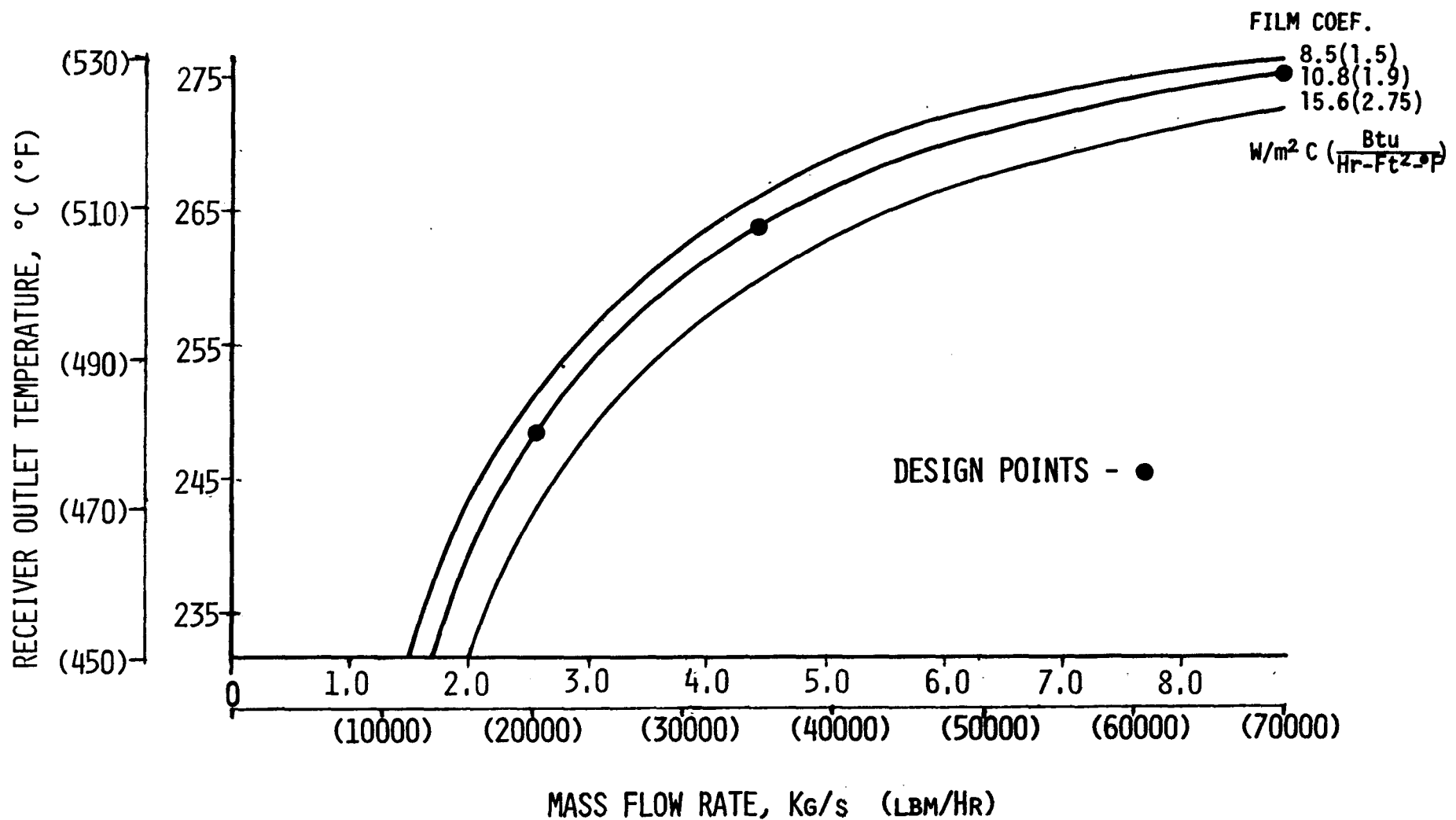
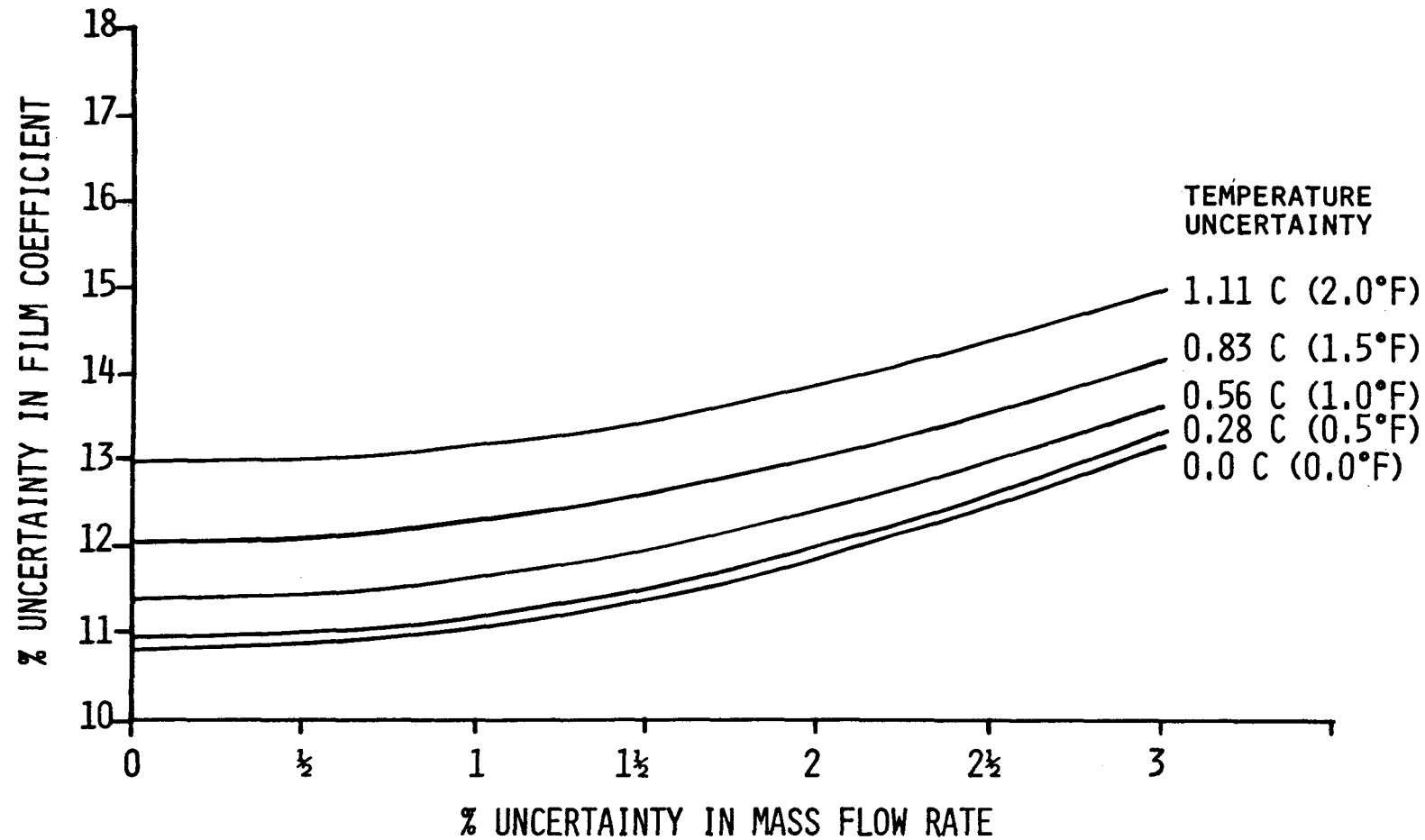
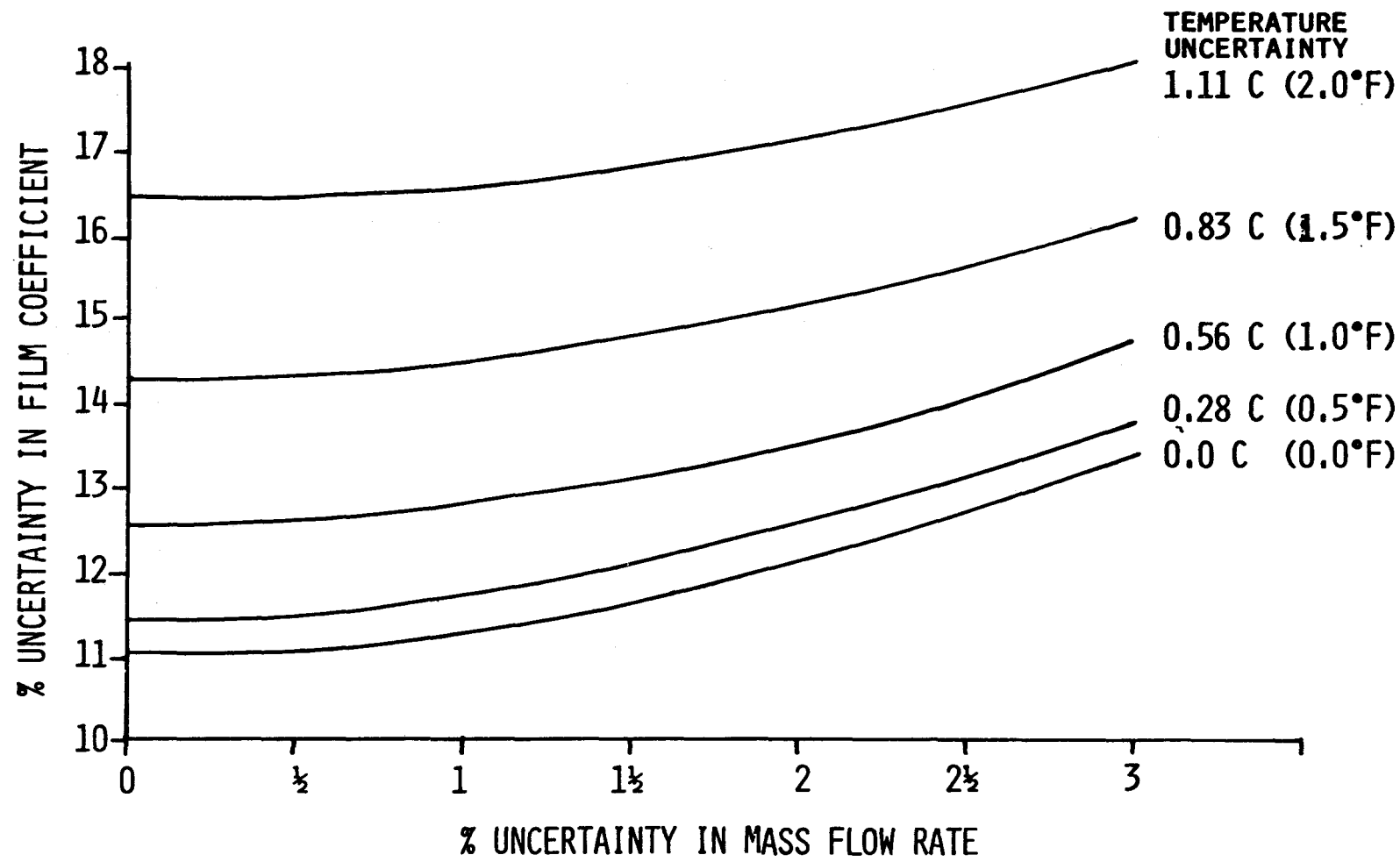


Figure III-76 Receiver Convection Experiment Parameters



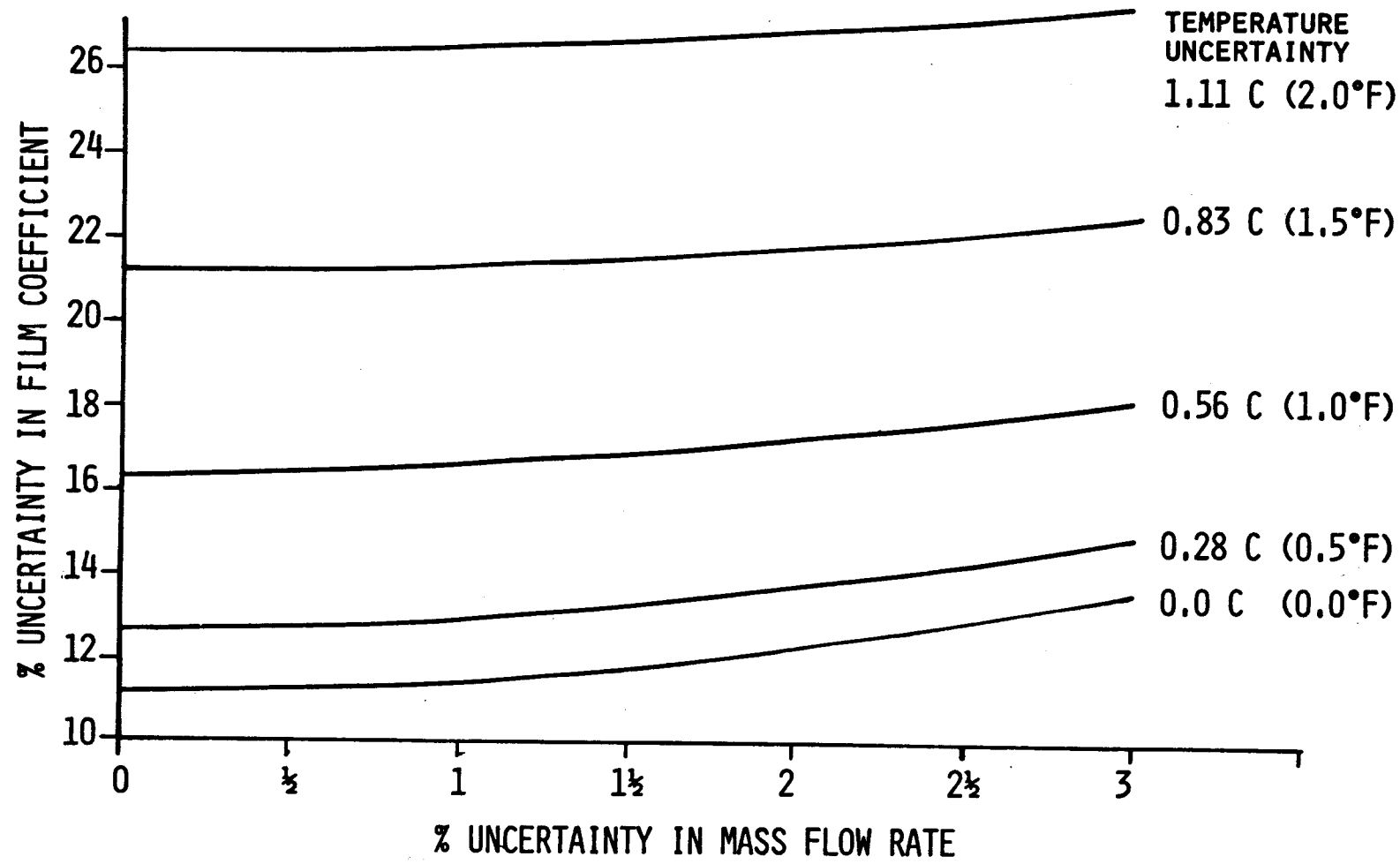
DESIGN POINT AT 2.52 Kg/s (20,000 LBM/HR)
TEMPERATURE DIFFERENCE ACROSS THE RECEIVER = 38.9 C (70°F)

Figure III-77 Receiver Convection Experiment Uncertainty Analysis



DESIGN POINT AT 4.41 Kg/s (35,000 LBM/HR)
TEMPERATURE DIFFERENCE ACROSS THE RECEIVER = 23.3 °C (42°F)

Figure III-78 Receiver Convection Experiment Uncertainty Analysis



DESIGN POINT AT 8.82 Kg/s (70,000 LBM/HR)
TEMPERATURE DIFFERENCE ACROSS THE RECEIVER = 12.2 C (22°F)

Figure III-79. Receiver Convection Experiment Uncertainty Analysis

F. STRESS ANALYSIS

The structural analysis discussed in this section was done to support the receiver SRE. Thermal stress analysis was performed on the receiver tubes because of the high solar flux impinging on the tubes. The heat flux reflected from the heliostats can raise the tube temperature up to 677°F (1250°F). Creep-fatigue damage to the material was also evaluated for the high temperature.

Receiver and cavity support structures were analyzed for critical wind loads of 44.7 m/s (147 ft/s) and the design was analyzed to meet ASME Section I design requirements.

1. Thermal Analysis and Creep-Fatigue Evaluation of Receiver Tubes

a. Design Criteria - The design guidelines for creep-fatigue damage on the tubes are based on the ASME Boiler Code, Code Case 1592. The total creep-fatigue damage is expressed as

$$\sum_{j=1}^P \left(\frac{n}{N_d} \right)_j + \sum_{k=1}^P \left(\frac{t}{T_d} \right)_k \leq 1.$$

where:

n - number of applied cycles;

N_d - number of design allowable cycles;

t - time duration of load condition, k; and

T_d - allowable time at a given stress intensity.

The creep-fatigue life of the receiver tubes is to be 30 years.

b. Analysis - The thermal stress analysis of the receiver tubes was performed using the finite-element computer program NASTRAN, which uses the temperature distributions around the tube to determine the thermal stresses at each point. The finite-element model used to predict stresses is shows in Figure III-80. Because of symmetry, only one-half of the tube was analyzed. The tube was divided into 96 isoparametric 'HEXA 8' elements. HEXA 8 is a three-dimensional, solid element in NASTRAN.

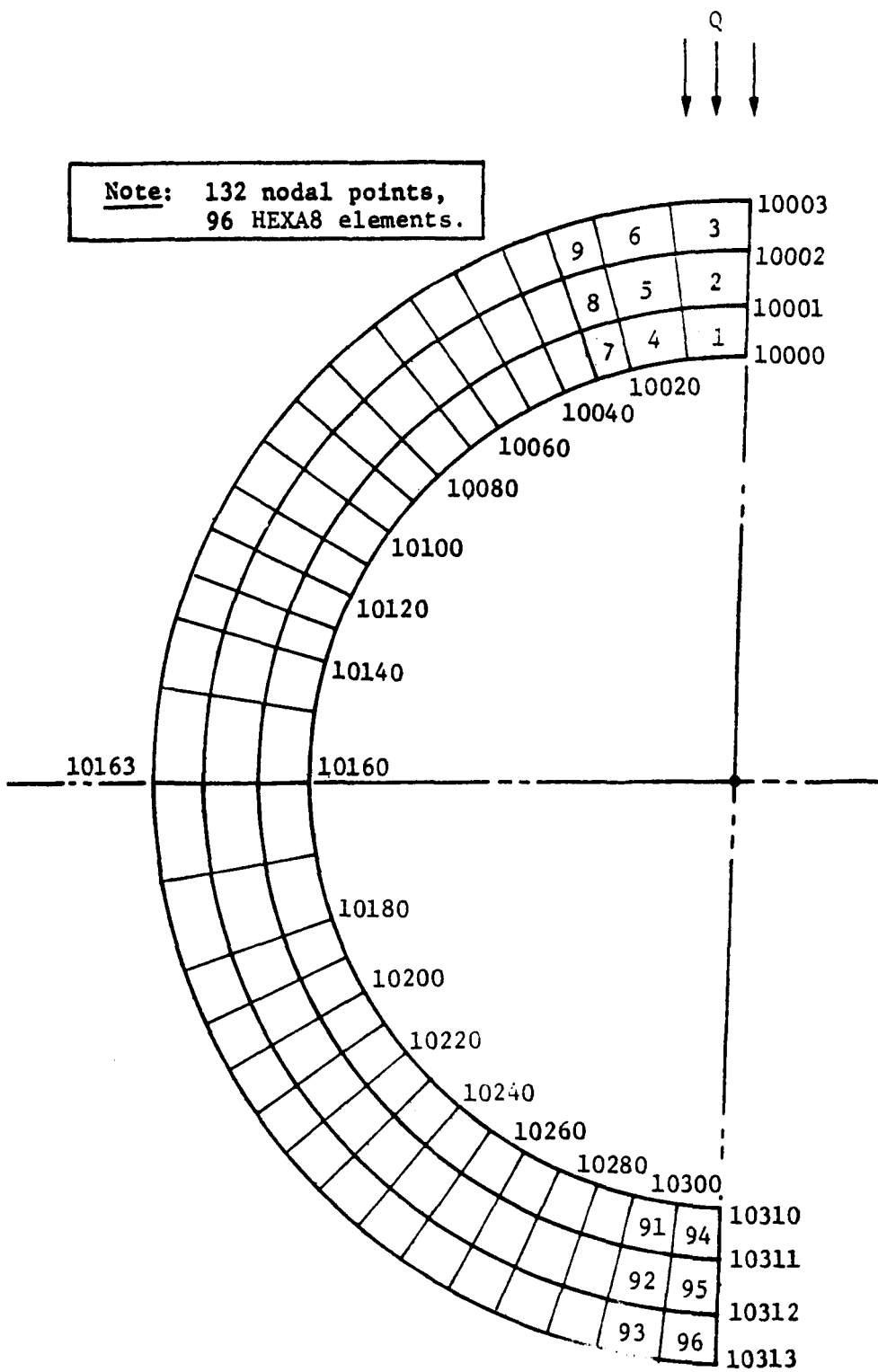


Figure III-80 Finite Element Model for Receiver Tube Stress Analysis

Very little information is available on Incoloy 800. Although Incoloy-800 is an acceptable material, the boiler code does not list creep and fatigue data for the alloy. The code does, however, show rupture life (T_d) and allowable cycles (N_d) graphs for Incoloy 800H. Since the material properties are nearly the same for 800 and 800H at 593°C (1100°F), the creep-fatigue data for 800H was used. This was justified by using the curves for slightly higher temperatures than the tubes are actually seeing, thus yielding conservative results.

As shown in the creep-fatigue damage equation, the creep-damage is defined as follows:

$$\Delta_c = \int_0^t \frac{dt}{T_d} = \frac{t}{T_d}$$

Accordingly, it would not be acceptable to simply determine the immediate stress level, find the corresponding allowable time, and therefore deduce that the total creep damage is $\Delta t/T_d$, where Δt equals the entire operation life. This is much too conservative an approach. In reality, the material is in a continuous state of creeping, or relaxing. Since the stress is strain dependent, the stress level is also continuously dropping.

In determining actual creep damage, the relaxation effect was accounted for by breaking the operating life into sufficiently small time intervals (as small as 1/10 of an hour during initial operation) and successively summing the ratios of Δt over the allowable time at the corresponding stress level. At each interval a new stress was found by using the Huntington Alloys Creep Ration Curve to determine the relaxing strain (creep) during that interval. The resulting summation represents a good approximation of the creep damage encountered during a given operation life.

Using this technique, the tubes were shown to be good for two and one-half cycles per day, ten hours per day, for 30 years; or a total of 27,375 cycles and 109,500 hours of operation:

$$\begin{aligned} \text{Fatigue Damage, } D_F &= 0.883 \\ \text{Creep Damage, } D_C &= 0.073 \\ 0.883 + 0.073 &= 0.956 < 1. \end{aligned}$$

(Note: N_d values for Fatigue Damage were found using Figure 1420-IC of Code Case 1592-10. T_d values for Creep Damage were found using Figure I-14.6C of Code Case 1592-10.)

2. Receiver Structural Analysis

a. Design Criteria - The receiver structure was designed according to Sections I and VIII, Division 2, of the ASME Boiler Code:

- 1) $P_m \leq k S_m$
- 2) $P_B + P_L \leq 1.5 k S_m$
- 3) $P_L + P_B + Q \leq 3 S_m$

where:

P_m = primary membrane stress intensity,

P_B = primary bending stress intensity,

P_L = primary local stress intensity,

Q = secondary (thermal) stress intensity,

S_m = allowable stress specified in the Boiler Code for given temperature, and

k = load condition factor (1.2 for wind).

Loading conditions applied to the receiver structure were:

1) Wind load - 44.7 m/s (147 ft/s), and

2) Seismic load - 1.5 gs applied to total weight.

b. Analysis - Thermal stress due to solar flux was analyzed for each individual tube of the receiver. Additional stress due to internal pressure and wind loads was calculated and combined with the thermal stress. The resulting moments are shown in Table III-4.

The upper and lower support headers were analyzed for both operating wind load plus flux load and for a 44.7 m/s (147 ft/s) maximum wind acting alone. The receiver tubes that are welded to the header stagger in a way that one tube comes in straight and the next in a 30 degree angle. Connection of tube and header was analyzed for bending stresses due to maximum wind load. The maximum stress was 107 MPa (15,500 psi) which is less than the allowable of 201 MPa (29,200 psi). The end plate of the header was analyzed for internal pressure and the stress was only 5.9 MPa (855 psi).

Each upper header support consists of two stainless steel flat plates. The thickness of each plate is 3.0 mm (0.125 in). The plates are welded to the header at one end and bolted to the fixture at the other end. Maximum moment at the fixed end was calculated to be 1072 Nm (908 ft-lbf) due to maximum wind with a corresponding stress of 143 MPa (20,800 psi) which leaves a 30% positive margin of safety for the plate. The lower header supports, on the other hand, are short, 3.8-cm (1.5-in) pipes welded to the lower header at one end with the other end free. The free end is restrained laterally only in the direction of the applied loads. The reaction force due to 44.7-m/s (147-ft/s) winds was calculated to be 552 n (124 lbf) and the stresses on both the pipe and the support angles were small compared with the allowables.

3. Receiver and Cavity Support Structures

a. Design Criteria - The factor of safety (FS) is defined by

$$FS = F_{ty}/f_{limit} \geq 2.0$$

Table III-4 Thermal and Wind Stresses on Receiver Tubes

		Flux	44.7 m/s (147 ft/s) Wind	17.9 m/s (58.7 ft/s) Wind	Flux + 17.9 m/s (58.7 ft/s) Wind
Moment at Top Header	Nm in 1b	+16.46 +145.7	-44.64 -395.0	-7.14 -63.2	+9.32 +82.5
Moment at Mid Span	Nm in 1b	+8.24 +72.9	+22.44 +198.6	+3.59 +31.8	+11.83 +104.7
Moment at Point 10	Nm in 1b	+6.33 +56.0	+25.19 +222.9	+4.03 +35.7	+10.36 +91.7
Deflection at Midspan	cm in	+3.188 +1.255	-5.019 -1.976	-.805 -.317	+2.383 +.938
Deflection at Point 10	cm in	+3.546 +1.396	-5.171 -2.036	-.828 -.326	+2.718 +1.070
Shear at Top Header	N 1b	-4.237 -.9525	+57.42 +12.91	+9.21 +2.07	+4.97 +1.12
Shear at Bottom Header	N 1b	+4.237 +.9525	+34.47 +7.75	+5.52 +1.24	+9.76 +2.19

Stresses were calculated using these moments and compared with the material allowables.

where F_{ty} is the allowable tensile yield stress and f_{limit} is the stress from either 44.7 m/s (147 ft/s) winds or 1.5 gs applied to the total weight.

b. Analysis - Both the receiver and cavity support structures are truss-type structures. Wide-flange beams were used as truss members. The receiver support structure was designed to support the vertical receiver tubes, which are welded together to form a bank of tubes in front of the truss. Normal maximum wind load was considered to be the most critical load and the stress was calculated for the maximum shear and/or binding at the critical member. The maximum stress calculated at the vertical member is 100.2 MPa (14,530 psi) which is less than the compressive yield allowable $F_{cy} = 241$ MPa (35,000 psi). Column buckling was also checked for the vertical members and the factor of safety is about 7. Welded attachment joints between cross and vertical members were analyzed and the stress is low. The natural frequency of the overall structure was determined to be about 15 Hz.

The cavity structure consists of four panels partly welded and partly bolted to the truss members. Maximum wind load was used as critical load for the analysis. The maximum stress calculated at the cross member of the top panel is 71.7 MPa (10,400 psi). The side panel stiffener maximum stress is 116.6 MPa (16,914 psi), which corresponds to a factor of safety greater than 2.0. The natural frequency of the cavity structure is about 26 Hz.

G. TEST PLANNING

In support of the planning for the receiver testing, we have completed a test plan draft, provided a draft of typical test procedures for several tests, and assembled a data package required by the CRTF.

1. Test Plan Summary

A list of the tests are in Table III-5. Checkout tests will be performed both in Denver and at ground level on the elevating module at CRTF. The majority of the checkout tests are on a component level, but the functional tests (CO-8 and CO-9) are system-level activities. The functional test with salt (CO-9) is designed to demonstrate that the system is ready for operation with a solar load.

Table III-5 Receiver SRE Tests

<u>Checkout Tests</u>
CO-1 Air Flow Distribution for Air Cooler (Denver)
CO-2 Hydrostatic and Leak Checks (Denver)
CO-3 Sump and Air Cooler Heaters (Denver)
CO-4 System Trace Heaters (Albuquerque)
CO-5 Thermocouples (Albuquerque)
CO-6 Functional Value Operation (Albuquerque)
CO-7 Electrical Control System (Albuquerque)
CO-8 Functional Test with Water (Albuquerque)
CO-9 Functional Test with Salt (Albuquerque)
<u>Preliminary Tests - Cavity</u>
1 PC-1 Partial Load - Tower Console Control
2 PC-2 Partial Load - Central Computer Control
3 PC-3 Maximum Load - Tower Console Control
4 PC-4 Maximum Load - Central Computer Control
5 PC-5 Maximum Load - Tower Console Control
6 PC-6 Maximum Load - Central Computer Control
7 PC-7 Partial Load with Emergency Shutdown
8 PC-8 Recovery from Simulated Cloud Passage
<u>Convection Tests - Cavity</u>
9 CC Convection Loss at 371°C (700°F)
<u>Performance Tests - Cavity</u>
10 PFC-1 Efficiency Tests at 35 to 100% of Maximum Load
11 PFC-2 Maximum Load for 20 hours
12 PFC-3 Recovery from Simulated Cloud Passage
<u>Performance Tests - Exposed</u>
13 PFE-1 Efficiency Tests at 45 to 100% of Maximum Load
14 PFE-2 Recovery from Simulated Cloud Passage
<u>Convection Tests - Exposed</u>
15 CE Convection Loss at 371°C (700°F)
<u>Special Tests - Exposed</u>
16 SE-1 Cycle Tests
17 SE-2 Endurance Test
18 SE-3 Extreme Cloud Conditions
19 SE-4 Lateral Support Shadowing
20 SE-5 High Localized Fluxes

At the conclusion of the checkout tests, the experiment will be taken to the 61-m (200-ft) level of the tower where all the remaining tests will be performed. The receiver will be tested first in the cavity configuration followed by tests in the exposed configuration. This sequence was chosen since the cavity is much safer than the exposed configuration relative to salt freeze-up problems. This is because the cavity is fitted with doors that will be closed during shutdown operations. With these doors shut, heat will be retained in the receiver for a considerably longer time than in the exposed configuration and therefore the risk of salt freeze-up is significantly reduced, an important consideration both in normal and emergency shutdown situations.

Preliminary tests are designed to be "shake down" tests and will provide the test crew with experience in controlling and operating the experiment. Performance tests will yield efficiency data for both the cavity and exposed configurations and demonstrate the ability to recover from cloud interruptions. Results from the performance tests will be used to estimate losses, but separate convection tests will be conducted to gain as much data as possible relative to the convective processes. Separate convection tests will be conducted with all the heliostats offline so that the uncertainty relative to the solar load can be eliminated from the energy balance on the receiver. The special tests are performed at the end of the test program since they will excessively stress the receiver. These tests will demonstrate the ability of the receiver to withstand load cycling and to operate at full load for a substantial length of time. Also, certain extreme conditions will be explored during the special tests such as high-flux conditions. The entire receiver test plan is included in Appendix A.

2. Test Procedures

Detailed step-by-step operating procedures will be written and integrated with the CRTF operating procedures. Example procedures for three typical tests were provided to Sandia and we are currently writing procedures for all the tests.

3. Data Package

A data package for the receiver SRE has been provided to CRTF. Contents of the package are shown in Table III-6.

H. FABRICATION

1. Receiver Subassembly

The receiver subassembly, without the support frame, is shown in Figure III-81. It was fabricated in accordance with the requirements of Section I of the ASME code. Use of the ASME code required that the following provisions be followed:

Table III-6 Receiver SRE Data Package Contents

SCOPE AND OBJECTIVES

- Test Article Description
- Operating Parameters
- Summary Schedule
- Expected Results

DESIGN DESCRIPTION

- System Components and Specification
 - Receiver
 - Cavity Structure
 - Air Cooler
 - Sump Tank
 - Pump
 - Lines
 - Air Heater
 - Control Console
- Drawings
- Engineering Analyses
 - Receiver Analyses
 - Solar flux
 - Stress and fatigue
 - Thermal/hydraulic
 - Air Cooler Analyses
 - Line Analysis
 - System Analyses

SAFETY ANALYSIS

- Failure Modes and Effects
- Hazards to Personnel and Equipment

QUALITY ASSURANCE

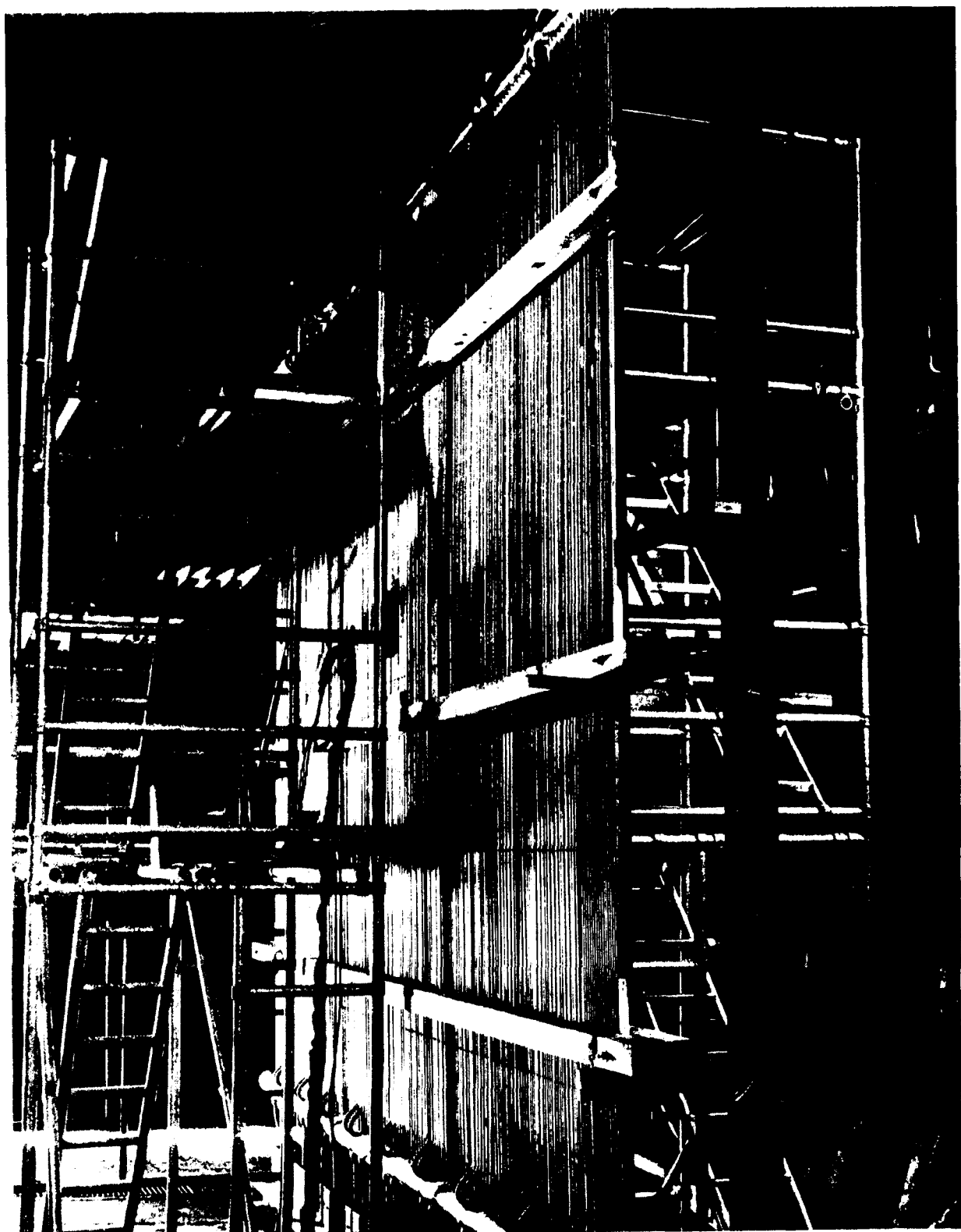


Figure III-81 Receiver Tubes and Headers Subassembly

- 1) Only certified and traceable material was used in the fabrication process;
- 2) Weld procedures were developed and both machines and welders were certified;
- 3) Various types of NDE (Non-Destructive Examination) were made of the final assembly; and
- 4) Following a hydrostatic pressure and leak test, the final assembly will be certified and given a code stamp.

The header sections were the first parts to be fabricated. After the sections were cut to the proper length, the end closure plates were welded in and each section was hydrostatically tested to 2.4 MPa (350 psig). Each section was then sent to an outside machine shop where all of the holes were machined in accordance with design requirements.

The receiver absorber tubes were purchased in random lengths and some of them had to be welded together to make up the required length. All welded tubes were hydrostatically tested to 2.4 MPa (350 psig) after welding. All tubes were sent to an outside vendor in Los Angeles for forming. To be able to weld all around each tube upon installation and still have the tubes fit side by side in a single plane, each tube had to be offset on one end, and in some cases on both ends. This was a critical process since the tubes had to fall into a single plane after installation. Thus each tube had to be offset exactly the same amount.

The header sections and tubes were then made ready to go together as an assembly. A carbon steel support fixture was fabricated to act as a support for the upper and lower header sections. The upper header sections with their flexure beam supports were installed first. The support fixture was carefully leveled and secured in place. Using transit and plumb lines, the bottom header sections were positioned and secured in place on their pipe supports. Welding the tubes in place started at the center and progressed toward both ends of the receiver. Each weld was dye-penetrant checked by quality control and necessary repairs were made. During the welding process, restraining fixtures were put between the header sections to prevent them from moving.

After the tube-to-header welds were completed, the header drain and purge lines were installed. A line for each drain and purge valve was welded to each header section. These lines were capped to allow hydrostatic testing of the completed assembly.

Next, the tubes were joined together to control cracks or open areas between them. The wood beams shown in Figure III-81 were used to align the tubes prior to starting the joining process.

The tube joining requirement was thoroughly studied before being started. Brazing with high-temperature filler alloy was first studied and test specimens for evaluation were made. All forms of brazing were dropped after testing showed that the joints were very brittle. It was thought that the thermal cycling of the tube assembly would cause the joints to crack. It was also very difficult to control the size of the fillet.

An evaluation of tungsten inert gas (TIG) weld joints was done and this proved to be the best way to join the tubes. Specimens were made and tested for strength and criteria were developed to control joint configuration. All welders were certified in accordance with the criteria before being allowed to weld on the receiver tubes. The tubes were joined together by approximately 3500 small weld joints in the configuration shown in Figure III-82. Each weld was checked to assure that it fell within those requirements. Figure III-83 is a closeup of the welded receiver tubes.

Clips were also welded to the back of some of the tubes to provide support for the heat flux sensors and LVDTs. The heat flux sensors will protrude between the tubes to the front surface of the receiver by means of a small dimple in the tube wall.

2. Main Structure

The main support structure shown in Figure III-84 consists of two structural steel towers that will be bolted together at the top and then secured to the floor of the CRTF elevator module. The towers were fabricated as completely welded assemblies and all of the structural steel meets the specification requirements as set forth in ASTM A-36. The towers were assembled in the horizontal position and then were set upright on a level surface where dimensional fit checks were made between them and the receiver support structure. These towers will be positioned directly in front of the air cooler and will serve as the primary support for the receiver subassembly. The receiver support frame will be bolted to the face of the towers after they have been installed on the elevator module. Also, a lot of the interconnecting piping, valves, access ladders, and platforms will be supported from the towers.

3. Air-Cooled Heat Exchanger

The heat exchanger assembly shown in Figure III-85 consists of four major parts: a fan housing assembly, tube bundle assembly, movable louver assembly, and movable insulated door assembly. The fan housing assembly was slightly modified to meet the requirements of this program and a new tube bundle was fabricated by the Happy Division of Therma Technology, Inc. (Tulsa, OK).

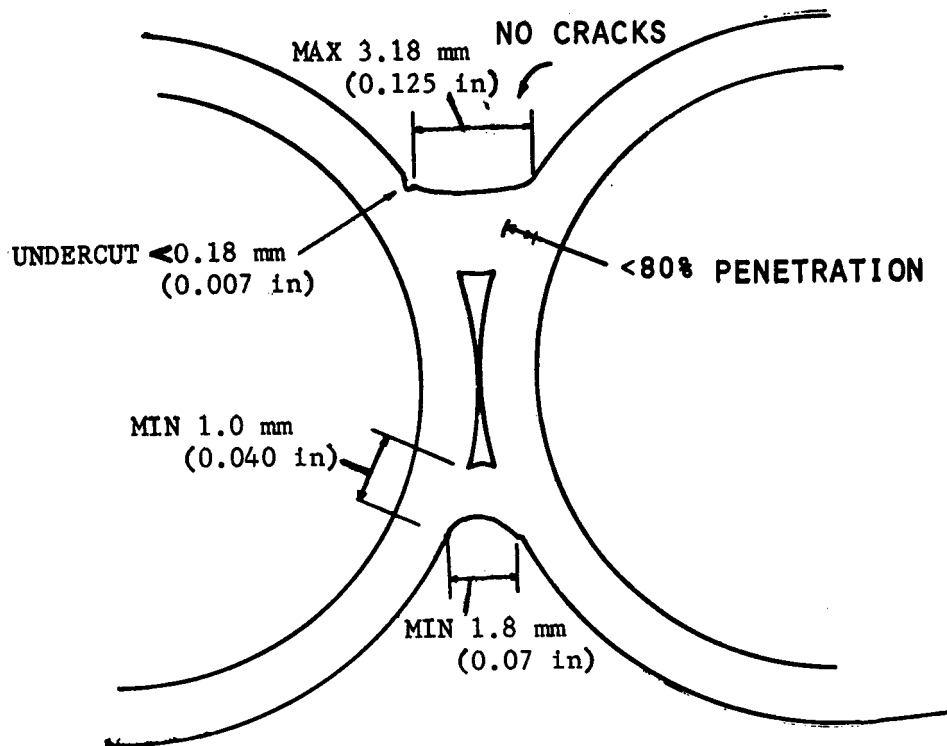


Figure III-82 Receiver Tube Weld Requirements

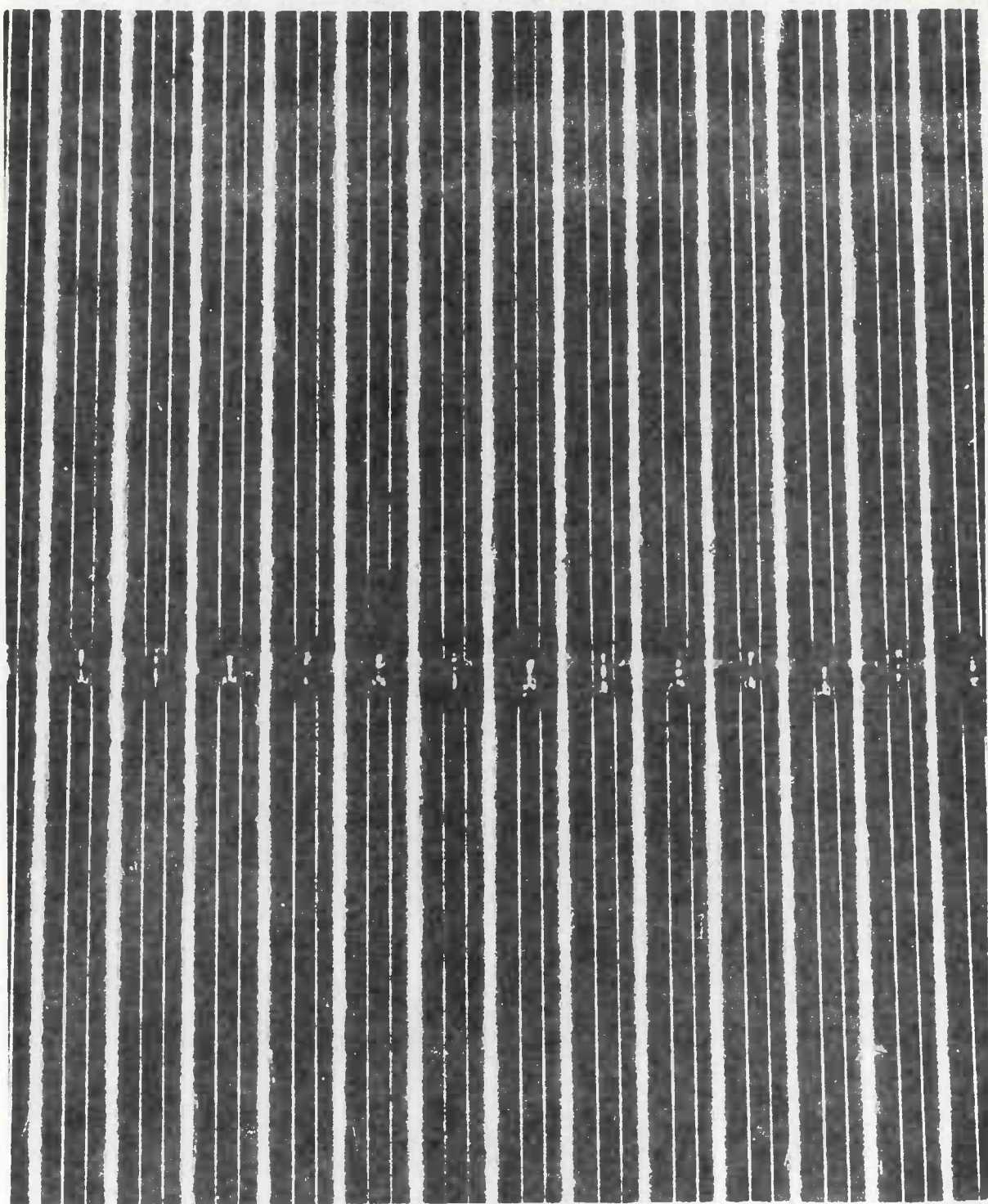


Figure III-83 Welded Receiver Tubes

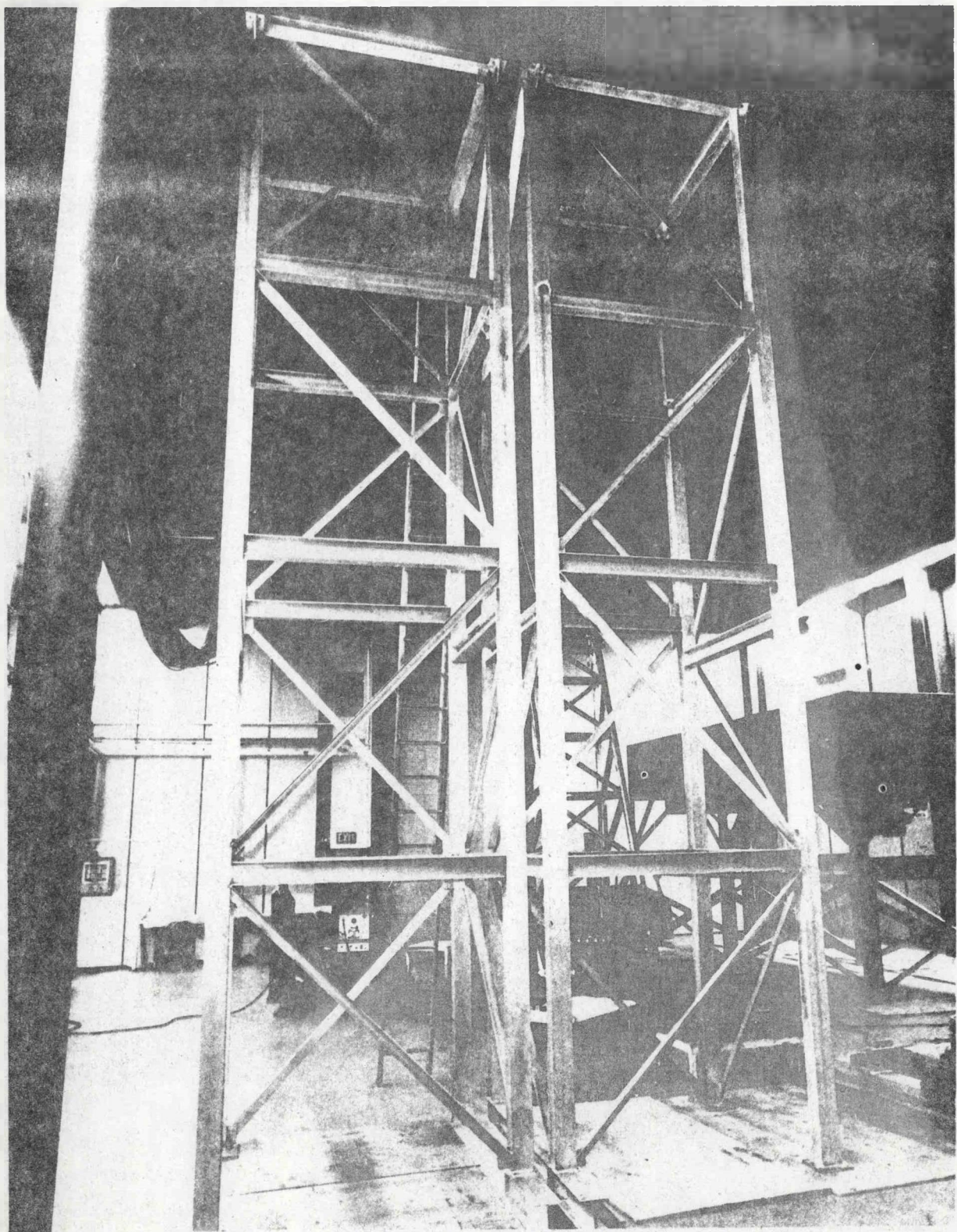


Figure III-84 Receiver Main Support Structure

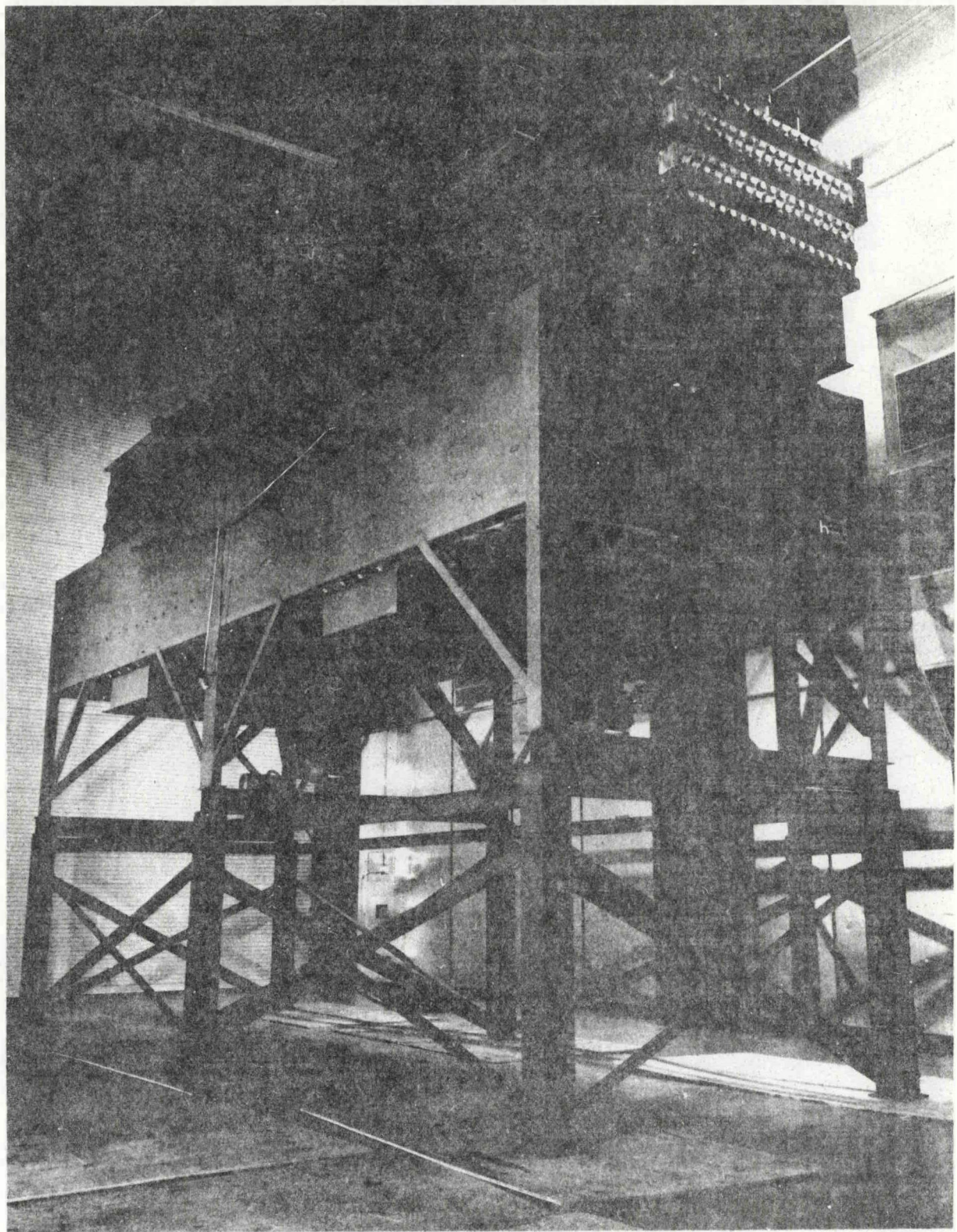


Figure III-85 Air-Cooled Heat Exchanger

The tube bundle assembly (Figure III-86), fabricated in accordance with the requirements set forth in Section VIII of the ASME code, is certified and stamped. Tubes and headers are constructed entirely from 316 stainless steel. The headers are rectangular and the seal area is extended to maintain a seal as the tubes and tube sheets thermally expand and contract. The individual tubes are first pre-rolled to a snug fit in the tube sheet of each header and then are seal welded to the tube sheet. The structural tie between the tube and tube sheet is accomplished by the tube rolling operation, which consists of inserting a mandrel into the end of each tube and expanding it against the tube sheet. The tube-to-tube sheet welds are then leak tested by means of a halogen leak tester using Freon-12 as a tracer gas. Each tube is then given a final roll to ensure a good structural connection with special care being taken not to overroll the tubes.

The individual headers are assembled within a framework and all tubes within a header assembly are fit in place before any tube rolling is done. The headers are also shown in Figure III-86. The outside plate on each header is called the plug sheet. There is a hole through the plug sheet in line with each tube allowing for installation of the rolling tool. The headers are then hydrostatically tested to 3.36 MPa (488 psi) by installing plugs in each hole in the plug sheet. The plugs in the plug sheet are welded in place and leak tested with a halogen leak tester. After all of the headers have been assembled within the support frame, the complete assembly is given a final halogen leak test with Freon-12 as the tracer gas.

If a leakage problem should develop with any of the tubes at the test site, there is a standard procedure for either plugging the tube or removing it and replacing it with a new tube. Access to a particular tube can be gained by grinding out the weld around the plug on the plug sheet, which is in line with the tube in question.

The louver assembly shown in Figure III-87 is fabricated within a support frame and attaches to the underside of the coil bundle. The insulated doors will be fabricated from standard materials by the vendor. The doors will set on rollers that ride in tracks extending across the top of the tube bundle. The doors can be moved remotely by means of pneumatically-actuated cable cylinders.

4. Pump/Sump Assembly

The sump, shown in Figure III-88, is fabricated from SA-285 Grade C alloy steel and is a completely welded assembly. Even though it is not an ASME-coded vessel, it was fabricated by the same processes and procedures as were used in fabricating the receiver subassembly. The pump, (Figure III-88) attaches to the flanged connection on the top of the sump by means of 28 3.2-cm (1.25-in.) diameter bolts. The pump, a standard design for this service, was manufactured by the Lawrence Pump Company and was completely assembled and checked out by the manufacturer prior to shipment. The pump will be fit checked to the sump prior to shipment to the test site.

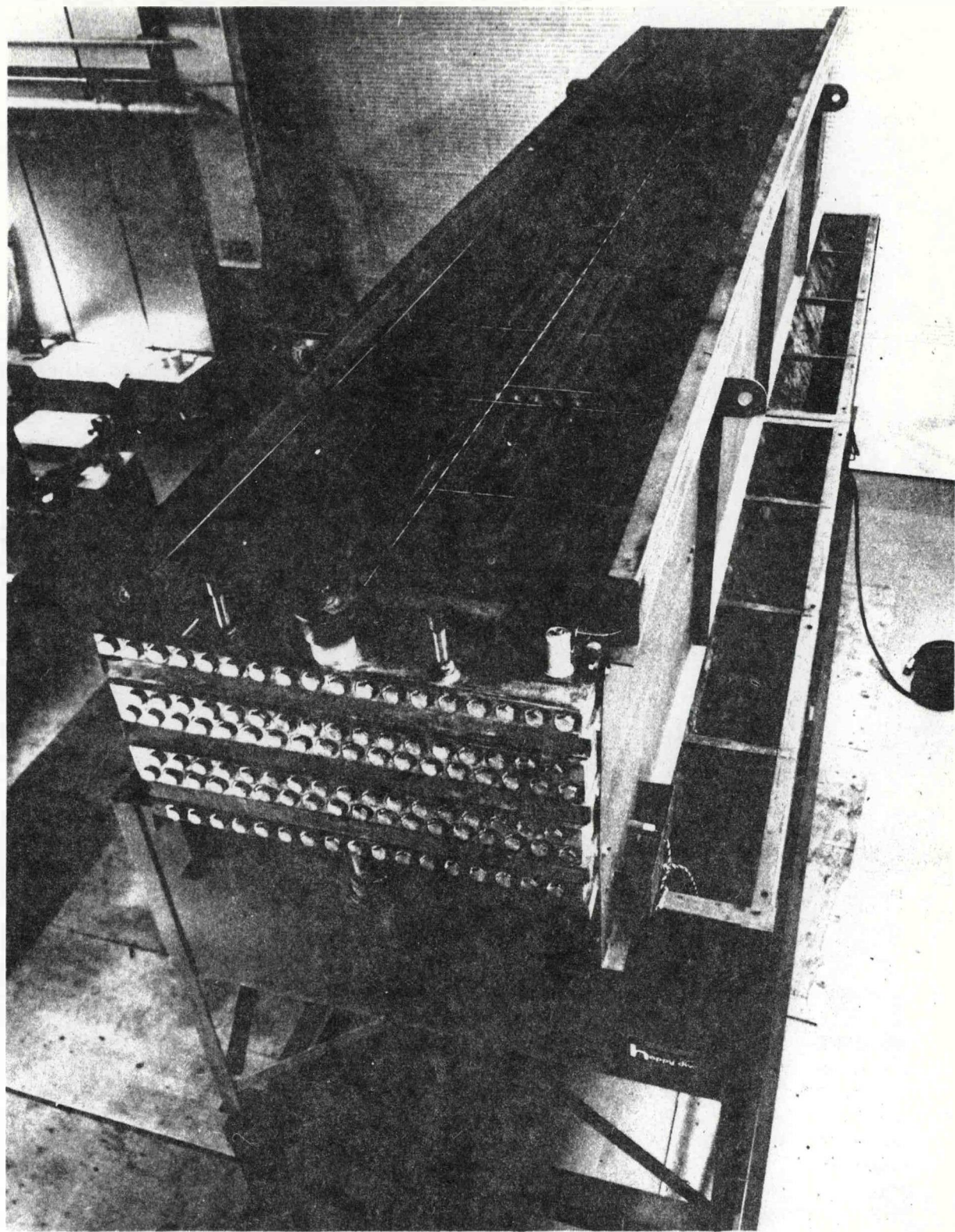


Figure III-86 Air Cooler Tube Bundle Assembly

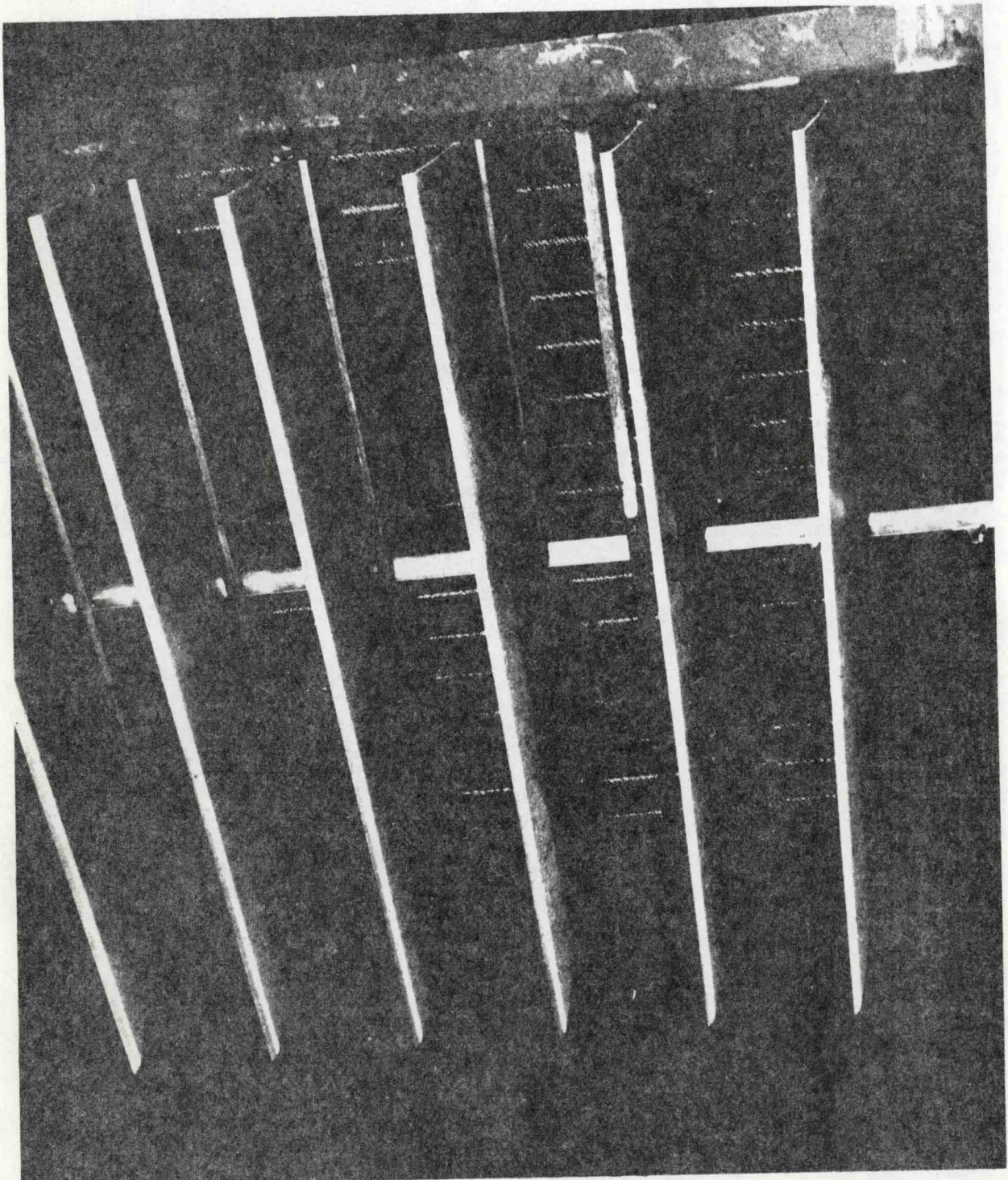


Figure III-87 Air Cooler Controllable Louvers

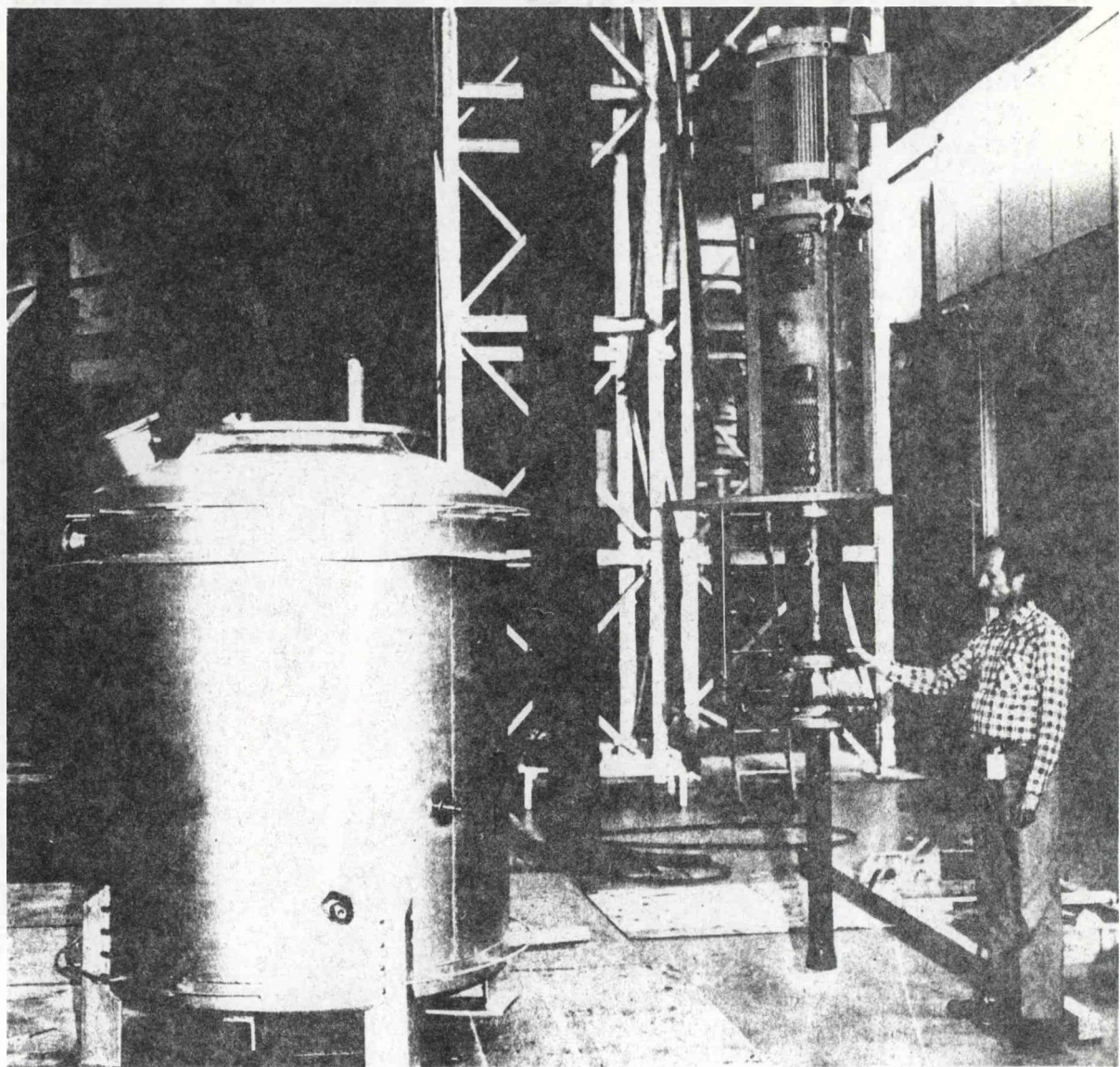


Figure III-88 Molten Salt Sump and Vertical Cantilever Pump

5. Control Console and Electrical Cabinets

The main control console (Figure III-89) is fabricated from carbon steel angle and channel that is welded together to form a frame assembly. Closure panels are bolted to all sides of the frame and a systems flow schematic engraved into the front face of the console. Cutouts throughout the flow schematic accommodate all the switches, indicator lights, and component control devices needed to operate the system during test. All of the components within the console are of standard off-the-shelf design. The components are wired to terminal strips mounted inside of the frame assembly by means of single conductor stranded wire. All connections are either soldered or screw-lugged.

Another smaller console, constructed in much the same manner as the main control console, contains indicator lights and switches for actuation of the trace heating circuits. It also contains the multipoint recorders used to monitor system temperatures during warmup. The signal conditioning equipment required to support the operation of the calibration pot load cell is also housed within this smaller console.

There are several junction box cabinets that are installed in the system for various reasons. There are four thermocouple junction boxes mounted on the back of the receiver support structure. All thermocouple lead wires are terminated inside of one of these junction boxes and at this point the wire is changed to a heavier gage and is referred to as thermocouple extension cable from the junction box back to the control center. There is a 0.9-m x 1.8-m (3-ft x 6-ft) steel junction box containing all the circuit breakers, contactors, fuses and relays that control and transmit the AC power required throughout the system. Another junction box, 1.8-m x 1.8-m (6-ft x 6-ft) contains all of the fuses, contactors, and relays required for operation of the system valves and flow control devices.

6. Cavity Assembly

The cavity assembly is a free-standing structure in front of the receiver assembly consisting of a frame with closure panels, two movable doors, a water-cooled aperture, and the RTAF. The cavity completely shields the receiver tube assembly. The cavity frame and panels are completely welded assemblies constructed entirely of carbon steel. The doors and their respective frames connect to the front of the cavity frame and are constructed of both carbon and stainless steel. The doors may be opened or closed using pneumatic actuators that are activated from the main control console. In case of an emergency shutdown during test operations, the doors would immediately be closed, preventing the receiver tubes from cooling as quickly as they would in an exposed configuration. The water-cooled aperture sits in front of the cavity doors and absorbs most of the stray energy that does not pass through the opening in the cavity. The RTAF, which is a water-cooled, Sandia-furnished structure sits in front of the water-cooled aperture. It contains a movable rake with many heat flux sensors attached. The rake moves back and forth across the cavity opening and maps the distribution of energy received from the heliostats. The total cavity assembly can be removed from the setup so that the receiver can be tested in an exposed configuration.

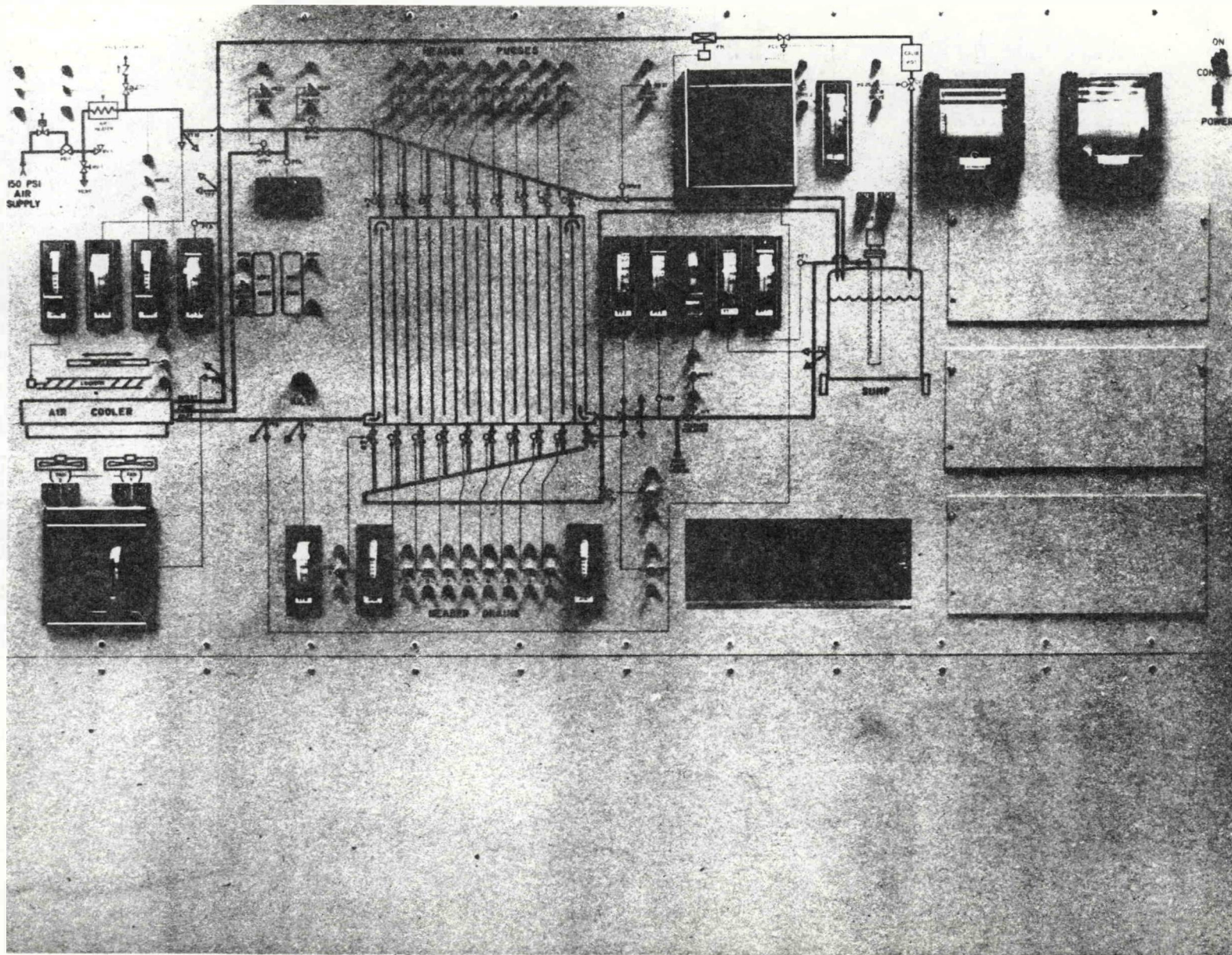


Figure III-89 Receiver SRE Main Control Console

7. Plans for Assembly and Checkout at the CRTF

All major subassemblies will be assembled as much as practical at Martin Marietta in Denver, with over-the-road transport being the limiting factor. The receiver tube assembly will be completely assembled, heat traced, instrumented, and will receive its ASME certification stamp prior to shipment to the CRTF. The air cooler and sump assemblies will be completely assembled and thermally checked before shipment to the CRTF. All piping sections will be partially assembled in Denver before shipment to CRTF. The control console and each of the components connected to it will be checked before shipment. Since there are no complete system-level checkout tests planned in Denver, the full integrity of the system to operate with molten salt will not be determined until the system is completely assembled at the CRTF.

After arriving at the CRTF, the complete system will be assembled on the elevator at ground level. This assembly operation will involve a combination of personnel from Martin Marietta and the CRTF. Verification of the operational readiness of the system will first be demonstrated by a series of water flow tests. These tests will show that the system is leak tight at low temperature, that all components will function upon command, and that instrumentation will respond to a change in temperature. These tests will be followed by a series of molten salt checkout tests also at ground level and without any heliostats. These tests will verify the integrity of the system to operate properly with molten salt up to 288°C (550°F). After these tests, the elevator module will be raised to the top of the tower and formal testing with solar energy, as described in the test planning section of this report, will be conducted.

IV. MATERIALS SUBSYSTEM RESEARCH EXPERIMENTS (SREs)

The Phase II materials SREs are designed to evaluate the compatibility of candidate solar thermal power plant construction materials with molten salt (60% sodium nitrate, 40% potassium nitrate) used as the solar heat transfer medium and storage fluid. This test program is a follow-on to testing begun in Phase I. The Phase II tests give more information on long-term compatibility of materials under thermal and fluid flow conditions representative of a commercial solar thermal power plant.

These experiments comprise two major efforts: the molten salt pumped fluid loop, and the static materials compatibility tests. The test plans for these can be found in Appendix B.

A. LONG-TERM MOLTEN SALT FLOW LOOP

1. Objectives

The purpose of the molten salt flow loop is to simulate the thermal and fluid flow characteristics of a full-scale solar central receiver power system to permit the study of materials compatibility and salt stability in a dynamic system. Specifically, the loop simulates:

- 1) Fluid velocity--3.5 m/s (11 ft/s) in the vicinity of the material samples,
- 2) Temperature profile--566°C (1050°F) at the hot end of the loop, 288°C (550°F) at the cold end, and
- 3) Materials--the loop is constructed of Incoloy 800 at the hot end and A516 carbon steel at the cold end.

The loop is designed to allow for the insertion and removal of sample coupons at various points in the flowing salt stream for analysis at 1000-hr intervals during the test. This dynamic testing will permit the investigation of:

- 1) Mass transport phenomena (if any) from the high to the low temperature part of the loop;
- 2) Materials compatibility and erosion in a flowing molten salt system;
- 3) Chemical stability of the molten salt in a flowing, thermally-cycled system; and
- 4) Electrolytic corrosion phenomena (if any) in a flowing molten salt system.

2. System Design

Figure IV-1 shows a schematic of the molten salt flow loop. The sump contains molten salt maintained at 288°C (550°F). A cantilever pump pumps the salt through the inside tube of a counterflow heat exchanger where it is heated to 482°C (950°F). The salt is heated to 566°C (1050°F) in a three-stage electric resistance heater tube, then cooled to 371°C (700°F) as it passes through the outer tube of the counterflow heat exchanger. It then flows through a finned-tube forced convection air cooler and is returned to the sump at 288°C (550°F). Seven sample ports are located at various points along the test loop to permit insertion and removal of metal coupons and salt sampling.

Figure IV-2 shows the assembled flow loop. The pump and sump are located at the lower left. The three long legs of the counterflow heat exchanger can be seen at the left and the heater is at the top left. The air cooler is near the center of the photo and the control console is at the lower right.

Figure IV-3 shows the cantilever pump on the molten salt sump. The sump is a stainless steel tank, 0.76 m (30 in.) in diameter and 0.76 m (30 in.) high, and holds the entire inventory of salt for the fluid loop, 0.34 m³ (12 ft³). To maintain the salt at 288°C (550°F), the sump is wrapped with temperature-controlled band heaters (which can be seen in the figure) and covered with fibrous insulation. The tank is vented to the atmosphere through a CO₂ and water vapor scrubber to prevent salt contamination.

The pump motor is rated at 5.6 kW (7.5 hp) and drives a cantilevered 316 stainless steel impeller and shaft. There are no bearings or seals submerged in the salt.

The heat exchanger is a counterflow tube-in-tube type. The inner tube is 1.9-cm diameter x 1.7-mm wall (0.75-in. diameter x 0.065-in. wall) Incoloy 800 tube, and is concentric with the outer tube, a 3.2 cm (1.25 in.) schedule 40 pipe of Incoloy 800. Salt enters the inner tube at 288°C (550°F) and is heated to 482°C (900°F) by the counterflowing salt in the outer tube that is cooled from 566°C (1050°F) to 371°C (700°F) at the inlet to the air cooler.

The total length for the four legs of the heat exchanger is 29.6 m (97.0 ft) and it is constructed to allow complete drainage of salt when the pump is turned off. This prevents any salt from solidifying on the internal surfaces of the loop when it cools. The heat exchanger is also heat traced so tubes can be preheated to 260°C (500°F) prior to starting the system from ambient temperature. Figure IV-4 shows the heat tracing being installed on one of the heat exchanger legs.

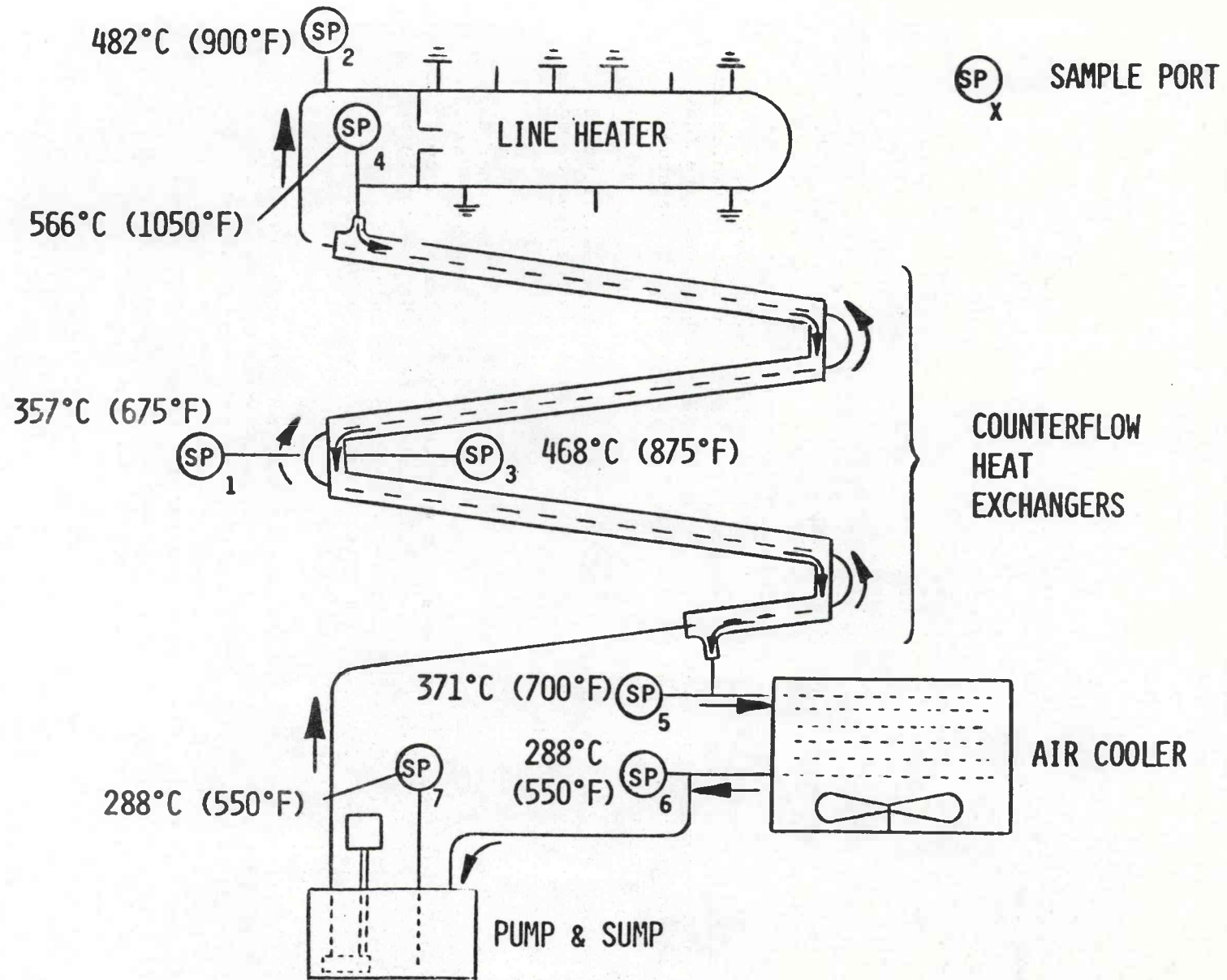


Figure IV-1 Long-Term Molten Salt Flow Loop Schematic

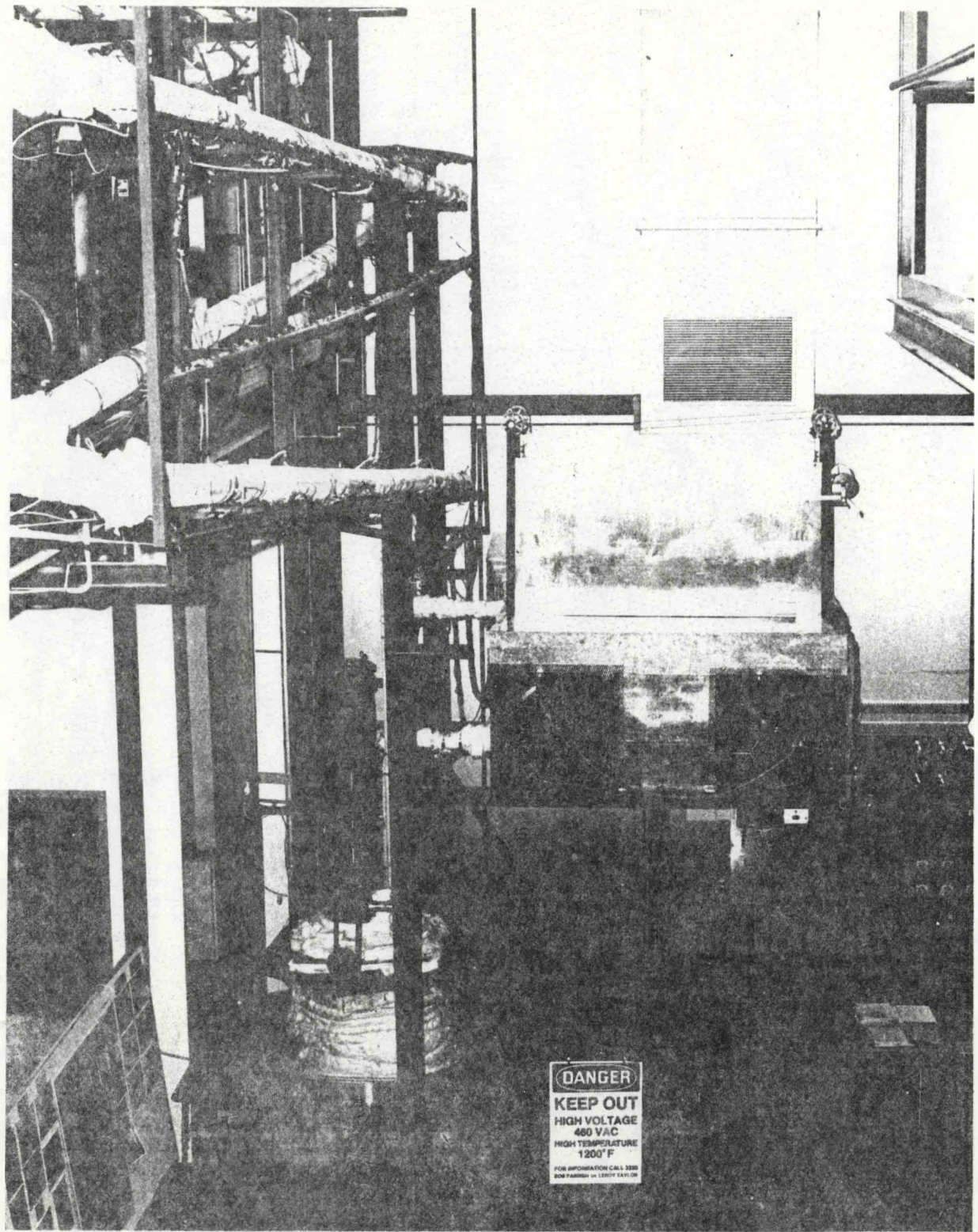


Figure IV-2 Long-Term Molten Salt Flow Loop

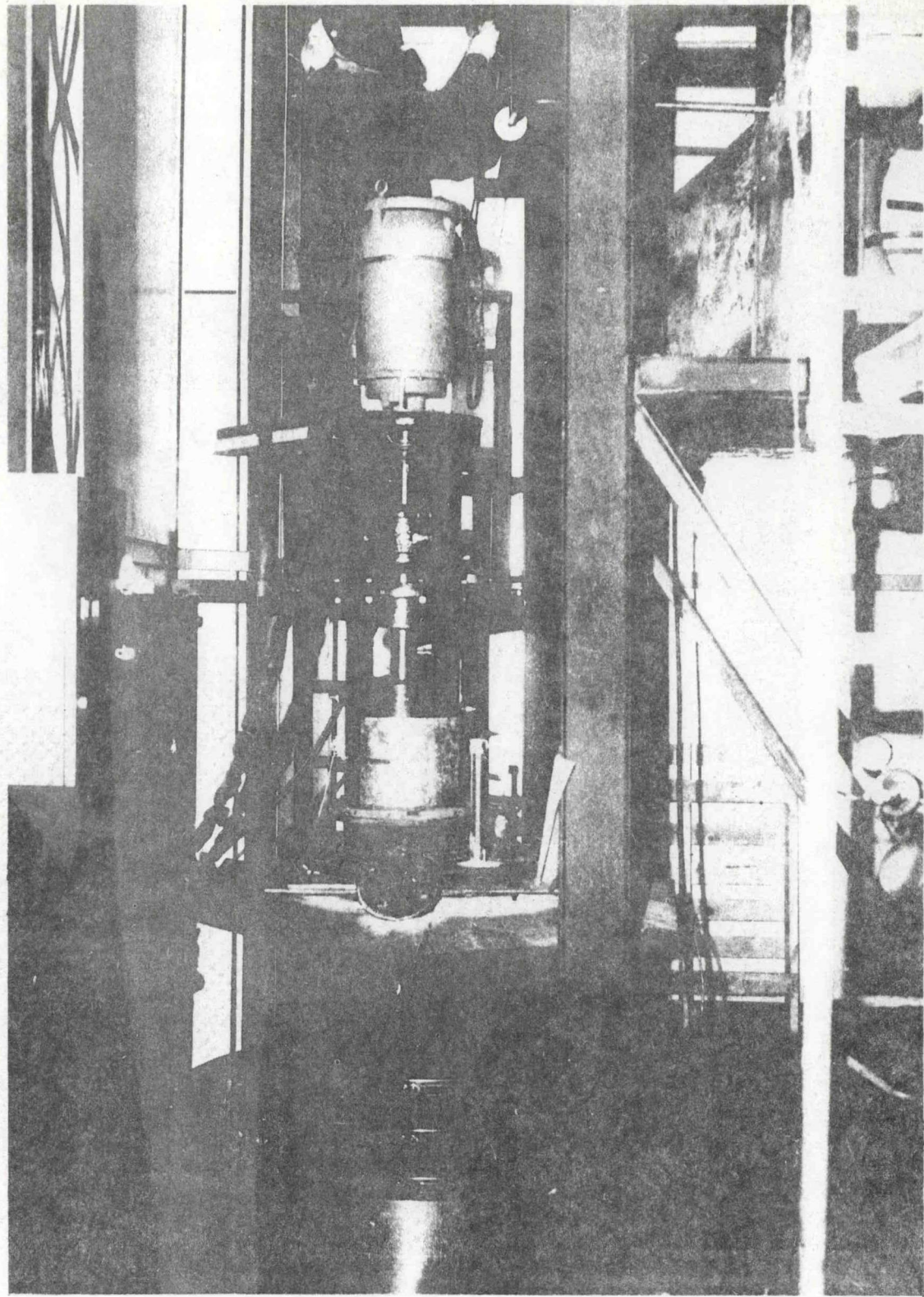


Figure IV-3 Molten Salt Loop Pump and Sump

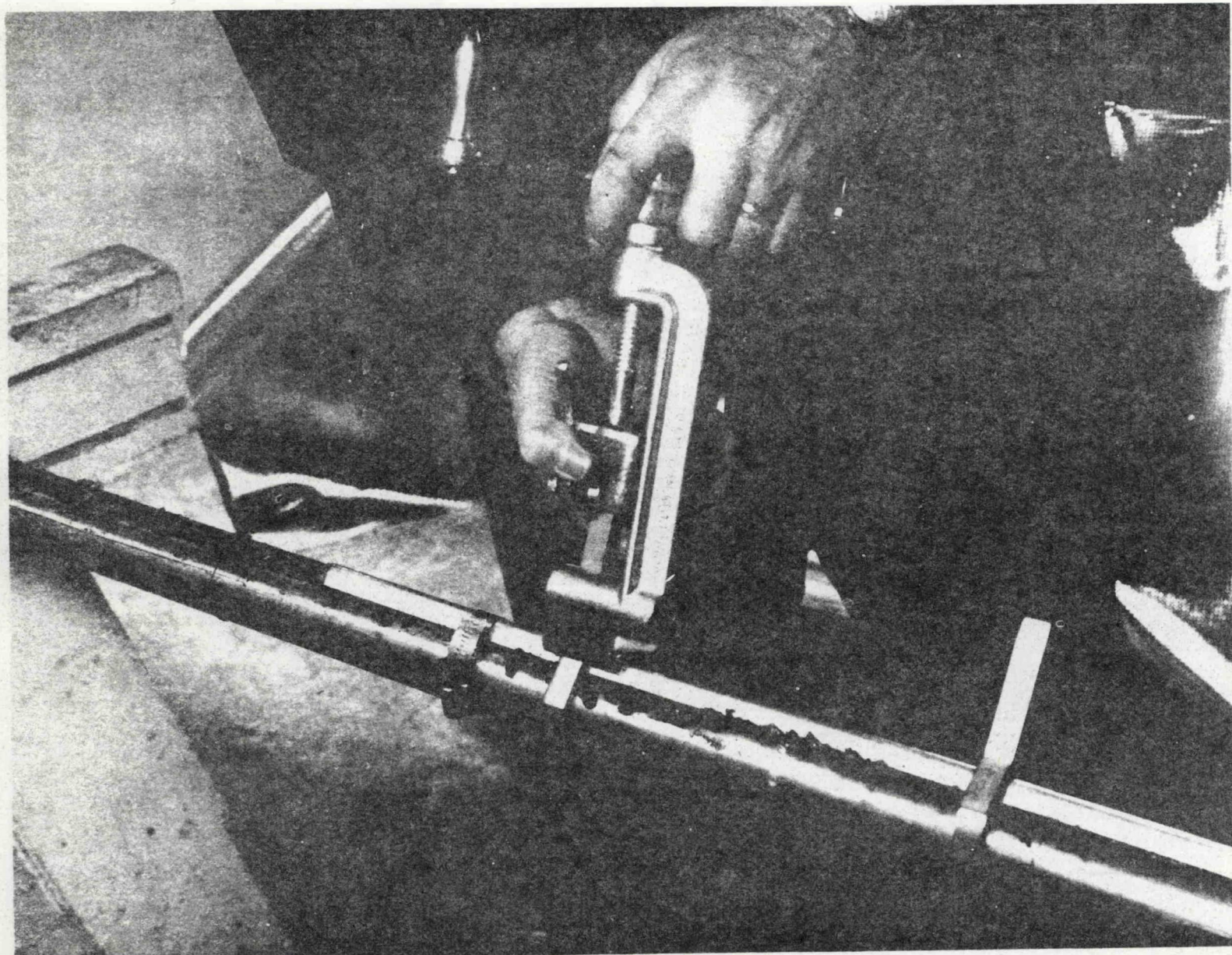


Figure IV-4 Trace Heating being Installed on Counterflow Heat Exchanger Leg

The line heater is a 1.9-cm diameter x 1.7-mm wall (0.75-in. diameter x 0.065-in. wall) Incoloy 800 tube that is resistively heated by passing high-amperage, low-voltage ac current through the tube itself. Salt enters at 482°C (900°F) and leaves at 566°C (1050°F). The line heater is 7.4-m (24.3-ft) long and consists of three independently-heated sections. Power for each section is supplied by a variable power source that feeds a transformer to step down the voltage and supply proper amperage. The power can be manually or automatically controlled on all three sections. Power is regulated by a power controller and each heater section is protected by an overtemperature kill to prevent the salt from exceeding 566°C (1050°F) during operation.

Power is supplied to the tubes via copper busbars that have been brazed to the Incoloy tubes. These are shown in Figures IV-5 and IV-6 (the heater is shown uninsulated). The busbars have been specially sized to permit proper current flow without overheating due to electrical resistance. Figure IV-6 shows a closeup of the area around the braze joints. These sections are semienclosed and purged with dry nitrogen to limit oxidation of the copper at high temperature. The opposite end of each busbar is water-cooled to prevent overheating due to the electrical resistance of the connection to the transformer cables.

After 1000 hours of testing it was discovered that the copper busbars were oxidizing at a greater rate than was expected around the braze joints. The busbars were removed and bolted outside of the insulation to 20-cm x 13-cm x 1.3-cm thick (8-in. x 5-in. x 0.5-in. thick) Incoloy 800 tabs that are welded to the line heater tubes. The water-cooled tabs, shown in Figure IV-7, are operating successfully and preventing the copper from oxidizing.

The air cooler is at the outlet of the outer jacket of the heat exchanger and is sized to reduce the salt temperature from 371°C (700°F) to 288°C (550°F) before returning the salt to the sump. The cooler consists of 11.0 m (36.0 ft) of 2.5-cm (1.0-in) diameter carbon steel tubing with a fin density of 236 fins per meter (6 fins per inch). A closeup of these tubes is shown in Figure IV-8. The tubes are sloped so salt in the air cooler will drain into the sump if the pump is turned off. A plenum chamber distributes the forced air from the dual fan system evenly over the finned tubes.

The cooler housing is insulated to prevent excessive cooling during operation. Insulated panels can also be lowered in front of the air inlet and outlet during startup. Trace heaters preheat the tubes prior to startup and can also be used to melt salt in the finned tubes if the salt freezes during an emergency situation. Figure IV-9 shows the air cooler and fans with the insulated panels in the raised (operating) position.

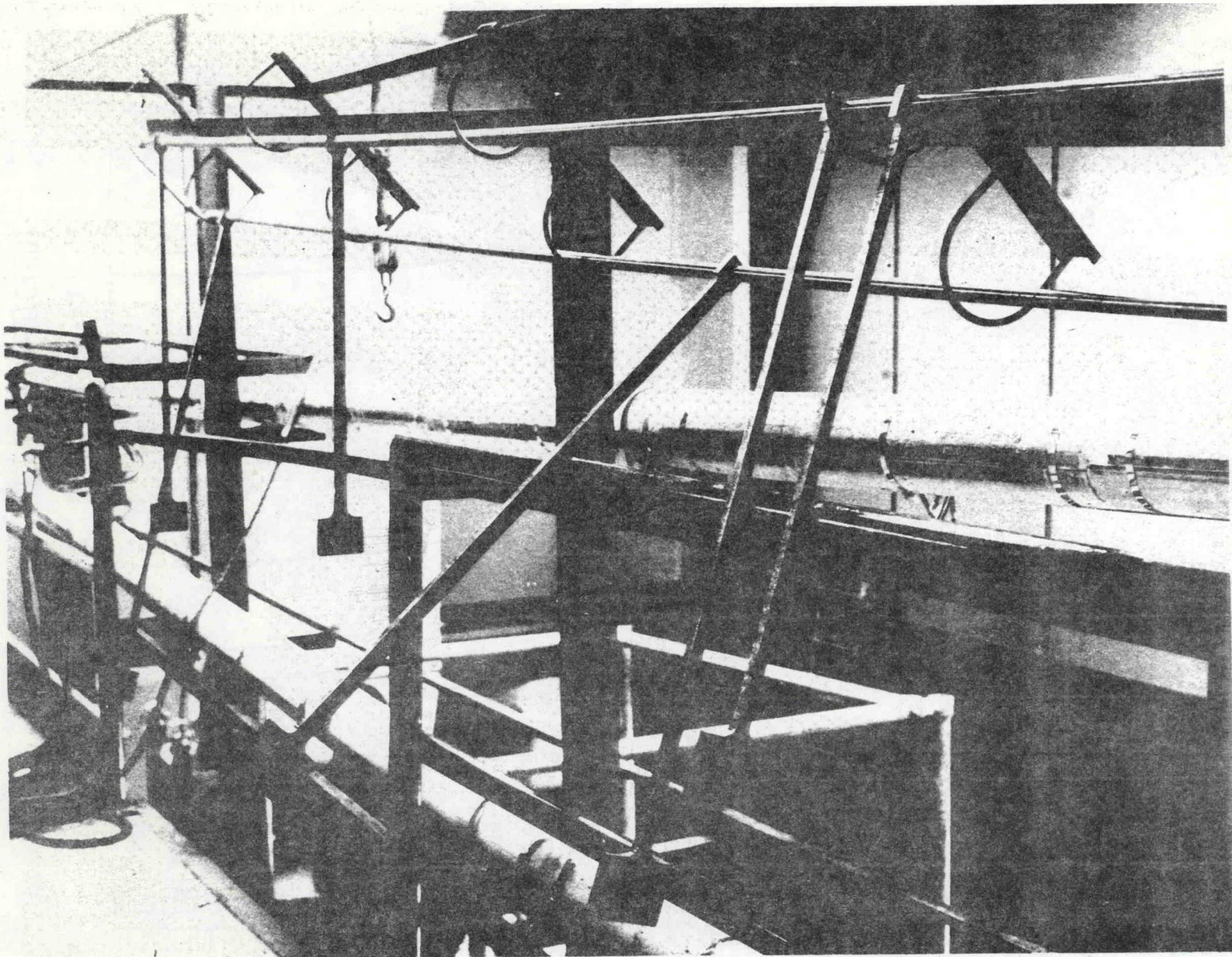


Figure IV-5 Copper Busbars on Molten Salt Loop Line Heater

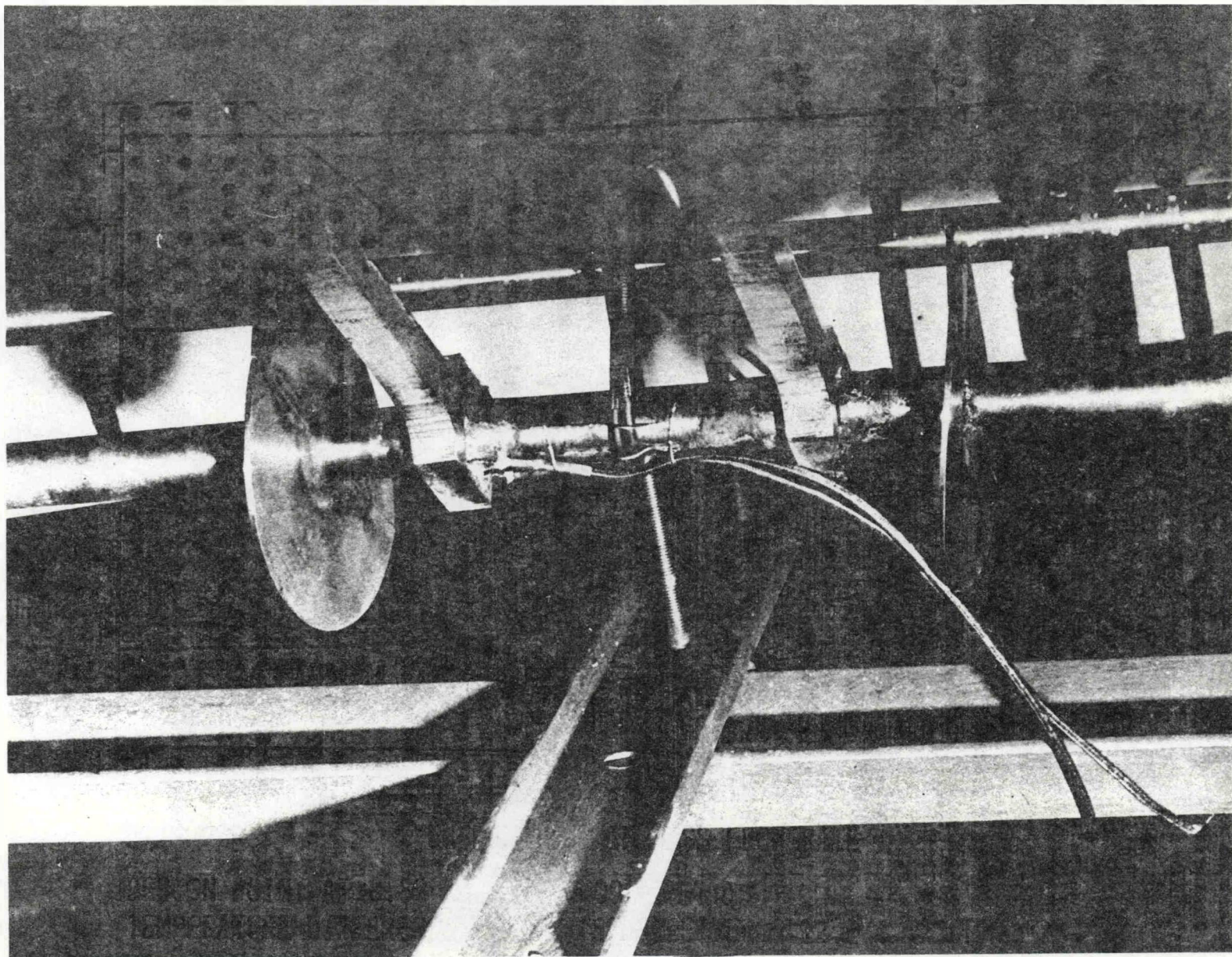


Figure IV-6 Closeup of Copper Busbars Brazed to Incoloy 800 Tube

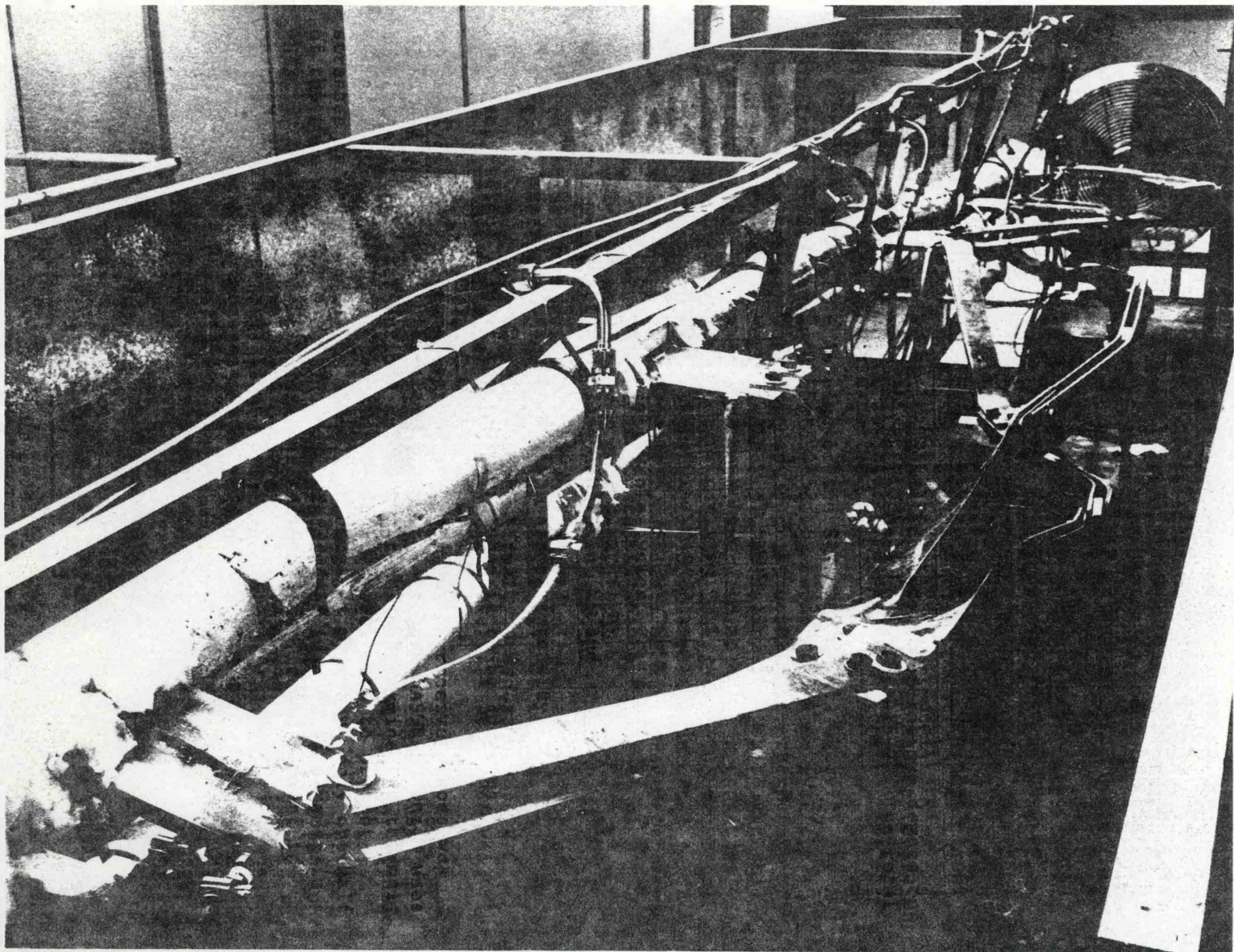


Figure IV-7 Line Heater with Incoloy 800 Tabs

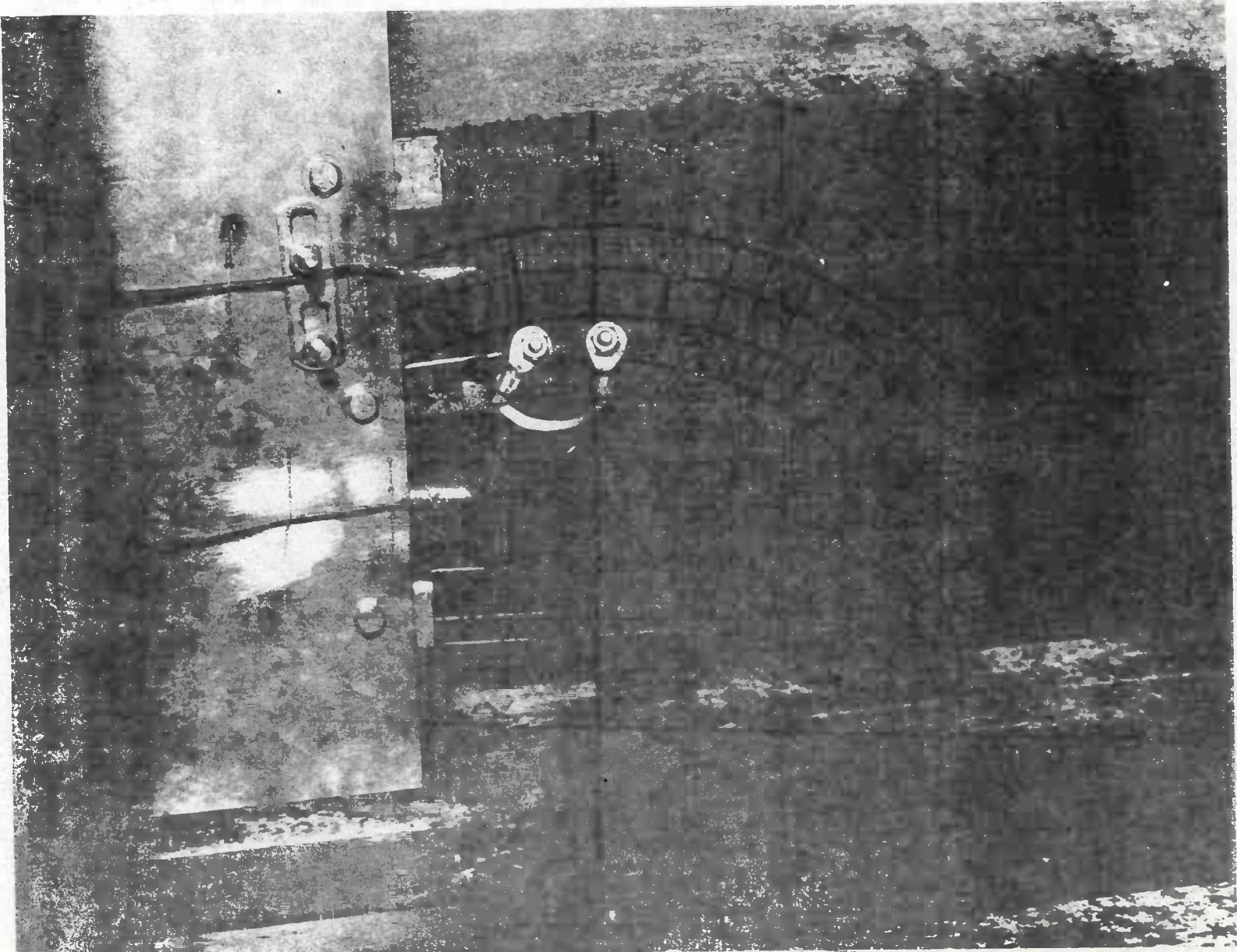


Figure IV-8 Closeup of Molten Salt Flow Loop Finned Air Cooler Tubes

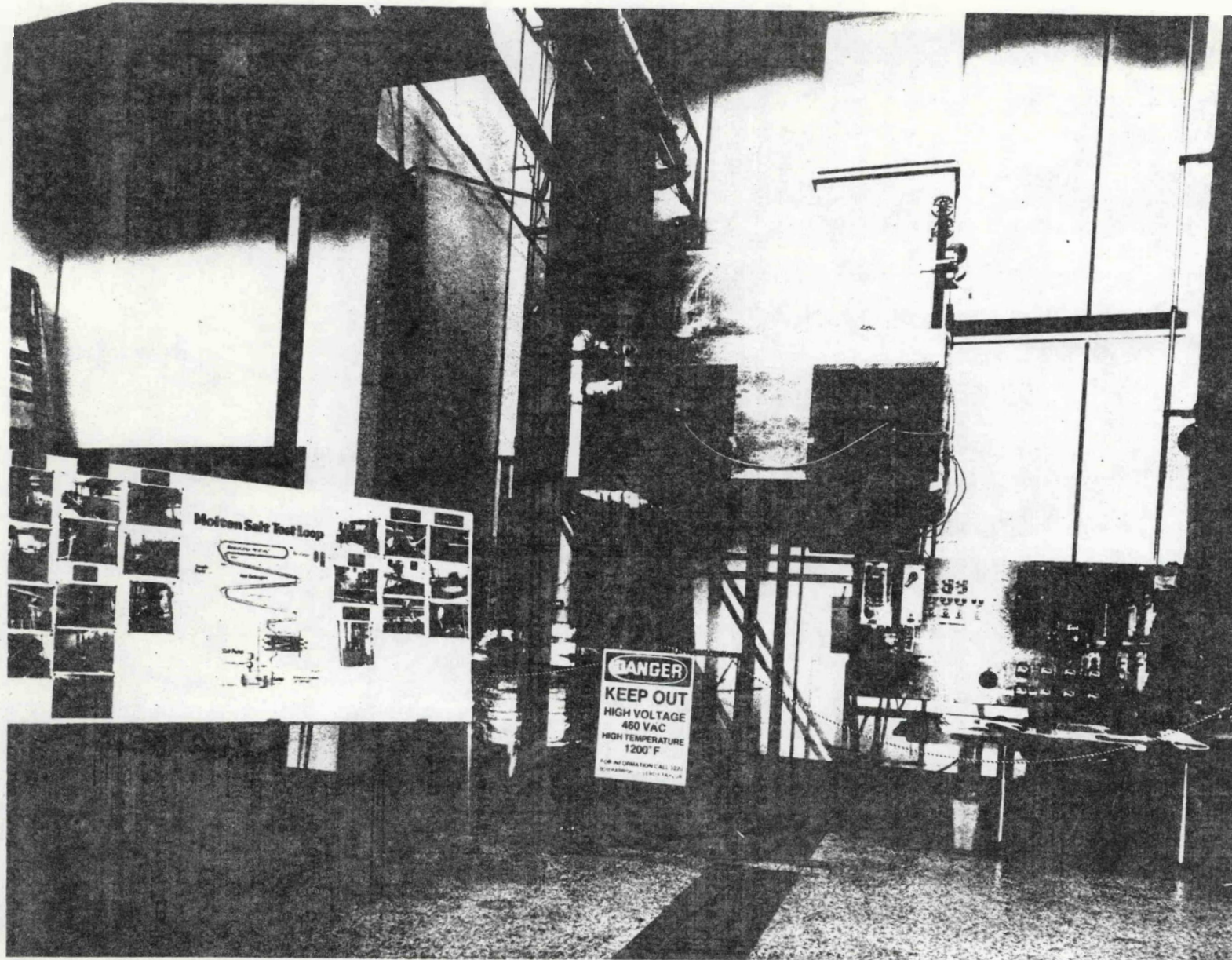


Figure IV-9 Air Cooler and Fans Showing Insulated Panels

There are seven sample ports at various locations in the salt loop. Sample ports 1-5 (refer to the schematic, Figure IV-1) have Incoloy 800 coupons inserted into the salt flow stream, ports 5 and 6 have carbon steel coupons, and port 7 is used to sample the molten salt in the sump. Sample ports are designed so the fluid velocity across the coupons is approximately 3.5 m/s (11 ft/s), which is the design velocity of the salt flow in the full-scale molten salt central receiver system. The coupons are held in the salt stream on a removable sample holder, shown in Figure IV-10. The coupons are placed in slots in the holder, then inserted into the sample port, as shown in Figure IV-11.

All lines in the loop are insulated and shielded with a thin sheet-metal shroud during operation as a safety precaution against possible leaks.

3. System Operation

Figure IV-12 shows the control panel and instrumentation for the fluid loop. On the left are the main power input and the controls for the pump, cooler fans, line heaters, and sump heaters. At top center are the Variacs used to control the trace heating during start-up. The temperature controllers for over- and under-temperature kill are at bottom center, and the four data loggers at right are used to monitor the over 120 thermocouples located at various points around the loop.

During start-up, the insulated panels on the air cooler are closed and the lines and cooler are preheated with the trace heating. When the lines are hot enough, the pump is turned on and salt flow through the system is verified. Power to the line heaters is then slowly increased while temperatures throughout the system are monitored until the temperature at the outlet of the line heaters stabilizes at about 566°C (1050°F). Heater power is then switched to automatic.

The system is designed for continuous unattended operation over a period of at least 5,000 hours. The material samples are checked every 1000 hours for weight change, and will be metallurgically and chemically checked after the test is complete and at other times if weight-change data indicates significant mass transport. Molten salt samples are taken every 1000 hours and analyzed chemically as required.

4. Results

Sample coupons were removed after 1000 hours of test and were visually inspected for corrosion effects. Although they were discolored, none showed any evidence of flaking, blistering, or pitting. It was discovered that some of the coupons had been ground down after the initial weighing prior to insertion, so no weight change data is available for the first 1000 hours.

IV-14

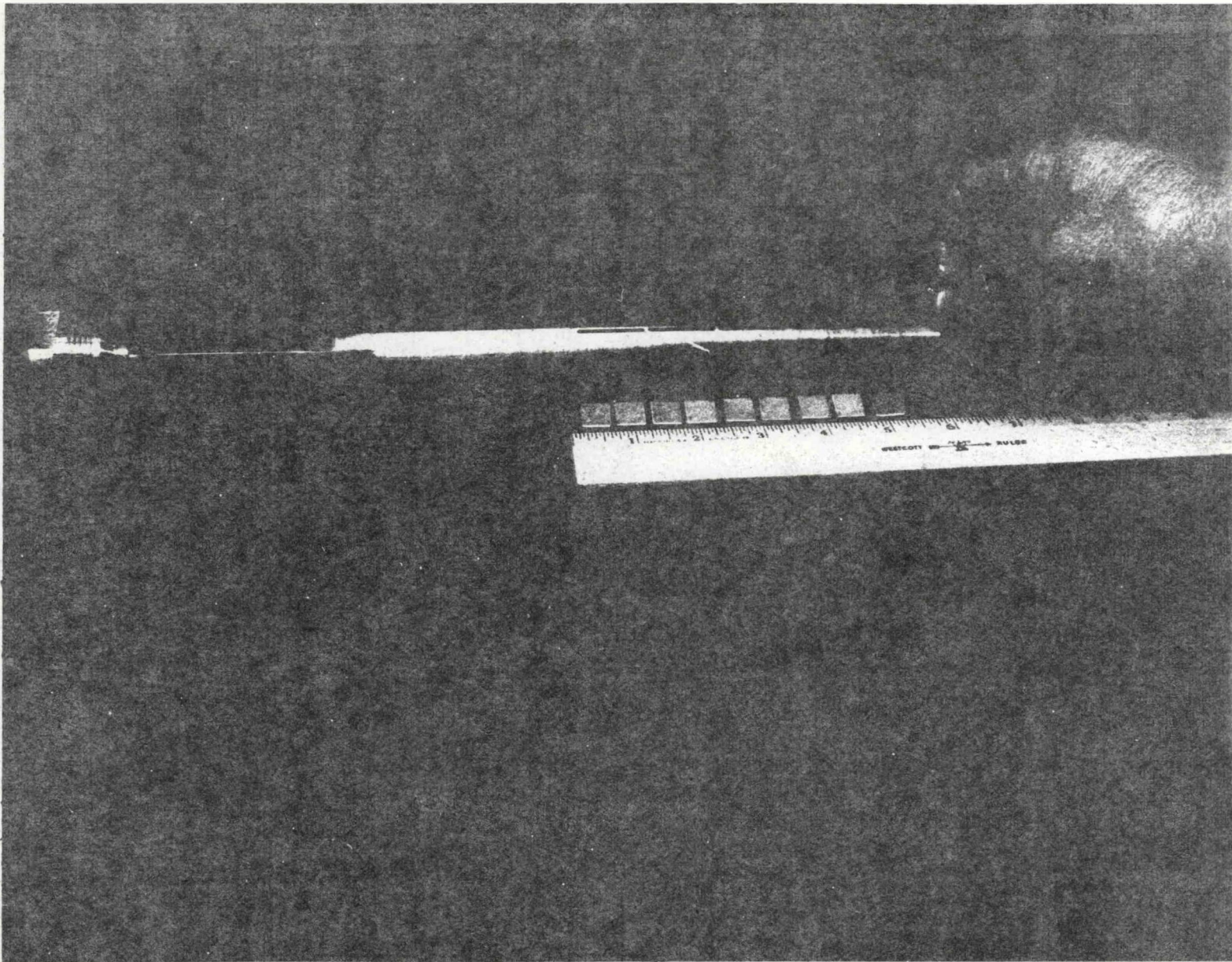


Figure IV-10 Removable Materials Sample Holder, with Samples



Figure IV-11 Removal of Materials Sample Holder from Flow Loop



Figure IV-12 Molten Salt Flow Loop Control Console

B. Static Materials Tests

1. Objectives

The purpose of the Phase II static materials compatibility tests is to extend the Phase I materials test program and to increase knowledge of both materials corrosion and molten salt stability. The Phase II program continues the testing of Incoloy 800 and carbon steel (the selected materials) as well as other candidate materials such as 347, 316L, and RA330 (which is similar to Incoloy 800). The 347 and 316L stainless steels were selected because of the added stabilizing elements Cb and Ta in 347, and the low carbon in 316L, which tend to make these steels less susceptible to sensitization at high temperatures.

Test descriptions and results to date for each test are discussed below. For a detailed test description, see the Materials Test Plan in Appendix B.

2. Test Descriptions and Results

a. Trace Contaminants Test - The purpose of this test is to create a better understanding of corrosion effects for trace amounts of anionic contaminants present in commercial nitrate salt. Such tests will indicate if there is a need to control certain impurities in the commercial-grade salts.

Test coupons are suspended in reagent-grade molten salt (60% NaNO₃, 40% KNO₃) that has been doped with the maximum concentrations of chloride ion, sulfate ion, hydroxide ion, and carbonate ion as specified for commercial salt. Figure IV-13 shows the test vessels used. They are all 3.2-cm (1.25-in.) diameter pipes, 0.38-m (15-in.) long made of the same material as the coupons being tested, and are vented to the atmosphere through CO₂/water vapor scrubbers. The tubes are placed in an insulated test oven with the tops protruding to keep them cool.

A test matrix for the trace contaminants tests is shown in Table IV-1. Each test vessel contains three welded sample coupons and three regular coupons. Coupons are removed every 1000 hours during the 4000-hour test, washed free of salt, weighed, and returned to the salt. If any coupons show unusual visual appearance or weight change, further microscopic or photographic examination is made. Salt samples are taken every 1000 hours so that they can be analyzed for further data should any coupons show a particular corrosion problem. Salt and dopant are replaced with a new solution 2000 hours into the test. Salt samples are analyzed for anion concentration at 2000 and 4000 hours.

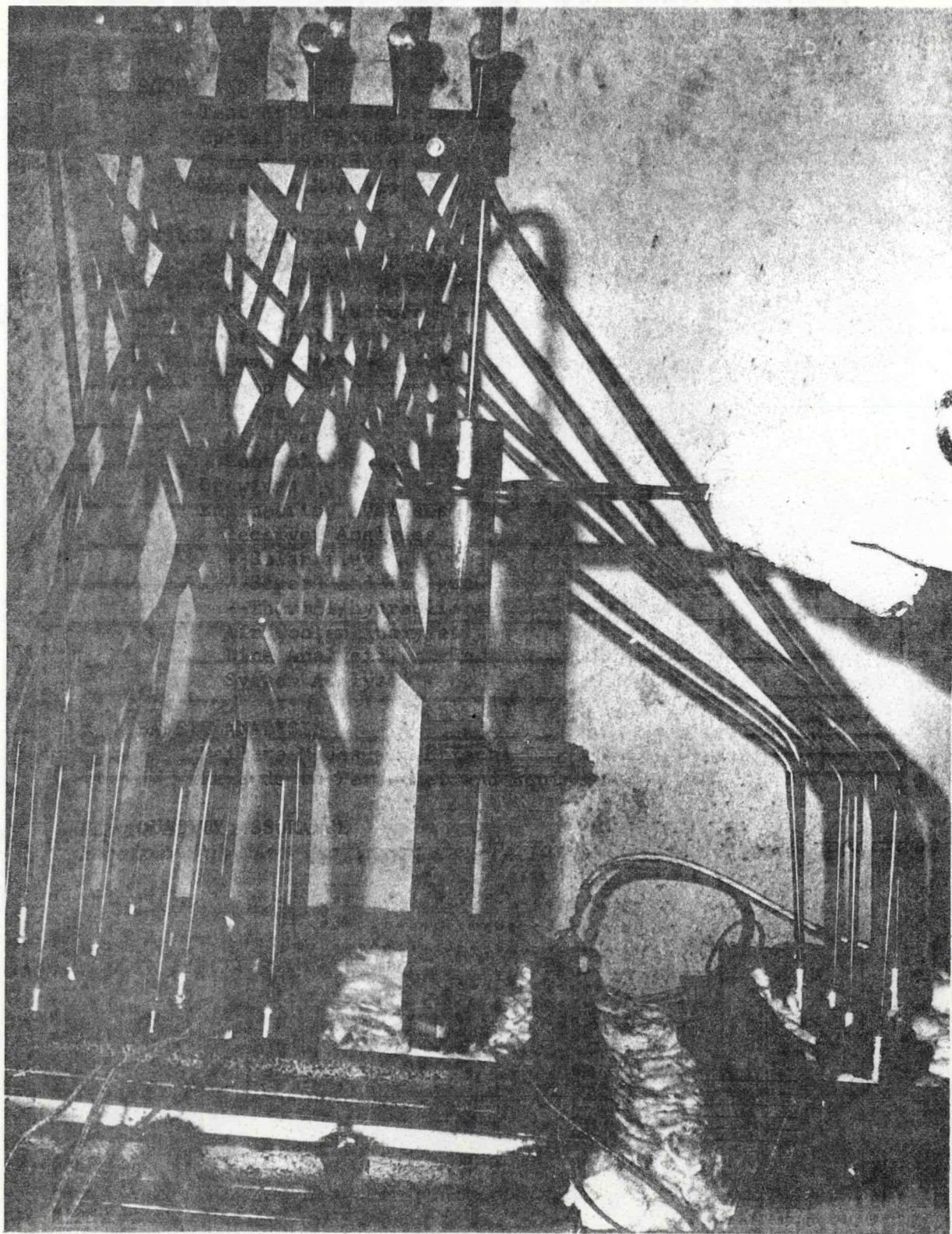


Figure IV-13 Test Vessel for Trace Contaminants Test

Table IV-1 Test Matrix for Trace Contaminants Test

DOPANT	WT %	TEMPERATURE		593°C	593°C	593°C	593°C	399°C
		SAMPLE	INCOLOY 800	RA330	316L SS	347SS	A516	
NaOH	0.50		X	X	X	X	X	
Na ₂ CO ₃	0.20		X	X	X	X	X	
Na ₂ SO ₄	0.35		X	X	X	X	X	
NaCl	0.25		X	X	X	X	X	
NaCl	0.50		X				X	
BLANK	--		X	X	X	X	X	
ALL OF ABOVE			X	X	X	X	X	

X EACH COMBINATION WILL HAVE SIX SAMPLES; THREE WITH WELDS AND THREE WITHOUT.

Table IV-2 shows weight-change data as of the 2000-hour work. In general the Incoloy 800 coupons all appeared very good visually and showed small positive weight gains. The RA 330 alloy also looked good with only surface discolorations noted and no blistering or flaking. The stainless steels varied in their ability to resist surface corrosion with 316L visually appearing good, but 347 showing surface pitting, minor blistering, and weld areas showing some cracking.

The A516 carbon steel showed severe blistering and flaking in all tests except the hydroxide-doped salt. Welds and heat-affected zones were especially corroded in the sulfate and chloride tests. Coupons immersed in salt with the maximum specification level of all dopants seemed to show slightly less corrosion than the blank (no dopants). We are not sure why at this time.

b. On-going Materials Tests (Long-Term Tests) - These on-going tests evaluate selected construction materials under longer periods of molten salt exposure than was possible in Phase I. Selected sample coupons from Phase I testing are being exposed for an additional twelve months to molten salt in the same Incoloy 800 immersion trays (see Figure IV-14). They are suspended in the molten salt with nichrome wires. Weight-change data is collected every 2000 hours, and the coupons will be microsectioned and optically analyzed at the end of the 12-month test, or before, if any unusual changes are noted.

The test matrix and results to date are shown in Table IV-3. After 2000 hours in Phase I of the on-going materials tests, the Incoloy 800, RA330, and 347 stainless steel do not show visual signs of degradation. The 316 stainless steel and especially the A516 carbon steel do, however, show signs of blistering and flaking. Weight changes in the A516 are especially erratic which indicate flaking or spalling of the passivation layer.

c. Stress Corrosion Test - The stress corrosion test determines the susceptibility of candidate materials (both parent metal (PM) and welds) to corrosion cracking under stressed conditions. Stress conditions are those required to produce a 1% deformation in three different time frames.

Dog-bone specimens, such as the one shown in Figure IV-15, are contained in a molten salt vessel made from a 5.1-cm (2.0-in.) pipe. A standard creep test machine is attached to both ends of the specimen to maintain a constant load throughout the test, and the test vessel is surrounded by a tube furnace controlled to keep the salt at 593°C (1100°F). See Figure IV-16. Table IV-4 shows a test matrix for the stress corrosion specimens.

Total creep strain is determined by measuring the cross-sectional areas of the specimen before and after testing. Each PM specimen will be tensile tested and metallographically analyzed. In addition to this, the weld specimens will be tested by a standard 180° bend test.

Currently, the Incoloy 800 stress corrosion samples are in test and the other materials will be put into test shortly. Results from these tests should be available in several weeks.

Table IV-2 Weight Change Data for Trace Contaminants Test After 2000 Hours

DOPANT	CARBON STEEL		INCOLOY 800		RA 330		347 STAINLESS STEEL		316L STAINLESS STEEL	
	1000 HR	2000 HR	1000 HR	2000 HR	1000 HR	2000 HR	1000 HR	2000 HR	1000 HR	2000 HR
.50% Na OH	2.47	3.51	0.83	0.84	1.69	1.87	2.00	4.01	1.07	1.37
.26% K ₂ CO ₃	2.69	2.76	0.63	0.77	1.70	1.90	1.07	3.05	0.90	1.46
.35% Na ₂ SO ₄	3.05	-0.63	0.61	0.75	1.41	1.67	1.39	2.92	0.82	1.14
.25% NaCl	2.32	2.87	0.44	0.61	0.320	0.45	0.46	0.63	0.88	1.01
.50% NaCl	2.49	3.07	0.45	0.65	-	-	-	-	-	-
BLANK	2.51	3.37	0.59	0.79	1.14	1.26	0.85	1.97	0.97	1.24
MAX. ALL	1.61	2.62	0.54	0.56	1.39	1.49	1.09	1.98	0.61	0.98
PHASE I PREVIOUS DATA	0.40	0.45	1.2	1.6	0.52	0.55	0.92	1.0		

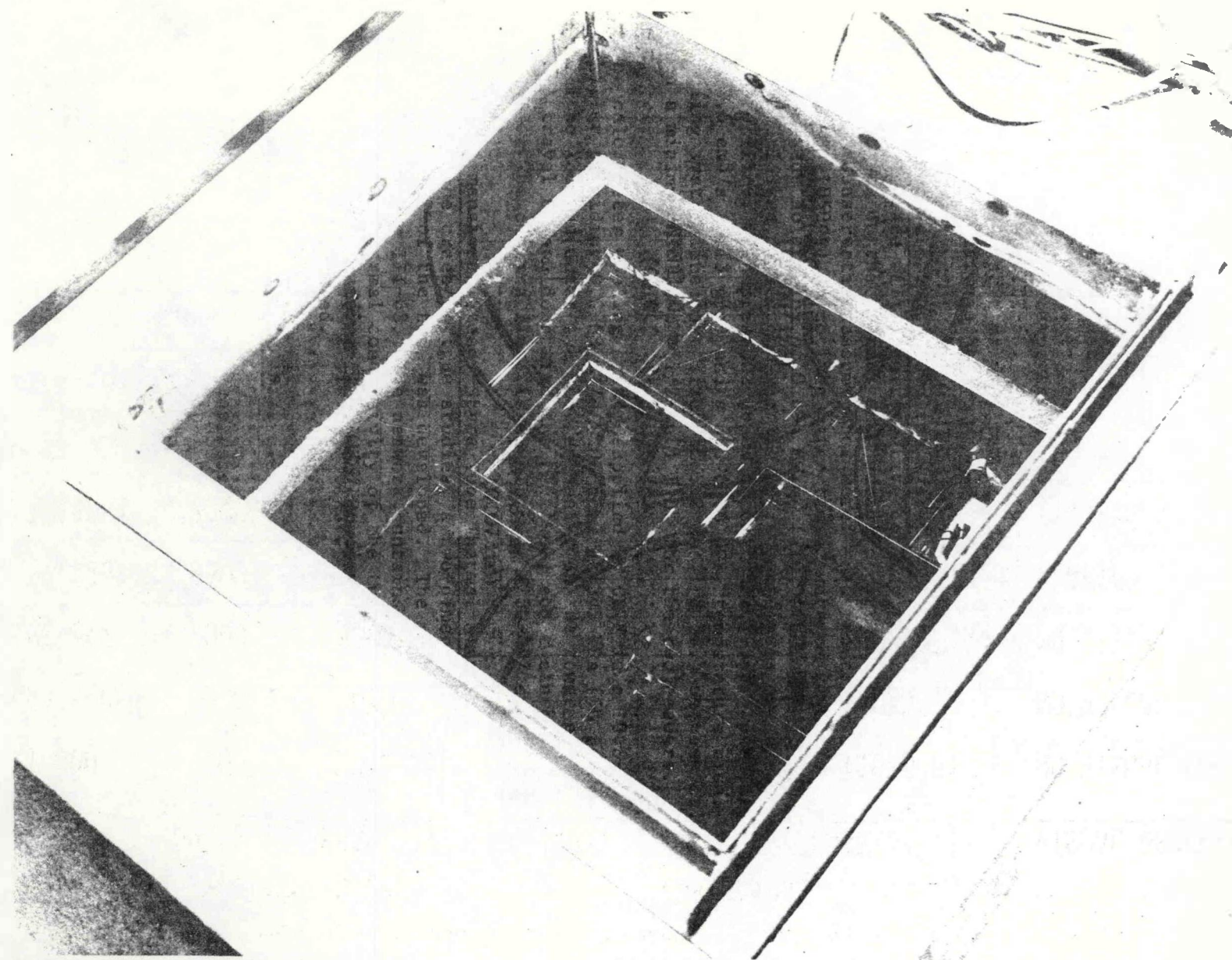


Figure IV-14 Incoloy 800 Materials Samples Immersion Trays in Test Oven

Table IV-3
Visual Results of On-going Materials Tests - 2000-Hour Examination

<u>ALLOY</u>	<u>NO. TEST HOURS</u>		<u>TEMPERATURE</u>		<u>VISUAL OBSERVATIONS</u>
	<u>PHASE I</u>	<u>PHASE II</u>	<u>PHASE I</u>	<u>PHASE II</u>	
I-800	5500	2000	593 C (1100°F)	579 C (1075°F)	NO VISUAL CHANGE
RA 330	2300	2000	593 C (1100°F)	579 C (1075°F)	NO VISUAL CHANGE
SS 347	2000	2000	593 C (1100°F)	579 C (1075°F)	NO VISUAL CHANGE
SS 316	9600	2000	621 C (1150°F)	579 C (1075°F)	FLAKING
A516	7200	2000	399 C (750°F)	399 C (750°F)	BLISTERING & FLAKING

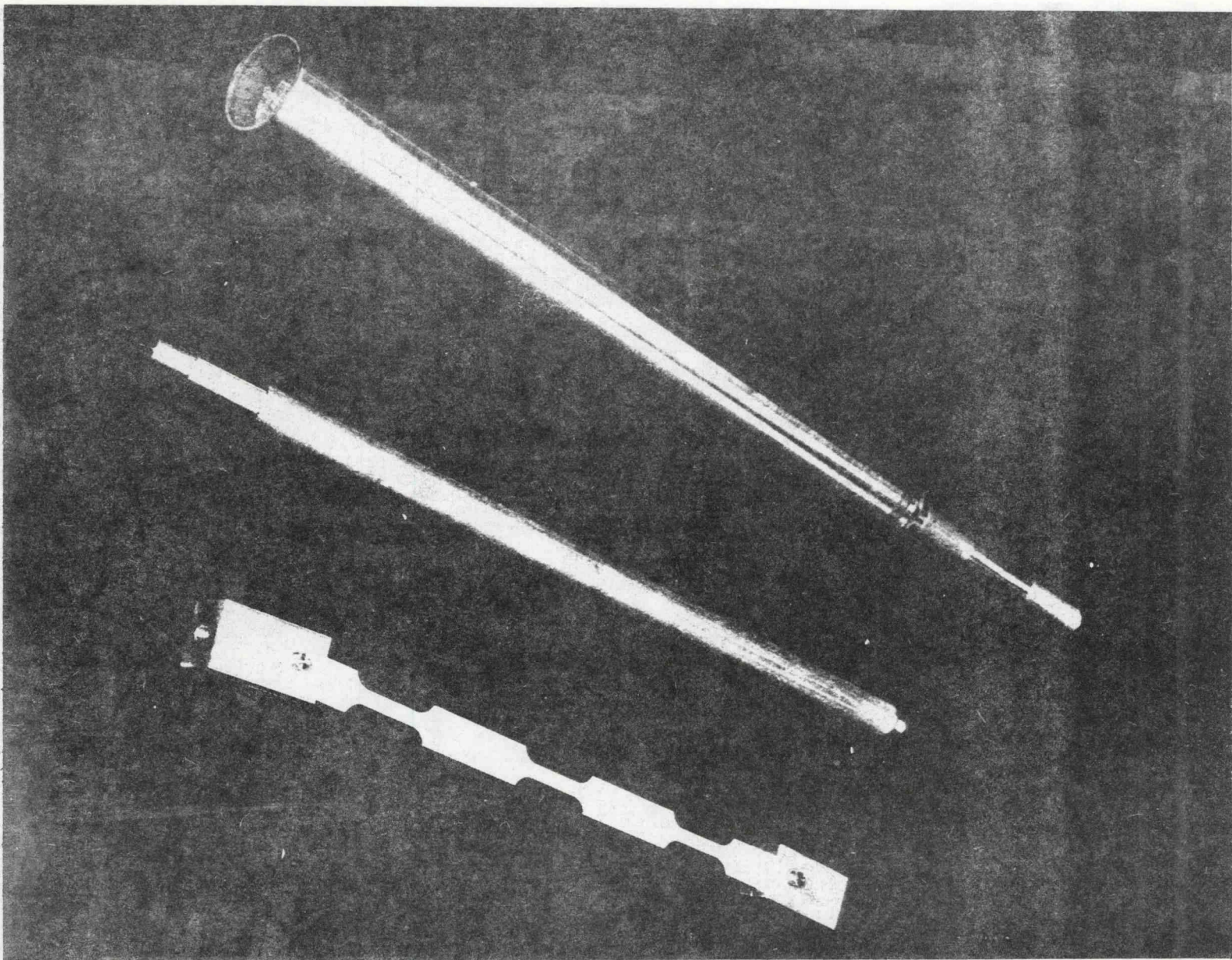


Figure IV-15 Dog-Bone Sample for Stress Corrosion Test

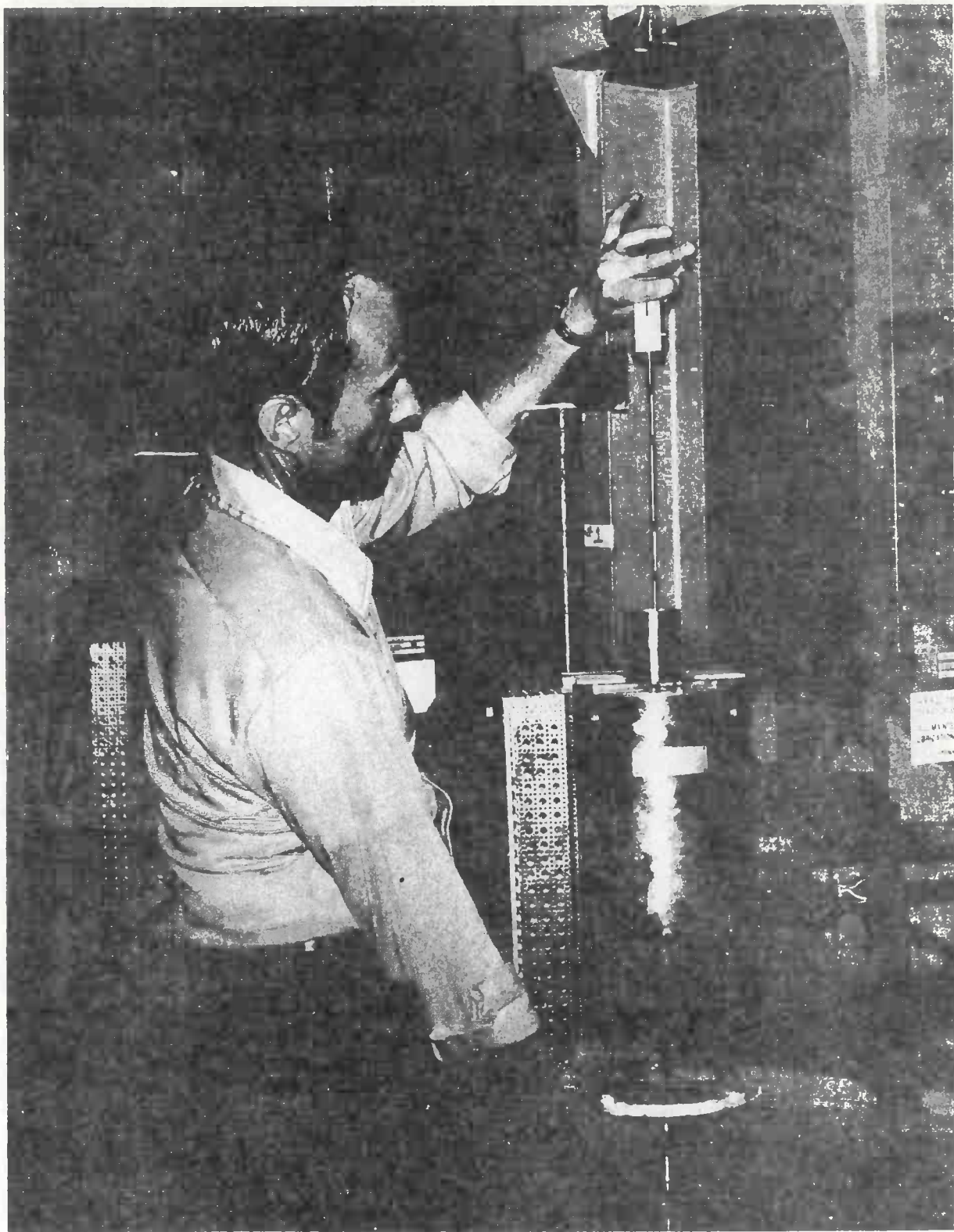


Figure IV-16 Stress Corrosion Test Fixture

Table IV-4 Test Matrix for Stress Corrosion Test

APPROXIMATE CREEP RATES

MATERIAL	0.001%/HR	0.01%/HR	0.1%/HR
I-800 PM	3	3	3
I-800 WELD	6	6	6
RA330 PM	3	3	3
RA330 WELD	6	6	6
SS-347 PM	3	3	3
SS-347 WELD	6	6	6

d. Carbon Dioxide - Water Vapor Effects on Salt Chemistry - The purpose of this test is to determine the effects of long-term exposure of the molten salt to ambient atmosphere.

Known quantities of CO_2 and water vapor are bubbled through approximately 300 g (0.66 lbm) of molten salt at 579°C (1075°F). The salt is contained in 3.8-cm (1.5-in.) Incoloy 800 pipes 0.38-m (15-in.) long that are heated in an insulated test oven. Figure IV-17 shows the test vessels in the oven. Their tops protrude to keep them below the freezing temperature of the salt so that it cannot escape. Small Incoloy 800 test coupons are placed in each test vessel to determine the effects of long-term exposure to high CO_3^{2-} and OH^- concentrations.

Table IV-5 shows a test matrix for this test. The salt is analyzed at the end of each test for hydroxides/oxides, carbonates, nitrates, nitrites, potassium, sodium, and chromium.

Table IV-6 shows the results for the one-, five-, and fifteen-week tests. This data will be supplemented shortly with the 6-month results. Testing will be terminated at this point since it appears that an equilibrium level of carbonate build-up is being approached. Both the carbonate and oxide/hydroxide seem to be approaching equilibrium levels in the salt that are below the solubility limits for these materials at the test temperatures. Test results indicate that hydroxides/oxides are readily converted to carbonate in the presence of CO_2 .

The chromium concentration has jumped significantly between the five- and 15-week results, probably because we have made a special effort on subsequent analyses to analyze bottom residue, which consists of 3-4% of total material left in the vessel after the salt is poured out. The analysis of these residues is not complete, but it appears there is a small amount of salt-insoluble chromium compound in the vessel bottoms. Carbon dioxide seems to lessen the amount of chromium present either in the total salt or the salt residue for reasons unknown at this time.

e. Salt Treatment Techniques - This test evaluates the "in situ" regeneration of molten salt containing carbonates and hydroxides/oxides by exposure to gaseous nitrogen dioxide.

Molten salt at 288°C (550°F) containing carbonate and hydroxide/oxide dopants is exposed to gaseous nitrogen dioxide in the Incoloy 800 bubbler vessels used for the CO_2 /water vapor tests. A test coupon of Incoloy 800 is placed in each vessel as well. The test matrix for this test is shown in Table IV-7.

Each salt sample is analyzed at the end of the test for CO_3^{2-} , OH^- , NO_3^- , NO_2^- , Cr, Ni, and Fe. The coupons are optically analyzed, and weighed to determine a weight gain or loss.

Salt treatment tests will be started after termination of the CO_2 /water vapor tests.

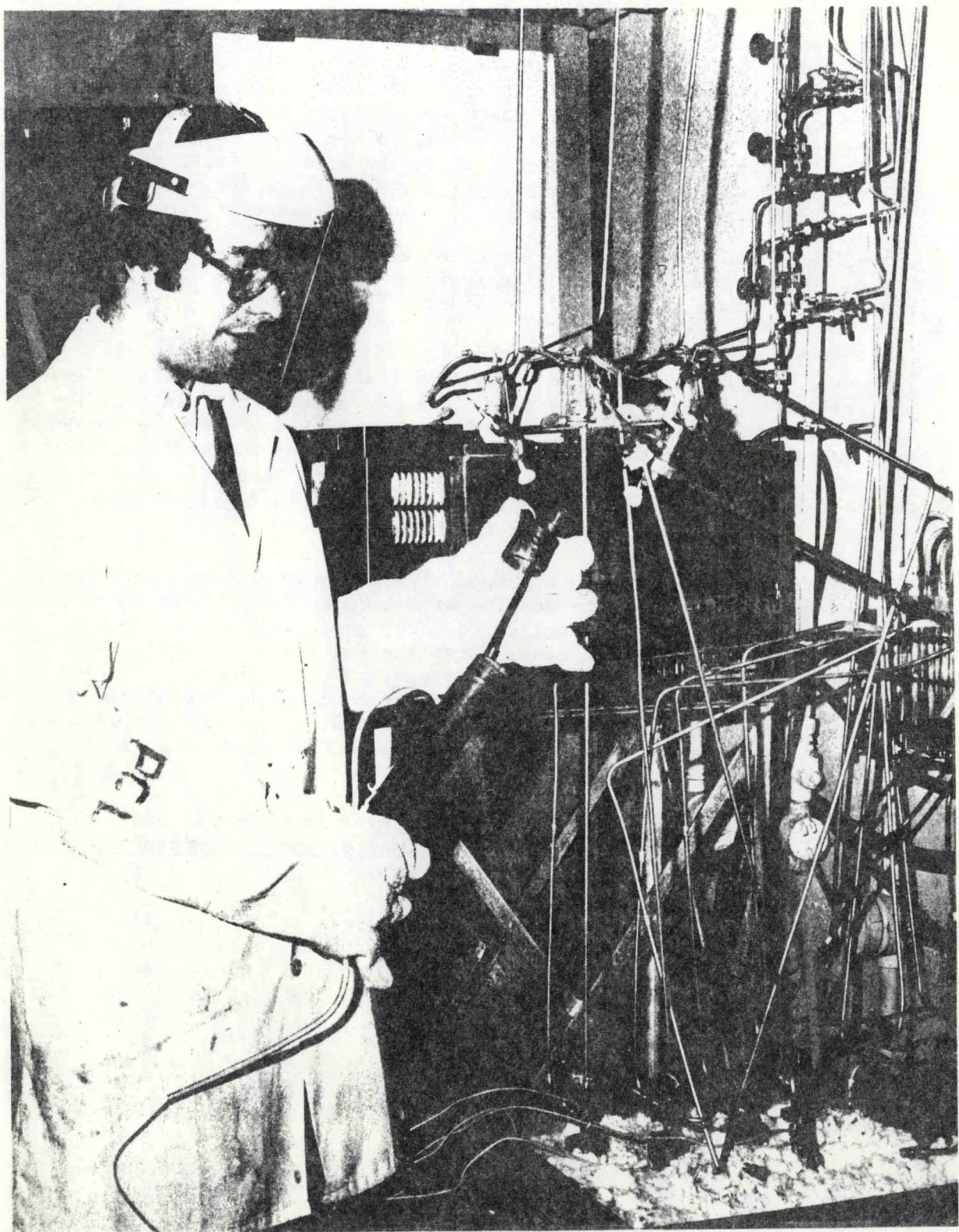


Figure IV-17 Test Fixture for Effects of CO_2 --Water Vapor on Salt Chemistry

Table IV-5 Test Matrix for CO_2 -Water Vapor Test

Test	Gas Purified Air	Composition H_2O	Vol % CO_2	Test Time
A1	100%	0	0	1 wk
A2				5 wk
A3				15 wk
A4				6 mo
A5	↓	0	0	12 mo
B1	Balance	100% R.H.	0	1 wk
B2				5 wk
B3				15 wk
B4				6 mo
B5	↓		↓	12 mo
C1	Balance	0	1.0%	1 wk
C2				5 wk
C3				15 wk
C4				6 mo
C5	↓		↓	12 mo
D1	Balance	100% R.H.	1.0%	1 wk
D2				5 wk
D3				15 wk
D4				6 mo
D5	↓		↓	12 mo

ANALYSIS - EACH SAMPLE WILL BE QUENCHED IN DISTILLED
WATER AND ANALYZED FOR CO_3^- , OH^- , NO_2^- ,
 NO_3^- , Na^+ , K^+ , Cr^{+++}

Table IV-6 Test Results for CO₂-Water Vapor Test

ANALYSIS	HOMOGENIZED PARTHERM 430	TEST CONDITIONS											
		ONE WEEK TEST				FIVE WEEK TEST				FIFTEEN WEEK TEST			
		DRY AIR	100% R.H.	1% CO ₂	100% R.H. 1% CO ₂	DRY AIR	100% R.H.	1% CO ₂	100% R.H. 1% CO ₂	DRY AIR	100% R.H.	1% CO ₂	100% R.H. 1% CO ₂
INSOLUBLE RESIDUES (WT %)	0.060	0.127	0.073	0.573	0.072	0.061	0.087	0.047	0.058				
OXIDE (WT %)	0.018	0.029	0.080	0.009	0.012	0.050	0.450	0.017	0.037	0.042	0.219	0.026	0.032
CARBONATE (WT %)	0.060	0.059	0.086	0.629	0.508	0.047	0.070	2.946	2.907	0.203	0.331	3.142	3.778
NITRITE (WT %)	0.348	4.582	4.143	3.814	3.361	4.311	4.367	3.928	3.587	5.209			
NITRATE (WT %)	68.39	65.40	65.03	65.05	65.80	63.42	63.40	62.06	60.84	62.20			
CHROMIUM (PPM)	1.5	123.9	84.2	60.7	43.2	176	225	70	48	439.6	351.2	137.4	140.7
WEIGHT CHANGE I-800 COUPON 4%	-	+.052	+.029	+.028	+.039	+.221	+.199	+.076	+.069	+.176	+.119	+.132	+.114

Table IV-7 Test Matrix for Salt Treatment Techniques

TEST #	SALT COMPOSITION	TEST TIME	NO ₂ ADDITION RATE
1	5 w/o CO ₃ ⁼	24 HR	5 CC/MIN
2	5 w/o OH ⁻	24 HR	5 CC/MIN
3	5 w/o CO ₃ ⁼ , 5 w/o OH ⁻	24 HR	5 CC/MIN
4	BLANK	24 HR	5 CC/MIN
5	5 w/o CO ₃ ⁼	5 DAYS	5 CC/MIN
6	5 w/o OH ⁻	5 DAYS	5 CC/MIN
7	5 w/o CO ₃ ⁼ , 5 w/o OH ⁻	5 DAYS	5 CC/MIN
8	BLANK	5 DAYS	5 CC/MIN
9	5 w/o CO ₃ ⁼ , 5 w/o OH ⁻	24 HRS	No NO ₂
10	5 w/o CO ₃ ⁼ , 5 w/o OH ⁻	5 DAYS	No NO ₂

f. Tensile/Intergranular Corrosion Tests - The purpose of this test is to assess the susceptibility of candidate materials to intergranular corrosion. Tensile specimens (both parent metal (PM) and weld) cut from 1.6 mm (1/16-in.) sheet stock are placed in trays of salt in a standard 0.51-m x 0.51-m (20-in. x 20-in.) test oven at 593°C (1100°F). The ovens are vented to the atmosphere through CO₂ and water vapor scrubbers. An equal number of samples (both PM and weld) are held at 593°C in air for reference testing at the end of the tests. Three salt-immersed PM samples of each alloy and three each of the air samples will be removed from test after 6 months and exposed to ASTM A262 accelerated intergranular corrosion (IGC) solution before analyzing. The rest of the samples will remain in test for a total of 12 months. Table IV-8 shows the test matrix.

Both parent metal and weld samples will be tensile tested at ambient temperature, microsectioned, and metallographically examined for IGC. A 180° bend test will also be performed on the weld samples.

The intergranular corrosion test samples are currently in test, and the 6-month analysis will be made in June.

g. Corrosion Fatigue Test - This test will provide fatigue data for candidate receiver metals immersed in hot molten salt. It is similar to the conventional tension fatigue test except that the sample is immersed in 593°C (1100°F) molten salt.

Three dog-bone samples of each material are tested at three different stress levels to define a stress/cycle (S-N) curve. The samples are cycled to failure for up to 10⁶ cycles at approximately one cycle/second. The cyclic loading is tension-tension with a "R" factor of 0.1. Table IV-9 shows the corrosion fatigue test matrix.

Corrosion fatigue S-N curves derived from this test will be compared to typical S-N curves for the metals at 593°C (1100°F) in air. Any tendency of the passivation layer to flake off will be evaluated by visual examination and by comparing post-test with pre-test specimen weights.

The corrosion fatigue test is scheduled to start in mid-March.

h. Thermal Cycling of Test Coupons - The purpose of this test is to demonstrate the tenacity of the oxide passivation layer of sample coupons during severe thermal shock.

Three coupons each of Incoloy 800, 316L, 347, RA330, and carbon steel are given a 2000-hour passivation layer and then heated in an oven to 593°C (1100°F) for the stainless steels and 399°C (750°F) for the carbon steel. They are then immediately quenched in ambient temperature water. This cycle is repeated 50 times. The coupons are checked for weight change after each ten quench cycles and the passivation layer is optically analyzed at the end of the test for any degradation.

The thermal cycling test will start in April.

Table IV-8 Test Matrix for Tensile/Intergranular Corrosion Test

MATERIALS -	<u>593°C (1100°F)</u>	<u>399°C (750°F)</u>
	INCOLOY 800	CARBON STEEL
	RA 330	
	SS 347	
	316L	

NUMBER OF SAMPLES

6 - PARENT METAL	- 3 PM - 6 Mo, 3 PM - 12 Mo
6 - WITH WELDS	- 6 WELDS - 10 Mo, 3 FOR 180° BEND
6 - PARENT METAL	- AIR EXPOSURE ONLY - 3 ACCELERATION TEST 6 Mo.

IV-33

Table IV-9 Test Matrix for Corrosion Fatigue Test

<u>MATERIAL</u>	<u>CONFIGURATION</u>	<u>STRESS LEVELS</u>	<u>ENVIRONMENT</u>	<u># SAMPLES</u>
I-800	PM DOGBONE	TBD (3)	593 C SALT	9
SS-347	PM DOGBONE	TBD (3)	593 C SALT	9
RA-330	PM DOGBONE	TBD (3)	593 C SALT	9

i. Nitrate Salt Decomposition Test - This test is done to determine the rate of decomposition of nitrate salt to oxides in a closed system.

A sealed Incoloy tube (approximately 1000 cm³ volume) with 500 g (1.1 lbm) of salt is connected to a pressure gage and a gas sample withdrawal septum, as shown in Figure IV-18. The tube is heated to 593°C (1100°F) in a test oven. Pressure is monitored every 24 hours and gas samples are taken every 100 to 1000 hours, depending on the pressure rise.

At the end of the test [1000 to 5000 hours or when the pressure exceeds 345 kPag (50 psia)], the salt will be analyzed for O⁼, CO₃⁼, NO₂, and NO₃⁼, and these results will be compared to the salt composition before the tests. Pressure increases and changes in salt composition will indicate whether or not the decomposition is reversible and can be controlled by adjustments in the molten salt cover gas.

The apparatus for the nitrate decomposition test is assembled and the test should start immediately.

j. Special Purpose Materials Immersion Tests - These tests will determine the compatibility of such limited-use materials as seals, gaskets, packing, and valve trim with molten salt. The test setup is the same as that for the on-going compatibility tests with the materials immersed in molten salt in Incoloy trays and heated to 399°C (750°F) in a test oven. The materials are weighted to determine weight change where possible, and all samples are visually examined every 1000 hours during the 5000-hour tests.

Several special-purpose materials have been evaluated and more are being added to test. Results to date are as follows:

1. Tungsten Carbide - potential pump seal. Results: material completely dissolved in 399°C (750°F) salt in less than 140 hr.
2. Stellite #6 - potential pump seal. Results: both weld and parent metal samples tested at 399°C (750°F) held up well. No visible change in surface except discoloration after 2000 hours of exposure.
3. Crane Grafitic #235 - packing material. Results: material dissolved completely after less than 340 hours immersion at 399°C (750°F).
4. Crane Style 100 Al - packing material. Results: no visible change after more than 800 hours at 399°C (750°F).
5. Crane Graphite Coated Asbestos. Results: coating dissolved immediately, asbestos gradually swelled and unraveled.
6. Crane Copper Packing - To be tested soon.
7. Silicon Carbide - possible pump seal. Results: presently in test; data not yet available.

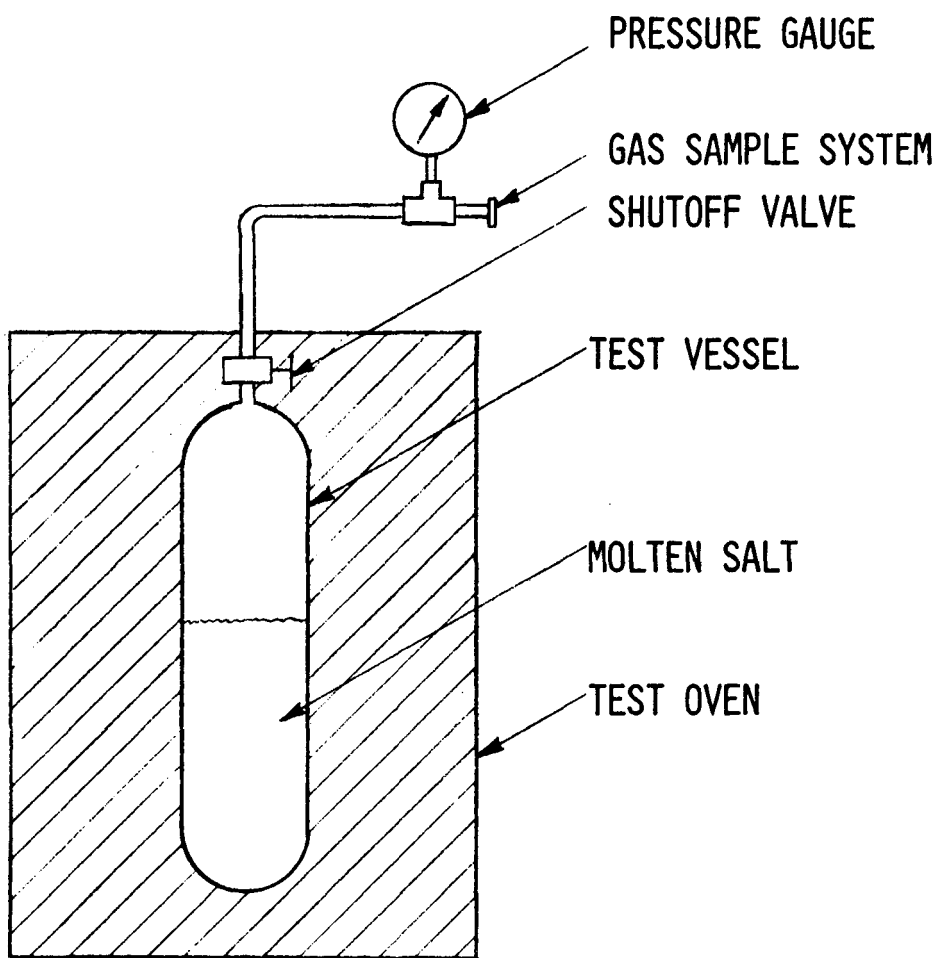


Figure IV-18 Nitrate Salt Decomposition Test Fixture

V. COMMERCIAL SYSTEM UPDATE

The purpose of this part of the program is to update the commercial system design developed during Phase I based on new data generated during Phase II. This will be done near the completion of the Phase II program. However, we did review the receiver selection (cavity vs exposed) early in Phase II to aid in the selection of the receiver SRE configuration. The results of this analysis are presented in Section III B of this report.

March 1980

APPENDIX A

TEST PLAN: RECEIVER SUBSYSTEM

RESEARCH EXPERIMENT

CONTENTS

	<u>Page</u>
1.0 Introduction	1-1
1.1 Test Objectives	1-1
1.2 Scope	1-2
1.3 Background	1-2
1.4 Test Program Summary	1-2 and 1-3
2.0 Experiment Description	2-1
2.1 General Description	2-1
2.2 Major Components	2-1 thru 2-18
3.0 Interface Definition	3-1
3.1 Overall CRTF Responsibilities	3-1
3.2 Overall Martin Marietta Responsibilities	3-2
3.3 Interfaces and Specific Responsibilities	3-3 thru 3-13
4.0 Test Program	4-1
4.1 Checkout Tests	4-2
4.2 Preliminary Tests - Cavity	4-5
4.3 Convection Tests - Cavity	4-15
4.4 Performance Tests - Cavity	4-17
4.5 Performance Tests - Exposed	4-19
4.6 Convection Tests - Exposed	4-21
4.7 Special Test - Exposed	4-22 thru 4-24
5.0 Test Program Schedule	5-1 thru 5-3

Figure

2-1 SRE Receiver	2-2
2-2 Plan View Layout	2-3
2-3 Receiver SRE Elevation Layout	2-4
2-4 Molten Salt Solar Receiver Experiment - Exposed Configuration	2-5
2-5 Molten Salt Solar Receiver Experiment - Cavity Configuration	2-6
2-6 Receiver SRE Schematic	2-7
2-7 Pump Design	2-8
2-8 Sump Design	2-9
2-9 Air Cooler	2-10

2-10	Air Cooler Fan Enclosure	2-11
2-11	Air Cooler Tube Bundle	2-12
2-12	Weigh Tank	2-15
2-13	Control Console	2-17
5-1	Test Schedule	5-3

Table

1-1		
2-1	Receiver Experiment Parameters	2-8
2-2	Instrumentation and Controls	2-14
2-3	Salt Properties	2-18
3-1	CRTF Power Requirements	3-4
3-2	Instrumentation List	3-6
3-3	Control List	3-9
3-4	Software Grouping	3-11
5-1	Ideal Test Spans	5-2

1.0 INTRODUCTION

This document describes the tests that will be performed with a solar central receiver subsystem research experiment. The heat transfer fluid used by the receiver is a eutectic salt mixture made up of 60% NaNO₃ and 40% KNO₃. The tests will be performed at the Central Receiver Test Facility (CRTF) in Albuquerque, New Mexico.

The major elements of this subsystem research experiment (SRE) include the receiver, a molten salt pump, a sump and an air cooler. The air cooler uses ambient air to reject the energy collected by the receiver. The nominal salt temperatures at the receiver inlet and outlet are 288°C (550°F) and 566°C (1050°F), respectively.

1.1 TEST OBJECTIVES

1.1.1 Primary Objective

The overall objective is to demonstrate that a solar receiver that utilizes molten salt as a heat transfer fluid can operate safely, reliably, and efficiently both in steady-state and transient modes and at temperatures and radiation flux levels consistent with commercial plants.

1.1.2 Specific Objectives

The specific objectives of this activity to be demonstrated are:

- 1) Performance at full load;
- 2) Performance at partial load;
- 3) System startup from "cold" conditions;
- 4) System overnight shutdown and startup;
- 5) System emergency shutdown;
- 6) Ability of the system to recover from cloud interruptions in a controlled manner;
- 7) Durability of receiver within the limitations of the test time available;
- 8) Performance comparison of cavity and exposed receivers.

The specific objectives of the activity that will be studied are:

- 1) Methods to prevent the salt from freezing;

- 2) Convection losses;
- 3) Design and fabrication techniques, particularly as they relate to commercial designs.

1.2 SCOPE

The purpose of this experiment is to demonstrate the performance of a molten salt receiver. Other elements of a commercial system such as the heliostats, boiler, tower, etc are not part of this demonstration. However, the molten salt pump, heat tracing, sump, piping, instrumentation, and controls will be demonstrated.

1.3 BACKGROUND

Martin Marietta has performed two studies of molten salt central receiver systems for the Department of Energy. The first was entitled Conceptual Design of Advanced Central Receiver Power System, Phase I, Contract EG-77-C-03-1724. The final report for this activity was released in September 1978. The second study was entitled Solar Central Receiver Hybrid Power System, Contract DE-AC-03-7SET21038. The work performed under this contract is documented in a final report dated September 1979. Both of these studies were concerned with commercial-size systems although both of these studies contributed a significant amount of information that was useful in the design of this test.

1.4 TEST PROGRAM SUMMARY

Table 1-1 lists the tests that will be performed during this program. The checkout tests will be performed both in Denver and at ground level on the elevating module at CRTF. Although the majority of the checkout tests are on a component level, the functional tests (CO-8 and CO-9) are system-level activities. The functional test with salt (CO-9) is designed to demonstrate that the system is ready for operation with a solar load.

At the conclusion of the checkout tests, the experiment will be taken to the 61-m (200-ft) level of the tower where all the remaining tests will be performed. The receiver will be tested first in the cavity configuration followed by tests in the exposed configuration. This sequence was chosen since the cavity is much safer than the exposed configuration relative to salt freezeup problems. This is because the cavity is fitted with doors that will be closed during shutdown operations. With these doors shut, heat will be retained in the receiver for a considerably longer time than in the exposed configuration and

therefore the risk of salt freezeup is significantly reduced. This is an important consideration both in normal and emergency shutdown situations.

The preliminary tests are designed to be "shakedown" tests and will provide the test crew experience in controlling and operating the experiment. The performance tests will yield efficiency data for both the cavity and exposed configurations and demonstrate the ability to recover from cloud interruptions. Although the results from the performance tests will be used to estimate losses, separate convection tests will be conducted to gain as much insight as possible relative to the convective processes. The convection tests will be conducted with all the heliostats off line to eliminate the uncertainty relative to the solar load from the energy balance on the receiver. The special tests will be performed at the end of the test program since they will "stress" the receiver. These tests will also demonstrate the ability of the receiver to withstand load cycling and to operate at full load for a substantial length of time.

Table 1-1 Tests To Be Conducted

<u>4.1 Checkout Tests</u>
4.1.1 CO-1 Airflow Distribution for Air Cooler (Denver)
4.1.2 CO-2 Hydrostatic and Leak Checks (Denver)
4.1.3 CO-3 Sump and Air-Cooler Heaters (Denver)
4.1.4 CO-4 System Trace Heaters (Albuquerque)
4.1.5 CO-5 Thermocouples (Albuquerque)
4.1.6 CO-6 Functional Valve Operation (Albuquerque)
4.1.7 CO-7 Electrical Control System (Albuquerque)
4.1.8 CO-8 Functional Test with Water (Albuquerque)
4.1.9 CO-9 Functional Test with Salt (Albuquerque)
<u>4.2 Preliminary Tests - Cavity</u>
4.2.1 1 PC-1 Partial Load - Tower Console Control
4.2.2 2 PC-2 Partial Load - Central Computer Control
4.2.3 3 PC-3 Maximum Load - Tower Console Control
4.2.4 4 PC-4 Maximum Load - Central Computer Control
4.2.5 5 PC-5 Maximum Load - Tower Console Control
4.2.6 6 PC-6 Maximum Load - Central Computer Control
4.2.7 7 PC-7 Partial Load with Emergency Shutdown
4.2.8 8 PC-8 Recovery from Simulated Cloud Passage
<u>4.3 Convection Tests - Cavity</u>
4.3.1 9CC Convection Loss at 700°F
<u>4.4 Performance Tests - Cavity</u>
4.4.1 10 PFC-1 Efficiency Tests at 35 to 100% of Maximum Load
4.4.2 11 PFC-2 Maximum Load for 20 Hours
4.4.3 12 PFC-3 Recovery from Simulated Cloud Passage
<u>4.5 Performance Tests - Exposed</u>
4.5.1 13 PFE-1 Efficiency Tests at 45 to 100% of Maximum Load
4.5.2 14 PFE-2 Recovery from Simulated Cloud Passage
<u>4.6 Convection Tests - Exposed</u>
4.6.1 15 CE Convection Loss at 700°F
<u>4.7 Special Tests - Exposed</u>
4.7.1 16 SE-1 Cycle Tests
4.7.2 17 SE-2 Endurance Test
4.7.3 18 SE-3 Extreme Cloud Conditions
4.7.4 19 SE-4 Lateral Support Shadowing
4.7.5 20 SE-5 High Localized Fluxes

2.0 EXPERIMENT DESCRIPTION

2.1 GENERAL DESCRIPTION

A simplified schematic of the SRE is shown in Figure 2-1. The experiment layouts are given in Figures 2-2 and 2-3, and artists' concepts are given in Figures 2-4 and 2-5. The experiment consists of a receiver, vertical cantilevered molten salt pump, sump, air cooler, and weigh tank. The air cooler rejects the solar energy collected by the receiver. The weigh tank is used to provide accurate salt flow rates. Since it is difficult to show analytically which type of receiver is optimum, cavity or exposed, the experiment is designed so both receiver types can be demonstrated and compared.

2.2 MAJOR COMPONENTS

The SRE schematic is shown in Figure 2-6. Note that valves PV-1 through PV-9 and DV-1 through DV-10 are used during filling and draining operations and are all closed during normal operation.

2.2.1 Receiver

The receiver experiment parameters are given in Table 2-1. The receiver is designed with a single inlet and a single outlet and has 18 fluid passes. The fluid passes are in series and each pass is made up of 16 tubes, which are in parallel.

2.2.2 Pump

The centrifugal pump is mounted vertically. Its nominal flow rate is $0.00757 \text{ m}^3/\text{s}$ (120 gpm) with a headrise of 1.17 MPa (170 psi). The power requirement is 44.8 kW (60 hp). A diagram of a typical pump is given in Figure 2-7.

2.2.3 Sump

The sump is placed at an elevation that will allow the molten salt throughout the system to drain by gravity into it at the end of each test day. The sump is heated and insulated to maintain the salt temperature overnight as well as to maintain the proper salt temperature at the receiver inlet. The sump is shown in Figure 2-8.

Figure 2-1
Air Cooler

2-2

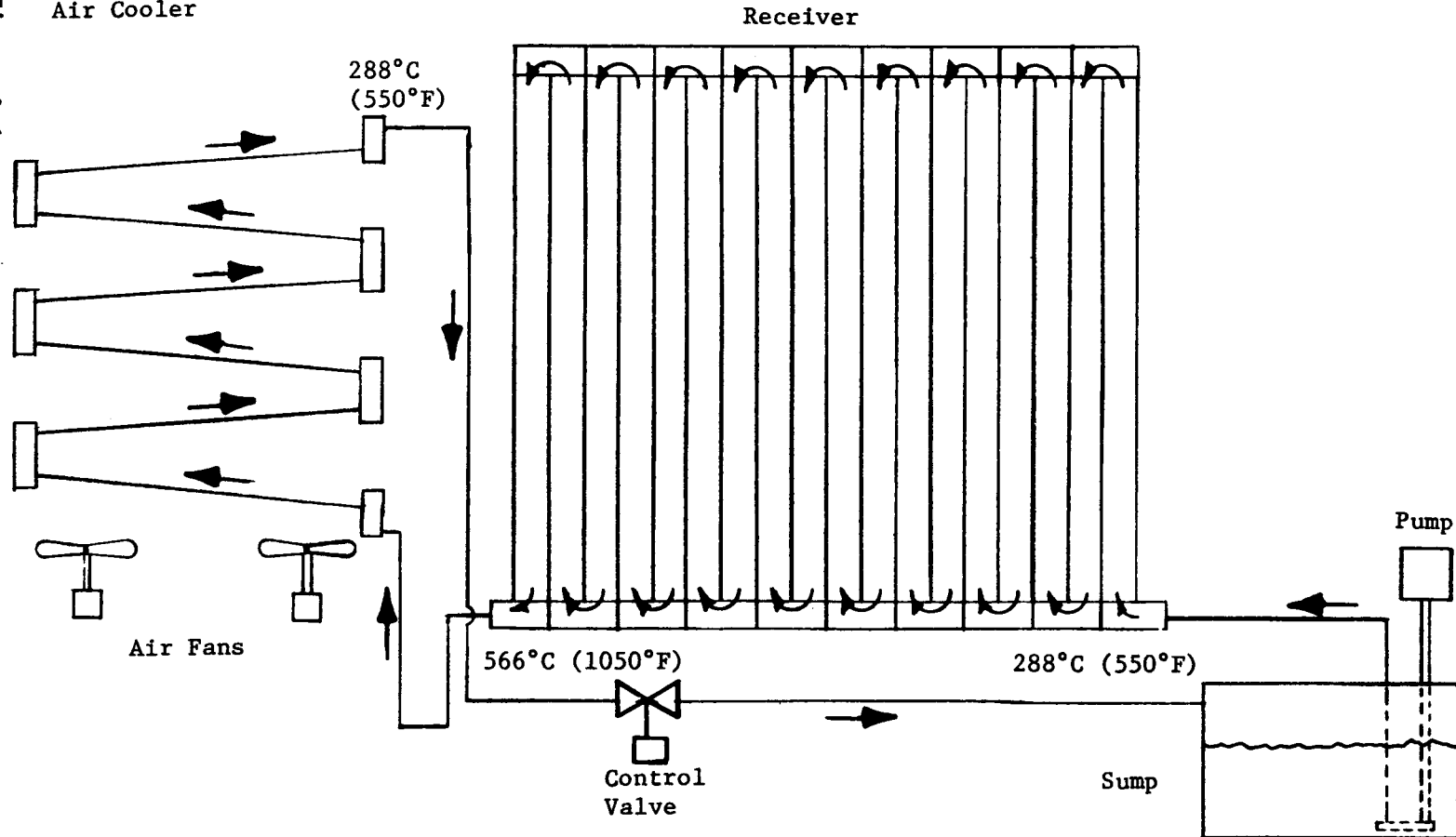
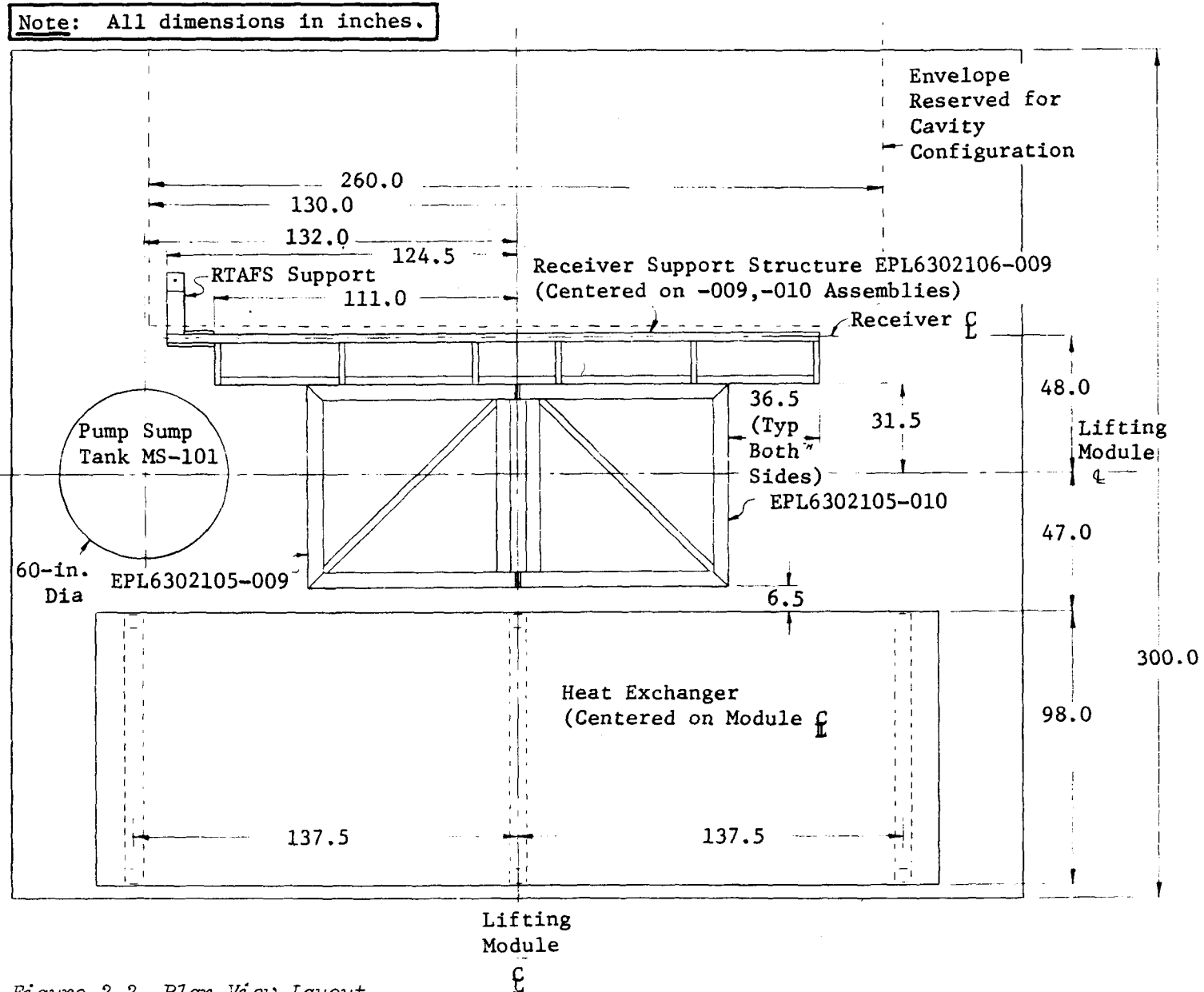


Figure 2-1 SRE Receiver

Figure 2-2



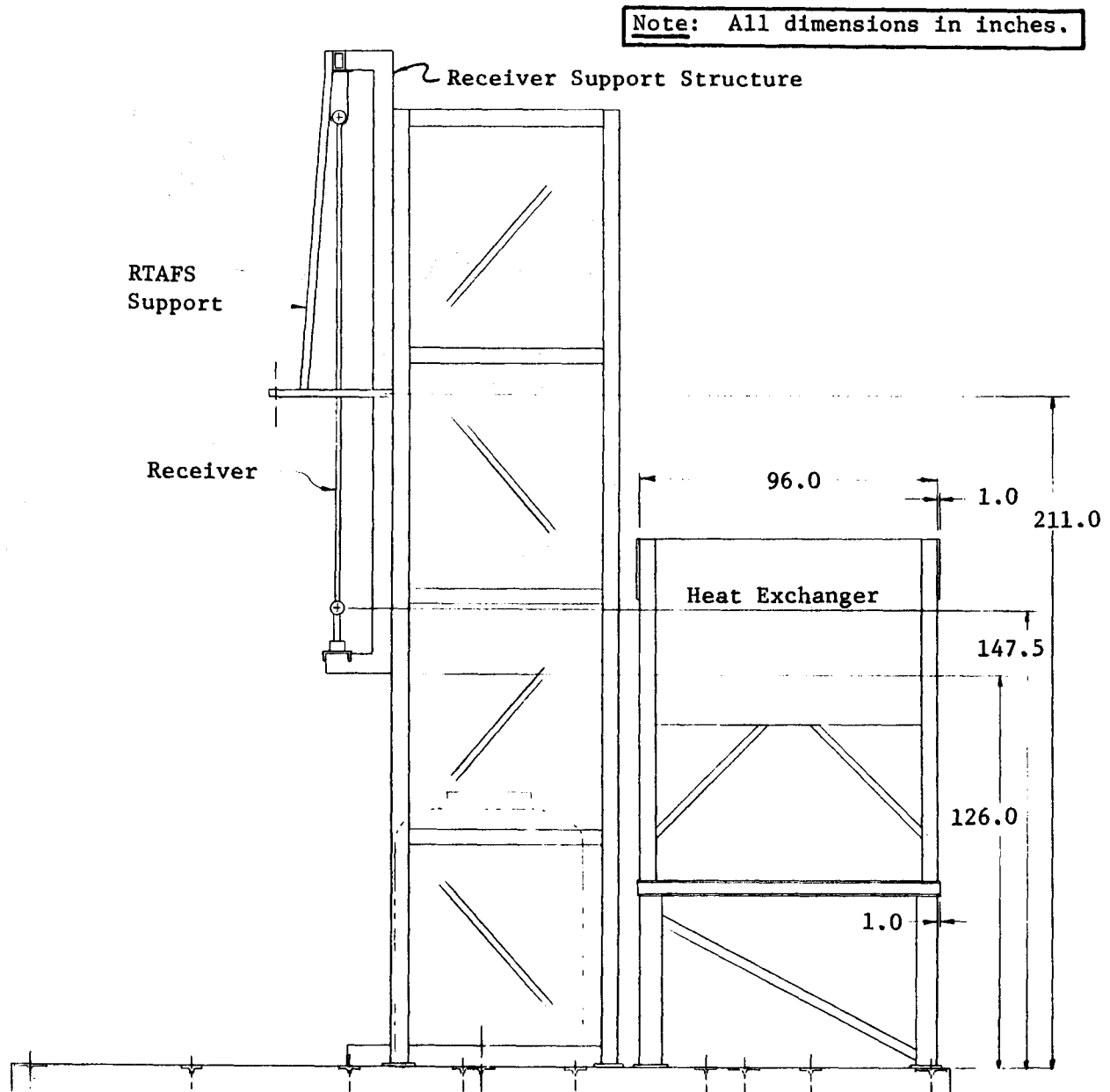


Figure 2-3 Receiver SRE Elevation Layout

Figure 2-4

Molten Salt Solar Receiver SRE—Exposed Configuration

2-5

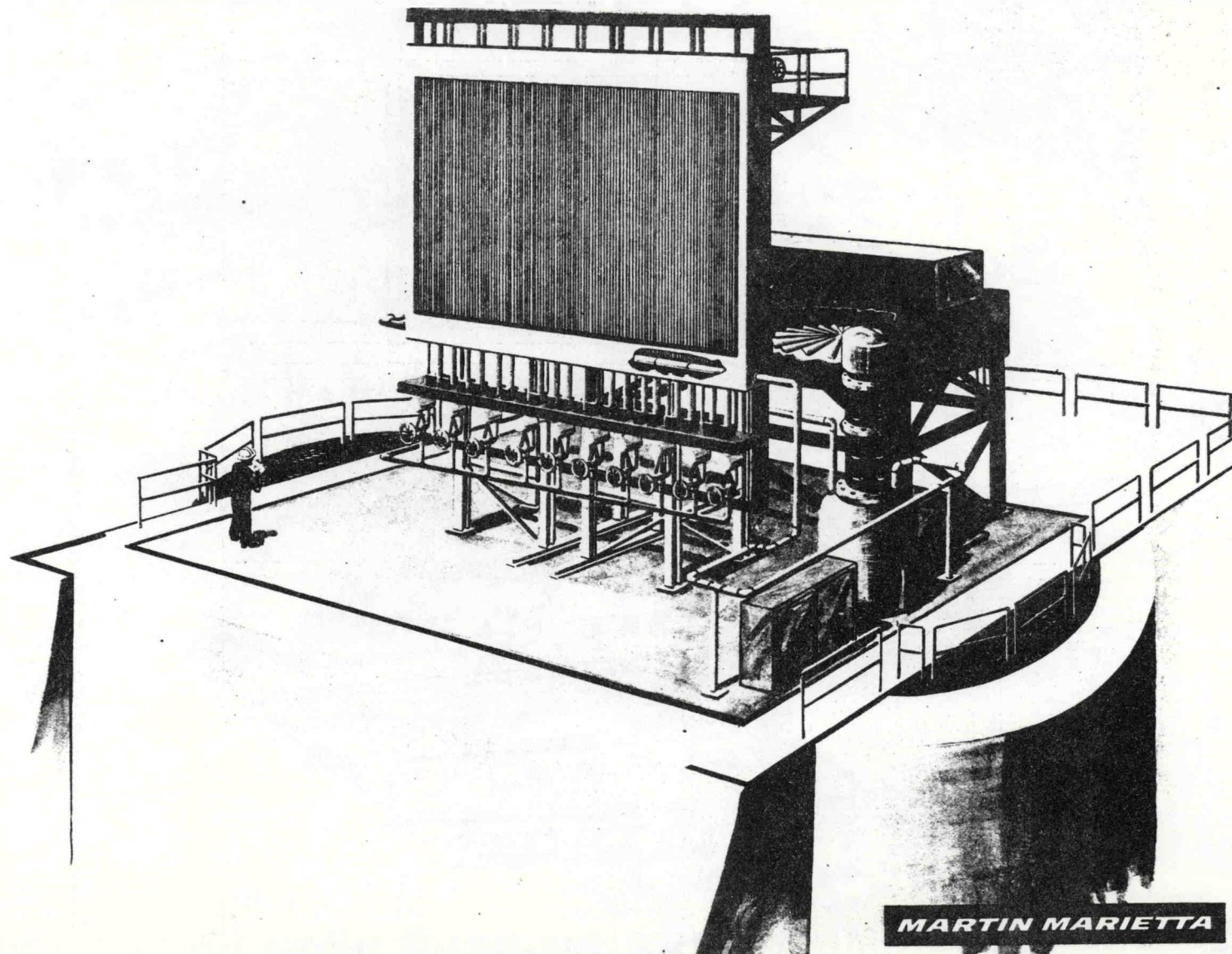
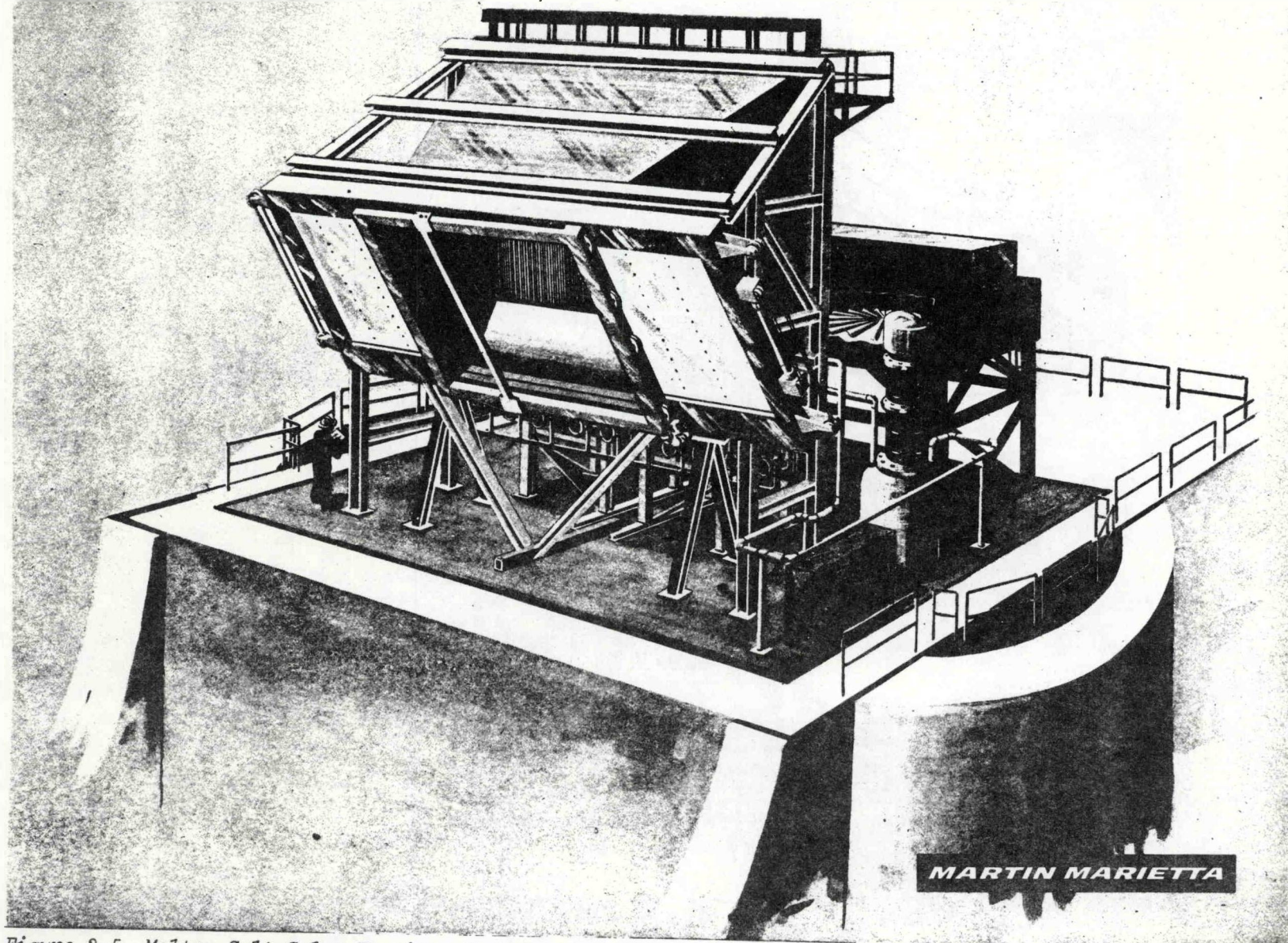


Figure 2-4 Molten Salt Solar Receiver Experiment - Exposed Configuration

Figure 2-5

Molten Salt Solar Receiver SRE—Cavity Configuration

2-6



MARTIN MARIETTA

Figure 2-5 Molten Salt Solar Receiver Experiment - Cavity Configuration

2-7

Figure 2-6

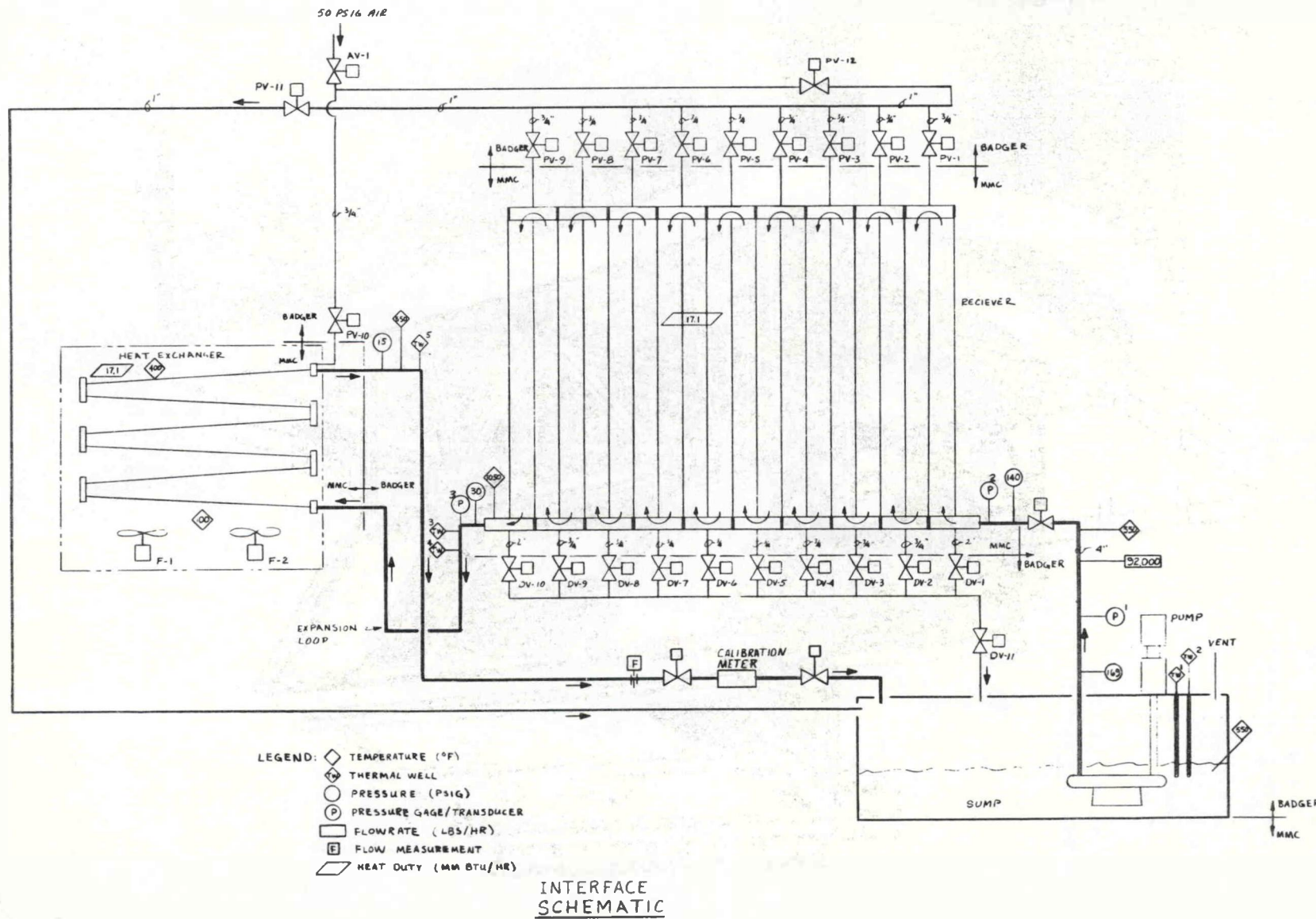


Figure 2-6 Receiver SRE Schematic

Table 2-1 Receiver Experiment Parameters

Nominal Thermal Rating	- 5 MWT (17.1×10^6 Btu/h)
Active Surface Dimensions	- 3.35 m (11 ft) x 5.49 m (18 ft)
Material	- Incoloy 800
Molten Salt Temperatures	- 561 K (550°F) to 839 K (1050°F)
Average Heat Flux (Approx)	- 0.315 MW/m ² (~100,000 Btu/h-ft ²)
Peak Heat Flux (Approx)	- 0.653 MW/m ² (~207,000 Btu/h-ft ²)
Tube Size	- 19.1 mm dia. x 1.651 mm Wall (0.75 in. dia x 0.065 in. Wall)
Number of Passes	- 18
Number of Tubes Per Pass	- 16

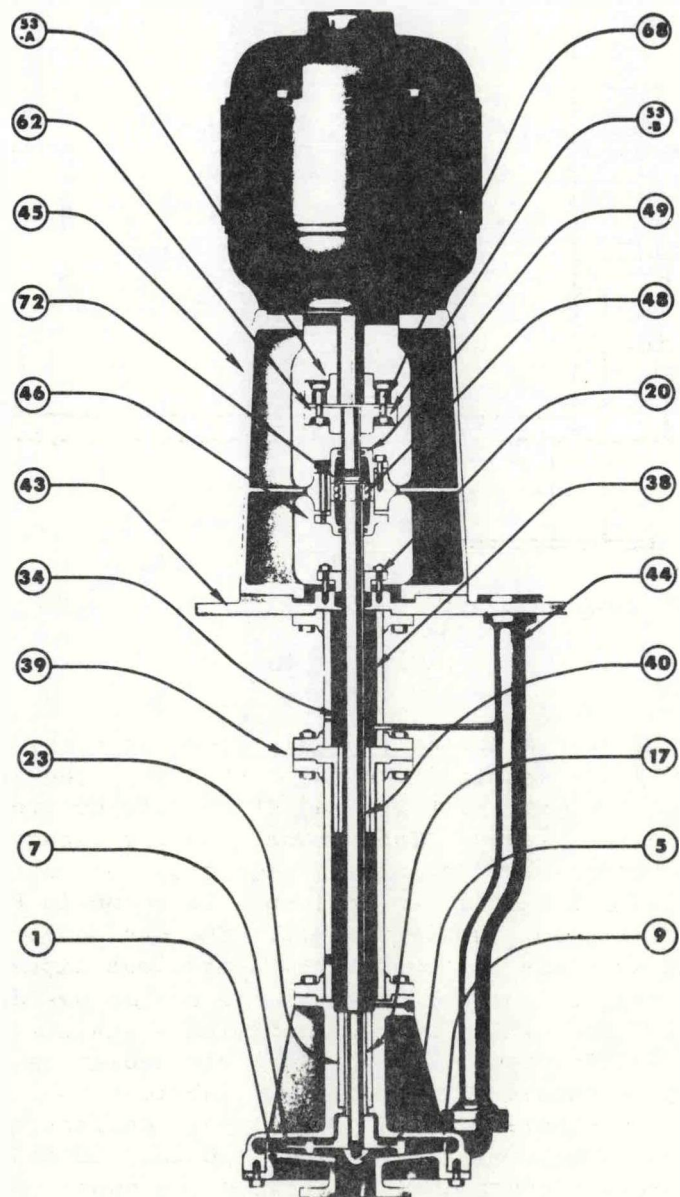


Figure 2-7 Pump Design

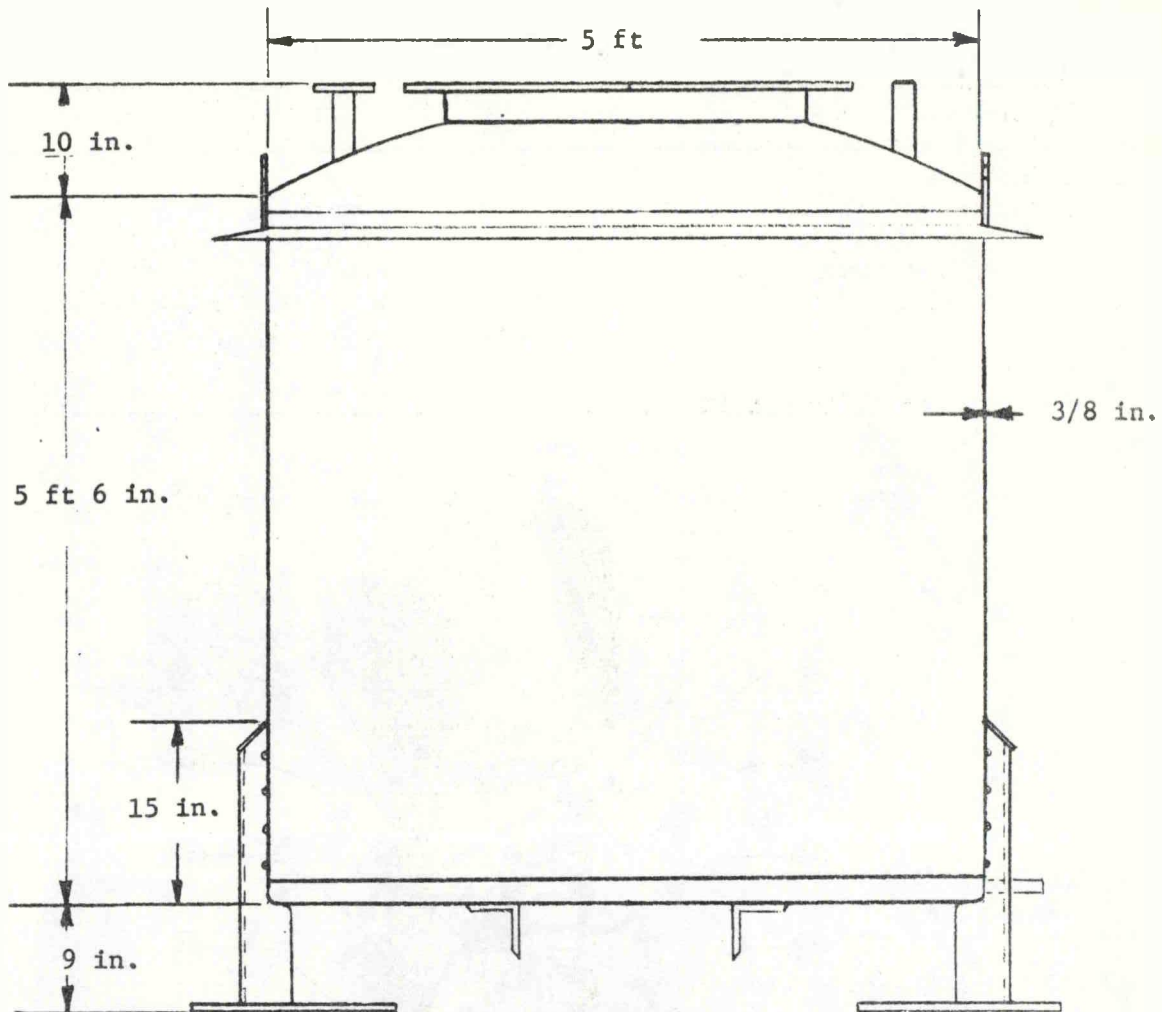


Figure 2-8 Sump Design

2.2.4 Air Cooler

The air cooler takes the molten salt from the receiver outlet at 566°C (1050°F) and cools it to 288°C (550°F). The heat is rejected to ambient air with the rejection rate controlled by varying the pitch of the fan blades. The nominal cooling capacity of the air cooler is 5 MW ($17.1 \times 10^6 \text{ Btu/h}$). A photograph of the air cooler is given in Figure 2-9, the fan enclosure is shown in Figure 2-10, and the tube bundle is shown in Figure 2-11. The fan enclosure structure (including the fans) is equipment from a previous experiment. The carbon steel tube bundle from the original air cooler was designed for water/steam service and had to be replaced with a stainless steel bundle for the molten salt system. The original air cooler as well as the replacement tube bundle is designed and fabricated by Therma Technology, Inc. The tube bundle for this experiment consists of 105 316 stainless steel tubes. The tubes are 2.54 cm (1.0 in.) OD and are finned. There are six passes through the cooler with the number of tubes per pass alternating between 18 and 17. Two fans force the air through the cooler; the fans are driven by two 14.9-kW (20-hp) motors.

Figure 2-9

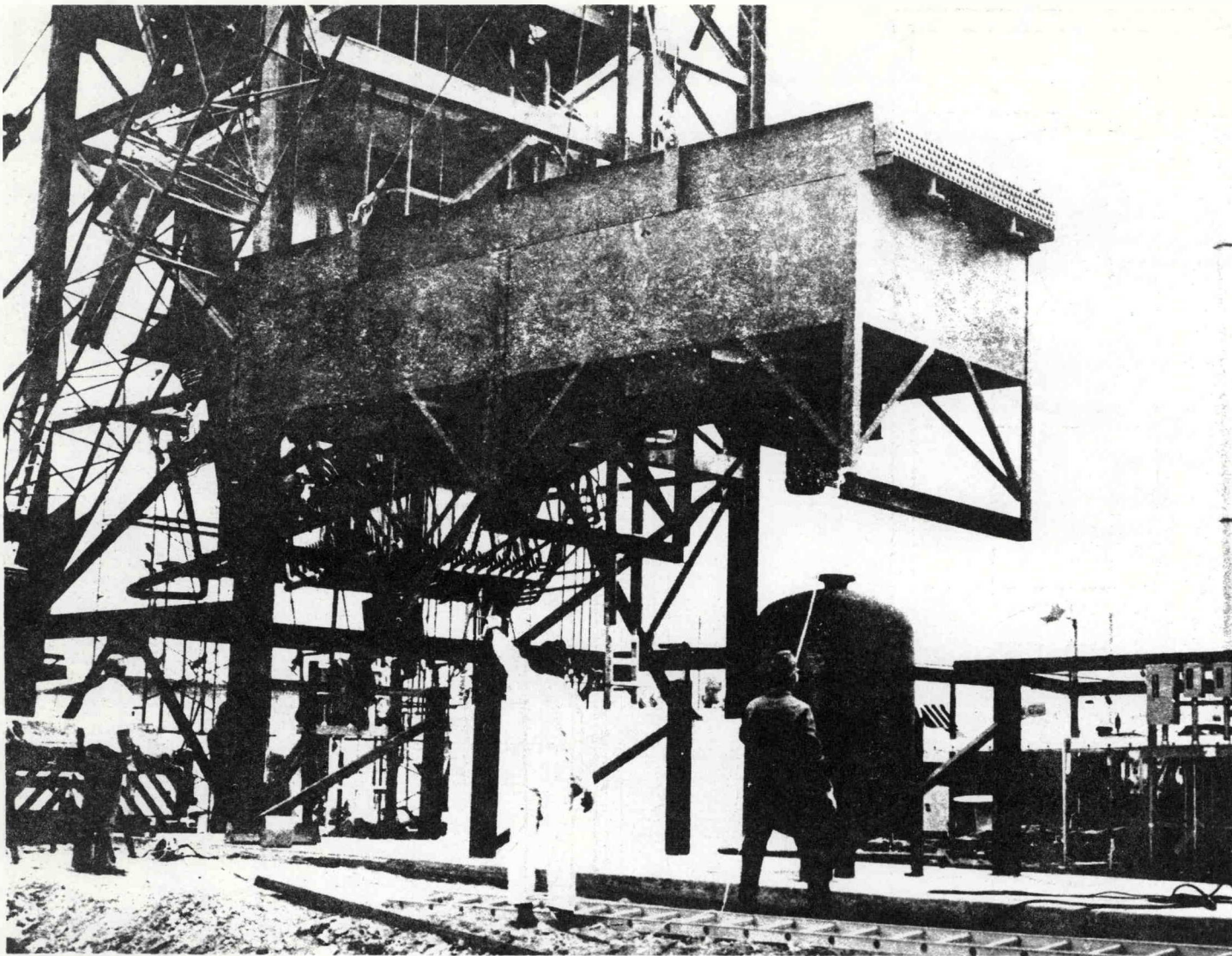


Figure 2-9 Air Cooler

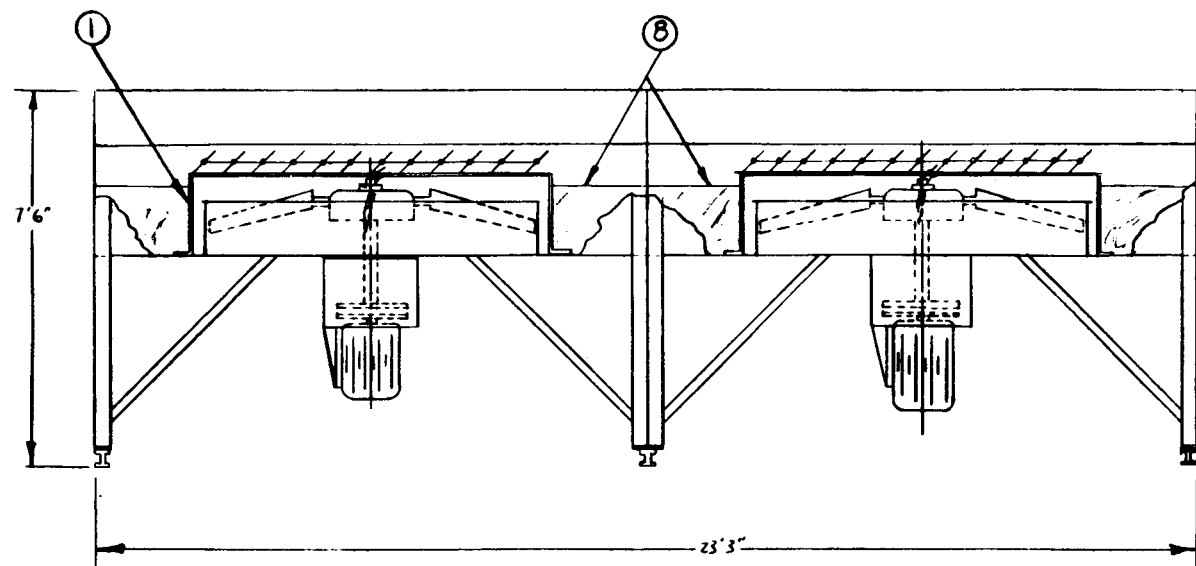
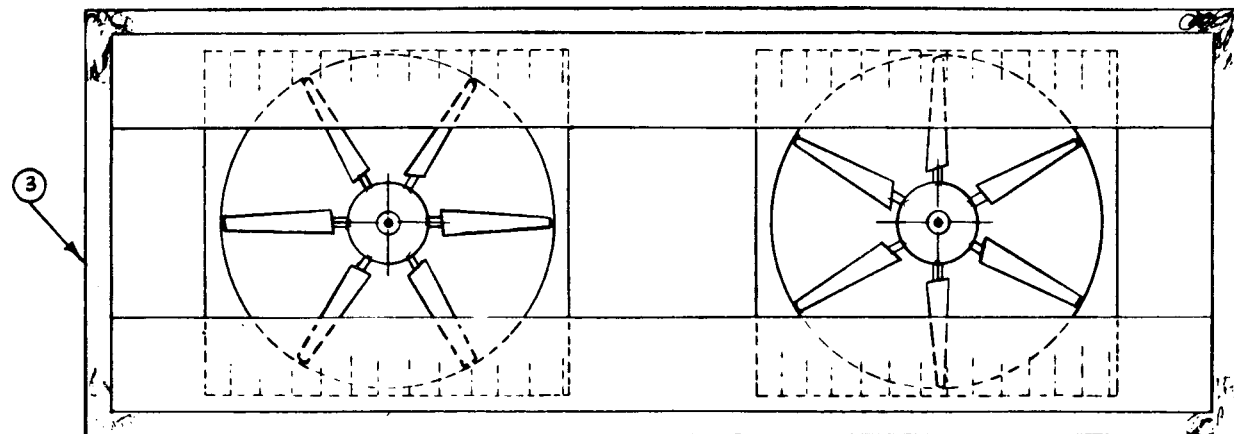


Figure 2-10 Air Cooler Fan Enclosure

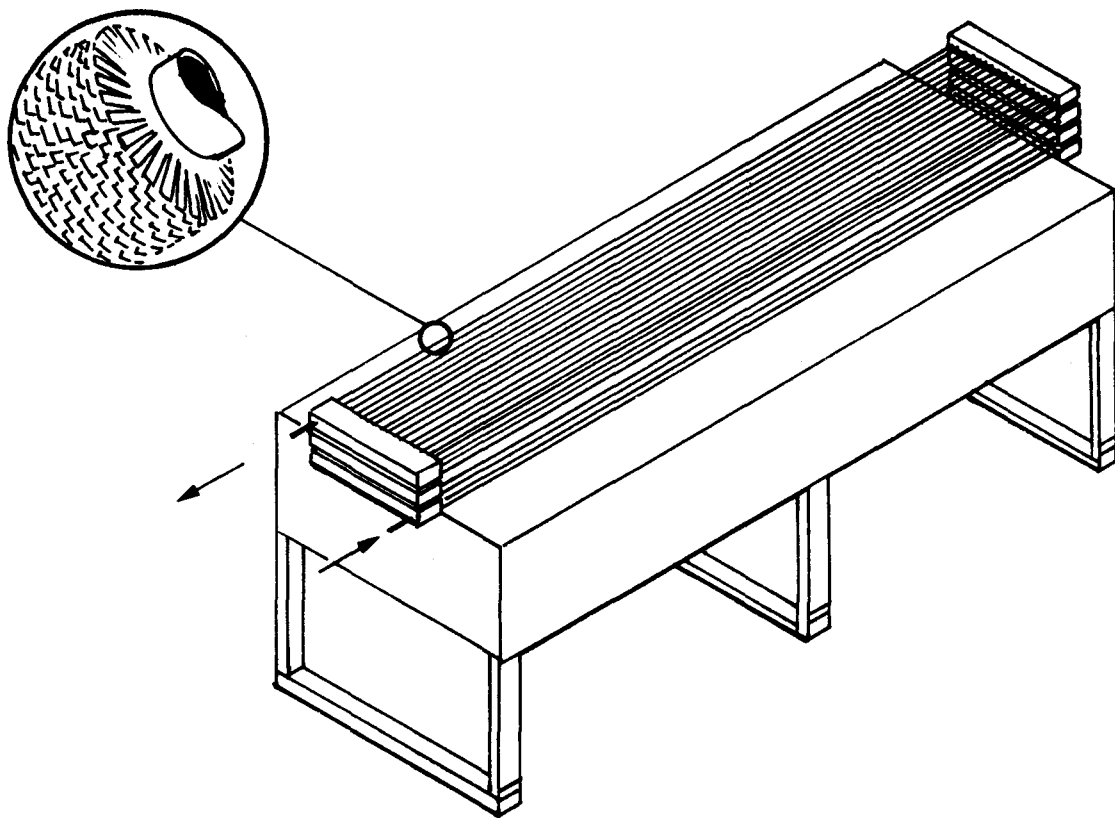


Figure 2-11 Air Cooler Tube Bundle

2.2.5 Instrumentation and Controls

2.2.5.1 Temperature - The temperature sensors selected for this experiment are all type K thermocouples but vary in configuration to meet the requirements of respective installations. The sensors in the interconnecting piping and sump tank are in thermowells and consist of an ungrounded junction, stainless steel-sheathed thermocouple. The absolute temperature measurements in support of the flux gages, and the absolute and differential temperatures on and between headers, are generated by ungrounded stainless steel-sheathed units that incorporate a 1.27x1.27-cm (0.5x0.5-in.) weld tab to facilitate installation. The ungrounded junction optimizes data acquisition via electronic high-speed multiplexing.

The differential temperature measurements between headers and respective tubes incorporate a combination of ungrounded junction and grounded junction weld-on units.

Different types of insulation on the thermocouple extension wires have been selected to match various environmental conditions.

2.2.5.2 Pressure and Flow - All molten salt pressures are obtained via pressure transmitters that are strain-gage, nonindicating instruments. The transmitters produce 4- to 20-mA signals proportional to pressure. The interface at the molten salt is a stainless steel diaphragm that couples the salt pressure to a silicone-filled line that connects the diaphragm to the pressure sensor. A differential pressure is taken across the segmented orifice for flow measurements.

2.2.5.3 Displacement - Eight linear variable differential transformers are used to detect displacement on tubes induced by thermal stresses.

The valve stem of the flow control valve has also been instrumented to monitor its motion during molten salt flow.

2.2.5.4 Flux Measurement - Eighteen miniature water-cooled flux gages (calorimeters) are located in the plane of the receiver tubes with the sensors protruding from the tubes and facing the receiver cavity.

2.2.5.5 Heat Tracing - The 26 heat-tracing circuits of this experiment are manually controlled from the tower control room. Each circuit is protected by a circuit breaker and is remotely energized by power contactors.

The magnesium-oxide-packed heater cables are stainless steel-sheathed and are individually designed to meet the required length and wattage.

Numerous thermocouples support the uniform preheating of the fluid system.

2.2.5.6 Valve Control - The control valves of this system are of the pilot-operated air-actuated diaphragm-type and are equipped with dual sets of open and closed limit switches. The design permits either local or remote control of the three-way solenoid valves. Each set of limit switches provides verification of valve-stem position for either the control console or CRTF computer.

Several valves are instrumented with pressure transducers that convert the 4- to 20-mA analog control signal to supply 20.7- to 103.4-kPa (3- to 15-psig) air pressure.

The instrumentation and data acquisition sensors are given in Table 2-2.

Table 2-2 Instrumentation and Controls

Item	Quantity	CRTF Interface		Data Acquisition						Console Control
		Thermo-Couple Channel	Copper Conductor	CRTF Computer	CRTF Data Logger	Martin Marietta Multipoint Recorder	Martin Marietta Data Logger	Console Recorder		
Temperature, Absolute										
- Piping	20	20	--	8	--	--	--	3	6	
- Header	19	19	--	19	--	--	--	--	--	
- Header	19	19	--	--	--	19	--	--	--	
- Trace Heat	110	110	--	--	--	--	110	--	--	
- Cavity	50	50	--	--	--	--	50	--	--	
- Flux Gage	18	18	--	18	--	--	--	--	--	
Temperature, Differential										
- Header	18	18	--	18	--	--	--	--	--	
- Header/Tube	288	--	576	--	200	88	--	--	--	
LVDT										
- Tubes	10	--	30	10	--	--	--	--	--	
- Valve	1	--	3	1	--	--	--	--	1	
Calorimeter	18	--	36	18	--	--	--	--	--	
Solenoids and Dual Microswitches	30	--	150	30	--	--	--	--	30	
Pressure	4	--	8	4	--	--	--	--	4	
Flowmeter	1	--	2	1	--	--	--	--	1	
Load Cell	1	--	4	1	--	1	--	--	--	

2.2.6 Weigh Tank

Since the molten salt flow rate is one of the quantities that determines the useful energy absorbed by the receiver's working fluid (energy absorbed = mass rate of flow x specific heat x temperature difference), it is important to accurately measure this quantity. A weigh tank is incorporated in the system to calibrate the segmented-orifice flowmeter. The weigh tank is attached to the structure at a single point through a load cell. All piping in and out of the weigh tank is designed so no forces can be transmitted to the tank from the piping system. This design is shown in Figure 2-12. When the valve at the bottom of the weigh tank is closed, the molten salt mass versus time is measured for approximately 35 seconds. This yields a basic salt flow rate measurement.

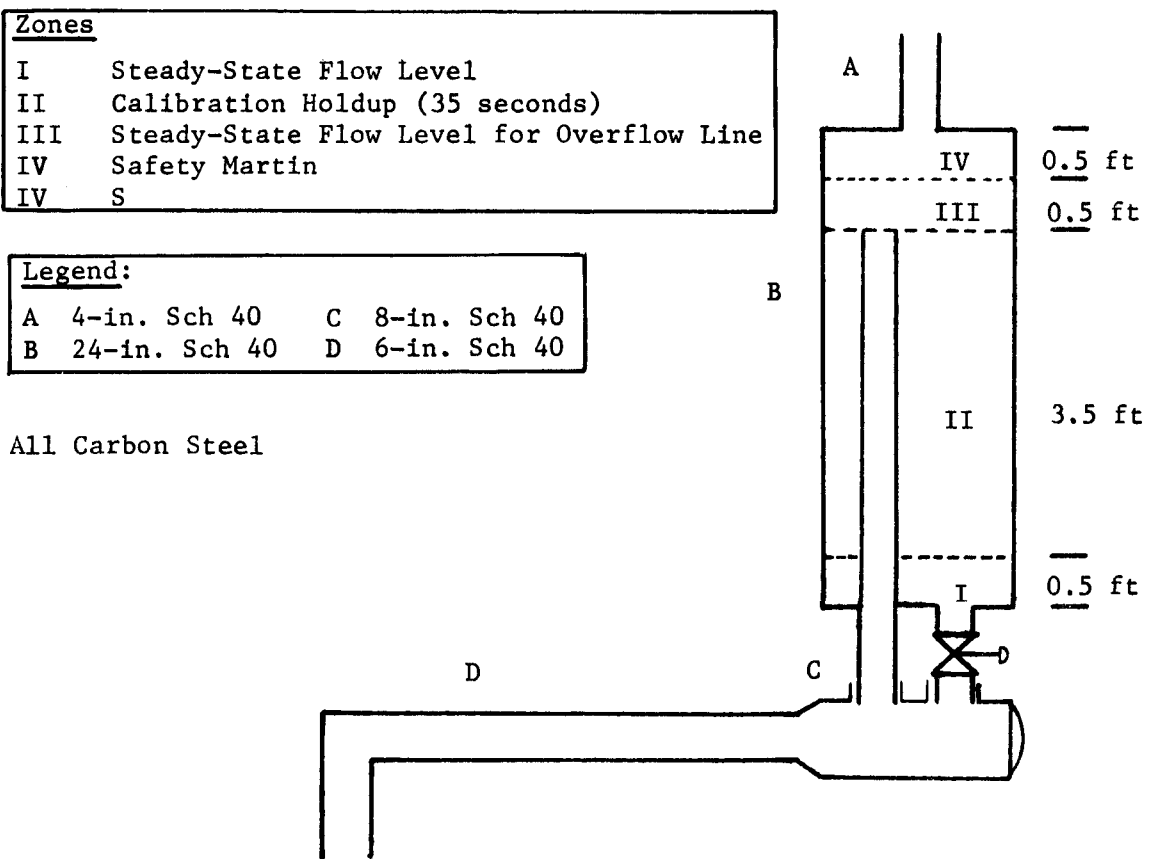


Figure 2-12 Weigh Tank

2.2.7 Control Console

The experiment control console will be located in the elevating module's data acquisition room. This console, shown in Figure 2-13, is designed to manually control and monitor the entire receiver experiment. Automatic control of the receiver outlet temperature and the air cooler is also provided for at the control console. This automatic control can be switched from the control console to the central computer.

The console contains all of the necessary manual valve control switches, process controllers and monitors, pump and cooler fan controls, valve position indicator lights, trace-heatin controls, process warning annunciator system and temperature recorders. A large and complete pictorial system diagram that allows the console operator an overall view of experiment performance has been incorporated on the front panel.

All receiver control functions, as well as computer input/output control functions, interface within the console on terminal boards. Only minimal analog recording of test parameters will be made on the console with the majority being digitally recorded by data logger techniques. A heliostat field scramble command capability has been incorporated in the control circuitry.

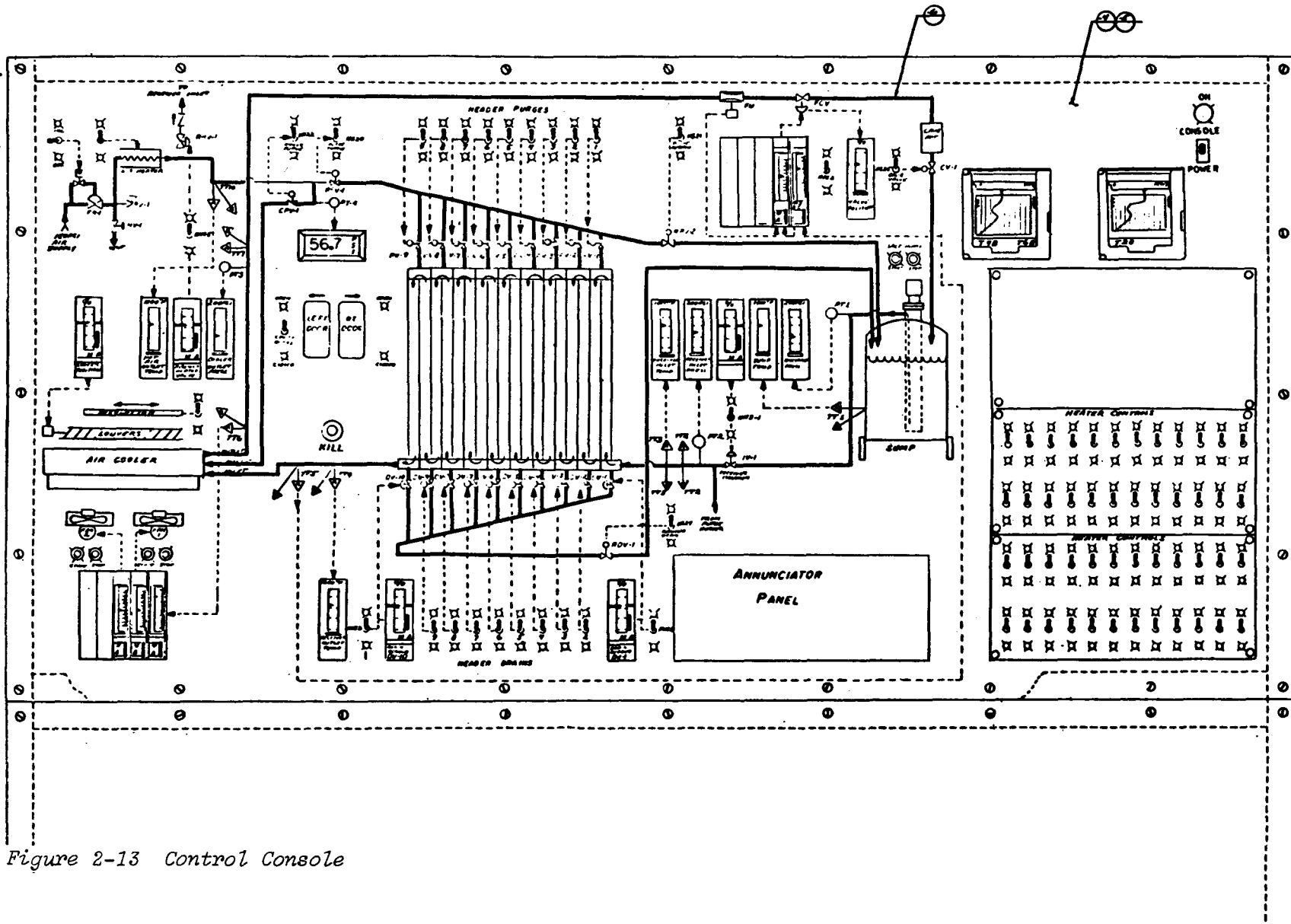
2.2.8 Heat Transfer Fluid

The heat transfer fluid is a eutectic mixture of 60% NaNO_3 and 40% KNO_3 . The mixture's melting temperature is 221°C (430°F).

Table 2-3 lists the properties of the salt as a function of temperature.

Figure 2-13

2-17



2.2.9 Trace-Heating Subsystem

Because the salt that will be used as the working fluid for this experiment has a relatively high freezing point, trace heating is provided to all components that contact the molten salt except for the receiver tubes. Heliostats will be used to preheat the receiver tubes for the majority of the startup situations. In one of the receiver tests a portion of the receiver tubes will be insulated from radiation by the heliostats. In this case a hot-air system will be used to preheat the receiver tubes by flowing heated air through the tubes.

Table 2-3 Salt Properties

T °C (°F)	ρ , $\frac{kg}{m^3}$ (lb/ft ³)	c_p , $\frac{J}{kg \cdot ^\circ C}$ $\frac{Btu}{lb \cdot ^\circ F}$	$\mu \times 10^3$, Pa-s $\frac{1b}{ft \cdot s}$	K, $\frac{W}{m \cdot ^\circ C}$ $\frac{Btu}{hr \cdot ft \cdot ^\circ F}$	Pr	$\beta \times 10^4$, $\frac{1}{^\circ C}$ $\frac{1}{^\circ F}$
260 (500)	1928.6 (120.4)	1553.3 (0.371)	4.00 (2.69)	0.398 (0.23)	15.62	3.4 (1.89)
316 (600)	1888.6 (117.9)	1553.3 (0.371)	2.80 (1.88)	0.398 (0.23)	10.92	3.4 (1.91)
371 (700)	1848.5 (115.4)	1553.3 (0.371)	2.05 (1.38)	0.398 (0.23)	8.01	3.5 (1.96)
427 (800)	1819.7 (113.6)	1553.3 (0.371)	1.65 (1.11)	0.398 (0.23)	6.45	3.6 (2.00)
482 (900)	1789.3 (111.7)	1553.3 (0.371)	1.45 (0.974)	0.398 (0.23)	5.66	3.7 (2.04)
538 (1000)	1741.2 (108.7)	1553.3 (0.371)	1.00 (0.674)	0.398 (0.23)	3.91	3.7 (2.08)
Solid						
38 (100)	1922.2 (120)	1553.3 (0.371)		0.363 (0.21)		
93 (200)	1922.2 (120)	1553.3 (0.371)		0.363 (0.21)		

where

ρ = density

c_p = specific heat

μ = viscosity

K = thermal conductivity

Pr = Prandtl number

β = coefficient of thermal expansion

3.0 INTERFACE DEFINITION

3.1 OVERALL CRTF RESPONSIBILITIES

The Central Receiver Test Facility in Albuquerque, N.M. will:

- 1) Provide information defining the CRTF capabilities and safety requirements;
- 2) Perform radiation analyses that will define the heliostat aiming strategy necessary to provide the required flux distribution on the receiver;
- 3) Develop the software that supports the experiment data acquisition and experiment control;
- 4) Provide a summary report on operation and control of the experiment;
- 5) Provide support in the area of data processing, including equipment and software. No manpower support will be provided except to place floating point data on tapes. CRTF's role is primarily to assist in processing the data necessary for test activities. CRTF is not responsible for data reduction relating to the reporting activities of Martin Marietta;
- 6) Provide special safety equipment and procedures to assure personnel and facility safety;
- 7) Provide design data relating to all the CRTF/experiment interfaces, including:
 - a) Mechanical/structural,
 - b) Electric power,
 - c) Cooling water,
 - d) Instrument and process air,
 - e) Air heat rejection system,
 - f) Instrumentation,
 - g) Controls,
 - h) RTAF,
 - i) Net radiometer;

- 8) Assist in the detailed test planning to assure that test conditions and data requirements are met;
- 9) Assist in development of the test operating procedures and sequences and in writing the integrated test procedures;
- 10) Review the required experiment documentation including:
 - a) Data package, including the experiment safety analysis,
 - b) Test plan,
 - c) Detailed procedures and training materials,
 - d) As-built drawings and quality assurance records;
- 11) Remove molten salt receiver components from transport vehicle and position on roof of the elevating module;
- 12) Operate facility in accordance with approved test procedures;
- 13) Disconnect receiver system from CRTF interfaces, remove from elevator, and store on CRTF site.

3.2 OVERALL MARTIN MARIETTA RESPONSIBILITIES

Martin Marietta will:

- 1) Design and fabricate the molten salt receiver system;
- 2) Leak-check and perform a functional test of the receiver system using both water and molten salt;
- 3) Provide the following documentation to CRTF,
 - a) Data package,
 - b) Test plan,
 - c) Detailed procedures and training materials,
 - d) As-built drawings and quality assurance records;
- 4) Deliver the receiver system to CRTF;
- 5) Connect the receiver system hardware on the top level of the CRTF elevator. Any welding required will be performed by Martin Marietta using appropriately qualified welders;
- 6) Define flux distribution and heliostat sequencing requirements on receiver;

- 7) Define instrumentation, experiment control, data displays, and system kill requirements, and supply all experiment sensors, control elements, and a control console;
- 8) Define experiment safety requirements;
- 9) Operate receiver tests in accordance with approved test procedures;
- 10) Perform real-time and posttest receiver performance analyses;
- 11) Disconnect the receiver system hardware after completion of tests and prepare system for storage;
- 12) Write final test report;
- 13) Maintain receiver system during the test operations.

3.3 INTERFACES AND SPECIFIC RESPONSIBILITIES

3.3.1 Heliostat Aim Point and Sequencing

Martin Marietta will define the desired flux distributions and perform radiation analyses with the TRASYS computer program. CRTF will check the TRASYS analyses with the HELIOS computer program and define the heliostat aim point (points) and heliostat sequencing necessary to meet the test requirements. Martin Marietta will transmit the heliostat requirements to CRTF via a separate document.

3.3.2 Mechanical/Structural

The major structural interfaces consist of attachment of the molten salt receiver system to the top level of the CRTF elevator and attachment of the RTAF to the receiver in both the exposed and cavity configurations. CRTF will supply structural drawings of the elevator and the RTAF. Martin Marietta will design the receiver system to match the structural requirements of the elevator and the RTAF. The mechanical and structural interfaces are defined in detail by Martin Marietta drawing EPL 6302122. CRTF will provide the handling equipment for moving the experiment components from the truck to the elevator. Martin Marietta will install the system on the roof of the elevating module.

The basic conditions considered relative to the structural design activities were:

- 1) Seismic loads of 1.5 g in any lateral direction while system is inoperative;
- 2) 17.8-m/s (40-mph) wind during system operation;
- 3) 44.7-m/s (100-mph) wind while system is inoperative;
- 4) Analysis of receiver tube stress and deflection due to solar flux assuming no wind loads.

3.3.3 Electric Power

The electric power interface for the experiment will be at the designated CRTF facility power panels. The power requirements are described in Table 3-1. The physical interfaces for the electric power subsystem are defined in Martin Marietta drawing EPL 6302122.

Table 3-1 *CRTF Power Requirements*

Item	Voltage	Power, kW	Normalized Power, kW, 480 Vac 3Ø	Requirement for Normalized Power, kW, 480 Vac 3Ø			
				Startup or Shutdown	Normal Operation	Overnight Standby	Emergency Shutdown
Salt Pump	480 Vac 3Ø	44.8	44.8	--	44.8	--	--
Cooling Fans	480 Vac 3Ø	29.8	29.8	--	29.8	--	--
Trace Heating							
Cooler	277 Vac 1Ø	31.5	10.5	10.5	--	10.5	--
Receiver	277 Vac 1Ø	4.5	1.5	1.5	--	1.5	--
Piping	277 Vac 1Ø	17.2	5.75	5.75	--	5.75	--
Sump	277 Vac 1Ø	12.1	4	4	--	4	--
Air Heater	48 Vac 3Ø	81	81	81	--	--	--
Controls	110 Vac 1Ø	3	3	3	3	3	3
Total Service			178 kW 214 A	103.5 kW 124 A	75.3 kW 90 A	24.8 kW 29.8 A	3 kW 3.6 A

3.3.4 Cooling Water

Cooling water (40% ethylene glycol, 60% water) will be supplied to the water-cooled aperture, the RTAF, and the flux sensors that are installed between the receiver tubes. The RTAF and the water-cooled aperture are connected in series. The required flow rates and inlet pressures are tabulated.

	Maximum Flow Rate	Inlet Pressure
Water-Cooled Aperture and RTAF	$1.89 \times 10^{-2} \text{ m}^3/\text{s}$ (300 gpm)	345 kPa (50 psig)
Flux Sensors	$5.17 \times 10^{-5} \text{ m}^3/\text{s}$ (0.82 gpm)	345 kPa (50 psig)

CRTF will connect the utility cooling water to the inlet and outlet experiment water lines. The physical interface for the cooling water system is given in Martin Marietta drawing EPL 6302122.

3.3.5 Instrument and Process Air

Instrument air is required for the system control valve and the drain valves. Process air is required to actuate these valves. Process air is also required to cool the salt pump bearings. The required pressures at the inlet to the receiver system and the flow rates are tabulated.

	Maximum Flow Rate	Inlet Pressure
Instrument Air	0.003 scms (7 scfm)	103 kPa (15 psig)
Process Air, Valves	0.0083 scms (17.8 scfm)	690 kPa (100 psig)
Process Air, Salt Pump Bearings	0.0095 scms (20 scfm)	69 kPa (10 psig)

Martin Marietta will connect the utility air line (lines) to the experiment inlet air lines. The physical interface for the instrument and process air is defined in Martin Marietta drawing EPL 6302122.

The CRTF will supply a backup system for instrument and process air. This will be accomplished by using gas bottles attached to a three-way valve that automatically actuates when a loss of normal supply air occurs.

3.3.6 Air Heating System

The air heat rejection system will be used to heat the tubes of the receiver when the system is in the exposed configuration with the RTAF in place. For this situation the receiver tubes will be thermally insulated (front and back) in the region outside the RTAF aperture area. For this condition during startup, the air from the heat rejection system will be heated to approximately 316°C (600°F) and introduced into the receiver inlet. This air will heat the insulated tubes on the inlet side of the receiver, will be reheated by energy from the heliostats in the uninsulated portion of the receiver, and then heat the insulated tubes on the outlet side of the receiver. The air heat rejection system is also required for purging the receiver system. The maximum flow rate required is approximately 0.23 kg/s (0.5 lbm/s). This will require one diesel compressor set of the air heat rejection system. The physical interface for the air heat rejection system is defined in Martin Marietta drawing EPL 6302122.

Since system draining and purging must be accomplished quickly, particularly under emergency conditions, the diesel compressor set that supplies air to the air heat rejection system must be on at all times during experiment operation.

3.3.7 Instrumentation

The instrumentation consists of sensors that measure temperature, pressure, molten salt flow rate, and receiver tube displacement. The instrumentation is summarized in Table 2-2. The instrumentation list is given in Table 3-2. Data from the instrumentation will flow to the central control room and to a console in the tower. The flow of the data is defined in the instrumentation list. Martin Marietta will handle the entire instrumentation and data system associated with the tower console. Martin Marietta will also provide the cabling from the various sensors to the CRTF central control room instrumentation interface in the tower. CRTF will provide the connectors for this interface (experiment sensors to central control room) and will make the connections.

Table 3-2 Instrumentation List

Measurement	Identification Code	Number of Channels	Experiment Location	Data Acquisition	Comments
Temperature*	TRH1DIC/TRHD18C	18	Receiver Headers	CRTF Multiplexer	Differential temperatures.
	T1P1D/T16P18D	288	Receiver Tubes	CRTF Data Logger	Differential temperatures. Back side of Tubes.
	TRH1C/TRH19C	19	Receiver Headers	CRTF Multiplexer	
	TRH1L/TRH19L	19	Receiver Headers	Martin Marietta Data Logger	
	TRFGU1C/TRFGU6C	6	Receiver Tubes	CRTF Multiplexer	Back side of tubes at upper flux gages.
	TRFGM1C/TRFGM6C	6	Receiver Tubes	CRTF Multiplexer	Back side of tubes at middle flux gages.
	TRFGL1C/TRFGL6C	6	Receiver Tubes	CRTF Multiplexer	Back side of tubes at lower flux gages.
	TRSSM1L/TRSSM6L	6	Receiver Tubes	Martin Marietta Data Logger	Front side (sun side) of tubes.
	TT-1BC	1	Sump	CRTF Multiplexer	Salt temperature on lower portion of sump.
	TT-2BX	1	Receiver Inlet	Console Recorder	Salt temperature.
	TT-3BC	1	Receiver Inlet	CRTF Multiplexer	Salt temperature.
	TT-4BX	1	Receiver Outlet	Console Recorder	Salt temperature.
	TT-5BC	1	Receiver Outlet	CRTF Multiplexer	Salt temperature.
	TT-6BX	1	Air Cooler Outlet	Console Recorder	Salt temperature.
	TT-7BC	1	Air Cooler Outlet	CRTF Multiplexer	Salt temperature.
	TT-8BC	1	Sump	CRTF Multiplexer	Salt temperature on middle portion of sump.
	TT-9BC	1	Sump	CRTF Multiplexer	Salt temperature on upper portion of sump.
	TT-10BC	1	Air Heater Outlet	CRTF Multiplexer	Air temperature.
	TA1RINC	1	Air Cooler Inlet	CRTF Multiplexer	Air temperature.
	TPUMPBL	1	Salt Pump Bearing	Martin Marietta Data Logger	
	TLCELLL	1	Load Cell	Martin Marietta Data Logger	
	T1ET1L/T2ET1L	2	Sump	Martin Marietta Data Logger	Trace heating.
	T1ET2L/T2ET2L	2			
	T1ET3L/T2ET3L	2			
	T1ET4L/T2ET4L	2			
	T1ET5L/T4ET5L	4			
	T1ET6L/T3ET6L	3	Air Cooler	Martin Marietta Multipoint	
	T1ET7L/T3ET6L	3			
	T1ET8L/T3ET8L	3			
	T1ET9L/T3ET9L	3			
	T1ET10L/T3ET10L	3			
	T1ET11L/T3ET11L	3			
	T1ET12L/T3ET12L	7			
	T1ET13L/T3ET13L	7			

Table 3-2 (concl)

Measurement	Identification Code	Number of Channels	Experiment Location	Data Acquisition	Comments
Temperature	T1ET14L/T8ET14L T1ET15L/T7ET15L T1ET16L/T3ET16L T1ET17L T1ET18L T1ET19L/T3ET19L T1ET20L/T6ET20L T1ET21L/T8ET21L T1ET22L/T3ET22L T1ET23L/T9ET23L T1ET24L/T10ET24L T1ACL/T20ACL TRB1L/TRB6L TRBMLL/TRBM6L TRBL1L/TRBL6L TRC1IL/TRC24IL TRC1ET/TRC24EL TJB1L/TJB4L	8 7 3 1 1 3 6 8 3 9 10 20 6 6 6 24 24 4	Piping Air Cooler Receiver Back Receiver Back Receiver Back Cavity Cavity T/C Junction Boxes	Martin Marietta Data Logger	Upper level. Middle level. Lower level. Interior. Exterior.
Pressure	PT-1C PT-2C PT-3C PT-4C	1 1 1 1	Pump Discharge Receiver Inlet Air Cooler Outlet Air Heater Outlet Flow Meter	CRTF Multiplexer CRTF Multiplexer CRTF Multiplexer CRTF Multiplexer CRTF Multiplexer	
Pressure	FMC	1			Differential pressure.
Force	LCC	1	Load Cell	CRTF Multiplexer and Martin Marietta Data Recorder	
Solar Flux	QRFG11C/QRFG16C	6	Receiver Tubes	CRTF Multiplexer	Lower level flux gages.
Solar Flux	QRFGMLC/QRFGM6C	6	Receiver Tubes	CRTF Multiplexer	Middle level flux gages.
Solar Flux	QRFGU1C/QRFGU6C	6	Receiver Tubes	CRTF Multiplexer	Upper level flux gages.
Displacement	LVDT1C/LVDT4C LVDTV1C LVDTV2C LVDTL1C LVDTL2C	4 1 1 1 1	Receiver Tubes Receiver Inlet Receiver Outlet Receiver Inlet Receiver Outlet	CRTF Multiplexer CRTF Multiplexer CRTF Multiplexer CRTF Multiplexer CRTF Multiplexer	Displacement at vertical centerline. Vertical displacement. Vertical displacement. Lateral displacement. Lateral displacement.
*All temperature measurements utilize thermocouples. The thermocouples recorded on the CRTF multiplexer are ungrounded. All other thermocouples are grounded. All thermocouples are type-K chromel/alumel.					

In Table 3-2, the final letter of the identification code defines the data acquisition equipment where the given signal terminates. C stands for CRTF multiplexer, D stands for CRTF data logger, L stands for Martin Marietta multipoint recorders or Martin Marietta data logger, and X stands for Martin Marietta console.

3.3.8 Control

The major elements or items that are controlled include the outlet salt temperature on the receiver, the outlet salt temperature on the air cooler, the salt flow rate, the various heater power levels, and the opening and closing of the purge/vent valves. The controls are summarized in Table 2-2. The control list is given in Table 3-3. The system will be designed so control of the experiment is provided either by the control console in the tower or by the central control room. During the early phase of the test program, system control will be handled at the tower console. As confidence is developed relative to overall performance of the system, control will be shifted to the central control room. Martin Marietta will install and connect the entire control system.

3.3.9 Software

The software for the molten salt receiver system is concerned with data that are transmitted to the central control room. Martin Marietta is responsible for defining the software requirements while CRTF is responsible for developing the software itself. The detailed software requirements will be defined in a document separate from this test plan. Martin Marietta views the software to be grouped into several categories with definite priorities associated with each group. These groups are listed in Table 3-4.

3.3.10 Real-Time Aperture Flux (RTAF) System

The interface between the CRTF and Martin Marietta relative to the RTAF is the mechanical attachment of the RTAF to the molten salt receiver structure. CRTF will connect the RTAF to the receiver structure and will be responsible for providing the necessary cooling water and instrumentation cabling as required. Martin Marietta will provide the structure to which the RTAF is mounted. The mechanical interface is defined in Martin Marietta drawing EPL 6302122.

3.3.11 Backup Systems

Backup systems must be provided to allow the receiver system to be shut down safely after failure of the primary electrical or pneumatic systems. Also if the primary heliostat control system fails, there must be provisions for defocusing the heliostats off the receiver. Martin Marietta will define the requirements for these systems. The specifics of how these systems are to be switched will be coordinated with CRTF and included in the test procedure.

Table 3-3 Control List*

Function Symbol	Component Description	Component Signal	Console Controller Signal	Computer	
				Input	Output
PT-1	Pressure Transducer	4 to 20-mA Output	4 to 20-mA Input	Share	--
PT-2	Pressure Transducer	4 to 20-mA Output	4 to 20-mA Input	Share	--
PT-3	Pressure Transducer	4 to 20-mA Output	4 to 20-mA Input	Share	--
PT-4	Pressure Transducer	4 to 20-mA Output	4 to 20-mA Input	Share	--
TT-1B	Thermo Couple	Millivolt	--	Direct	--
TT-3B			--		--
TT-5B			--		--
TT-7B			--		--
TT-9B			--		--
TT-10B			--		--
TT-1A			4 to 20-mA Output		--
TT-2A			--		--
TT-3A			4 to 20-mA Output		--
TT-4A	(Spare)		--	4 to 20-mA	--
TT-5A			--		--
TT-6A			--		--
TT-7A			--		--
TT-8A			--		--
TT-9A	(Spare)		--	4 to 20-mA	--
TT-10A			4 to 20-mA Output		--
FM			4 to 20-mA Output		--
LC	Differential Pressure Transducer	Millivolt	--	Share	--
IV-1	Load Cell I/P	4 to 20-mA Input	4 to 20-mA Output	Share	4 to 20-mA
DV-1					
DV-10					
FAN-1					
FAN-2					
RHV-1					
LONV					
FCV					
FCP	Linear Potentiometer	4 to 20-mA	4 to 20-mA	Share	--

Table 3-3 (concl)

Function Symbol	Component Description	Component Signal	Console Controller Signal	Computer	
				Input	Output
DV-1	Contact Closures	0 to 5 V	--	Direct	--
DV-2			--		--
DV-3			--		--
through					
DV-10			--		--
PV-1			--		--
PV-2			--		--
PV-3			--		--
through					
PV-9			--		--
IV-1			--		--
RHV-1			--		--
FCV-1			--		--
ROV-1			--		--
RPV-1			--		--
RPV-2			--		--
CPV-1			--		--
CV-1			--		--
PR-1			--		--
INSUL			--		--
CAV. Door-R			--		--
CAV. Door-L			--		--
Loss of Pneumatics	Pressure Switch	--	--	--	Warning
Computer "Watchdog"		--	--	--	Warning
Receiver		--	--	--	Kill
Tube					
Over Temp					

*Symbols are identified in Figure 2-13.

Table 3-4 Software Grouping

Priority	Software
1	Basic data in engineering units (temperature, flow rates, pressures, displacements, and power input), control displays, control signals, alarms, kills, and limit monitoring.
2	Performance data, - Receiver power output, m Cp T, - Solar input (from RTAF) in Btu/h-ft ² , - Flow rate computed from weigh tank measurements.
3	Data averaging and max/min discrimination (average temperatures on each pass of receiver and determine maximum and minimum temperatures).
4	Generation of system schematic with key temperatures, pressures, and flow rates shown.
5	Overall system heat balance calculations.

3.3.11.1 Electrical Backup - The primary and backup electrical systems are defined as tabulated.

	Primary	Backup
MCS		
Power Control	Diesel Generator Diesel Generator	Commerical Commerical
Tower Experiment		
Power Control	Commercial Commercial	None Battery

Both primary and backup electrical systems will be provided by and will be the responsibility of CRTF, except the experiment backup battery that will be provided by and will be the responsibility of Martin Marietta.

3.3.11.2 Pneumatic Backup - Two primary pneumatic systems are provided by CRTF--instrument and process air at 552 kPa (80 psig) and 0.0095 scms (20 scfm) and heating system air at 1035 kPa (150 psig) up to 0.227 kg/s (0.5 lb/s).

CRTF will provide two K-bottles with regulators and switchover valves and plumbing as a backup system for the instrument and process air.

Since Martin Marietta will require only one of the three compressors used to provide heating system air, the two unused compressors will be the pneumatic backup for the heating system air.

3.3.11.3 Heliostat Sequencing Backup - Heliostat sequencing is computer-controlled from the MCS and is therefore powered by a diesel generator with commercial power as backup. Should computer control be lost, the heliostats will defocus and sequence to the stowed position. It will be CRTF's responsibility to provide primary and backup heliostat sequencing to defocus the heliostats during control system failure.

3.3.12 Personnel Safety

The design, manufacturing, and operation of the research experiment will be in strict compliance with the latest issue of the Operating and Safety Procedures for CRTF Solar Operations document prepared and maintained by CRTF personnel.

Specific design features oriented toward personnel safety include:

- 1) A configuration envelope consistent with the boundaries of the elevating module so all assembly, checkout, and reconfiguration of the experiment can be accomplished at ground level;
- 2) Provisions for containment of molten salt spillage on the top of the tower (CRTF will construct a dam around the edge of the elevating module and around roof penetrations. Martin Marietta will install a salt containment dam around the sump);
- 3) Walkways, platforms and handrails for safe access to manual override valves, insulation attachments, etc that must be used during emergency situations;
- 4) Attachments for safety hooks that can be slid across structural members such as the RTAF sensor bar.

The following operational safety provisions will be included in the Martin Marietta test procedures as a minimum:

- 1) Personnel accountability system - The Martin Marietta test engineer will be responsible for knowing the whereabouts of all Martin Marietta personnel assigned to the test during both sun-on and sun-off operations;
- 2) A buddy system will be strictly enforced for access to the top of the tower;
- 3) Flags such as "Note", "Caution" and "Warning" will be incorporated in the test procedures to alert operating personnel to potential hazards or requirements for emergency steps to be taken during all test operations;
- 4) Preplanned and rehearsed emergency procedures will be established to effect safe shutdown of equipment should the operations/safety engineer or console operator exercise his option to terminate the test due to safety concerns;

- 5) Personnel performing duties on the top of the tower will be in constant audio communication with the Martin Marietta test engineer or other supervisory personnel designated by him;
- 6) CRTF will provide lightning protection for the experiment.

3.3.13 Maintenance

Martin Marietta will provide a maintenance schedule for the molten salt receiver system components and will provide the maintenance materials.

3.3.14 Spares

Martin Marietta will provide spare parts for the critical components of the receiver experiment system.

3.3.15 Audio Communication System

Audio communication is required between the central control room and the control console in the tower. CRTF will provide this communication system.

4.0 TEST PROGRAM

All of the tests defined in this section will be performed at the top level of the tower with the exception of the checkout tests. The system-level checkout tests will be conducted at ground level with the receiver system mounted on the roof of the elevating module. A portion of the component-level checkout tests will be conducted in Denver.

There are three basic test configurations--the exposed configuration without the real-time aperture flux (RTAF) system, the exposed configuration with the RTAF and the cavity configuration with the RTAF. Because of inadequate space and the possibility of limited crane capability on the top level of the tower, the elevating module will bring the experiment to ground level for each changeover to a different test configuration. The tests have been sequenced to minimize this operation. Under the present plan the experiment will be brought to ground level after the cavity convection test and the exposed performance tests.

Data will be taken and recorded from all installed sensors for all tests, other than the checkout tests, at the data system's minimum scan rate. The data will include:

- 1) Molten salt temperatures and pressures;
- 2) Receiver tube temperatures;
- 3) Receiver insulation from the flux sensors installed between the receiver tubes;
- 4) Receiver tube deflections;
- 5) Molten salt flow rates.

Special data collection requirements such as RTAF measurements and weigh tank data will be specified, as needed, for individual tests. All the data will be presented in English units.

General requirements that apply to all tests are that the first two rows of heliostats will not be used and that salt will be maintained in a molten state in the sump throughout the entire test period.

It is also important to note that all backup systems will be checked to verify that they function properly. This will be done before the system-level testing.

4.1 CHECKOUT TESTS

The system-level checkout tests will be conducted at ground level with the receiver system mounted on the roof of the elevating module. A portion of the component-level checkout test will be conducted in Denver. All tests other than the checkout tests will be conducted with the receiver system at the 61-m (200-ft) level.

The checkout test objectives are:

- 1) Check quality of system fabrication and assembly;
- 2) Check performance of subsystem components;
- 3) Perform functional test of system with particular attention given to filling and draining operations;
- 4) Provide test crew training.

4.1.1 Test CO-1 - Airflow Distribution Test for Air Cooler

This test will be conducted in Denver rather than at CRTF depending on schedules. The air cooler to be used for this testing is an existing unit that was originally designed for a water/steam solar system. The modifications of this original system to make it compatible with the molten salt system include a new tube bundle and the removal of three of the six fan blades on each fan. Therefore it is essential to verify the balance of the fans in the three-blade configuration before the flow distribution tests. After the balance has been verified, an anemometer will be used to check the air velocity on the upstream side of the tube bundle. This test will be conducted with the anemometer positioned at several locations across the tube bundle outlet and at several fan blade pitch settings. If the airflow distribution is unsatisfactory, baffles will be positioned in the airstream and the flow tests repeated.

4.1.2 Test CO-2 - Hydrostatic and Leak Check

Hydrostatic tests of the following subsystems will be conducted in Denver per the ASME process plan:

- 1) Receiver tubing;
- 2) Headers;
- 3) Purge and drain lines.

The hydrostatic tests will be conducted with gaseous helium at a pressure of 2.5 Pa (364 psig) and ambient temperature. At the conclusion of each hydrostatic test, a bubble leak check will be conducted.

A system-level bubble check will be performed on the completed system after the assembly and installation at CRTF. This leak check will be conducted with helium gas at 690 kPa (100 psig) and ambient temperature. The final leak check will be conducted before the system water flow functional test.

4.1.3 Test CO-3 - Sump and Air-Cooler Heaters

A checkout of the sump and air-cooler heaters will be conducted in Denver. The purpose will be to verify their operation and establish their capabilities. Power will be applied to the heaters and the temperature will be slowly increased to $371 \pm 28^\circ\text{C}$ ($700 \pm 50^\circ\text{F}$). The power will then be removed and the tank returned to ambient temperature.

4.1.4 Test CO-4 - System Trace Heaters

To allow for system warmup before initiation of the salt flow, all subsystems with the exception of the receiver tubes will be heat-traced. All subsystems will have power applied to the heat tracing to establish a temperature of $371 \pm 28^\circ\text{C}$ ($700 \pm 50^\circ\text{F}$). At the conclusion of this checkout, all power will be removed and the temperature returned to ambient.

While the system is at temperature all thermocouples should be monitored to verify there are no cold spots.

4.1.5 Test CO-5 - Thermocouples

End-to-end checkouts of all thermocouples will be conducted to verify that the junctions and connections are completed and that no opens exist. This checkout will also verify the proper location of each thermocouple. A heat gun will be used to apply heat to each thermocouple junction and the response will be verified using the data system.

4.1.6 Test CO-6 - Functional Valve Operation

All subsystem valving will be functionally operated and checked out to verify proper positioning and actuation. Any valves that do not seat properly will be adjusted. The outputs of all electropneumatic controllers will also be verified.

4.1.7 Test CO-7 - Electrical Control System

Before conducting the functional water flow test, as many system controls will be verified as possible. Numerous controls will already have been verified during previous checkouts. An example is valve operation. Items such as outlet temperatures and heater power levels will be checked out as much as possible but will require the functional operating temperature for final verification. All adjustments that can be will be made before that test. These checkouts will be made just before initiating the functional tests and will include the completed tower control console checkout and central computer checkout.

4.1.8 Test CO-8 - Functional Test with Water

The complete molten salt control receiver will be assembled on the roof of the elevating module with all of its subsystems operational. Before flowing molten salt, it will be necessary to check out the operation with water. This procedure will accomplish the following objectives:

- 1) Verify pump operation;
- 2) Verify system flow rate vs pressure drop predictions;
- 3) Check calibration of segmented-orifice flowmeter with weigh tank;
- 4) Verify valve sequencing and operation;
- 5) Provide partial test procedure checkout;
- 6) Develop fill and drain procedures;
- 7) Provide training to test personnel.

The segmented orifice will be initially checked out during this functional water test. With the orifice flowmeter in line, the weigh tank will be suspended from a load cell. After the water flow has stabilized, the weigh tank outlet valve will be closed and a reading of the load cell recorded. Water will be allowed to flow into the weigh tank with a load cell reading taken at approximately 2-second intervals. The weigh tank data will be converted to flow rate and then compared with the segmented-orifice flow rate measurements. This operation will be conducted for flow rates of approximately 25, 60, 75 and 100% of maximum flow. Two data points at each flow setting will be obtained. During the functional molten salt flow test, this operation will be performed as previously described except that in this case the test medium will be molten salt.

At the conclusion of this test, the system must be completely purged and drained.

4.1.9 Test CO-9 - Functional Test with Salt

A functional molten salt test will be conducted following the purging and drying operations. This test will verify the system's capabilities to flow molten salt at 288°C (550°F), establish a 5.68×10^{-3} to $6.94 \times 10^{-3} \text{ m}^3/\text{s}$ (90- to 110-gpm) flow rate, and check for any leakage or cold spots with molten salt. The air heater system will also be checked out to establish its capability for heating the receiver tubes to approximately 288°C (550°F) at a flow rate of approximately 0.23 kg/s (0.5 lbm/s). Electric power supplied by the CRTF electrical system will provide the heating source and the air heat rejection system will be used as the air supply. The procedural steps necessary to accomplish this test are:

- 1) Completely purge and dry the system;
- 2) Install and melt salt in the sump;
- 3) Adjust all trace-heater controls to slowly achieve 288°C (550°F) on all components except the receiver tubes;
- 4) Bring receiver tubes to approximately 299°C (550°F) using the air heat rejection system;
- 5) Open the purge and drain valves when all systems are stabilized at 299°C (550°F);
- 6) Start the salt pump and allow the system to fill with molten salt;
- 7) Close the purge and drain valves when the receiver indicates all tubes are full of molten salt;
- 8) Allow system to flow molten salt while performing the following operations,
 - a) Inspect for any leaks,
 - b) Conduct segmented-orifice flow calibrations,
 - c) Check for any cold spots,
 - d) Check flow control valve operation while operating both from the tower control console and the central computer,
 - e) Check all instrumentation;
- 9) Shut off salt pump and activate purge system;
- 10) Turn off all trace heaters except for those on the sump;
- 11) Secure the system.

4.2 PRELIMINARY TESTS - CAVITY

The receiver configuration and test conditions are:

- 1) Cavity configuration with the entire receiver illuminated, 3.35x 5.49 m (11x18 ft);
- 2) The real-time aperture flux (RTAF) system attached to the receiver;
- 3) The first two rows of heliostats not used;

- 4) Single-point heliostat aim strategy used with the maximum flux limited to 6.93 W/cm (220,000 Btu/h/ft²).

The test objectives are to:

- 1) Check out system and components;
- 2) Familiarize the test crew with system operation;
- 3) Determine system operational characteristics;
- 4) Demonstrate control stability;
- 5) Check out instrumentation;
- 6) Check out software;
- 7) Check out drain and purge system;
- 8) Demonstrate emergency shutdown operation;
- 9) Demonstrate recovery from simulated cloud passage.

4.2.1 Test 1 PC-1 - Partial Load, Tower Console Control

Outlet receiver temperature will be slowly increased to a maximum of 482°C (900°F) with solar input limited to approximately 1/2 of maximum. The air-cooler outlet temperature and receiver inlet temperature will be maintained at approximately 343°C (650°F). System control will be provided by the tower control console.

The specific test conditions are:

- 1) Test will be performed during periods when shadowing of heliostat field by clouds is not probable;
- 2) Test will be terminated if shadowing of heliostat field by clouds is likely;
- 3) Experiment control will be handled by tower console.

The specific test objectives are to:

- 1) Familiarize test crew with system operations;
- 2) Determine molten salt flow distribution through the receiver tubes at partial load;
- 3) Calibrate segmented-orifice flowmeter using the weigh tank;
- 4) Demonstrate receiver outlet temperature control and air-cooler control via the tower control console;

- 5) Demonstrate that the receiver can be brought to approximately 1/2 of its maximum power by slowly increasing the outlet temperature;
- 6) Perform an initial tuning of the console controllers.

The test sequence is as follows:

- 1) Heat all molten salt lines, air cooler, receiver headers and sump to approximately 343°C (650°F). The salt will have been previously melted in the sump and the sump temperature maintained at approximately 343°C (650°F) continuously. During system heatup the air-cooler louvers and top insulation will be in their closed positions;
- 2) Heat receiver tubes with heliostats so the minimum tube temperature is greater than 288°C (550°F) while the maximum tube temperature is less than 593°C (1100°F). The particular heliostats and the aim strategies used for this operation will be chosen so the flux distribution on the receiver tubes is as uniform as possible;
- 3) Fill the system with molten salt;
- 4) Monitor the trace-heating system and shut off heaters as required;
- 5) Start molten salt flow through system. Set flow at rate consistent with receiver's maximum power;
- 6) Monitor trace-heating system and shut off heaters as required;
- 7) Bring on line 20 additional heliostats. The heliostats used for this operation will be chosen so the basic flux distribution is uniform across the majority of the receiver's surface;
- 8) Open the air-cooler louvers and top insulation and start fans with zero pitch on fan blades. Adjust pitch on fan blades until air-cooler outlet salt temperature is approximately 343°C (650°F) and steady;
- 9) Bring on line 20 additional heliostats as in item 7;
- 10) Adjust pitch on fan blades until air-cooler outlet temperature is approximately 343°C (650°F) and steady;
- 11) Repeat items 9 and 10 until approximately 110 heliostats are operating;
- 12) Check temperature distribution on all receiver tubes;
- 13) Perform a molten salt flow calibration test using the weigh tank;

- 14) Adjust molten salt flow rate until receiver outlet temperature is approximately 482°C (900°F), maintaining air-cooler outlet at approximately 343°C (650°F);
- 15) Check temperature distribution on all the receiver tubes;
- 16) Tune console controllers;
- 17) Perform a molten salt flow calibration test using the weigh tank;
- 18) Switch air cooler to automatic control on the tower control console with the air-cooler outlet salt set point temperature at 343°C (650°F) and operate for at least 10 minutes;
- 19) Return air cooler to manual control;
- 20) Switch receiver outlet temperature to automatic control on the tower control console with the set point at 482°C (900°F) and operate for at least 10 minutes;
- 21) Switch air cooler to automatic control on the tower control console with the air-cooler outlet salt set point temperature at 343°C (650°F) and operate for at least 10 minutes;
- 22) Bring slowly off line all heliostats except those defined in item 2. During this operation the air cooler will be on automatic control while the receiver outlet temperature will be on manual control;
- 23) Operate system until the molten salt temperature throughout the system is approximately 288°C (550°F);
- 24) Simultaneously close main control valve, shut off molten salt pump, close air-cooler louvers, and close air-cooler top insulation;
- 25) Turn on purge air heater and drain molten salt from system into sump;
- 26) Bring off line the remaining heliostats;
- 27) Secure system.

4.2.2 Test 2 PC-2 - Partial Load, Central Computer Control

Outlet receiver temperature will be slowly increased to a maximum of 482°C (900°F) with solar input limited to approximately one-half of maximum. The air-cooler outlet temperature and receiver inlet temperature will be maintained at approximately 343°C (650°F). System control will be provided by the central computer.

The specific test conditions include:

- 1) Test will be performed during periods when shadowing of heliostat field by clouds is not probable;
- 2) Test will be terminated if shadowing of heliostat field by clouds is likely;
- 3) Experiment control will be handled by the central computer.

The specific test objectives are to:

- 1) Familiarize test crew with system operation;
- 2) Demonstrate receiver outlet temperature control and air-cooler control via central computer.

The test sequence is the same as Test 1 PC-1 (4.2.1) except for the following items:

- 16) Eliminate controller tuning;
- 18) Switch air cooler to automatic control on the central computer and operate for at least 10 minutes;
- 20) Switch receiver outlet temperature to automatic control on the central computer and operate for at least 10 minutes;
- 21) Switch air cooler to automatic control on the central computer and operate for at least 10 minutes.

4.2.3 Test 3 PC-3 - Maximum Load, Tower Console Computer

Outlet receiver temperature will be slowly increased to a maximum of 566°C (1050°F) with solar input up to the maximum capability of the heliostats. System control will be provided by the tower control console.

The specific test conditions are:

- 1) Test will be performed during periods when shadowing of heliostat field by clouds is not probable;
- 2) Test will be terminated if shadowing of heliostat field by clouds is likely;
- 3) Experiment control will be handled by the tower control console.

The specific test objectives are to:

- 1) Operate receiver at maximum power level;

- 2) Demonstrate receiver outlet temperature control and air-cooler control via the tower control console at maximum power conditions;
- 3) Determine molten salt flow distribution through receiver tubes at maximum power conditions;
- 4) Calibrate segmented-orifice flowmeter at maximum flow conditions using the weigh tank;
- 5) Demonstrate that the receiver can be brought to its maximum power by slowly increasing the outlet temperature;
- 6) Perform final tuning of console controllers.

The test sequence is the same as Test 1 PC-1 (4.2.1) except for the following items:

- 11) Repeat items 9 and 10 until all functioning heliostats, except the first two rows, are operating. The last step in this sequence will probably bring on line less than the 20 heliostats called out in item 9. At the beginning of this step the air-cooler outlet temperature will be reduced to approximately 288°C (550°F) via control console manual control. After all heliostats are on line, the receiver outlet temperature will be manually adjusted to approximately 566°C (1050°F);
- 14) Delete this step;
- 15) Delete this step;
- 17) Delete this step;
- 18) Switch air cooler to automatic control on the tower control console and operate for at least 10 minutes;
- 20) Switch receiver outlet temperature to automatic control on the tower control console with the set point at 566°C (1050°F) and operate for at least 10 minutes;
- 21) Switch air cooler to automatic control on the tower control console with the air-cooler outlet salt set point temperature at 288°C (550°F) and operate for 10 minutes;
- 22) Bring slowly off line all heliostats except the heliostats defined in item 2 (Test 1 PC-1, 4.2.1). During this operation the air cooler will be on automatic control while the receiver outlet temperature will be on manual control.

4.2.4 Test 4 PC-4 - Maximum Load, Central Computer Control

The outlet receiver temperature will be slowly increased to a maximum of 566°C (1050°F) with solar input up to the maximum capability of the heliostats. System control will be provided by the central computer.

The specific test conditions are:

- 1) Test will be performed during periods when shadowing of the heliostat field by clouds is not probable;
- 2) Test will be terminated if shadowing of the heliostat field by clouds is likely;
- 3) Experiment control will be handled by the central computer.

The specific test objectives are to:

- 1) Demonstrate receiver outlet temperature control at maximum power condition via the central computer;
- 2) Demonstrate air-cooler control at maximum power condition via the central computer.

The test sequence is the same as Test 3 PC-3 (4.2.3) except for the following items:

In steps 18, 20, and 21 (4.2.3) change automatic control by tower control console to automatic control by central computer.

4.2.5 Test 5 PC-5 - Maximum Load, Tower Console Control

Power will be slowly increased to maximum value with the receiver outlet temperature held constant at the nominal value of 566°C (1050°F). System control will be provided by the tower control console.

The specific test conditions are:

- 1) Test will be performed during periods when shadowing of heliostat field by clouds is not probable;
- 2) Test will be terminated if shadowing of heliostats by clouds is likely;
- 3) Experiment control will be handled by the tower control console.

The specific test objectives are to:

- 1) Demonstrate that the receiver can be brought to its maximum power with a slow increase in incident solar energy and with the receiver outlet temperature held constant at the nominal value of 566°C (1050°F);
- 2) Demonstrate that the receiver and air cooler can be automatically controlled via the tower control console during the transient from minimum to maximum power conditions.

The initial test sequence is the same as the system startup given by sequence items 1 through 8 from Test 1 PC-1 (4.2.1).

The following items from Test PC-1 will change:

- 9) Manually adjust molten salt flow rate and air-cooler outlet temperature until receiver outlet temperature is approximately 566°C (1050°F) and the air-cooler outlet salt temperature is approximately 288°C (550°F);
- 10) Switch air cooler to automatic control on the tower control console and switch receiver outlet temperature to automatic control on the tower control console;
- 11) Bring on line 20 additional heliostats. The heliostats used for this operation will be chosen so the basic flux distribution is uniform across the majority of the receiver's surface. Temperature will be held for at least 10 minutes before proceeding to next step;
- 12) Repeat item 11 until all functioning heliostats except the first two rows are operating. The last step in this sequence will probably bring on line less than the 20 heliostats called out in item 11;
- 13) Operate system at maximum power with the receiver outlet temperature at approximately 566°C (1050°F) for 1/2 hour;
- 14) Bring off line all heliostats except those defined in item 2 (Test 1 PC-1, 4.2.1). During this operation the air cooler will be on automatic control (tower control console) while the receiver outlet temperature will be on manual control;
- 15) Shut down system per items 23 through 27, Test 1 PE-1 4.2.1).

4.2.6 Test 6 PC-6 - Maximum Load, Central Computer Control

Power output will be slowly increased to maximum value with the receiver outlet temperature held constant at the nominal value of 566°C (1050°F). System control will be provided by the central computer.

The specific test conditions are:

- 1) Test will be performed during periods when shadowing of heliostat field by clouds is not probable;
- 2) Test will be terminated if shadowing of heliostats by clouds is likely;
- 3) Experiment control will be handled by the central computer.

The specific test objective are to:

- 1) Demonstrate that the receiver can be brought to its maximum power with a slow increase in incident solar energy and with the receiver outlet temperature held constant at the nominal value of 566°C (1050°F);
- 2) Demonstrate that the receiver and the air cooler can be controlled automatically via the central computer during the transient from minimum to maximum power conditions.

The test sequence will be identical to that of Test 5 PC-5 (4.2.5) except for the following item:

In step 10 (4.2.5) change automatic control by tower control console to automatic control by central computer.

4.2.7 Test 7 PC-7 - Partial Load with Emergency Shutdown

This test will be conducted the same as Test 1 PC-1 except that an emergency shutdown will be performed.

The specific test conditions are:

- 1) Tests will be performed during periods when shadowing of the heliostat field by clouds is not probable;
- 2) Test will be terminated if shadowing of heliostats by clouds is likely;
- 3) Experiment control will be handled by the tower control console.

The initial test sequence is the same as the system startup given by sequence items 1 through 11 from Test 1 PC-1 (4.2.1). The remainder of the test sequence is as follows:

- 12) Adjust molten salt flow rate until the receiver outlet temperature is approximately 482°C (900°F), maintaining the air-cooler outlet at approximately 343°C (650°F);
- 13) Simultaneously take all heliostats off line, stop the molten salt pump, and stop the air-cooler fans;

- 14) Ten seconds after initiation of commands associated with step 13, close air-cooler louvers, air-cooler top insulation, and cavity doors;
- 15) Monitor receiver temperatures and selectively drain receiver passes if salt temperature for pass is below 371°C (700°F);
- 16) Open flow control valve (FCV) and weigh tank butterfly valve (CV-1) and allow time for line from air-cooler outlet to sump to drain. Then close flow control valve;
- 17) Monitor air-cooler temperatures and receiver tube temperatures on the outlet pass of the receiver. When all air-cooler temperatures and all the receiver tube temperatures on the outlet pass of the receiver are below 371°C (700°F), drain the air cooler and the outlet pass of the receiver;
- 18) After the system is totally drained into sump, secure system.

4.2.8 Test 8 PC-8 - Recovery from Simulated Cloud Passage

The specific test conditions are:

- 1) Test will be performed during periods when shadowing of heliostat field by clouds is not probable;
- 2) Test will be terminated if shadowing of heliostats by clouds is likely;
- 3) Experiment control will be handled by the tower control console and the central computer.

The specific test objective is to demonstrate recovery from simulated cloud passage while operating at approximately one-half load with a receiver outlet temperature of approximately 482°C (900°F) and an air-cooler outlet salt temperature of approximately 343°C (650°F).

The initial test sequence is the same as the system startup given by sequence items 1 through 11 from Test 1 PC-1 (4.2.1). The remainder of the test sequence is as follows:

- 12) Adjust molten salt flow rate until the receiver outlet temperature is approximately 482°C (900°F), maintaining the air-cooler outlet at approximately 343°C (650°F);
- 13) Switch receiver outlet temperature and air-cooler outlet temperature to automatic control on the tower control console. The set points are the temperatures given in item 12);
- 14) Simulate a cloud passage from west to east traveling at approximately 2.2 m/s (5 mph). Starting with the west heliostat columns 13

and 14, bring off line approximately one-half the operating heliostats in this group. Four seconds after this operation, bring off line approximately one-half the operating heliostats in west columns 11 and 12. Continue this process until approximately one-half of the initially operating heliostats in the entire field are brought off line and operate in this condition for at least 10 minutes;

- 15) Starting with the west heliostat columns 13 and 14, bring on line the heliostats in this group that were brought off the line in item 14. Four seconds after this operation bring on line the heliostats in west columns 11 and 12 that were brought off line in item 14. Continue this process until the heliostat field is in the same condition as at the beginning of item 14 and operate in this condition for at least 10 minutes. Note that the first two rows of heliostats are not used;
- 16) Repeat items 13, 14 and 15 with the receiver and air cooler controlled automatically by the central computer;
- 17) Shut down system per items 22 through 27, Test 1 PC-1 (4.2.1).

4.3 CONVECTION TESTS - CAVITY

The convection tests are intended to provide an insight into the convection processes. These tests will be conducted with all heliostats off line to eliminate the uncertainties associated with the solar input to the receiver. For this class of test it is desirable to obtain an energy balance on the receiver during steady-state operation. To provide an unlimited period for steady-state operation, the heat input to the experiment via the trace-heating system would have to be equal to the total system losses. This is not the case for this experiment since a trace-heating system with a capability equal to the total system losses, particularly the receiver, would be prohibitively large. However, steady-state conditions can be provided for a sufficient time to conduct meaningful convective loss tests utilizing the fluid transit lag time through the system. This is accomplished by slowing the molten salt flow rate to a low value at the point in the test when the entire system is at approximately 371°C (700°F). Also at this time the cavity doors are opened allowing convection to the ambient. At this beginning point there will be a slug of 371°C (700°F) molten salt in the air cooler, sump, and interconnecting piping from receiver outlet to receiver inlet. For the time it takes this slug to flow past the receiver inlet, the temperature at the receiver inlet will remain essentially constant at 371°C (700°F). This time can also be increased by utilizing the weigh tank to hold up the flow through the system. It turns out that the receiver inlet temperature can be held constant for approximately 13 minutes. Since this is enough time for

the receiver outlet temperature to come to steady-- state conditions, the convective losses can be readily obtained.

The receiver configuration and overall test conditions are:

- 1) Cavity configuration;
- 2) The real-time aperture flux (RTAF) system attached to the cavity.

The overall objective is to determine the convective losses from the receiver in the cavity configuration.

4.3.1 Test 9CC - Convection Loss at 371°C (700°F)

The initial test sequence is the same as the system startup given by sequence items 1 through 6 from Test 1 PC-1 (4.2.1). The remainder of the sequence is as follows:

- 7) Bring off line the startup heliostats and close the cavity doors;
- 8) Use the trace-heating system to increase the average molten salt temperature throughout the system to approximately 371°C (700°F);
- 9) Reduce the molten salt flow rate to yield a Reynolds number in the receiver tubes of approximately 4000 (slightly turbulent);
- 10) Perform a molten salt flow calibration test using the weigh tank;
- 11) Open the cavity doors;
- 12) Close the butterfly valve on the weigh tank consistent with the time it takes the fluid to travel from the receiver outlet to the weigh tank inlet (approximately 6 minutes after cavity doors are opened);
- 13) Measure receiver temperatures until receiver inlet temperature has changed by more than $\pm 2.7^\circ\text{C}$ ($\pm 5^\circ\text{F}$) from its initial value;
- 14) Close cavity doors;
- 15) Drain and secure system.

Note that convection tests will be performed either separately or in series to provide five data points at various wind conditions.

4.4 PERFORMANCE TESTS - CAVITY

The overall test conditions and receiver configuration include:

- 1) Cavity configuration;
- 2) Real-time aperture flux (RTAF) system attached to the cavity;
- 3) The first two rows of heliostats not used;
- 4) Single-point heliostat aim strategy will be used with the maximum flux limited to 69.3 W/cm^2 ($220,000 \text{ Btu/h-ft}^2$);
- 5) Experiment control will be handled by central computer.

The test objectives are to:

- 1) Determine the efficiency of the receiver in the exposed configuration at several load conditions;
- 2) Demonstrate performance of receiver at maximum load;
- 3) Demonstrate ability of receiver to recover from actual or simulated cloud passages.

The specific test objective is to develop the data so a curve of receiver output versus input can be plotted.

4.4.1 Test 10 PFC-1 - Efficiency Tests with Receiver in Cavity Configuration

The test sequence is:

- 1) Heat all molten salt lines, air cooler, receiver headers, and sump to approximately 288°C (550°F). The salt will have been previously melted in the sump and the sump temperature maintained at approximately 288°C (550°F) continuously. During system heat-up, the air-cooler louvers and top insulation will be in their closed position;
- 2) Heat uninsulated receiver tubes to approximately 288°C (550°F) using eight to 10 heliostats. The particular heliostats and their aim strategies for this operation will be chosen so the flux distribution on the receiver tubes is as uniform as possible;
- 3) Fill system with molten salt;
- 4) Monitor trace-heating system and shut off heaters as required;
- 5) Start molten salt flow through system. Set flow at rate consistent with receiver's maximum power. Monitor trace-heating system and shut off heaters as required;

- 6) Bring on line 20 additional heliostats. The heliostats used for this operation will be chosen so the basic flux distribution is uniform across the majority of the receiver's surface;
- 7) Open the air-cooler louvers and top insulation and start fans with zero pitch on fan blades. Adjust pitch on fan blades until air-cooler outlet salt temperature is approximately 288°C (550°F) and steady;
- 8) Manually adjust molten salt flow rate and air-cooler outlet temperature until receiver outlet temperature is approximately 566°C (1050°F) and the air-cooler outlet salt temperature is approximately 288°C (550°F);
- 9) Switch air cooler to automatic control on the central computer and switch receiver outlet temperature to automatic control on the central computer;
- 10) Bring on line a set of heliostats so the receiver power levels will be between 25 and 35% of full load. At this setting operate system until pseudo-steady-state is achieved. At or near steady-state record all receiver temperatures, the receiver radiation emission, salt flow rate (using the segmented orifice), and the heliostat input power from the RTAF. Calculate and display the receiver efficiency;
- 11) Bring on line a set of heliostats so the receiver power level will be between 35 and 45% of full load and operate this test segment as described in item 10. Repeat this process by moving to power levels between 45 and 55%, 55 and 65%, etc until full power is achieved. Operate this test (it will undoubtedly require several days) until efficiency data are obtained for at least two data points in each efficiency range;
- 12) Bring off the line all heliostats except those defined in item 2 of this sequence. During this operation the air cooler will be on automatic control (central computer) while the receiver outlet temperature will be on manual control;
- 13) Shut down system per items 23 through 27, Test 1 PC-1 (4.2.1).

4.4.2 Test 11 PFC-2 - Maximum Power Tests with Receiver in Cavity Configuration

The specific test objective is to demonstrate system performance at maximum load for a minimum of 20 hours.

The test sequence is the same as Test 10 PFC-1 (4.4.1) except to increase the receiver to maximum power as rapidly as practical and continue tests until a minimum of 20 hours have been accumulated.

4.4.3 Test 12 PFC-3 - Demonstrate Recovery from Simulated Cloud Passage, Cavity Configuration

The specific objectives are to:

- 1) Demonstrate recovery from simulated cloud passage while operating at 75% of maximum power with the receiver outlet temperature set at 537.8°C (1000°F) and the air-cooler outlet temperature set at 315.5°C (600°F);
- 2) Cloud speed is approximately 4.4 m/s (10 mph).

The test sequence is the same as Test 8 PC-8 (4.2.8) except the cloud speed is 4.4 m/s (10 mph) instead of 2.2 m/s (5 mph), the load is 75% of maximum instead of 50%, the receiver outlet temperature is changed to 537.8°C (1000°F), and the air-cooler outlet temperature is changed to 315.5°C (600°F). Also for this test cloud travel from east to west, west to east, north to south, and south to north will be simulated. Note that it is likely that cloud conditions similar to those defined here will have occurred during the test periods of 10 PFC-1 or 11 PFC-2. If this is the case, system performance data will have been obtained for cloud conditions similar to those of this test and this test need not be performed.

4.5 PERFORMANCE TESTS - EXPOSED

The overall test conditions and receiver configuration include:

- 1) Exposed configuration with the center 3.35x3.35-m (11x11-ft) portion of the receiver illuminated;
- 2) Real-time aperture flux (RTAF) system attached directly in front of and in the center of the receiver. The receiver tubes outside the aperture of the RTAF will be insulated on the heliostat side of the tubes;
- 3) The first two rows of heliostats will not be used;
- 4) Single-point heliostat aim strategy will be used with the maximum flux limited to 69.3 W/cm² (220,000 Btu/h-ft²);
- 5) Experiment control will be handled by central computer.

The test objectives are to:

- 1) Determine the efficiency of the receiver in the exposed configuration at several load conditions;

- 2) Demonstrate ability of receiver to recover from actual or simulated cloud passages.

The specific test objective is to develop the data so a curve of receiver output versus input can be plotted.

4.5.1 Test 13 PFE-1 - Efficiency Tests with Receiver in Exposed Configuration

The test sequence is:

- 1) Heat all molten salt lines, air cooler, receiver headers, and sump to approximately 288°C (550°F). The salt will have been previously melted in the sump and the sump temperature maintained at approximately 288°C (550°F) continuously. During system heat-up, the air-cooler louvers and top insulation will be in their closed position;
- 2) Heat uninsulated receiver tubes to approximately 288°C (550°F) using eight to 10 heliostats. The particular heliostats and their aim strategies for this operation will be chosen so the flux distribution on the receiver tubes is as uniform as possible;
- 3) Heat insulated receiver tubes using the air heater and the air supply from the air heat rejection system. Continue this process until all receiver tubes are approximately 288°C (550°F);
- 4) Fill system with molten salt, monitor trace-heating system, and shut off heaters as required;
- 5) Start molten salt flow through system. Set flow at rate consistent with receiver's maximum power. Monitor trace-heating system and shut off heaters as required;
- 6) Bring on line 20 additional heliostats. The heliostats used for this operation will be chosen so the basic flux distribution is uniform across the majority of the receiver's surface;
- 7) Open the air-cooler louvers and top insulation and start fans with zero pitch on fan blades. Adjust pitch on fan blades until air-cooler outlet salt temperature is approximately 288°C (550°F) and steady;
- 8) Manually adjust molten salt flow rate and air-cooler outlet temperature until receiver outlet temperature is approximately 566°C (1050°F) and the air-cooler outlet salt temperature is approximately 288°C (550°F);
- 9) Switch air cooler to automatic control on the central computer and switch receiver outlet temperature to automatic control on the central computer;

- 10) Bring on line a set of heliostats so the receiver power levels will be between 25 and 35% of full load relative to this partially exposed configuration. At this setting operate system until pseudo-steady-state conditions are achieved. At or near steady-state, record all receiver temperatures, the receiver radiation emission, salt flow rate (using the segmented orifice), and the heliostat input power from the RTAF. Calculate and display the receiver efficiency;
- 11) Bring on line a set of heliostats so the receiver power level will be between 45 and 55% of full load and operate this test segment as described in item 10. Repeat this process by moving to power levels between 55 and 65%, 55 and 75%, etc until full power is achieved. Operate this test (it will undoubtedly require several days) until efficiency data are obtained for at least two data points in each efficiency range;
- 12) Bring off the line all heliostats except those defined in item 2 of this sequence. During this operation the air cooler will be on automatic control (central computer) while the receiver outlet temperature will be on manual control;
- 13) Shut down system per items 23 through 27, Test 1 PC-1 (4.2.1).

4.5.2 Test 12 PFE-2 - Recovery from Simulated Cloud Passage, Exposed Configuration

The specific objectives are to:

- 1) Demonstrate recovery from simulated cloud passage while operating at 75% of maximum power with the receiver outlet temperature set at 537.8°C (1000°F) and the air-cooler outlet temperature set at 315.5°C (600°F);
- 2) Cloud speed is approximately 4.4 m/s (10 mph).

The test sequence is the same as Test 12 PFC-3 (4.4.3) except the receiver configuration is exposed instead of cavity. Note that it is likely that cloud conditions similar to those defined here will have occurred during the periods of Test 13 PFE-1. If this is the case, system performance will have been obtained for cloud conditions similar to those of this test and this test need not be performed.

4.6 CONVECTION TESTS - EXPOSED

The exposed convection test receiver configuration and overall test conditions include:

- 1) Exposed configuration with entire receiver surface area open to the environment, 3.35x5.49 m (11x18 ft);
- 2) The real-time aperture flux (RTAF) system is not attached to the receiver.

The overall objective is to determine the convective losses from the receiver in the exposed configuration.

4.6.1 Test 15 CE - Convection Loss at 371°C (700°F)

The initial test sequence is the same as the system startup given by sequence items 1 through 6 from Test 1 PC-1 (4.2.1). The remainder of the sequence is as follows:

- 7) Bring on line a set of heliostats that will cause the average molten salt temperature throughout the system to increase to approximately 371°C (700°F). The trace-heating system, along with the heliostats, will be used to achieve this condition;
- 8) Reduce the molten salt flow rate to yield a Reynolds number in the receiver of approximately 4000 (slightly turbulent);
- 9) Perform a molten salt flow calibration test using the weigh tank;
- 10) Bring all heliostats off the line;
- 11) Close butterfly valve on the weigh tank consistent with the time it takes the fluid to travel from the receiver outlet to the weigh tank inlet (approximately 6 minutes after heliostats are removed in item 10);
- 12) Measure receiver temperature until receiver inlet temperature has changed by more than $\pm 2.7^\circ\text{C}$ ($\pm 5^\circ\text{F}$) from its initial value;
- 13) Drain and secure system.

Note that convection tests will be performed either separately or in series to provide five data points at various wind conditions.

4.7 SPECIAL TEST - EXPOSED

The overall test conditions and receiver configuration are:

- 1) Exposed configuration with the entire receiver surface area illuminated, 3.35x5.49 m (11x18 ft);

- 2) The real-time aperture flux (RTAF) system not attached to the receiver.

The test objectives are to:

- 1) Demonstrate performance of receiver under extreme conditions;
- 2) Subject receiver to rapid cyclic conditions;
- 3) Obtain as much maximum power receiver operation time as the test program schedule will permit.

4.7.1 Test 16 SE-1 - Cycle Tests

The specific test conditions are:

- 1) Receiver operating at maximum power;
- 2) Experiment control via central computer;

The specific objective is to demonstrate receiver capability to undergo 1000 cycles.

The test sequence is to bring all heliostats off line at full power and after 1 minute bring all heliostats on line. Keep heliostats on line for 1 minute and repeat cycle. Continue this process until 1000 cycles have been accumulated over the entire test program.

4.7.2 Test 17 SE-2 - Endurance Tests

The specific test conditions are:

- 1) Receiver operating at maximum power and design temperatures;
- 2) Experiment control via central computer.

The specific test objective is to demonstrate the receiver's capability to operate at maximum power for 100 hours.

The test sequence is the same as Test 13 PFE-1 (4.5.1).

4.7.3 Test 18 SE-3 - Extreme Cloud Conditions

The specific test conditions are:

- 1) Receiver operating at maximum power and design temperatures;
- 2) Experiment control via central computer.

The specific test objective is to demonstrate that the receiver can recover from extreme cloud conditions while operating at maximum power and at design temperature levels.

This test will be conducted in a similar manner as Test 14 PFE-2 except that the system will be operated at maximum power, the receiver outlet temperature will be set at 566°C (1050°F), and the receiver outlet temperature will be set at 288°C (550°F). Also the full sets of operating heliostats will be brought off the line in each region as the "cloud" passes over the heliostat field. The time that the "cloud" will cover the entire heliostat field will be 2 minutes.

4.7.4 Test 19 SE-4 - Lateral Support Shadowing

The specific test conditions are:

- 1) Receiver operating at maximum power;
- 2) Lateral support shadows provided by refractory material.

The specific objective is to demonstrate the effect of shadowing that would occur in commercial design on the receiver tubes.

The sequence is similar to Test 13 PFE-1 (4.5.1). Three tests will be performed with shadows at different locations for each test.

4.7.5 Test 27 MC-6 - High Localized Fluxes

The specific test condition is to aim heliostats to yield a flux of approximately 94.5 W/cm² (300,000 Btu/h-ft²) in the center of the receiver. The test will proceed until pseudo-steady-state conditions are achieved.

The specific test objective is to demonstrate the effect of high fluxes on receiver tubes.

The test sequence is similar to Test 13 PFE-1 (4.5.1).

5.0 TEST PROGRAM SCHEDULE

Table 5-1 lists the tests that will be conducted during this program. The table includes an estimate of the days required to conduct each of the tests assuming ideal-weather (solar) conditions and no effect on test time due to problems with the test system. As the program proceeds, experience will enable the tests to be conducted in relatively shorter periods of time. It should be noted that the checkout tests do not require operation of the heliostats and these tests will be performed in Denver or at ground level at CRTF. These checkout tests, which are scheduled for Albuquerque, will also be conducted in series with the system buildup operations. The current plan is to perform the system buildup and the checkout tests over a period of approximately 1 1/2 months.

Figure 5-1 is an overall schedule for the test operations. The rationale used to obtain the span times for the tests is as follows. Starting with the ideal test times from Table 5-1, the individual times for each of the major test categories (preliminary tests, convection tests, etc) are summed. These span times are then adjusted on a monthly basis to account for Albuquerque weather conditions. This adjustment is based on Table 2 from the Central Receiver Test Facility Experiment Manual entitled "Typical Albuquerque Sunshine (Compiled from 38-Year Record)." For the preliminary tests, only clear days will be used for testing so the cloudiness factor applied to the ideal test times is (days in a month/clear days in a month). For the remainder of the tests the cloudiness factor is [days in a month/(clear days in a month + 1/2 partly cloudy days in a month)].

In other words, for all solar tests except the preliminary tests, it is assumed that partly cloudy days will provide a half day of testing. The final adjustment of test spans is a learning curve factor. This factor accounts for the experience of the test crew and provides a means of factoring this experience into the test span times. The values assumed for this factor are tabulated.

Test	Learning Curve Factors
Preliminary Test - Exposed	2.0
Convection Tests - Exposed	2.0
Performance Tests - Exposed	1.5
Performance Tests - Cavity	1.5
Convection Tests - Cavity	1.5
Special Tests - Cavity	1.2

An example of the calculation to provide the span time for the exposed performance tests is:

Ideal test time = 5.0 days

Cloudiness factor (Aug) = $[31/(14 + 0.5 \times 12)] = 1.55$

Learning curve factor = 1.5

Adjusted span time = $5.0 \times 1.55 \times 1.5 = 11.63 = 12$ days
(all times are rounded to nearest whole number).

Table 5-1 Ideal Test Spans

			Days
<u>4.1 Checkout Tests</u>			
4.1.1	CO-1	Airflow Distribution for Air Cooler (Denver)	1.0
4.1.2	CO-2	Hydrostatic and Leak Checks (Denver)	2.0
4.1.3	CO-3	Sump and Air-Cooler Heaters (Denver)	2.0
4.1.4	CO-4	System Trace Heaters (Albuquerque)	2.0
4.1.5	CO-5	Thermocouples (Albuquerque)	2.0
4.1.6	CO-6	Functional Valve Operation (Albuquerque)	0.5
4.1.7	CO-7	Electrical Control System (Albuquerque)	1.0
4.1.8	CO-8	Functional Test with Water (Albuquerque)	2.0
4.1.9	CO-9	Functional Test with Salt (Albuquerque)	1.0
<u>4.2 Preliminary Tests - Cavity</u>			
4.2.1 1	PC-1	Partial Load - Tower Console Control	1.0
4.2.2 2	PC-2	Partial Load - Central Computer Control	1.0
4.2.3 3	PC-3	Maximum Load - Tower Console Control	1.0
4.2.4 4	PC-4	Maximum Load - Central Computer Control	1.0
4.2.5 5	PC-5	Maximum Load - Tower Console Control	1.0
4.2.6 6	PC-6	Maximum Load - Central Computer Control	1.0
4.2.7 7	PC-7	Partial Load with Emergency Shutdown	1.0
4.2.8 8	PC-8	Recovery from Simulated Cloud Passage	1.0
<u>4.3 Convection Tests - Cavity</u>			
4.3.1	9CC	Convection Loss at 700°F	3.0
<u>4.4 Performance Tests - Cavity</u>			
4.4.1 10	PFC-1	Efficiency Tests at 35 to 100% of Maximum Load	3.0
4.4.2 11	PFC-2	Maximum Load for 20 Hours	5.0
4.4.3 12	PFC-3	Recovery from Simulated Cloud Passage	2.0
<u>4.5 Performance Tests - Exposed</u>			
4.5.1 13	PFE-1	Efficiency Tests at 45 to 100% of Maximum Load	3.0
4.5.2 14	PFE-2	Recovery from Simulated Cloud Passage	2.0
<u>4.6 Convection Tests - Exposed</u>			
4.6.1 15	CE	Convection Loss at 700°F	3.0
<u>4.7 Special Tests - Exposed</u>			
4.7.1 16	SE-1	Cycle Tests	5.0
4.7.2 17	SE-2	Endurance Test	13.0
4.7.3 18	SE-3	Extreme Cloud Conditions	0.5
4.7.4 19	SE-4	Lateral Support Shadowing	3.0
4.7.5 20	SE-5	High Localized Fluxes	0.5

Test Sequence	Weeks from Start of Solar Testing																	
	1	2	3	4	5	6	7	8	9	10	11	12	13	14	15	16	17	18
4.1 Checkout Test (Nonsolar Tests)																		
4.2 Preliminary Tests - Cavity																		
4.3 Convection Tests - Cavity																		
4.4 Performance Tests - Cavity																		
Configuration Changeover																		
4.5 Performance Tests - Exposed																		
Configuration Changeover																		
4.6 Convection Tests - Exposed																		
4.7 Special Tests - Exposed																		

Figure 5-1 Test Schedule

Revision C

February 28, 1980

APPENDIX B

TEST PLAN: MATERIALS SUBSYSTEM

RESEARCH EXPERIMENTS

TEST PLAN

MATERIALS SUBSYSTEM RESEARCH EXPERIMENTS

SOLAR THERMAL POWER PROGRAM

I. INTRODUCTION

This test plan covers Phase II materials subsystem research experiments. These experiments are designed to evaluate the compatibility of candidate solar thermal power plant construction materials with molten salt (60% sodium nitrate, 40% potassium nitrate) used as the solar heat transfer and storage fluid.

These experiments are divided into two major parts: the molten salt pumped fluid loop, and the static materials compatibility test programs.

This test program is a follow-on to testing started in Phase I materials test program. The Phase II tests were designed to give more information on the long-term compatibility of materials under conditions representative of actual thermal and flow characteristics of a commercial thermal power plant.

The main objective of the Phase II materials test program is to provide the materials test data that is needed to commercialize a full-scale molten salt solar thermal power plant. In particular, these data shall include:

- A. The chemical stability of molten nitrate salt over all anticipated operating conditions for 30 years of system lifetime.

- B. Specific procedures for regeneration of the salt (if required) or conditions required for stabilization of the salt composition.
- C. The compatibility of materials of construction with molten salt under all anticipated conditions including: temperature, fluid velocity, galvanic potentials, salt impurities, and cyclic stresses.

II. BACKGROUND

The Phase I materials test program consisted of an isothermal fluid loop test, static coupon immersion compatibility tests, and a number of tests devised to study the stability of molten draw salt.

The results of these tests are given in the Advanced Central Receiver Power System, Phase I Final Report, Martin Marietta Sept. 1978. Briefly, the results of Phase I testing showed that molten draw salt was quite stable at the anticipated operational temperatures, 260° to 566°C (500 to 1050°F). A simple equilibrium relationship was demonstrated between alkali nitrates and nitrites which was dependent on oxygen concentration of the atmosphere over the salt. In general, the nitrate melts were stable, not very corrosive, and easy to handle.

Incoloy 800 was tested in a flowing molten salt loop at 566°C (1050°F) and exhibited good stability toward molten salt erosion and corrosion. Also, good stability to thermal stress and shock was

demonstrated by the Incoloy 800 passivation layer during dynamic thermal cycling in the test loop and during rapid water quenches from 800°F to ambient temperatures. These and other Phase I test data indicate Incoloy 800 is a prime candidate for solar receiver construction. Also, the Phase I testing indicated that relatively inexpensive mild steel such as A516 could be used for the solar thermal power system in places where temperatures do not exceed 399°C (750°F).

Other high temperature candidate materials such as 304 stainless steel and 321 stainless steels showed either poor corrosion resistance, high temperature sensitization or cracking and flaking of the passivation layer.

III. PHASE II TEST SUMMARY

The Phase II testing program is divided into two major test efforts: (1) the molten salt pumped loop, and (2) the static materials tests.

The purpose of the molten salt fluid loop is to simulate a fully operational solar thermal power generating system. The molten salt pumped fluid loop will simulate solar receiver temperatures of 566°C (1050°F) on the hot side and 299°C (550°F) on the cold side. The fluid loop is designed to allow the insertion and removal of sample coupons into the flowing salt stream for analysis during the 10,000-hour test schedule. This dynamic test will allow the study of possible material transport phenomena from

hot to cold sections of the loop and also provide more detailed information on corrosion/erosion of construction materials in a flowing molten salt loop. Additional information will be gained on the stability of the salt under dynamic thermal cycling conditions.

In addition to the material test loop, Phase II of the materials test program will include a series of materials compatibility tests designed to increase knowledge of both materials corrosion and the stability of the molten salt. Phase II tests will continue to test Incoloy 800 and carbon steel as well as other candidate materials such as 316L, 347, and RA330 steels. The selection of 316L and 347 stainless steels was made because of the added stabilizing elements Cb and Ta in 347, and the low carbon in 316L which tend to make these materials less susceptible to sensitization at high temperatures. These tests consist of:

- A. A trace contaminants test will be conducted with molten salt doped at maximum concentrations of contaminants present in the commercial salt. Coupon materials will be exposed to these doped melts for corrosion evaluation. Both butt weld samples and overlap weld crevice corrosion samples are included in this test.
- B. Long term coupon immersion tests will be run utilizing metal coupons exposed in Phase I, but continuing the salt exposure to gain long-term exposure data. The coupons will be withdrawn and analyzed periodically during the twelve month test.

- C. A stress corrosion test will yield corrosion information on materials exposed to molten salt environments and stressed by a nonrelieving, constant load method.
- D. Carbon dioxide and water vapor effects on the decomposition of nitrate salts will be studied in this test to determine the long-term stability of molten salt exposed to ambient atmosphere.
- E. Salt regeneration tests will be run to test the feasibility of regenerating decomposed salts by bubbling nitrogen dioxide through the molten salt mixture doped with carbonates and hydroxides. Analysis of the exposed salts will give an indication of the feasibility of "in situ" regeneration of nitrate salts.
- F. Tensile and metallographic analysis of candidate materials will be run after six and twelve months' exposure to molten salt environments. These tests will determine the susceptibility of the alloys to intergranular corrosion. Samples of exposed candidate materials and control samples will be tested for percent elongation, tensile strength, and ultimate strength; also metallographic analysis and 180° bend tests will be included.
- G. Stress fatigue test where candidate receiver alloys will be exposed to cycling stresses in the salt environment. This test

will compare corrosion fatigue in the salt environment with typical S-N curves at 593°C (1100°F) in air.

- H. Thermal shock test where candidate test coupons will be exposed to molten salt at 593°C (1100°F) for 2000 hours to build up an oxide layer. The coupons will then be thermally cycled by alternate heating to 593°C and quenching in water to determine oxide layer tenacity.
- I. Nitrate salt decomposition test--this test will determine the rate of thermal decomposition of mixed alkali nitrates to oxides in a closed system. This information is useful in predicting possible problems due to gas evolution in the receiver and overall thermal stability of the molten salt system.
- J. Special materials tests--these tests will be simple immersion tests for limited use material in the molten salt system. These materials will include gaskets, valve packings and seals and will be tested at 399°C (750°F) and 593°C (1100°F).

A sample for the above tests is shown in Figure I.

Individual test procedures will be written for each test and will include details of testing including test materials, facilities, special safety precautions, and step-by-step procedures.

The fluid loop test will be constructed of the most promising candidate materials to be used in a full-scale system and the loop will have the capability for placing various sample test coupons in the flow stream.

The static materials tests will be conducted in special 20"x20" stainless steel ovens constructed to minimize molten salt contamination by atmospheric or other sources.

The immersion tests and the tensile test will all be run in 4"x4" Incoloy 800 trays.

The trace contaminant test will be conducted in specially constructed 20"x20" ovens containing holes through the top to accommodate individual vessels made for 1 1/4" pipe. Each vessel will be made of the same alloy as the test coupons it contains, and each vessel will be constructed to eliminate salt creep and atmospheric contamination.

The carbon dioxide and water effects test will also be run in test vessels constructed of pipe and inserted through the top of a 20"x20" oven. The pipe vessels in the case will be 1 1/2" diameter Incoloy 800, and will have special gas inlet and exit tube constructed in the cap (see Part IV - Test Plan). The salt regeneration test will utilize the oven and vessels from the carbon dioxide-water effects tests, as they become available.

The stress corrosion tests will require construction of special vessels to hold stress specimens at temperatures in the molten salt environment while the specimens are stressed in a creep test machine. These vessels will be 2" diameter pipe vessels containing three test specimens each, attached in series.

IV. TEST PLAN

A. Long-Term Molten Salt Pumped Fluid Loop

1. Objective

The objective of the molten salt fluid loop is to provide a test apparatus which will simulate a full-scale solar thermal power system as closely as possible and allow the study of materials compatibility and stability under a dynamic flowing system. In particular, the objectives are to investigate:

- a. Mass transport phenomena (if any) from high to low temperature parts of loop.
- b. Construction material compatibility in a flowing molten salt system.
- c. Stability of molten salt in a dynamic thermal cycling system.
- d. Electrolytic corrosion phenomena (if any) in a flowing molten salt system.

2. Test Description

The molten salt test loop is shown schematically in Figure II; refer to this schematic for further details.

Partherm 430 salt consisting of 60% NaNO_3 and 40% KNO_3 will be heated to 288°C (550°F) in the pump sump. This salt is then circulated through the inside tube of the jacketed heat exchanger and is heated by the counterflow salt. The salt flow exits the jacketed exchanger at 482°C

(900°F) and enters a 3-part resistance heated tube. The salt exits the heater at 566°C (1050°F). This flow then passes through the outside portion of the counterflow heat exchanger and decreases in temperature to 371°C (700°F). It is then cooled to 288°C (550°F) as it passes through an air cooler before returning to the pump sump.

Sample ports are located at seven locations in the test loop. Sample ports 1-5 will have Incoloy 800 coupons inserted in the salt flow stream. Ports 5-6 will contain carbon steel coupons and Port 7 will be used to sample the molten salt in the sump. The velocity of the salt across the sample coupon will be controlled to approximately 3.3 meters per second (11 feet per second). This velocity will represent the design velocity of the salt flow in the full-scale solar molten salt receiver. The samples will be checked every 1000 hours for weight change and metallurgically and chemically examined after the 10,000 hour test is completed and at other times if the weight change data shows significant mass transport. Molten salt samples will be taken every 1000 hours and analyzed as required.

3. Equipment Requirements

a. Pump and Sump

The pump sump can hold the entire inventory, 340 liters (12 ft³)) of molten salt for the fluid loop SRE.

This salt can be heated to a temperature of 288°C (550°F)

and maintained at that temperature throughout the SRE using a system of band heaters, temperature controllers and insulation. The sump is a 30" diameter by 30" high stainless tank and has a vent to atmosphere through a CO_2 and H_2O scrubber to prevent pressure buildup and salt contamination.

The pump motor is rated at 7.5 HP and drives a cantilevered 316 stainless steel impeller and shaft. There are no bearings or seals submerged in the salt.

b. Heat Exchanger

The heat exchanger is a counterflow tube in tube type. The outer tube is made of 1 1/4" Schedule 40 Incoloy 800 pipe. The salt enters this tube at 566°C (1050°F) and is cooled to 371°C (700°F) as it travels through the exchanger by the counterflowing salt. The counterflow salt enters the inner 3/4" diameter Incoloy 800 tube at 287°C (550°F) and is heated to its exit temperature of 482°C (900°F) by the counterflow salt in the outer jacket.

The salt travels at a flow velocity of 0.49 meters per second (1.6 fps) in the outer jacket and 1.67 meters per second (5.5 fps) in the inner jacket.

Sample ports SP1, SP2, SP3, SP4, SP5, and SP6 are located in the heat exchanger at approximate temperature levels of 357°C (675°F), 482°C (900°F), 556°C (1050°F),

440°C (825°F), 371°C (700°F), and 287°C (550°F), respectively.

The total length of the jacketed exchanger is 29.6 meters (97 feet). It is constructed to allow complete drainage when the pump is turned off. The salt in the inner jacket will flow directly into the pump sump and the salt in the outer jacket would flow through the air cooler unit and into the pump sump. The exchanger is designed to eliminate any residual salt from collecting and solidifying on any internal surfaces of the exchanger when it cools to ambient temperature.

The entire heat exchanger is heat traced to pre-heat the jackets to at least 260°C (500°F) prior to starting the system from ambient conditions.

A thin sheet metal shroud will surround the entire fluid loop as a safety precaution against possible leaks.

c. Line Heater

The line heater is part of the 1.96 m (3/4 in.) Incoloy 800 tube loop which will be resistively heated directly by high amperage, low voltage AC current. The line heater consists of three independently heated sections. All three sections can be manually controlled and the third section can also be automatically controlled.

The salt enters the line heater at 482°C (900°F) and exits at 566°C (1050°F). The flowrate through the line

heater is 20.23 liters per min. (5.34 gpm) at a velocity of 1.7 meters per second (5.6 fps). The total length of the heater is 7.41 meters (24.3 feet) which will completely drain when the pump is turned off.

Each heater section is controlled by an RI power supply which feeds a transformer to step the voltage and provide the proper amperage. The power is regulated by a power controller, and each heater is protected by an overtemperature kill. This would prevent the salt temperature from exceeding 566°C (1050°F) during normal operation.

d. Air Cooler

The air cooler is sized to reduce the temperature of the salt flow from 371°C (700°F) to 288°C (550°F). It is located at the outlet of the outer jacket of the heat exchanger. The cooler consists of 36 ft of 2.54 cm (1.0 in.) diameter carbon steel tubing with a fin density of 236 fins per meter. The finned tube is arranged in a manner to allow the air cooler to completely drain into the pump sump when the pump is turned off.

A plenum chamber distributes the forced air from the dual fan system evenly over the finned tubes.

The total heat rejection capacity of this air cooler is 92,240 watts (315,000 Btu/hr), which includes a 20% margin over the input load.

The air cooler will be designed with inlet and outlet insulation panels which can be manually removed during loop startup. The cooler housing will be insulated to prevent it from excessive cooling during operation.

The air cooler will be heated to allow the finned tubing to be preheated prior to starting. The heater will also have the capability of melting the salt in the finned tubes if the salt freezes during an emergency condition.

4. System Requirements

This system is designed for continuous unattended operation over a period of at least 10,000 hours. Where possible, all connections are welded to prevent any leaks from mechanical fittings. These welds will be checked with dye penetrant for any cracks or potential leak paths. In addition, the entire system will be helium leak checked.

The system will be heat traced to allow the pipe and components to warm up to 260°C (500°F) prior to circulating the molten salt at 288°C (550°F). The interconnecting pipe will also be insulated with a minimum of one diameter thickness of insulation. The temperature of the pipe will be sensed at many locations by redundant thermocouples and displayed on a multiple channel temperature console. The heat tracing is operated only in the manual mode. If the pump is shut down, the system will automatically drain the circulating molten salt into the pump sump. This draining is facilitated by an automatic air purge system to help the salt rapidly drain into the sump.

Over temperature kill switches for the line heaters and cooler will be provided. If the temperature of the salt exceeds 579°C (1075°F) leaving the line heater or 302°C (575°F) leaving the air cooler, the system will automatically shut off and the loop system will drain. If the temperature of the salt leaving the air cooler reaches 274°C (525°F), the system will automatically shut down.

The air cooler is also connected to the pump operation. If the pump motor is shut off, the air cooler blower will automatically shut down and the louvers will automatically close. This will isolate the finned tubing in the air cooler and maintain a temperature greater than 260°C (500°F) to allow the molten salt from the piping loop to flow to the pump sump

without freezing in the air cooler. This system will also have a manual override for checkout purposes.

Dry air with low carbon dioxide content will be used to assist in the draining of the system during an emergency shutdown. An inlet port will be located midway in the line heater. This port will have a pneumatic solenoid valve in line and interconnected with the pump motor. If any one of a number of safety kills is activated during normal operation, the solenoid valve will open pressurizing the molten salt loop, and returning the molten salt to the pump sump. The maximum pressure of the air is 10 psig.

5. Safety Requirements

a. Personnel

To protect the personnel in the test area, a thin sheet-metal shroud will surround the entire fluid loop. This will prevent the possibility of hot salt impinging on personnel. Caution signs warning personnel of the high temperature and high voltage will be displayed near the test setup. The test area will be roped off to prevent personnel from approaching the test hardware. A salt containment dam will be built to prevent any possibility of a large salt spill from leaving the area surrounding the sump.

b. Equipment

A system of shutdowns will be incorporated to protect

the system from possible freeze-up. The freezing temperature of the salt is 221°C (430°F).

A temperature greater than this must be maintained to prevent the salt from solidifying in the pipes. The system will be designed to completely drain automatically into the pump sump if one of the following system shutdown modes is activated.

- 1) High salt temperature on line heaters 579°C (>1075°F).
- 2) Low salt temperatures on outlet of air cooler 260°C (>500°F).
- 3) Loss of pump cooling water.
- 4) Loss of power to:
 - a) Heaters
 - b) Pump
 - c) Fan
- 5) High pump bearing temperature.

6. Analysis

Analysis of the metal coupons in the loop will be accomplished at 1000 hour intervals.

The coupons will be withdrawn from the fluid loop (see diagram, Fig. III), washed, dried, and checked for change in weight from previous weighing. If the weigh change follows previous static immersion tests, the coupon will be replaced. However, weigh changes significantly different from the static tests may require further metallurgical and/or chemical analysis. Particular attention will be paid to the thickness and condition of the passivation layer.

The salt will be sampled at the start of test and every 1000 hours thereafter. Every other sample will be analyzed for $\text{CO}_3^{=}$, OH^- , NO_2^- , $\text{NO}_3^{=}$, K, Na and Cr. The remaining samples will be held as backups in case further testing is necessary. The amounts of oxide/hydroxide are of particular interest since these may indicate gradual decomposition of the nitrate salts which would have to be replenished or regenerated during the projected 30 year lifetime of a full-scale plant.

Parts of the loop will be sectioned and metallurgically analyzed at the end of the test. Welds and dissimilar joints will be studied to determine if there is any significant galvanic corrosion.

B. Static Materials Test

1. Trace Contaminants Test

The objective of the trace contaminants test is to understand the corrosion effects of trace amounts of different anionic contaminants that are present at low concentrations in commercial nitrate salt. This test is of considerable importance in determining the corrosivity of certain materials known to be present in commercial salt.

The test will determine if there exists a need to control certain impurities in the commercial salts. The test will be conducted with reagent grade (60% NaNO_3 , 40% KNO_3) draw salt doped with maximum amounts of chloride ion, sulfate ion, hydroxide ion, and carbonate ion, as speci-

fied in commercial grade salt. Test coupon specimens will be suspended in these salt mixtures during the 4000 hour tests. Each 1000 hours the coupons will be washed free of salt, dried, and weight changes determined.

If the coupons show any unusual visual appearance or weight change data, further microscopic or photographic examination will be made. The coupons will then be put back into the salt plus dopant for the next 1000 hour interval. Fresh salt plus dopant will replace the old salt 2000 hours into the test. At the test conclusion the coupons will be sectioned and examined metallographically.

A test matrix is shown below:

Dopant Wt %	Temp. Sample	1100°F (593°C)	1100°F (593°C)	1100°F (593°C)	1100°F (579°C)	750°F (593°C)
		Incoloy 800	RA330	316L	347	A516
NaOH	0.50	xxx xxx	xxx xxx	xxx xxx	xxx xxx	xxx xxx
Na ₂ CO ₃	0.20	xxx xxx	xxx xxx	xxx xxx	xxx xxx	xxx xxx
Na ₂ SO ₄	0.35	xxx xxx	xxx xxx	xxx xxx	xxx xxx	xxx xxx
NaCl	0.25	xxx xxx	xxx xxx	xxx xxx	xxx xxx	xxx xxx
*NaCl	0.50	xxx xxx				xxx xxx
Blank		xxx xxx	xxx xxx	xxx xxx	xxx xxx	xxx xxx
Max. Spec of All		xxx xxx	xxx xxx	xxx xxx	xxx xxx	xxx xxx

*Double the max. spec. level

The carbon steel coupon test described in the above matrix will be terminated after 3000 hours. In place of these coupons (same vessels) new circular machined surface coupons (3 PM, 3 Weld each) of A516 and A570 will be placed. In addition to these six machined coupons of each alloy, one coupon of each alloy with a rolled surface will be contained in each test vessel. The salt dopant exposure will be identical with the above matrix but the oven temperatures will be held at 288°C (550°F).

One other series of coupon tests will be run in separate vessels with A287 coupons. These vessels will also contain 3 machined parent metal coupons, 3 machined butt weld coupons and one rolled finish parent metal coupon. This test will be exposed to all the dopants listed above, the temperature will be 399°C (750°F).

Each vessel will contain three regular and two weld sample coupons 3/4" square by 1/16" thick. A third weld coupon will be constructed for crevice corrosion testing as described below. The vessel will consist of a 15" long by 1 $\frac{1}{4}$ " diameter pipe with pipe cap and vent tube to control atmospheric exposure (see Fig. IV). The vessel will be made, as closely as possible, of the same material as the sample coupons. Crevice corrosion coupons will be made by welding two overlapping 3/4 inch square coupons along one edge in such a manner as to create a $\frac{1}{2}$ " crevice for crevice corrosion examination. All high alloy coupons will be cleaned and passivated by EPG 50042 which is a solvent degrease, and a chromate passivation procedure.

The sample vessels will be flushed before testing with dry, CO₂ free air. During the test, the sample vessels will be vented through a manifold system to prevent CO₂ and water from entering the sample vessels.

Salt samples will be taken from each vessel after each 1000 hour test. If a particular corrosion problem is noted with the test coupons, then the corresponding salt will be available for analysis. In addition salt samples will be analyzed at the end of 2000 hour and 4000 hour tests for anions only.

2. Ongoing Materials Tests (Long Term Test)

The objective of this ongoing test is to evaluate selected construction materials under longer periods of exposure to the molten salt environment than was possible in Phase I tests.

Selected sample coupons from Phase I testing will be continued under immersion exposure conditions for an additional twelve months. The test matrix is shown below:

<u>593°C Oven (1100°F)</u>	<u>399°C Oven (750°F)</u>
Incoloy 800	A516 carbon steel
RA330	
SS 347	

The sample coupons will be continued in the same Incoloy 800 immersion trays and will be suspended into the molten salt with nichrome wires.

Weight change data will be collected every 2000 hours. The sample coupons will be microsectioned and analyzed by optical methods at the end of test (12 months), or before, if any unusual changes are noted in the coupons or the passivation layers.

4. Stress Corrosion Test

The purpose of the stress corrosion test is to determine the susceptibility of candidate materials, both parent metal (PM) and welds, to corrosion cracking under stressed conditions. The stress conditions will be those required to produce approximately a 1% deformation in three different time frames.

Specially constructed dog bone specimens approximately 4" long by 1/2" x 1/16" will be contained in a molten salt vessel made from 2" pipe (see Fig. VII). A standard creep testing machine will attach to the ends of the specimens and maintain the required constant load throughout the test.

The samples will be kept at the test temperatures in molten

salt by use of a tube furnace built into the creep rack machine. The tests will be run in molten salt at 593°C (1100°F). The alloys and creep rates to be tested are shown in the matrix below:

		Creep Rates			Total No. of Specimens
<u>Material</u>		<u>0.001%/hr</u>	<u>0.01%/hr</u>	<u>0.1%/hr</u>	
I-800	PM	XXX	XXX	XXX	9
I-800	Weld	XXX	XXX	XXX	18
		XXX	XXX	XXX	
RA330	PM	XXX	XXX	XXX	9
RA330	Weld	XXX	XXX	XXX	18
		XXX	XXX	XXX	
SS-347	PM	XXX	XXX	XXX	9
SS-347	Weld	XXX	XXX	XXX	18
		XXX	XXX	XXX	

The loads placed on the specimens will be sufficient to obtain creep rates on the order of 0.001%, 0.01%, and 0.1%/hr to a total strain of approximately 1%. Actual total creep strain will be determined by measuring cross-sectioned areas prior to, and after testing. Creep strain will then be calculated using the constant volume condition. Each PM specimen will be tensile tested and metallographically analyzed. The weld specimens will be tested by a standard 180° bend test in addition to the above tests.

5. Carbon Dioxide - Water Vapor Effects on Salt Chemistry

Objective:

The objective of this test is to determine the effects of long-term exposure of molten salt to the ambient atmosphere.

Test Approach:

Vessels containing molten salt at 579°C (1075°F) will be exposed to known amounts of CO₂ and water vapor over selected test periods (see matrix). The exposed salts will be analyzed and compared with a blank salt (purified air exposure) in test for a similar time period. The salts exposed to CO₂ or H₂O or both may decompose to form carbonates or hydroxides which will be analyzed for concentration versus time of exposure.

Matrix:

Test	Gas Purified Air	Composition H ₂ O	Vol % CO ₂	Test Time
A1	100%	0	0	1 wk
A2				5 wk
A3				15 wk
A4				6 mo
B1	Balance	100% R.H.	0	1 wk
B2				5 wk
B3				15 wk
B4				6 mo
C1	Balance	0	1.0%	1 wk
C2				5 wk
C3				15 wk
C4				6 mo

Test	Gas <u>Purified Air</u>	Composition		Vol % <u>CO₂</u>	Test Time
		<u>H₂O</u>	<u>100% R.H.</u>		
D1	Balance			1.0%	1 wk
D2					5 wk
D3					15 wk
D4					6 mo

If the concentrations of these products build up with time, atmospheric components may have to be excluded from molten salt contact or a method of regeneration of the converted salt must be employed.

The test setup will consist of eight salt test vessels constructed from Incoloy 800 1½" pipe (see Fig. VI) 15 inches long. The vessels are constructed to maintain the salt sample at 579°C (1075°F), but not to let the salt creep out of the container. This is accomplished by allowing the top part of the vessel to extend above the oven and cool below the freezing temperature of the salt. An Incoloy ¼" gas inlet tube will bubble the gas mixtures through the salt sample ~ g. salt. A test schematic is shown in Fig. VI.

Analysis:

The salt will be analyzed at the end of each test for hydroxide/oxide, carbonates, nitrite, nitrate, potassium, sodium, and chromium. Small test coupons of Incoloy 800 will be placed in each test vessel for analysis of exposure to high CO₃⁼ and OH⁻ concentrations.

6. Salt Treatment Techniques

Objective:

The objective of these tests is to evaluate the "in situ" regeneration of molten salts containing carbonates and hydroxides/oxides by exposure to gaseous nitrogen dioxide.

Approach:

Molten salt (Partherm 430) at 288°C (550°F) containing carbonates and oxides/hydroxide dopants will be exposed to gaseous nitrogen dioxide in the Incoloy 800 bubbler vessels used for the CO₂-H₂O effects test (see Fig. V). The test matrix is shown below:

Matrix

Test #	Salt Composition	Test Time	NO ₂ Addition Rate
1	5% CO ₃ ⁼	24 hrs	Approx. 5 cc/min.
2	5% OH ⁻	24 hrs	Approx. 5 cc/min.
3	5% CO ₃ ⁼ , 5% OH ⁻	24 hrs	Approx. 5 cc/min.
4	Blank	24 hrs	Approx. 5 cc/min.
5	5% CO ₃ ⁼	5 days	Approx. 5 cc/min.
6	5% OH ⁻	5 days	Approx. 5 cc/min.
7	5% CO ₃ ⁼ , 5% OH ⁻	5 days	Approx. 5 cc/min.
8	Blank	5 days	Approx. 5 cc/min.
9	5% CO ₃ ⁼ , 5% OH ⁻	24 hrs	No NO ₂
10	5% CO ₃ ⁼ , 5% OH ⁻	5 days	No NO ₂

Each sample will be analyzed for $\text{CO}_3^{=}$, OH^- , NO_3^- , NO_2^- , Cr, Ni, Fe. Test coupon on Incoloy 800 will be placed in each vessel. Changes in weight and optical analyses will be performed on each coupon at the end of the test.

7. Tensile/Intergranular Corrosion (IGC) Test

Objective: The objective of this test is to assess the susceptibility of candidate materials to intergranular corrosion in the molten salt environment.

Approach:

Tensile test specimens cut from 1/16" sheet stock will be placed in test in a standard 20"x20" oven. The samples will be stacked on top of each other separated by pieces of nichrome wire (6 samples per tray). The oven will be purged with CO_2 - H_2O free air prior to test start and the CO_2 and water vapor limited by use of a scrubber on the oven vent. Six samples of each alloy (both PM and weld) will be placed in test and an equal number of samples will be held at 1100°F in air for reference testing at the end of test and for accelerated testing after 6 months. Three PM salt immersion samples will be pulled from test at the end of 6 months and exposed to ASTM A262 accelerated IGC solution before testing. The remaining immersion samples will be tested without ASTM A262 exposure at the end of 12 months. In addition, 3 PM samples of each alloy exposed to 1100°F in air (no salt) for 6 months will be exposed to solutions to accelerate the IGC (ASTM A262 Test). All tensile tests will be run at ambient

temperatures. Sample analysis will include tensile testing and microsectioning for the parent metal samples and an additional 180° bend test for the weld samples.

IGC Test Matrix Salt Exposure

Material		Exposure	Time	Analyses	
PM	Incoloy 800	Salt, 579°C (1100°F)	6 Mo;12 Mo	6 Tensile & Microstructure	6 pm
Weld	Incoloy 800	Salt, 579°C (1100°F)	12 Mo	3 Tensile & Micro; 3-180° bend	6 weld
PM	RA 330	Salt, 579°C (1100°F)	6 Mo;12 Mo	6 Tensile & Microstructure	6 pm
Weld	RA 300	Salt, 579°C (1100°F)	12 Mo	6 Tensile & Micro; 3-180° bend	6 weld
PM	SS 347	Salt, 579°C (1100°F)	6 Mo;12 Mo	6 Tensile & Microstructure	6 pm
Weld	SS347	Salt, 579°C (1100°F)	12 Mo	3 Tensile & Micro; 3-180° bend	6 weld
PM	SS 316	Salt, 579°C (1100°F)	6 Mo;12 Mo	6 Tensile & Microstructure	6 pm
Weld	SS 316	Salt, 579°C (1100°F)	12 Mo	3 Tensile & Micro; 3-180° bend	6 weld
PM	SS 316L	Salt, 579°C (1100°F)	6 Mo;12 Mo	6 Tensile & Microstructure	6 pm
Weld	SS 316L	Salt, 579°C (1100°F)	12 Mo	3 Tensile & Micro; 3-180° bend	6 weld

In addition, 6 PM samples of each alloy (5) will be held at 1100°F in air. Three of each alloy will be tested after 6 months and three each will be tested after 12 months.

Analysis:

At the test completion, all test specimens will be tested by standard testing techniques for:

1) Tensile Properties

- a) Percent elongation
- b) Yield strength
- c) Ultimate strength

2) Metallographic examination for IGC after microsectioning.

3) All welds will be subjected to 180° bend test.

The six month salt exposure specimens (3 PM each alloy) and three of each 1100°F air exposure specimens will be subjected to an accelerated IGC test (ASTM A262) before the above testing takes place.

8. Corrosion Fatigue

Objective:

The cyclic stresses in a solar receiver would be thermal in nature. These stresses may combine with residual stresses due to fabrication. While extensive data are available on the fatigue strength of various materials in the air, the objective of this test would be to obtain fatigue data for metals immersed in the hot salt environment.

Approach:

The corrosion fatigue test will be similar to a conventional tension fatigue test except that the sample would be immersed in nominal molten salt at 593°C (1100°F). The cyclic loading would be tension-tension with an "R" factor of 0.1. Specific stress levels will be determined later. Tests would be conducted to failure for up to 10^6 cycles, at approximately 1 cycle/sec. Three samples of each material would be tested. Three stress levels would be investigated to define the stress/cycle (S-N) curve. The information to be derived is allowable fatigue strength in molten salt for

the materials to be tested. The test will be performed to compare corrosion fatigue curves with typical S-N curves at 593°C (1100°F) in air. Any tendency of the passivation layer to flake off would be evaluated by direct visual examination and by comparing post-test specimen weights with pretest weights and calculated passivation layer weights. Only candidate receiver materials will be tested.

Matrix

Material	Sample Config.	Cycles at 1 Hz	Stress Level	Environment	No. Samples	Time
Incoloy 800	Parent metal dog bone	TBD	TBD	1100°F Molten Salt	9	12 days max.
RA 330	"	TBD	TBD	"	9	"
347 SS	"	TBD	TBD	"	9	"

9. Thermal Cycling of Test Coupons

Objective

Demonstrate the tenacity of the oxide passivation layer during severe thermal shock conditions.

Test

Heat metal coupons (3 each) containing a 2000 hour passivation layer to 593°C (1100°F), in oven, then quench immediately in ambient water. Repeat cycle 50 times. Carbon steel will be heated to 399°C (750°F).

Material: Incoloy 800
 SS 316L
 SS 347
 RA 330
 Carbon Steel

Analysis

The coupons will be analyzed for weight change after each ten quench cycles and the passivation layer will be optically analyzed at end of test.

10. Nitrate Salt Decomposition Test

Objectives:

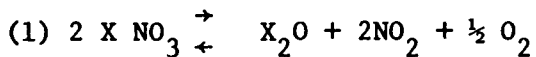
To determine the rate of decomposition of nitrate salt to oxides in a closed system.

Approach:

A sealed Incoloy tube (~1000 cc. volume) containing 500 g. of draw salt, a pressure gauge and a gas sample withdrawal septum (see Fig. VIII) will be heated to 593°C (1100°F) in a test oven. The pressure will be monitored every 24 hours and a gas sample will be taken every 100 to 1000 hours (depending on pressure rise).

At the end of the test (1000 to 5000 hours or when pressure exceeds 50 psig) the salt will be analyzed for $O^{=}$, $CO_3^{=}$, NO_2^{-} and NO_3^{-} and these results will be compared with salt composition samples before the test. An increase in pressure due to NO_2 or O_2 should correspond to an increase in X_2O and yield rate data on nitrate decomposition.

Decomposition can be followed by pressure buildup.



If the pressure steadily increases, the reaction (1) may not be reversible at reasonable pressures, but if the pressure builds up to a low level and stays constant then (1) is a reversible reaction and decomposition can be controlled by adjustments in salt atmosphere.

11. Special Purpose Materials Immersion Test

Objective:

To test limited use materials like seals, gaskets and packings, and valve trim for compatibility in molten salt.

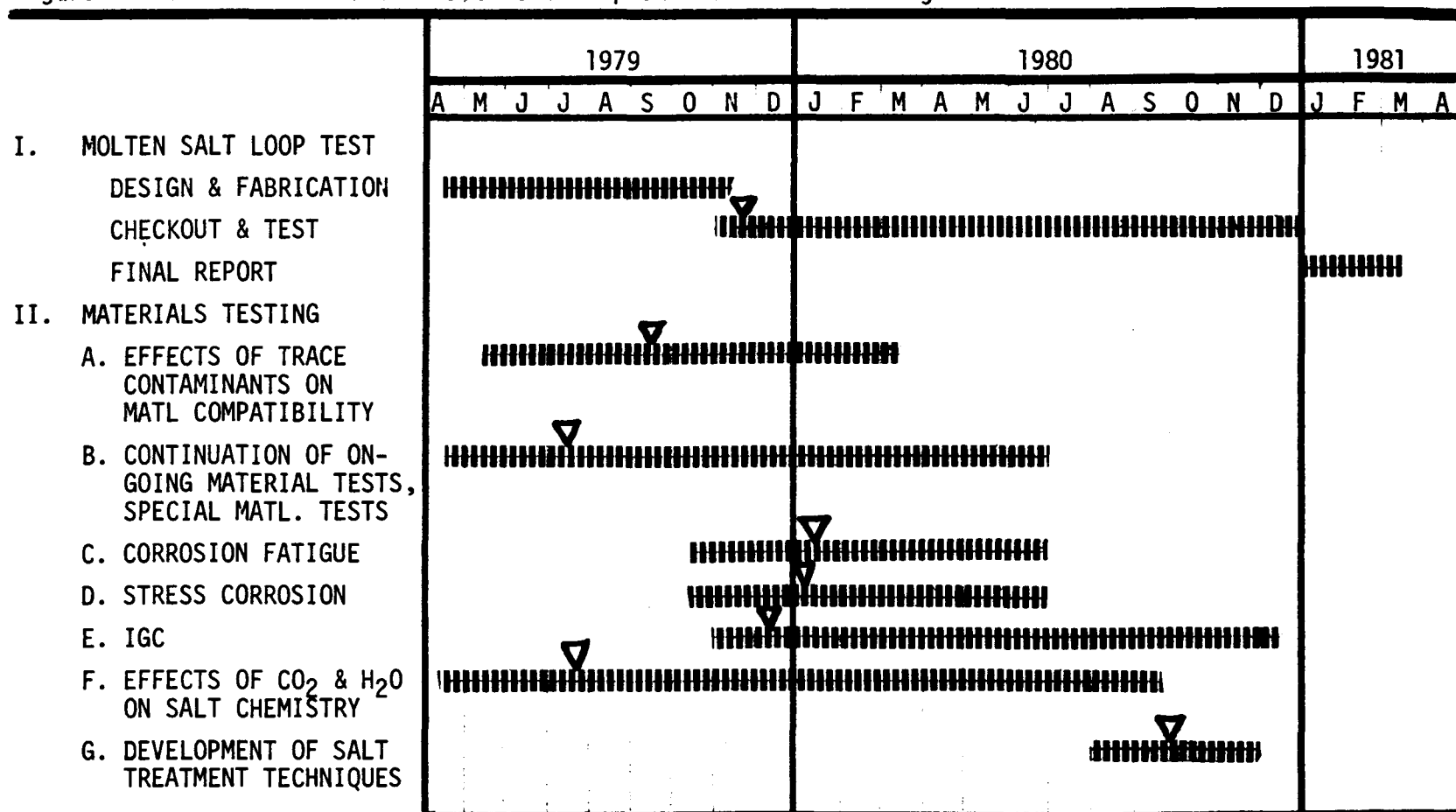
Approach:

The same molten salt immersion technique will be used as described for ongoing tests. Materials will be weighed periodically for weight change where possible, and all will be visually examined every 1000 hours of test time. The total test time will be 5000 hours.

MATRIX

<u>Material</u>	<u>Environment</u>	<u>Test</u>
Asbestos	399°C (750°F) Salt	Visual
Copper	399°C (750°F) Salt	Wt Δ, Visual
Aluminum	399°C (750°F) Salt	Wt Δ, Visual
Tungsten Carbide	399°C (750°F) Salt	Wt Δ, Visual
Stellite #6	399°C (750°F) Salt	Wt Δ, Visual

Figure I Schedule for Molten Salt Test Loop and Materials Testing



▼ - INDICATES TEST START DATES

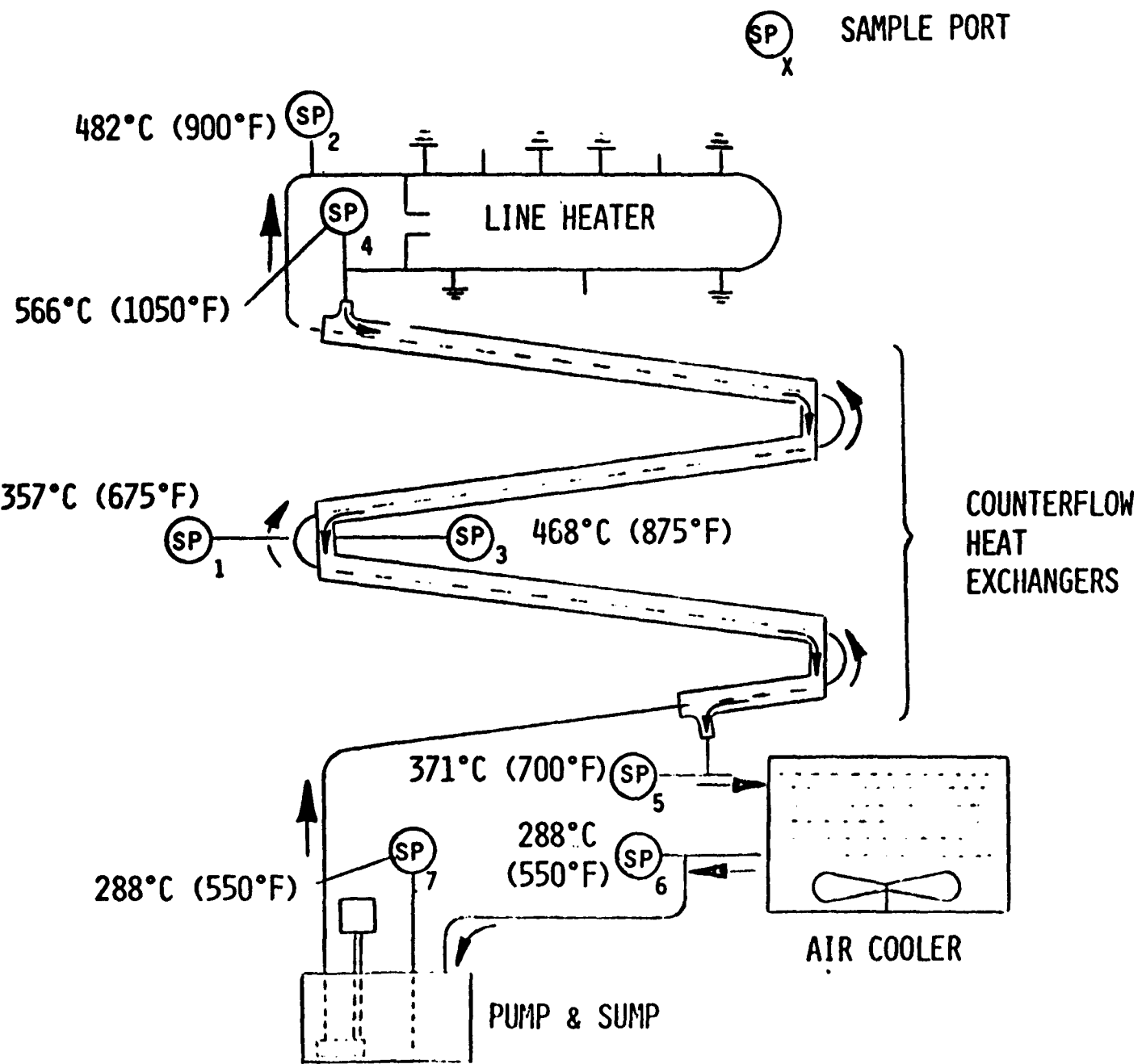
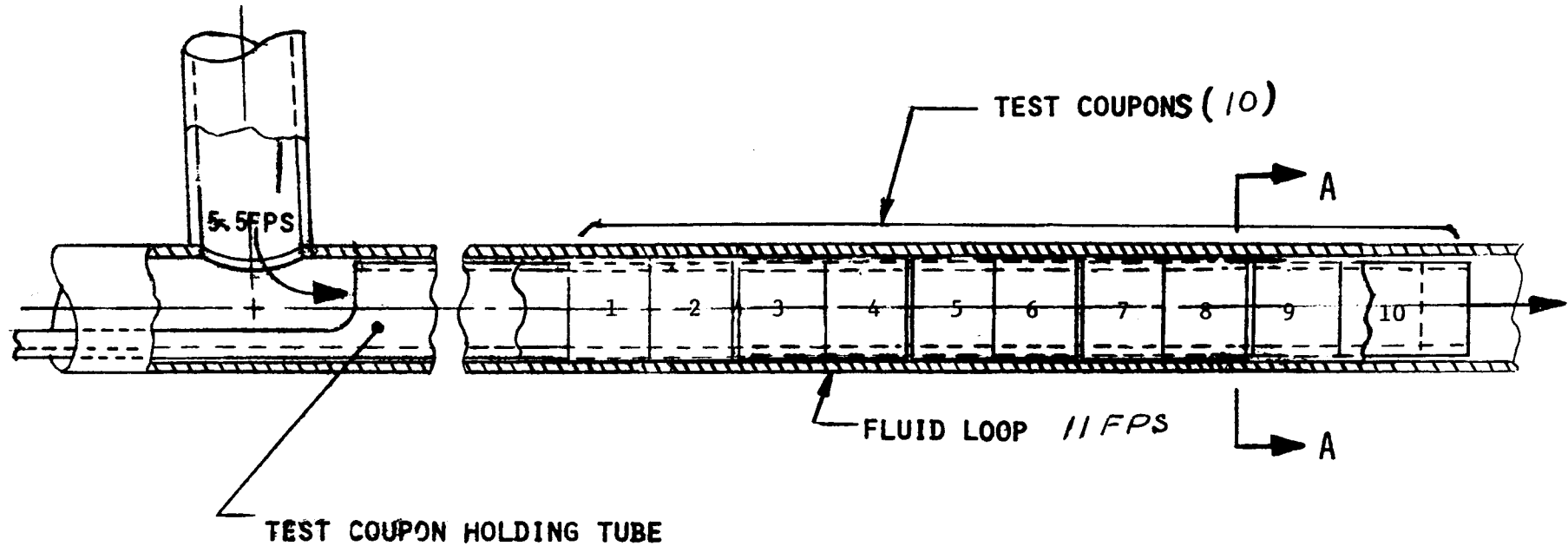
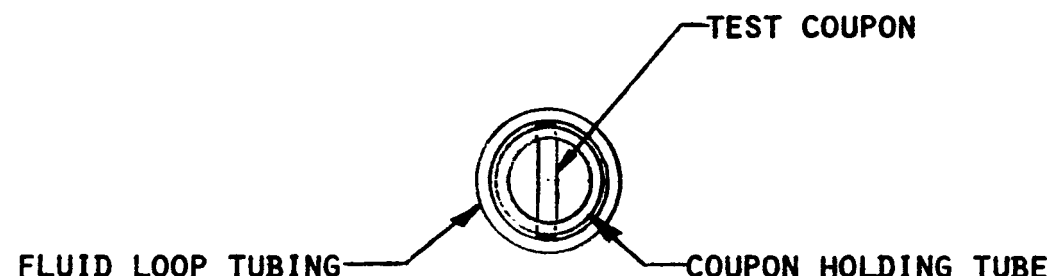


FIGURE II TEST LOOP SCHEMATIC

FIGURE III
MOLTEN SALT FLUID LOOP TEST COUPON INSTALLATION



33



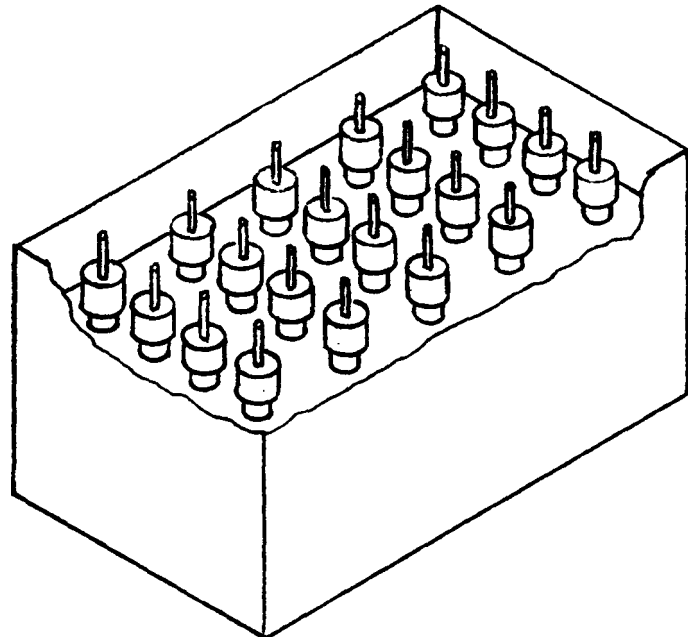
SECTION A-A

MARTIN MARIETTA

FIGURE IV

TRACE CONTAMINANTS TEST - OVEN AND TEST VESSELS DRAWING

34

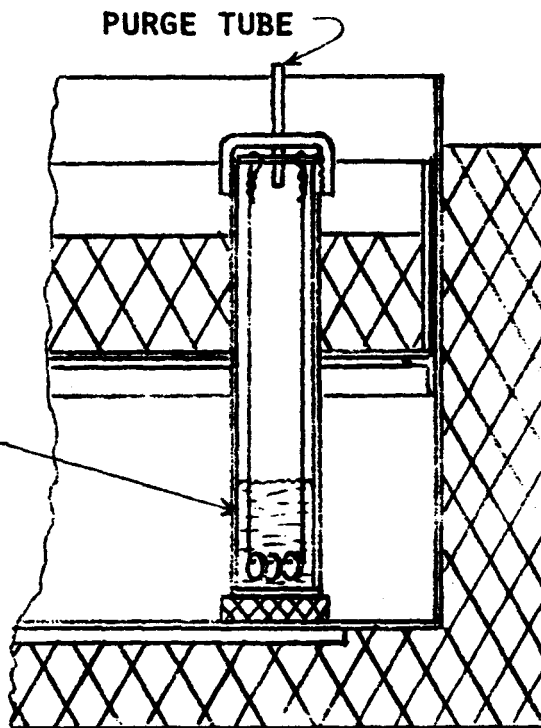


OVEN WITH TEST VESSELS

TEST VESSEL

OVEN AND VESSEL
SECTIONAL VIEW

INSULATION



MARTIN MARIETTA

FIGURE V

TEST VESSEL FOR CO_2 - H_2O TESTS AND SALT TREATMENT TESTS

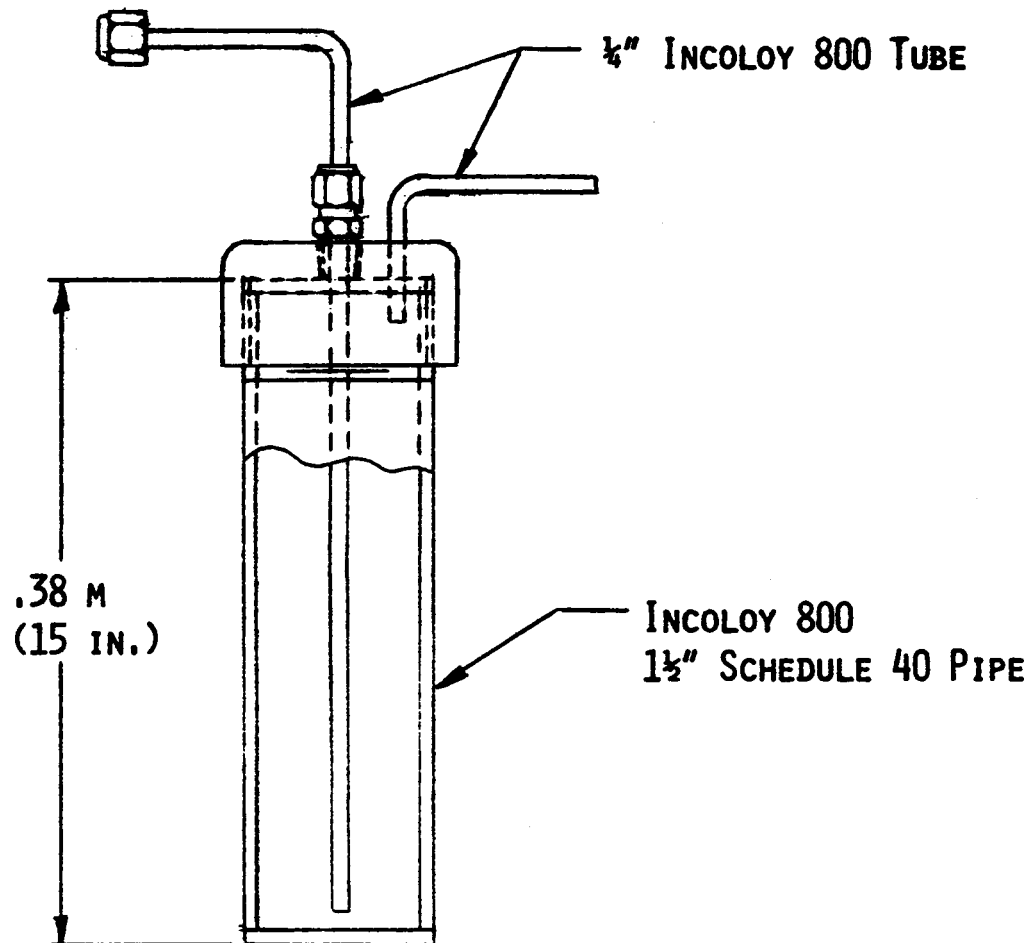
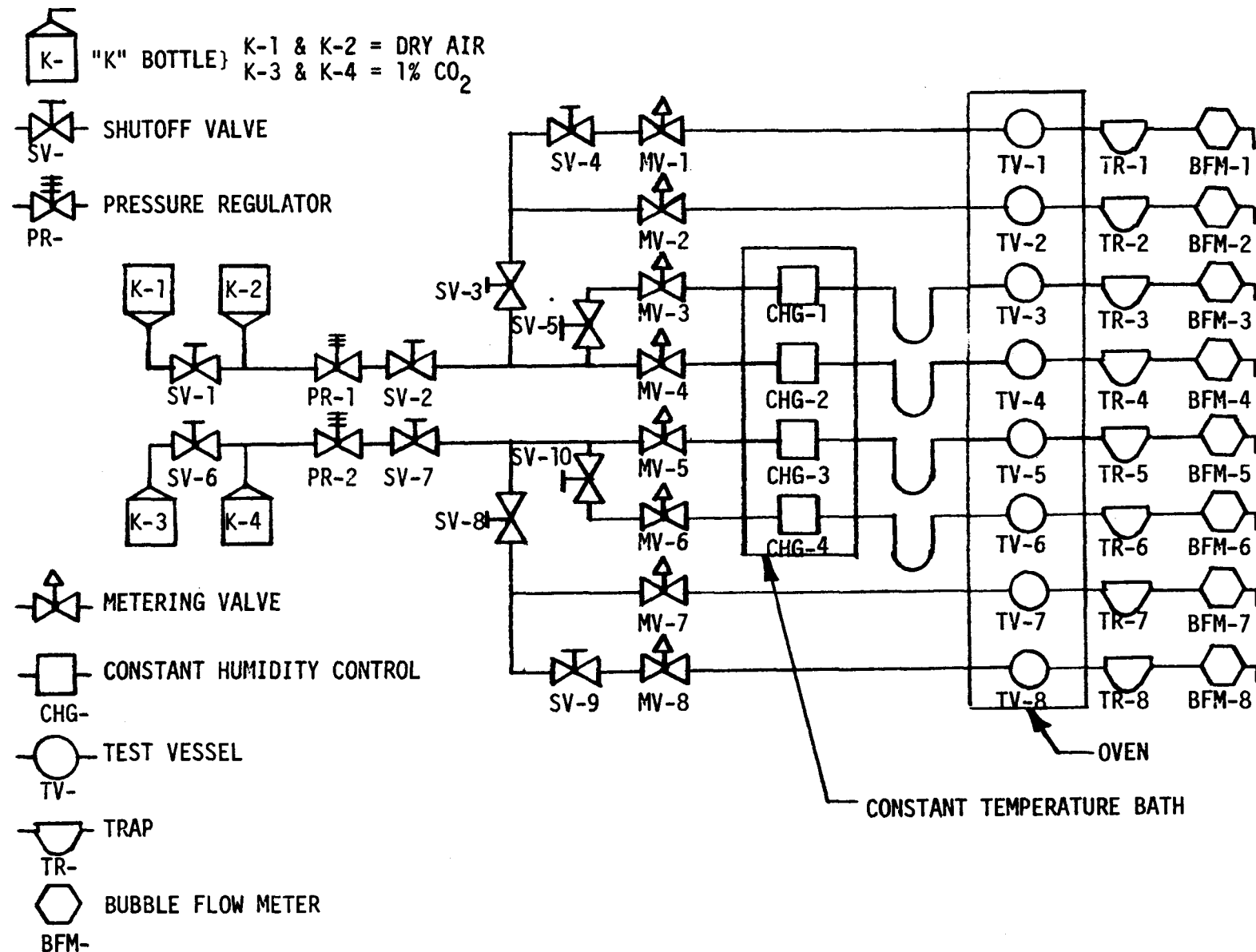


Figure VI. CO_2 - H_2O Chemistry Tests - Flow Schematic



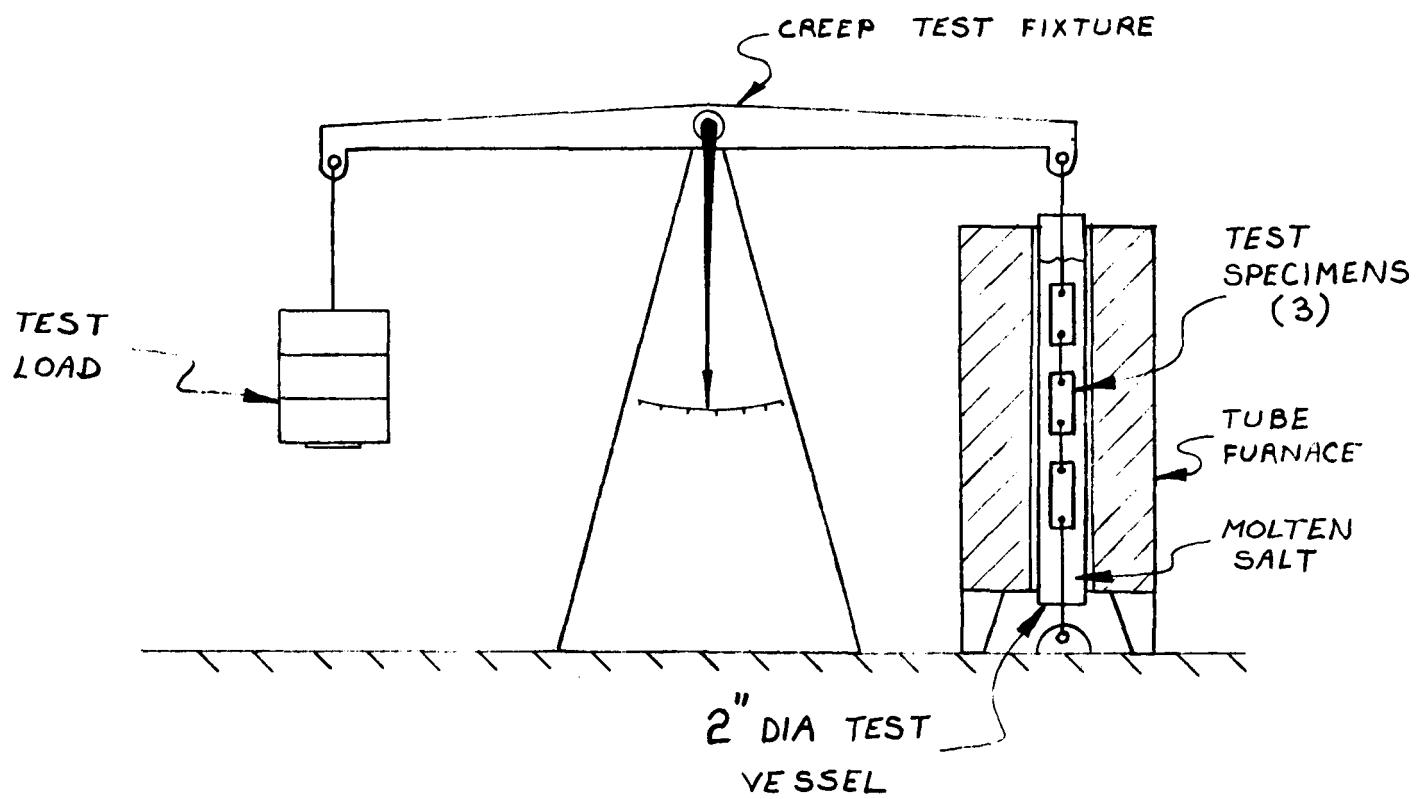


FIGURE VII STRESS TEST SCHEMATIC

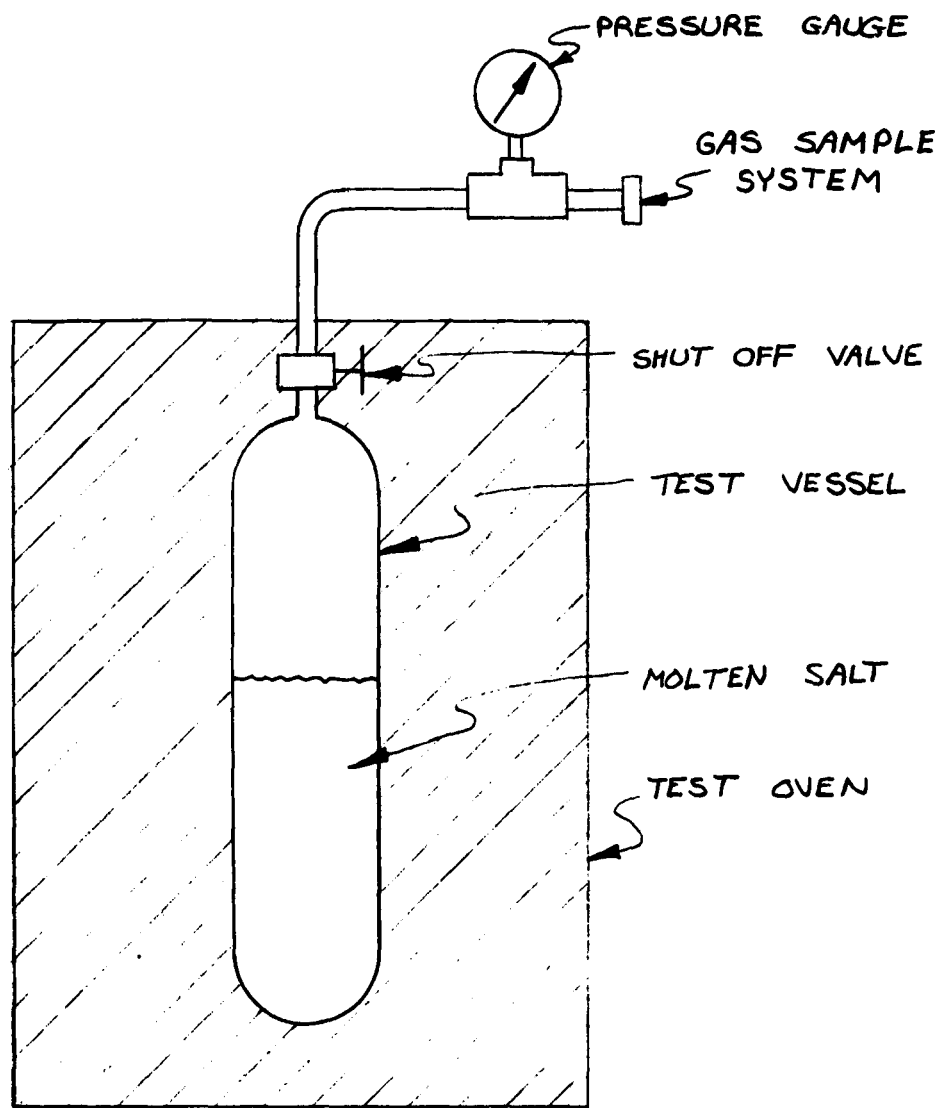


FIGURE VIII OXIDE TEST SCHEMATIC

*U.S. GOVERNMENT PRINTING OFFICE:1980 -740 -145 618 REGION NO.4